

~~JUN 1971~~



NATIONAL AERONAUTICS AND SPACE ADMINISTRATION

ORIGINAL CONTAINS
COLOR ILLUSTRATIONS

18
6/24

SECOND ANNUAL

EARTH RESOURCES AIRCRAFT PROGRAM

STATUS REVIEW

COLOR ILLUSTRATIONS REPRODUCED
IN BLACK AND WHITE

VOLUME I

GEOLOGY AND GEOGRAPHY

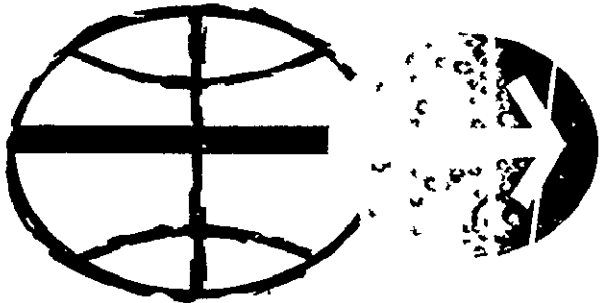
Presented at the

NASA Manned Spacecraft Center
Houston, Texas

September 16 to 18, 1969

N71-19251 - N71-19268

FACILITY FORM 602	(ACCESSION NUMBER)	34	(THRU)	63
	(PAGES)	669B	(CODE)	13
	(NASA CR OR TMX OR AD NUMBER)		(CATEGORY)	



MANNED SPACECRAFT CENTER
HOUSTON TEXAS

Reproduced by
NATIONAL TECHNICAL
INFORMATION SERVICE
Springfield, Va 22151

FOREWORD

On September 16, 17, and 18, a review of various aspects of the Earth Resources Program was held at the Manned Spacecraft Center, Houston, Texas. Particular emphasis was placed on the results of analysis of data obtained with the Manned Spacecraft Center and other aircraft which have contributed data to the program

The review was arranged in conjunction with the Department of Interior, Department of Agriculture and the Department of the Navy. Attendees and participants at the meeting included program investigators, their immediate associates, and program representatives from the above named agencies and ESSA and NASA

The review was divided into the disciplinary areas of Geology, Geography, Hydrology, Agriculture and Forestry, and Oceanography. An additional session was held on instrumentation. Program investigators presented the results of their work in each of these areas. The material presented is being published in three volumes:

Vol I - GEOLOGY AND GEOGRAPHY

Vol II - AGRICULTURE, FORESTRY, AND SENSOR STUDIES

Vol III - HYDROLOGY AND OCEANOGRAPHY

The review provided a current assessment of the program for both management and technical personnel. It is important to note that the material presented represented the current status on ongoing programs and consequently complete technical analyses will be available at a later date

CONTENTS OF VOLUME I

Section		Page
	FOREWORD	111
1	GEOLOGIC APPLICATIONS PROGRAM — SUMMARY OF RECENT PROGRESS AND PLANS	1-1 ✓
	By William R Hemphill	
2	APPLICATION OF COMPUTER PROCESSED MULTISPECTRAL DATA TO THE DISCRIMINATION OF LAND COLLAPSE (SINKHOLE) PRONE AREAS IN FLORIDA	2-1 ✓
	By A E Coker, R Marshall, and N. S Thomson	
3	DIGITAL COMPUTER TERRAIN MAPPING FROM MULTI- SPECTRAL DATA, AND EVALUATION OF PROPOSED EARTH RESOURCES TECHNOLOGY SATELLITE (ERTS) DATA CHANNELS, YELLOWSTONE NATIONAL PARK PRELIMINARY REPORT	3-1 ✓
	By Harry W Smedes, Kenneth L Pierce, Marc G Tanguay, and Roger M Hoffer	
4	GEOLOGIC ANALYSIS OF THE X-BAND RADAR MOSAICS OF MASSACHUSETTS	4-1 ✓
	By Lincoln R Page	
5	THERMAL INFRARED INVESTIGATIONS, MILL CREEK AREA, OKLAHOMA	5-1 ✓
	By L C Rowan, T W Offield, Kenneth Watson, R D Watson, and P J Cannon	
6	REMOTE SENSING TECHNIQUES AS APPLIED TO COASTAL SEDIMENTATION, SOUTH TEXAS	6-1 ✓
	By Henry L Berryhill, Jr	
7	REMOTE DETECTION OF GEOCHEMICAL SOIL ANOMALIES	7-1 ✓
	By F C Canney	
8	GEOLOGIC UTILITY OF SMALL-SCALE AIRPHOTOS	8-1 ✓
	By Malcolm M Clark	

PRECEDING PAGE BLANK NOT FILMED

Section		Page
9	EFFECTIVE RADAR LOOK-DIRECTION FOR GEOLOGIC INTERPRETATION By H C McDonald	9-1 ✓
10	CARTOGRAPHY . By Alden P. Calvocoresses	10-1 ✓
11	SUMMARY OF OBJECTIVES AND PROGRESS IN THE GEOGRAPHIC APPLICATIONS PROGRAM By Arch C Gerlach	11-1 ✓
12	REMOTE SENSING ANALYSIS OF GRASSLAND FIRE PHENOMENA. THE FLORIDA TEST SITES, 1968-69 . By Merle C Prunty	12-1 ✓
13	THEMATIC LAND USE MAPPING: SOME POTENTIALS AND PROBLEMS By David S Simonett	13-1 ✓
14	IMPERIAL VALLEY LAND USE STUDIES: A CONTINUUM FROM MISSION 73 TO APOLLO IX By Claude W Johnson	14-1 ✓
15	HOUSING QUALITY IN URBAN AREAS: DATA ACQUISITION AND CLASSIFICATION THROUGH THE ANALYSIS OF REMOTE SENSOR IMAGERY By Frank E Horton and Duane F Marble	15-1 ✓
16	SURFACE ENERGY EXCHANGE PHENOMENA INTERPRETED FROM IR EXPERIMENTS By Robert W Pease	16-1 ✓
17	GEOGRAPHY PROGRAM REVIEW AND INTEGRATION By Robert H. Alexander	17-1 ✓

CONTENTS OF VOLUME II

Section		Page	
18	VEGETATION RESOURCE -- USER REQUIREMENTS VERSUS REMOTE-SENSING CAPABILITIES	18-1	
	By Robert Colwell and William Draeger		
19	MULTISTAGE SAMPLING OF FOREST RESOURCES BY USING SPACE PHOTOGRAPHY	19-1	
	By Philip G Langley, Robert C Aldrich and Robert C Heller		
20	RANGE RESOURCE INVENTORY FROM SPACE AND SUPPORTING AIRCRAFT PHOTOGRAPHY	20-1	
	By Charles E Poulton		
21	MULTIPLE RESOURCE INVENTORY ON SPACE AND HIGH-ALTITUDE PHOTOGRAPHY	21-1	
	By Lawrence R Pettinger		
22	INTERACTION OF ELECTROMAGNETIC ENERGY WITH AGRICULTURAL CROPS	22-1	
	By Craig L Wiegand, Harold W Gausman, William A. Allen, and Ross W Leamer		
23	APPLICATION OF AUTOMATIC RECOGNITION TECHNIQUES TO EARTH RESOURCES	23-1	
	By R B MacDonald		
24	AUTOMATIC PROCESSING OF EARTH RESOURCE DATA	24-1	
	By D. A Landgrebe		
25	MULTISPECTRAL DATA COLLECTION AND INSTRUMENTATION STUDIES	25-1	
	By D. S Lowe		

Section	Page
26 AIRBORNE INFRARED SPECTRAL STUDY OF IGNEOUS ROCKS IN SONORA PASS TEST SITE	26-1 <i>WJ</i>
By I A Kilinc and R J P Lyon	
27 DATA PROCESSING AND PATTERN-RECOGNITION STUDIES OF MULTISPECTRAL SIGNALS	27-1 <i>WJ</i>
By M Holter	
28 USE OF PASSBAND INTERFERENCE FILTERS IN MULTISPECTRAL PHOTOGRAPHY	28-1 <i>WJ</i>
By Philip N Slater and Dean B McKenney	
29 MULTISPECTRAL VIEWERS	29-1 <i>WJ</i>
By Edward Yost	
30 MICROWAVE STUDIES AND INSTRUMENTATION FOR THE EARTH RESOURCES PROGRAM	30-1 <i>WJ</i>
By John C Blinn III	
31 GROUND TRUTH/SENSOR CORRELATION	31-1 <i>WJ</i>
By Peter Chapman, Jack Quade, and Peter Brennan	
32 RADAR AND DATA PROCESSING	32-1 <i>WJ</i>
By Richard K Moore	
33 RECENT PROGRESS IN TANK, SHIPBOARD, AND HELICOPTER TESTS OF THE FRAUNHOFER LINE DISCRIMINATOR	33-1 <i>WJ</i>
By George E Stoertz and William R. Hemphill	
34 EXPERIMENTAL RESULTS IN THE REMOTE SENSING OF GASES FROM HIGH ALTITUDES	34-1 <i>WJ</i>
By A R. Barringer and J H Davies	

CONTENTS OF VOLUME III

Section		Page	
35	APPLICATION OF INFRARED IMAGERY IN STUDYING THERMAL CHARACTERISTICS OF A COOLING RESERVOIR	35-1	<i>[Handwritten mark]</i>
	By J. F. Turner		
36	COLOR INFRARED AND THERMAL INFRARED SENSING OF HYDROLOGIC FEATURES IN NORTHERN COOK INLET, ALASKA	36-1	<i>[Handwritten mark]</i>
	By W. W. Barnwell		
37	RELATION OF REMOTE SENSING TO TRANSPIRATION OF FLOOD PLAIN VEGETATION	37-1	<i>[Handwritten mark]</i>
	By Richard C. Culler and Raymond M. Turner		
38	SYNOPTIC REMOTE SENSING SURVEY OF LAKES IN WEST-CENTRAL FLORIDA	38-1	<i>[Handwritten mark]</i>
	By J. W. Stewart		
39	REMOTE SENSING OF OFFSHORE SPRINGS AND SPRING DISCHARGE ALONG THE GULF COAST OF CENTRAL FLORIDA	39-1	<i>[Handwritten mark]</i>
	By J. D. Hun and R. N. Cherry		
40	THE USE OF COLOR INFRARED PHOTOGRAPHY AND THERMAL IMAGERY IN MARSHLAND AND ESTUARINE STUDIES	40-1	<i>[Handwritten mark]</i>
	By Richard R. Anderson		
41	A THERMAL SURVEY OF THE CONNECTICUT RIVER ESTUARY	41-1	<i>[Handwritten mark]</i>
	By F. H. Ruggles, Jr		
42	MULTISPECTRAL DATA COLLECTION AND PROCESSING TECHNIQUES APPLIED TO HYDROBIOLOGICAL INVESTIGATION, EVERGLADES NATIONAL PARK, FLORIDA	42-1	<i>[Handwritten mark]</i>
	By M. C. Kolipinski		

Section	Page
43 SNOW AND ICE SENSING WITH PASSIVE MICROWAVE AND GROUND TRUTH INSTRUMENTATION: RECENT RESULTS, SOUTH CASCADE GLACIER	43-1 ✓✓✓
By A. T. Edgerton and M. Meier	
44 USE OF INFRARED RADIOMETRY IN MEASURING GROUND-WATER INFLOW TO STREAMS, DELMARVA PENINSULA, MARYLAND AND DELAWARE	44-1 ✓✓✓
By E. F. Hollyday	
45 PRELIMINARY REPORT ON REMOTE SENSING IN WATER-RESOURCES STUDIES IN YELLOWSTONE NATIONAL PARK, WYOMING	45-1 ✓✓✓
By Edward R. Cox	
46 SNOWFIELD MAPPING WITH K-BAND RADAR	46-1 ✓✓
By William P. Waite and Harold C. McDonald	
47 PASSIVE MICROWAVE STUDIES	47-1 ✓✓✓
By James P. Hollinger	
48 RADAR AND OCEANOGRAPHY	48-1 ✓✓
By Richard K. Moore	
49 SEA-SURFACE TEMPERATURE AND HEAT FLOW - BOMEX	49-1 ✓✓
By E. D. McAlister	
50 EXPERIMENTAL RESULTS OF THE REMOTE MEASURE- MENT OF OCEAN FLOOR	50-1 ✓✓✓
By Peter G. White	
51 EXPERIMENTS IN OCEANOGRAPHIC AEROSPACE PHOTOGRAPHY BEN FRANKLIN SPECTRAL FILTER TESTS	51-1 ✓✓✓
By D. S. Ross and R. C. Jensen	

Section		Page	
52	DEPTH DETERMINATION BY MEASURING WAVE SURFACE EFFECTS	52-1	<i>AK</i>
	By F C Polcyn		
53	THE STUDY OF COASTAL ECOLOGY USING REMOTE PHOTOGRAPHY	53-1	<i>AK</i>
	By Mahlon G Kelly		

TABLES

Table		Page
2-1	COLOR KEY FOR SINK AREA VEGETATION	2-8
2-2	COLOR KEY FOR FALSE COLOR THERMAL CONTOURING IN SINK AREA	2-9
3-1	WAVELENGTH BANDS OF UNIVERSITY OF MICHIGAN MULTISPECTRAL SYSTEM	3-3
3-2	CHANNELS USED IN THE TERRAIN CLASSIFICATION AND MAPPING, AND TO SIMULATE THE ERTS DATA CHANNELS	3-10
7-1	METAL CONTENT OF RED SPRUCE (AND SUPPORTING SOIL) USED FOR REFLECTANCE MEASUREMENTS	7-6
7-2	METAL CONTENT OF BALSAM FIR (AND SUPPORTING SOIL) USED FOR REFLECTANCE MEASUREMENTS	7-6
9-1	ANALYSIS OF LOOK-DIRECTION PANAMA IMAGERY	9-14
13-1	DETECTABILITY OF ROADS BY WIDTH ON APOLLO SPACE PHOTOGRAPH	13-21
13-2	PERCENT OF VISIBLE ROADS ON APOLLO SPACE PHOTOGRAPH TEXAS COUNTIES	13-21
13-3	ROADS NOT DETECTED AND FALSE ALARM MILES IDENTIFIED ON APOLLO SPACE PHOTOGRAPH (TEXAS COUNTIES)	13-22
13-4	DALLAS-FORT WORTH AREA VISIBLE ROADS AND FALSE ALARM ERROR ON COLOR, FALSE COLOR AND MULTI-BAND APOLLO SPACE PHOTOGRAPHS	13-23
13-5	COMPARISON OF ROAD DETECTION USING MULTIPLE SPACE PHOTOGRAPHS DALLAS- FT. WORTH AREA, TEXAS	13-24
13-6	SUMMARY OF CAPABILITY TO DUPLICATE SAMPLED MAPS USING SPACE DATA	13-25
13-7	COMMERCIAL AGRICULTURE	13-26
13-8	MIXED COMMERCIAL-SUBSISTENCE AGRICULTURE	13-27

Table		Page
13-9	BAYESIAN CONTINGENCY PREDICTION TABLE USING UNNORMALIZED DATA AND CATEGORIES	13-28
13-10	BAYESIAN CONTINGENCY PREDICTION TABLE USING UNNORMALIZED DATA AND CATEGORIES	13-29
13-11	BAYESIAN CONTINGENCY PREDICTION TABLE USING NORMALIZED DATA AND CATEGORIES	13-29
14-1	CORRELATION OF LAND-USE IDENTIFICATION WITH GROUND SURVEY CHECK APOLLO 9 CIR IMPERIAL VALLEY IMAGE (MARCH 11, 1969)	14-6
14-2	SUMMARY OF CORRELATION BETWEEN REPORTED AND DETECTED AGRICULTURAL CROP ACREAGE IN THE IMPERIAL VALLEY (MARCH 15, 1969)	14-7
14-3	AGRICULTURAL LAND-USE CODE	14-10
15-1	STRUCTURAL AND ENVIRONMENTAL VARIABLES UTILIZED IN THE LOS ANGELES STUDY	15-7
15-2	ESTIMATED VALUES OF SEVEN VARIABLE DIS- CRIMINANT FUNCTION COEFFICIENTS FOR FIVE HOUSING QUALITY CLASSES	15-8

FIGURES

Figure		Page
2-1	The shaded area outlines the approximate area in Florida covered by University of Michigan's airborne multispectral scanner on September 5th and 6th, 1967	2-10
2-2	Sand-filled sinkholes formed in limestones of the Hawthorn formation underlie the study area at depths as much as 50 feet beneath the land surface	2-11
2-3	One of two homes lost in land collapse in Bartow, Florida, May 22, 1967	2-12
2-4	Sinkhole formed along the west side of US Highway 98 is in the test site in the center of the photograph	2-13
2-5	Location map of training sets in a karst area near Bartow, Fla.	2-14
2-6	The circular patterns along US Highway 98 to the left of the center part of the photograph show the area of active subsidence	2-15
2-7	The concentric and cooler surface temperature zones form patterns along the west side of US Highway 98 in the center of the photograph and show the area of active subsidence	2-16
2-8	Cooler surface temperature zones delineate the dry areas of deeper water levels and subsidence	2-17
3-1	Diagram of optical-mechanical scanner and spectrometer used by University of Michigan in gathering data for this study	3-19
3-2	Gray-scale video display of reflectance from channel 9	3-20
3-3	Ten-level gray-scale digital computer display of reflectance from channel 9 as obtained by LARS-Purdue	3-21

Figure		Page
3-4	Histograms of reflectance of talus in channels 1, 2, and 5	3-22
3-5	Comparison of spectral reflectance of training areas of four classes of material	3-23
3-6	Index map of test area	3-24
3-7	Aerial photograph of test area	3-25
3-8	Panorama of test area, looking west	3-26
3-9	Photograph of part of hand-colored computer printout of terrain maps, north-central Yellowstone Park	3-27
3-10	Bedrock exposures	3-28
3-11	Talus of rhyolite tuff near Floating Island Lake	3-29
3-12	Blocks of rhyolite tuff in talus, showing contrast between fresh surfaces and surfaces coated with dark lichens	3-29
3-13	Vegetated rock rubble	3-30
3-14	Glacial kame, showing grass, mineral soil, weeds, dead vegetation, elk manure, and sagebrush debris	3-31
3-15	Glacial till, showing sand, rock chips, and boulders in mineral soil, grass, sagebrush, weeds, and twigs	3-32
3-16	Comparison of wavelength bands used in this computer study	3-33
3-17	Segment of terrain map obtained by using computer-selected best set of four channels of reflective data	3-34
3-18	Segment of terrain map obtained by using simulations of ERTS 4-channel scanner data	3-35

Figure		Page
3-19	Segment of terrain map obtained by using simulations of ERTS 3-RBV camera data	3-36
3-20	Segment of terrain map obtained by combining one thermal infrared and three reflective channels of data	3-37
4-1	Side looking radar mosaic of Massachusetts (east looking, uncontrolled, raw imagery, no enhancement)	4-7
4-2	Side looking radar mosaic of Massachusetts (west looking, uncontrolled, raw imagery, no enhancement)	4-8
4-3	Side looking radar mosaic of Massachusetts (east looking, uncontrolled, enhanced)	4-9
4-4	Side looking radar mosaic of Massachusetts (west looking, uncontrolled, enhanced)	4-10
4-5	Lineaments traced from side looking radar mosaic of Massachusetts (east looking)	4-11
4-6	Lineaments traced from side looking radar mosaic of Massachusetts (west looking)	4-12
4-7	SLAR imagery - central Massachusetts and Connecticut	4-13
4-8	Lineaments from SLAR imagery - central Massachusetts and Connecticut	4-14
4-9	Massachusetts/Connecticut maps a. Geologic map of south-central part of Massachusetts and north-central Connecticut	4-15
	b. Reinterpretation of geologic map using SLAR imagery	4-15
4-10	Lineaments interpreted from two side looking radar mosaics of western Massachusetts (east looking and west looking)	4-16
4-11	Aeromagnetic map of western Massachusetts	4-17

Figure		Page
4-12	Aerial photomosaic of south-eastern New England	4-18
4-13	Geologic map of Massachusetts and Rhode Island	4-19
5-1	Tishomingo anticline area	
	a. Index map	5-15
	b. Geologic map	5-16
	c. Geologic map of South Flank area	5-17
5-2	Precambrian-Ordovician stratigraphic section, Tishomingo anticline area	5-18
5-3	Photomosaic showing rock-type occurrence, Tishomingo anticline area	5-19
5-4	Infrared images of Tishomingo anticline area	5-20
5-5	Isodensitracing of limestone-dolomite area on nighttime infrared image, Tishomingo anticline area	5-21
5-6	Topographic map showing cool linear zones	5-22
5-7	Infrared images of South Flank area	5-23
5-8	Strike computed from theoretical models for enhanced thermal contrast and enhanced isolation contrast	5-24
5-9	Theoretical cooling curves constructed using thermal inertias	5-25
6-1	Index map of the south Texas coast and key to figures	6-8
6-2	Effects of hurricane erosion and rates of healing	
	a. Inlets opened by Hurricane Beulah, September 1967 and storm tide deltas	6-9
	b. Amount of healing by sedimentation over the 15-month period	6-9
	c. Print from Ektactrome infrared film taken December 1968	6-9

Figure		Page
6-3	Sediment effluence	
	a. Corpus Christi ship channel	6-10
	b. Port Isabel ship channel	6-10
	c. Same general area as Port Isabel	6-10
6-4	Sediment patterns	
	a. Section of central Padre Island taken on Ektachrome film	6-11
	b. Nearby area taken on Ektachrome infrared film	6-11
6-5	Circulation vortex in western part of Corpus Christi Bay	
	a. Print from Ektachrome regular film	6-12
	b. Print from Ektachrome infrared film	6-12
6-6	Section of northern Laguna Madre showing com- parison of techniques for water penetration	
	a. Print from Ektachrome regular color film	6-13
	b. Print from Ektachrome infrared film	6-13
6-7	Thermal characteristics of bay and lagoonal water entering the Gulf of Mexico	
	a. Corpus Christi ship channel	6-14
	b. Natural inlets cut by storm erosion at southeast end of Corpus Christi Bay	6-14
	c. Port Isabel ship channel	6-14
6-8	Generalized environmental map of South Bird Island Quadrangle made from color aerial photographs	6-15
6-9	View of Texas coast facing southward, taken by Apollo 9, March 1969	6-15
7-1	Photograph showing method of obtaining reflectance data in a downward-looking orientation	7-7
7-2	Reflectance of Red Spruce	7-8
7-3	Reflectance of Balsam Fir	7-8

Figure		Page
8-1	Locations and approximate coverage of high altitude photographs shown in figures and plates	8-22
8-2	Oblique photo taken from 60,000 feet	8-23
8-3	Small-scale view of the Garlock fault (A-A') near Searles Valley	8-24
8-4	Geologic map of Pleistocene glacial deposits near Virginia and Green Creeks	8-25
8-5	Relations between flying height, angular field of view, and terrain hidden from view of aerial cameras	8-26
 Plate		 Page
8-1	Koehn Lake, a playa crossed by the Garlock fault	8-27
8-2	Portion of the Garlock fault	8-28
8-3	Southeast end of Coyote Creek fault	8-29
8-4	Southeast portion of Coyote Creek fault. Plate 8-4 forms a stereo pair with Plate 8-3	8-30
8-5	Mono Lake and drainages of Virginia and Green Creeks	8-31
8-6	Bridgeport Basin	8-32
8-7	Green and Virginia Creeks	8-33
8-8	Wisconsin moraines near Green Creek	8-34
8-9	San Andreas fault at Carrizo Plain	8-35
8-10	Several stream channels offset by San Andreas fault	8-35
8-11	San Andreas fault at Cholame Valley. A group of deflected stream courses	8-36

Plate		Page
8-12	San Andreas fault at Cholame Valley. An old erosion surface, now being dissected	8-36
8-13	Southern part of San Francisco Bay	8-37
8-14	Stereo pair of Garlock fault zone taken with superwide-angle lens	8-38
8-15	Stereo pair of Garlock fault zone taken with normal wide-angle lens	8-39
Figure		Page
9-1	Sketch diagram Typical side-looking airborne radar system	9-15
9-2	Shadowing characteristics associated with SLAR imaging systems	9-16
9-3	Geometry of slant range and ground presentation	9-17
9-4	Effect of near-range compression on geometric shape, La Palma Peninsula, Darien Province, Panama	9-18
9-5	Spanish Peaks, Colorado	
	a. Look-direction, north	9-19
	b. Look-direction, south	9-19
9-6	Central Humboldt Range, Nevada	
	a. Look-direction, south	9-20
	b. Look-direction, north	9-20
9-7	Multiple flight coverage, Boston Mountains, Arkansas	
	a. Look-direction, west	9-21
	b. Look-direction, north	9-21
	c. Look-direction, northwest	9-21
10-1	An example of automated snow mapping	10-5

Figure		Page
10-2	An example of automated vegetation mapping	10-6
10-3	An example of underwater detail enhanced by photolab procedures	10-7
10-4	Simplified drawings illustrating displacements in satellite imagery	10-8
11-1	Power spectra signatures by optical processing	11-9
11-2	Geographer consultants in remote sensing, by regions	11-11
11-3	Geographer participants in remote sensing institutes	11-12
12-1	Location of test site areas in Florida and Georgia	12-6
12-2	Vegetation types; Pipeline Road, Deseret Farms, Florida	12-7
12-3	Burns, Pipeline Road, Deseret Farms, Florida, 1967-1968	12-8
12-4	Pipeline Road Area, Deseret Farms, Florida, March 1968	12-9
12-5	Pipeline Road Area, Deseret Farms, Florida, October 1968	12-10
12-6	Pipeline Road Area, Deseret Farm, Florida, March 1969	12-11
12-7	Pipeline Road Area, Deseret Farm, Florida, April 1969	12-12
13-1	Comparison of air photo mosaics with red separation plate enlargements of the Gemini color photo of the Alice Springs region, Central Australia	13-30
13-2	Color photograph of the Alice Springs area, Central Australia	13-31

Figure		Page
13-3	Landscapes northwest of Alice Springs, Central Australia. Modified slightly from R. A. Perry (1961), Pasture Land Map	13-32
13-4	Landscapes northwest of Alice Springs, Central Australia. Boundaries and categories based upon space photography	13-33
13-5	Comparison of boundaries delineated on space photograph and Perry's (1961) map of the pasture lands of the Alice Springs region	13-34
13-6	Roads detected on a space photograph and color separation plates of the Dallas- Fort Worth area, Texas	13-35
13-7	This map depicts the area covered by the space photograph	13-36
13-8	Apollo VI color photograph of the Dallas-Fort Worth area, Texas	13-37
13-9	Photographs of Dallas-Fort Worth, Texas and vicinity of Cape Kennedy, Florida	
	a. Dallas-Fort Worth area	13-38
	b. Titusville and vicinity near Cape Kennedy, Florida	13-38
13-10	Aerial photographs, brought to a common scale of 1:25,000, illustrate the variations in the size, shape, and arrangement of spatial elements which occur in differing world environments	13-39
13-11	Time available for aerial photography in July	13-40
13-12	Number of hours lost to radar in July through precipitation equal to or exceeding 0.25 inches per hour	13-41
13-13	Color infrared photography of an area near Lawrence, Kansas, July 31, 1967	13-42

Figure	Page
13-14	Means and standard deviations for six crops, using unnormalized density data for the three dye layers of color infrared film 13-43
15-1	Study areas in Los Angeles 15-9
15-2	Flow chart for steps in analysis 15-10
15-3	Color infrared image of Firestone area 15-11
15-4	Mapping metropolitan land use from Apollo color IR photo 15-12
15-5	Mapping metropolitan land use from Apollo color IR photo (Phoenix, Arizona) 15-13
16-1	A comparison of black and white multi- spectral photographs with multispectral separations from color infrared film 16-6
16-2	The principle involved in making multispectral separations from multilayer film 16-7
16-3	Spectral sensitivities of the dye- forming layers of color infrared film compared with the effective sensitivities that occur in black and white multi- spectral systems 16-8
16-4	Enlarged portions of Figure 16-1 that compare resolution and tone 16-9
16-5	A comparison of IDECS readouts from CIR multispectral separations of the area shown in Figure 16-4 with B/W multispectral readout for an adjoining area 16-10
16-6	A color print from type 8443 CIR film processed successfully to a negative and the set of multispectral separa- tions derived from the same negative 16-11

Figure		Page
16-7	An IDECS readout from transparencies derived directly by separation methods from the CIR negative of Figure 16-6	16-12
16-8	Continuing investigation of value of multispectral separation process	16-13
16-9	Quantitative calibration of remote radiation sensors at Barbados	16-14
16-10	Other instruments for making ground to air correlations	16-15
16-11	Cross-calibration of radiation sensors	16-16
17-1	Geographic Applications Program, aircraft missions	17-10
17-2	Geographic Applications Program; test sites	17-11
17-3	Mapping land use from Gemini color photos	17-12
17-4	Airborne measurements of air pollutant (NO ₂) over Los Angeles Basin	17-14
17-5	Mapping urban areas from K-band radar	17-16
17-6	Recognition of gross surface temperature patterns by analysis of passive microwave radiometry	17-18
17-7	Regional land use classification from Gemini color photography	17-20
17-8	Sensor/applications matrix, Geographic Applications Program	17-22
17-9	Discipline research matrix, geography and cartography	17-23

SECTION 1

GEOLOGIC APPLICATIONS PROGRAM--SUMMARY OF
RECENT PROGRESS AND PLANS*

by

William R Hemphill
U S Geological Survey
Washington, D CIntroduction

The Geologic Applications Program, supported jointly by the U S Geological Survey and by NASA, is aimed at evaluating the application of airborne and satellite-borne remote-sensing systems to the discrimination and identification of geologic materials. During FY 1969 the program involved about 58 professional project personnel from the Geologic Division of the Geological Survey. Eleven technical reports describing the results of this effort were transmitted to NASA in FY 1969, about 30 additional reports are in preparation.

Contract and purchase-order agreements with nine universities and industrial firms were issued during the year for the procurement of the following services and equipment:

1. Compilation of a radar mosaic of Massachusetts
2. Field spectral reflectance measurements of geochemically stressed areas
3. Field spectral reflectance measurements of selected igneous and sedimentary rocks
4. Automatic data processing and image enhancement
5. Infrared emission studies of mineralized areas.
6. Evaluation of microwave radiometry applications to geology
7. Purchase of an infrared emission spectrometer

Studies Conducted During FY69

Airborne multiband line-scan imagery of Yellowstone National Park, acquired by the University of Michigan, was analyzed by automatic data-processing techniques at both Purdue and Michigan data-processing facilities (H. W. Smedes and K. L. Pierce, unpub. data). The results of this work are encouraging. Nine categories of materials, including four rock types, were automatically classified and symbolically displayed on a two-dimensional computer printout or "map" of the area. Some success was also achieved using only the three spectral bands of the Michigan scanner data that are analogous to the multispectral television system to be included in the first Earth Resources Technology Satellite (ERTS), tentatively scheduled for launch in 1972. Results from data-processing experiments such as this one will contribute to expeditious handling and analysis of satellite data when it becomes available.

Studies along the Atlantic and Gulf coasts are aimed at evaluating remote-sensor methods in observing the dynamics of sediment movement and the rates of deposition and erosion of shore areas (H. L. Berryhill, unpub. data). The results of these and similar studies could be of

*Publication authorized by the Director, U S. Geological Survey

N71-19252

direct importance in such diverse activities as prospecting for offshore placers, assessing the susceptibility of a coastal area to water pollutants, and changes of importance to coastal land use and development. Satellite observation could be particularly suited to this kind of work for two reasons

1. Some changes in coastal areas are sufficiently rapid to be observed on the repetitive imagery that long-lived satellites will provide routinely,
- 2 The size of many targets of interest to marine geologists are of sufficient size to be observed from orbital altitudes

Some success has been achieved in relating near infrared spectral reflectance of balsam fir and red spruce growing at the Catheart Mountain, Maine, test site to geochemical anomalies in the soil supporting the plants (F C Canney, unpub data) Although near infrared reflectance has been exploited for years in early detection of agricultural plant disease, this is the first attempt to relate plant stress to geochemical constituents that are mildly toxic to the plant.

Analysis of aerial photographs on a scale smaller than 1:120,000 shows that such photographs often reveal geologic information, particularly structural information, that might otherwise be overlooked on a photograph having a larger scale and therefore a smaller area (Clark, 1969) The data and conclusions acquired in the study of small-scale photographs are directly analogous to uses of orbital photographs in recognizing some regional geologic information that cannot be routinely acquired in any other way

Analysis of a radar mosaic of Massachusetts also demonstrates the value of radar as a medium for revealing geological relationships that commonly are available only in a synoptic view (L R Page, unpub data)

The work being conducted at the Mill Creek, Oklahoma, test site is the beginning of a continuing program to use remote sensors at sites where rocks of simple mineralogy are well exposed. Early work is being done at quartz and carbonate sites, more complicated mineralogies will be introduced later. Study of the infrared emission spectra and the modifications of spectra introduced by variations of grain size, surface roughness, and other variables, will hopefully someday permit interpretation of these spectra in terms of the gross mineral composition of at least some rock types.

A soils association map covering 150,000 square miles of the southwestern United States and northern Mexico, was compiled from Gemini and Apollo photography. The map demonstrates the value of synoptic photography acquired from orbit in achieving an internal consistency among

mapped units more readily than is possible on maps compiled by conventional means where several sources of data must be used (Morrison, 1969). This effort, moreover, is producing the kind of topical data of regional importance that we can expect to acquire from orbital satellite imagery when it becomes available on a routine basis.

Field evaluation of radio telemetry of data from ground instruments, strategically located in active earthquake and volcano areas, to a central reception center is the first phase in assessing the value of relaying similar information via satellite. Radio telemetry, conceivably, would be cheaper to install and maintain than land lines, which tend to be unreliable at the time of disaster. A satellite relay would also reduce the number of ground telemetry receiving stations that would be required in an all ground-based system.

The Fraunhofer line discriminator is the first so-called remote-sensing instrument to permit detection of solar-excited luminescing material from aircraft. The instrument appears to have application not only for quantitatively monitoring current dynamics and sediment movement, of interest to marine geologists, but also for studies of water and air pollution and possibly, for the detection of luminescing minerals (Stoertz, 1969).

FY70 Program

For FY70, work of the Geologic Applications Program has been consolidated into three NASA tasks, in order to facilitate administration of the program and to better reflect the kinds of geologic information that we can expect to acquire from space. These three tasks are as follows

1. Study of regional and continental geology and geophysics
This task involves assessing the use of the synoptic overview of satellite photography and other imaging remote sensors, to observe large-scale features that may reveal geological relationships of regional significance.
2. Monitoring changing geologic features This task involves study of active time-variant geologic processes such as coastal sedimentation and erosion, shoreline modification caused by major storms, seasonal variations in vegetation and snow that may enhance some geologic features, and monitoring changing trends in the events of historically active volcanoes
3. Fundamental field and laboratory studies. This task is designed to gain a more complete understanding of how the interaction of electromagnetic energy with rocks and other natural materials may be modified by such variables as grain size, surface roughness, weathering, temperature, and other variables.

REFERENCES

- Clark, Malcolm, 1969, Geologic utility of small-scale aerial photographs U S Geol. Survey open-file report
- Morrison, Roger, 1969, Photointerpretive mapping from space photographs of Quaternary geomorphic features and soil associations in northern Chichuahua and adjoining New Mexico and Texas New Mexico Geological Society Guidebook, (in press).
- Stoertz, George, 1969, Fraunhofer line discriminator--an airborne fluorometer U. S Geol Survey open-file report.

SECTION 2

APPLICATION OF COMPUTER PROCESSED MULTISPECTRAL DATA TO THE DIS-
CRIMINATION OF LAND COLLAPSE (SINKHOLE) PRONE AREAS IN FLORIDA 1/By A E Coker 2/, R Marshall 3/, and N S Thomson 3/

ABSTRACT

N71 - 19253

The U S Geological Survey and the Infrared and Optical Sensor Laboratory of the University of Michigan jointly collected data near Bartow, Florida, for the purpose of studying land collapse phenomena using remote sensing techniques. Data obtained using the multi-spectral scanner system consisted of various combinations of 18 spectral bands ranging from 0.4 to 14.0 micron and several types of photography.

Patterns that are hypothesized to be indicators of deeply buried relic sinks were chosen from photographic strips of imagery representative of 18 spectral bands. Data recorded in these spectra contain information about vegetation physiology and soil conditions, and, after special processing, these data may be used as indicators of hydrogeologic conditions related to the occurrence of sinkholes (circular land collapse features). Test sites within these patterns were chosen for multispectral image enhancement and discrimination studies.

The data were processed for the recognition of soil and vegetation characteristics through use of the University of Michigan's multi-spectral computer processor. The processor computes as much as eight Gaussian density functions with as much as 12 spectral bands. A likelihood function is then computed and tested using these functions. The results are in the form of video signals and are printed on film to show the pattern of distribution of the proposed hydrogeologic indicators.

Terrain temperature patterns (obtained from processed 8-14 micron data), when compared with moisture stressed vegetation patterns (obtained from processed 1-2.6 micron data), show distinctive patterns that correlate with the areas of known sinkhole formation in the Bartow area. These patterns also correlate with areas where sinkhole formation has been predicted based on a study of National Aeronautics and Space Administration data. Additional indicators of impending land collapse may be derived from the multispectral data after further detailed analyses.

1/ This study was prepared for the National Aeronautics and Space Administration under contract No. R-146-09-020-011.

2/ U S Geol Survey, Tampa, Fla.

3/ Infrared and Optical Sensor Laboratory, University of Michigan, Ann Arbor, Mich.

INTRODUCTION

The study area is in the headwaters of the Alafia and Peace River basins, near Bartow, Florida (fig 1) Carbonate rocks underlying the area have in the geologic past and, are undergoing solution by circulating ground water. Much of the sinkhole formation that occurred during previous periods of emergence of peninsular Florida has been buried beneath as much as 300 feet of interbedded sand, silt, clay, and marl. The area is presently emerged and sinkholes are forming.

Quartz sand of Pleistocene age blankets the surface, which is underlain by phosphatic clays and sands of the Bone Valley Formation. Locally, the Bone Valley Formation unconformably overlies the Hawthorn formation, in which many sinkholes have formed. The sinkholes developed in the Hawthorn formation are probably the result of solution of the underlying carbonate rocks. Buried sinkholes formed in the top of the Hawthorn formation underlie this area of present day sinkhole occurrence and development (fig 2, J B Cathcart, written commun, 1969).

Ground water in surficial sand percolates through semipermeable confining beds of the Bone Valley and Hawthorn formations into the underlying carbonate (Floridan) aquifer. Downward movement of this water is concentrated in places where these confining beds are thin, absent, or breached by sand-filled sinkholes.

The larger voids with the limestones of the Floridan aquifer and relic sinkholes may be filled or partly filled with porous sand so that the overall vertical permeability of the geologic section, from land surface to deep in the Floridan aquifer, is greater than in adjacent areas. Ground water in near surface aquifers should infiltrate into an underlying carbonate aquifer (the Floridan aquifer) more readily at these places of greater permeability.

Water levels in surficial unconfined aquifers in these areas of greater vertical permeability should decline more than in surrounding areas and a cone of depression, somewhat similar to that formed in the vicinity of a discharging well, should form. Because of continued drainage, the water content of the soils overlying these areas of greater vertical permeability is reduced considerably more than in the soils of surrounding and less well-drained areas.

During seasons of heavy rainfall, the percolation of somewhat acid water into the Floridan aquifer through these zones of greater vertical permeability should allow progressive carbonate solution of the Floridan aquifer. Such chemical solution can enlarge the underground conduits and weaken the roof that supports the overlying material. However, during rainy seasons when the recharge exceeds discharge, hydrostatic pressure within the aquifer will be increased. This increased pressure helps support the weakened roof and prevents collapse by reducing stress on the rocks.

During dry seasons as the water levels decline, hydrostatic pressure partially supporting cavern and conduit roofs may decline enough, so that the load stress caused by the overlying material exceeds mechanical strength of the cavern roofs and collapse occurs (fig 3) In the test area, industrial and agricultural expansion has led to a marked increase in the use of water from the Floridan aquifer This continuing increase in use of water coupled with a 6-year drought has caused a progressive decline of hydrostatic pressure, which has probably accelerated the natural process of sinkhole formation

A greater probability for the formation of sinkholes is hypothesized to occur in areas underlain by buried relic sinkholes, and sinkholes should tend to form during and shortly after time of greatest hydrostatic pressure or water-level decline. The objective of the study was to test this hypothesis and develop techniques by which land collapse may be anticipated and predicted by using the techniques of remote sensing

Because areas prone to active sink collapse are often not detectable from apparent surface expression of hydrology and geology prior to actual collapse, it was necessary to apply indirect methods to the problem of detecting the surface effects caused by water-pressure decline in the areas of active sinkhole development An experiment was begun to collect and process data for the purpose of testing the hypothesis that areas of active sinks could be detected at the land surface from the integrated effects of water loss at depth on vegetation and terrain temperature difference due to water availability

Multispectral imagery data was acquired by the University of Michigan's airborne 18-channel optical-mechanical scanner over a test area near Bartow, Florida, on September 5, 1967, at 1224 hours, and September 6, 1967, at 0647 hours Each flight was made at an altitude of 2000 feet above terrain (fig 4) These data have been processed using multispectral techniques in order to detect water-stressed vegetation and to enhance surface thermal effects The processed results have been correlated with hydrogeologic field data to determine the capability of using the processing techniques to identify and locate areas of sinkhole collapse This paper will be devoted to an interpretation of the processed images obtained by the automatic computer processing techniques at the Infrared and Optics Laboratory of the University of Michigan Detailed descriptions of the methods of collection and processing of the imagery are published in papers by Holter and Polcyn (1964), Holter and Wolfe (1960), Lowe and Braithwaite (1966), Malila (1968, and Marshall (1969)

The equipment and techniques employed were developed under several contracts, with the Army (Ft Monmouth), Air Force (Wright Patterson AFB), and the Department of Agriculture

The applications presented in this report have involved intensive collaboration of personnel engaged in remote-sensing techniques at the Infrared and Optics Laboratory, University of Michigan, and those Geological Survey hydrologists familiar with the hydrogeology of the Bartow area near Tampa, Florida. Very close cooperation across the disciplines involved proved to be extremely important for significant progress in this research.

The investigation was performed under the general direction of C S Conover, District Chief, Tallahassee, Florida, and J S Rosenshein, Subdistrict Chief, Tampa, Florida, Water Resources Division, U S Geological Survey.

THREE CHANNEL REFLECTIVE INFRARED PROCESSING

Four training set areas were selected that apparently represented four different vegetation moisture stress conditions thought to have been induced by sinkhole formation (fig 5).

The training set areas chosen were

- 1 Dry marsh vegetation
- 2 Dry grass vegetation along west edge of relic sinkhole
- 3 Dry grass vegetation near the center of sinkhole
- 4 Dry grass vegetation near east edge of sinkhole

Spectral signatures of these areas were obtained by the University of Michigan's processor (Spectral Analyzer and Recognition Computer) using the near IR spectral band (1.0 - 1.4 μm (micrometer), 1.5 - 1.8 μm , 2.0 - 2.6 μm). These signatures consisted of the mean and variance of each of the training sets in each spectral band (covariances were not included).

The computer was programmed to compute the sum of the square of the deviations about the mean for each point and to accept or reject the point on the basis of the magnitude of the sum. The decision level was arbitrarily set to yield a satisfactory and estimated ratio of target detection and background rejection.

Each signature was employed one at a time, to make strip maps. Color coded ozalid prints representative of each of the four recognition signatures were made from these maps and overlaid to form a composite recognition map of apparent moisture stressed vegetation (fig 6, table 1).

TEMPERATURE SLICING PROCESSING

Using the University of Michigan's processor, 12 separate images were produced from 8-14 μ m data with each separate image representative of an increment of apparent surface temperature between 77°F and 98.5°F. Although the actual ground temperatures within each separate image are not known, relative temperature information can be inferred from the data. Each temperature separate was assigned a different color and copied on an ozalid colored transparency (table 2). These color ozalids were overlaid and displayed against an 8-14 μ m black and white video background to form a 12 - color composite thermal map (fig 7).

ANALYSIS

The data were collected during a drought, when the shallow water table had markedly declined. Test drilling indicates that the soils in the test area have similar drainage properties. They are mixtures of silty organic matter and fine-to medium-grained sands.

Moist soils have a greater conductivity of heat than dry soils and are heated to greater depths during daylight hours. Consequently, moist soils do not cool as completely as dry soils and are warmer during the early morning hours. Therefore, zones of similar surface temperature may be indicative of soil-moisture similarities, especially during early morning hours.

Measurements of water levels in wells shows that the water table slopes downward toward areas where sinkhole are present and forming. Excluding minor irregularities caused by puddling and topographic anomalies, surface temperature conditions should reflect the general water-table configuration. The thermal imagery was collected on September 6, 1967, at 0647 hours. During this time, dry and well-drained soils which should be cooler may indicate deeper water levels than beneath moist soils. Moisture stressed vegetation should be rooted mainly in dry soils and should serve as additional indicators of areas deficient in water. The degree of vegetation stress should vary with the degree of the deficiency in water.

The circular patterns of moisture-stressed vegetation obtained from processed data in the reflective IR range correspond in shape and area with those of apparent surface temperatures obtained from processed thermal IR data. From examination of the thermal map, several different zones of cooler (80 °F, 85 °F and 86 °F) surface temperatures delineate the area of sinkhole activity (figs 7 and 8). From examination of the reflective IR recognition map, moisture-stressed vegetation occurs mainly in dryer soils of the cooler thermal zones (figs 6 and 7). Both patterns of moisture-stressed vegetation and cooler surface temperature zones delineate areas of active sinkhole formation. (For example, the sinkhole area is the area delineated by the red coded signature in training set 3 within the area delineated by the cooler thermal zone.) The area of sinkhole formation is underlain by a mantle of sand and a lime-sink, or buried relic karst, topography (fig 2).

Other oval patterns observed in the reflective and thermal IR recognition maps (made from data collected in September 1967) delineated an area where subsidence began in the late summer of 1968 (fig 8). This area of most recent subsidence is about 3000 feet north of the sinkhole area identified in figures 6 and 7.

CONCLUSIONS

Multispectral scanning and processing should prove to be useful for conducting hydrogeologic surveys of karst areas. From this study it is concluded that locating areas of future land subsidence by multispectral remote-sensing techniques is feasible. Of particular significance is the successful application of the techniques of multispectral scanning and processing of data acquired from an airborne platform to the determination of sinkhole formation that may be related to hydrogeologic conditions that occur several hundreds of feet beneath the surface of the earth.

SELECTED REFERENCES

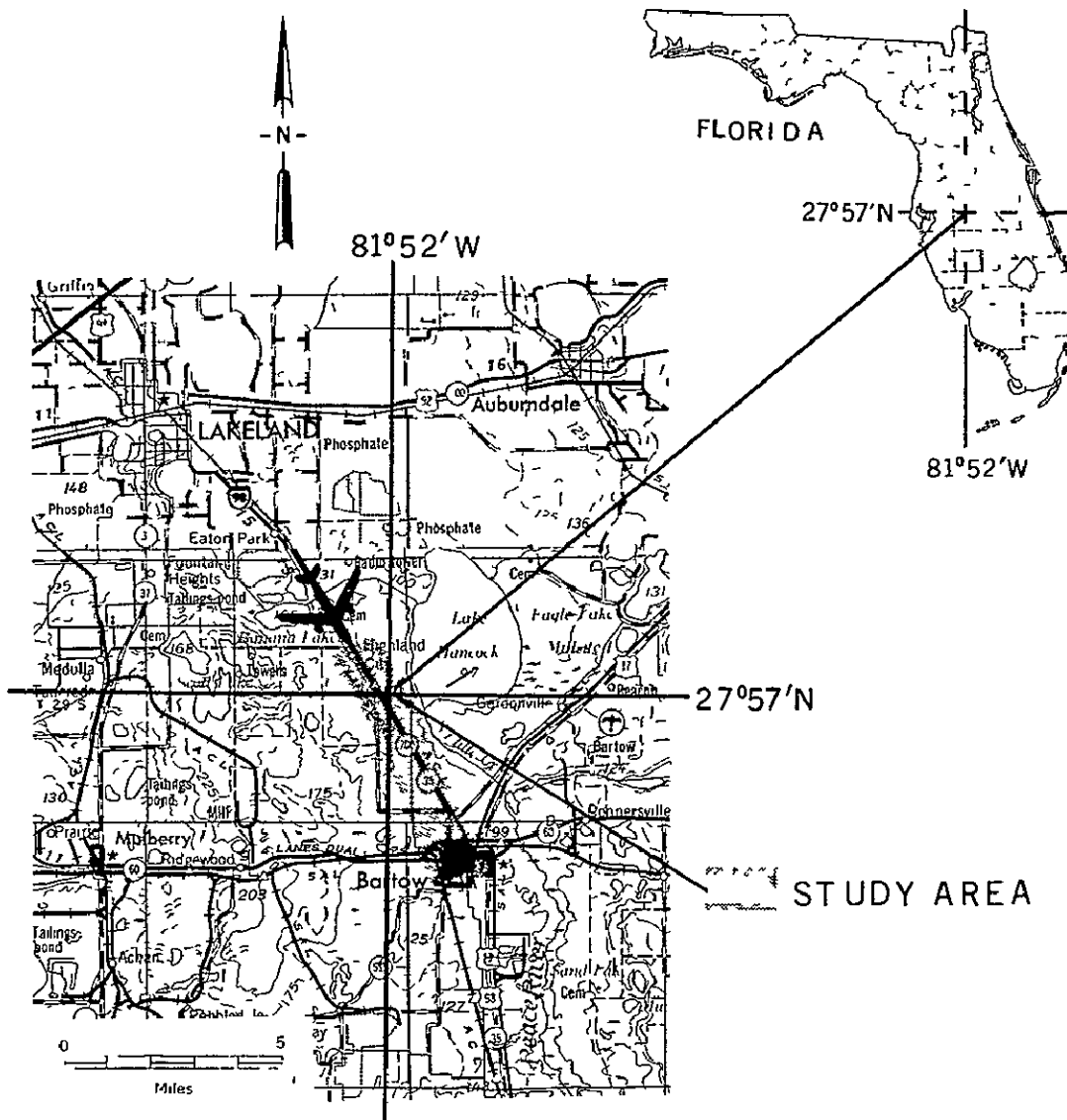
- Cathcart, J B , 1966, Economic geology of the Fort Meade quadrangle, Polk and Hardee counties, Florida. U S Geol Survey Bull. 1207, 97 p
- _____ 1964, Economic geology of the Lakeland quadrangle, Florida
U S Geol Survey Bull. 1162-G, p. G1-G128
- Coker, A E , 1968, Application of remote sensing to occurrence of collapse sinkholes in the Alafia and Peace River basins, Florida
NASA Earth Resources Aircraft Program Status Review , v. III,
p. 22A-1-14
- Holter, M R and Polcyn, F C 1964, Comparative multispectral sensing
(Classified Report) Univ of Michigan Infrared and Optics Lab
Rept No 2900-484-S 11 p
- Holter, M R and Wolfe, W L 1960, Optical-mechanical scanning
techniques Univ of Michigan Infrared and Optics Lab Rept No
2900-154-R, 13 p
- Kaufman, Mathew I , 1967, Hydrologic effect of ground-water pumpage in
the Peace and Alafia River basins, Florida 1934-1965 Florida Geol
Survey Rept Inv 49, 32 p
- Lowe, D S and Braithwaite, J G N 1966, Spectrum matching techniques
for enhancing image contrast. Applied Optics, v 5 p 893-898
- Malila, W A., 1968, Multispectral techniques for image enhancement
and discrimination Photogrammetric Engineering v 34, p. 566-575
- Marshall R E , 1969, Application of multispectral recognition
techniques for water resource in Florida Purdue Centennial on
Information Processing, v. 11, p 719-731, Purdue University, Indiana

TABLE 1 Color key for sink area vegetation

<u>Training Set</u>	<u>Color</u>	<u>Feature</u>
1	Blue	Dry marsh vegetation
2	Green	Dry grass vegetation along west edge of relic sinkhole
3	Red	Dry grass vegetation near the center of sinkhole.
4	Brown	Dry grass vegetation near east edge of sinkhole

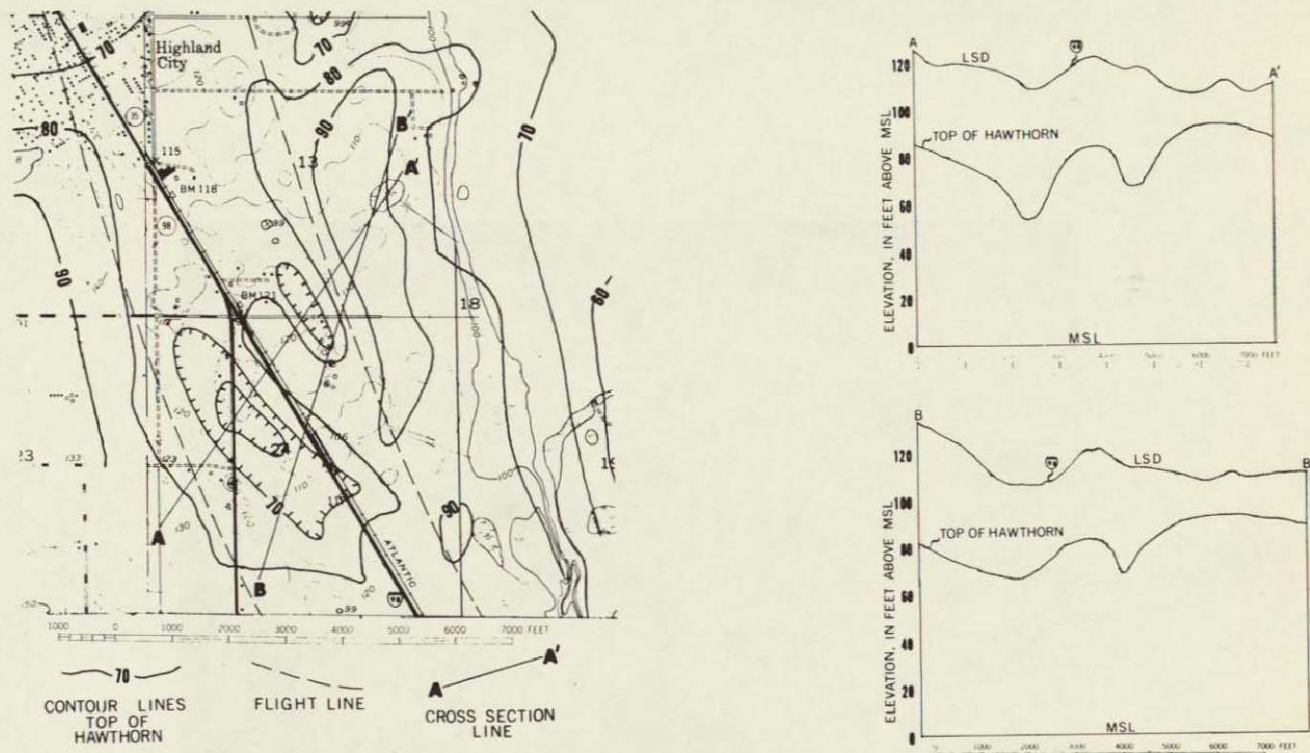
TABLE II Color key for false color thermal contouring in sink area

<u>Color</u>	<u>Average apparent surface temperature (°F)</u>
Cyan	77.0
Violet	79 0
Orange	80 5
Black	82 0
Yellow	83 5
Red	85 0
Blue green	86 5
Dark brown	88 0
Yellow green	90 0
Magenta	93 0
Olive	96 0
Dark blue	98 5



INDEX MAP OF STUDY AREA

Figure 1. The shaded area outlines the approximate area in Florida covered by University of Michigan's airborne multispectral scanner on September 5th and 6th, 1967



MAP AND CROSS SECTION OF RELIC KARST TOPOGRAPHY

Figure 2. Sand-filled sinkholes formed in limestones of the Hawthorn formation underlie the study area at depths as much as 50 feet beneath the land surface. Land collapse is hypothesized to occur more frequently in areas underlain by buried relic sinkholes, as indicated by the configuration of top of the Hawthorn formation (From unpublished map by Cathcart).



Figure 3. One of two homes lost in land collapse in Bartow, Florida, May 22, 1967. Sinkhole that formed was 520 by 125 feet and 60 feet deep.



Figure 4. Sinkhole formed along the west side of US Highway 98 is in the test site in the center of the photograph. The hydrogeologic conditions associated with highway subsidence that occurred 3000 feet north of this area are not discernible from interpretation of this photography.

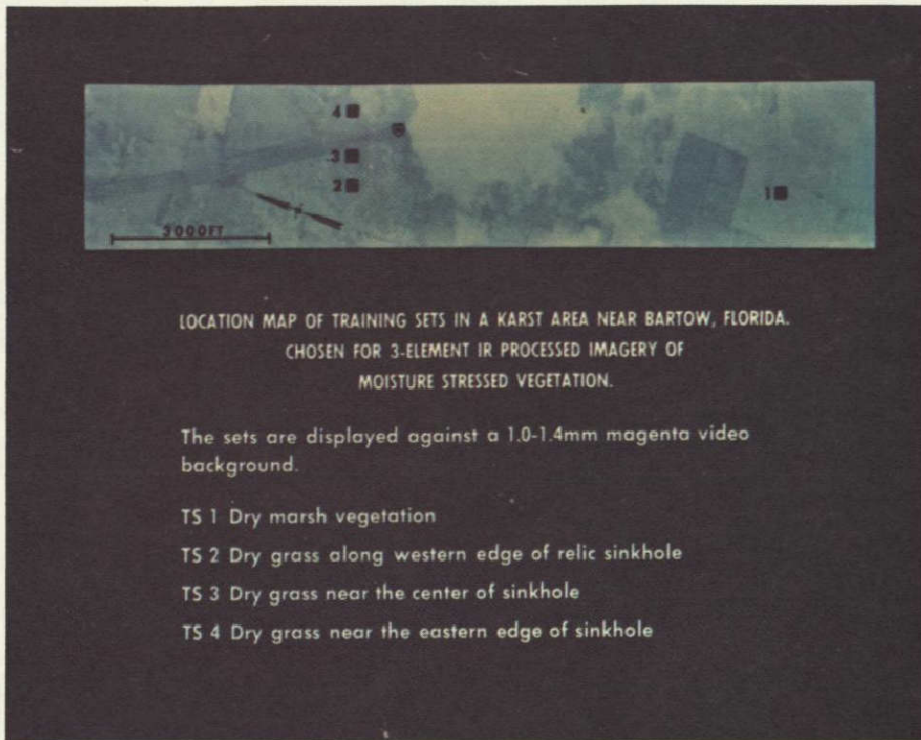


Figure 5. Location map of training sets in a karst area near Bartow, Fla.

NOT REPRODUCIBLE

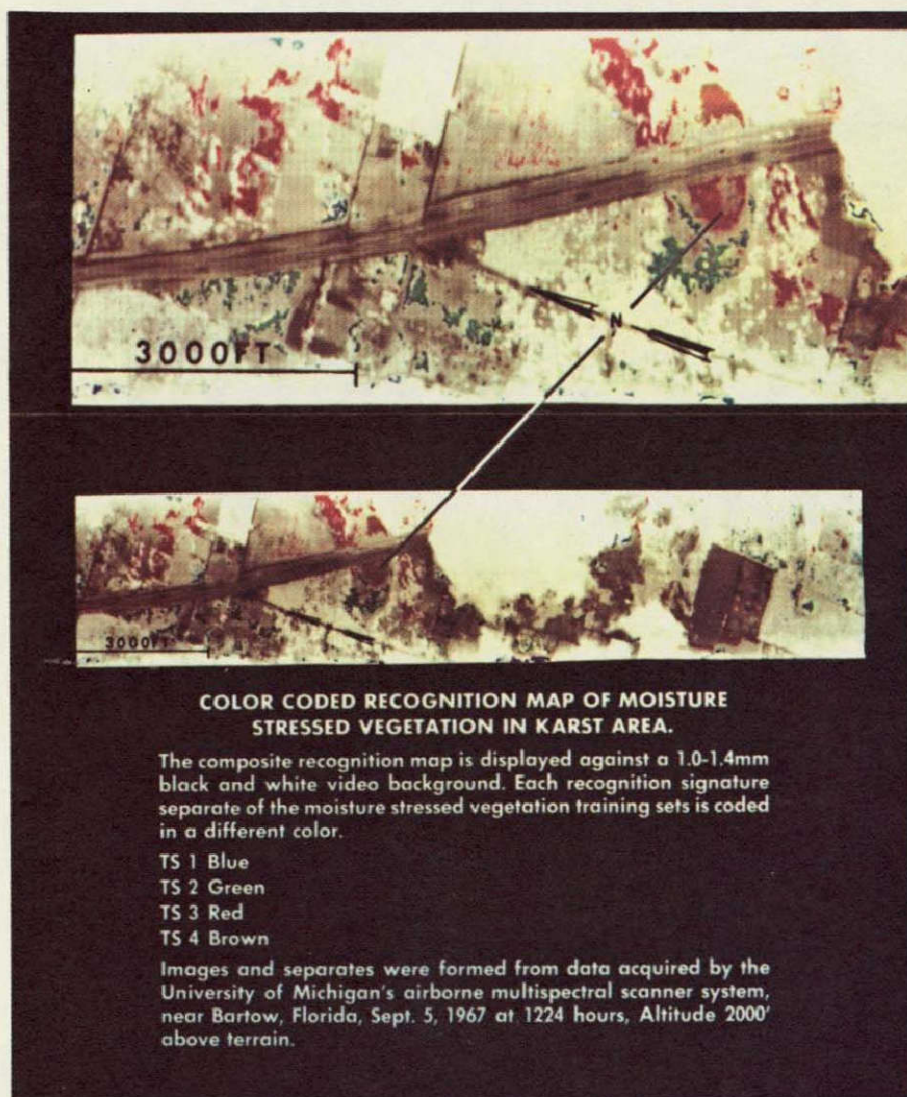


Figure 6. The circular patterns along US Highway 98 to the left of the center part of the photograph show the area of active subsidence. Less obvious patterns suggest sinkhole formation, about 3000 feet north.

NOT REPRODUCIBLE



Figure 7. The concentric and cooler surface temperature zones form patterns along the west side of US Highway 98 in the center of the photograph and show the area of active subsidence. Other patterns, suggestive of sinkhole formation, occur about 3000 feet north.

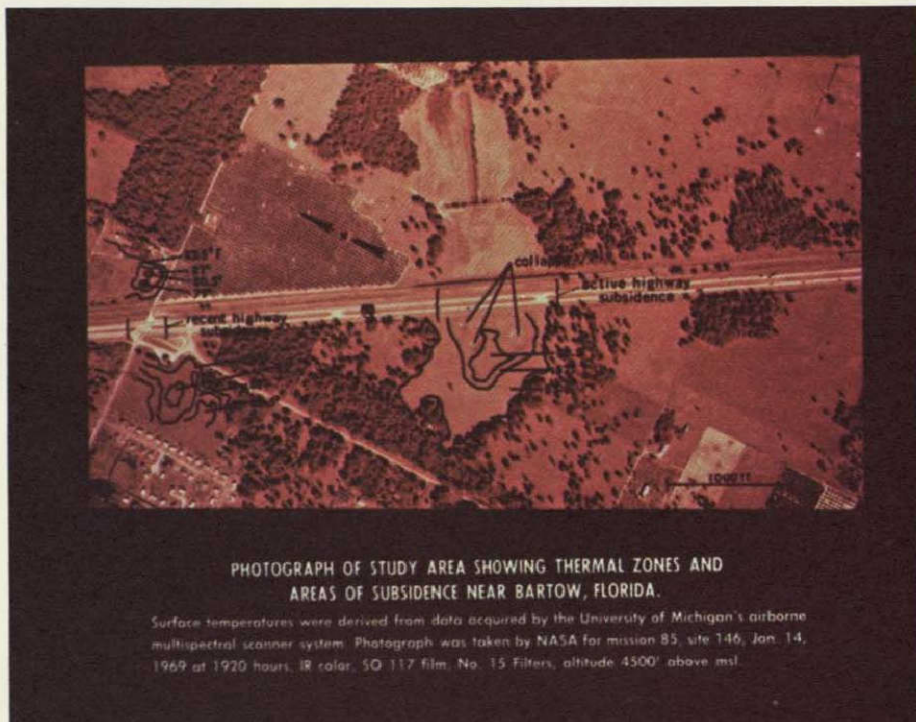


Figure 8. Cooler surface temperature zones delineate the dry areas of deeper water levels and subsidence.

NOT REPRODUCIBLE

SECTION 3

DIGITAL COMPUTER TERRAIN MAPPING FROM MULTISPECTRAL DATA,
AND EVALUATION OF PROPOSED EARTH RESOURCES TECHNOLOGY SATELLITE (ERTS)
DATA CHANNELS, YELLOWSTONE NATIONAL PARK. PRELIMINARY REPORT*

by

Harry W. Smedes, Kenneth L. Pierce,
Marc G. Tanguay, and Roger M. Hoffer

N71-19254

ABSTRACT

Digital computer processing of 12 wavelength bands of visible and reflective infrared scanner data has resulted in successful automatic computer mapping of eight terrain units in a Yellowstone National Park test site

Target areas in the scene were selected for training the computer. Statistical parameters of radiance such as mean, standard deviation, divergence, and covariance were computed for each category of material. These data were used in the computer program to determine which channels are most useful for recognition of all object categories studied, and to actually classify all the unknown data points into the known categories.

The following terrain types have been mapped with greater than 80 percent accuracy in a 12-square-mile area with 1,800 feet of relief: bedrock exposures, talus, vegetated rock rubble, glacial kame terrace, glacial till, forest, bog, and water, and shadows. In addition, shadows of clouds and cliffs are depicted

In addition, studies were made of the effectiveness of the proposed Earth Resources Technology Satellite (ERTS) data channels as compared to the computer-selected best four channels in the automatic recognition and mapping of the same terrain types based on simulations, using the same set of data.

These simulations resulted in maps whose accuracies were only a few percent less than that using the best set of four channels, they indicate that the ERTS data channels are likely to be successful for terrain analysis of a wide variety of categories encompassing a broad range of spectral reflectance

These studies also indicate that, for a broad range of terrain categories, many combinations of 3 or 4 channels of data would be satisfactory. We need worry about careful selection of specific wavelength bands only if there is a specific category being sought.

PURPOSE AND SCOPE

This report summarizes the preliminary results and current status of studies of digital computer processing of airborne multispectral data, the success of automatic recognition and mapping of the distribution

of eight different terrain types, and the effectiveness of the proposed Earth Resources Technology Satellite (ERTS) data channels as compared to the computer-selected best four channels in the automatic recognition and mapping of the same terrain types based on simulations, using the same set of data.

This study involves the data from one flight over a test area of about 12 square miles in a region of moderate relief (1,800 feet) comprising a wide variety of terrain types.

The data were acquired and processed in analog form by the Institute of Science and Technology of the University of Michigan, and were processed in digital form by the Laboratory for Agricultural Remote Sensing (LARS) at Purdue University. This report is concerned only with the preliminary study of the digital processing. This and other aspects of automatic data processing will be described in more detail in a later report.

The U.S. Geological Survey conducted field studies before, during, and after the flight, and actively participated in the computer processing.

DATA ACQUISITION

A multispectral survey was made of selected test areas in Yellowstone National Park during flights by the University of Michigan in September, 1967, on a NASA-sponsored contract to the U.S. Geological Survey.

The University of Michigan 12-channel scanner in the 0.4 to 1.0 μ m range (table 1) provided the principal data for the computer processing described in this report. In addition, two scanner systems recorded a total of five channels of reflective and thermal infrared data in the region beyond 1.0 μ m. A simplified diagram of the scanner-spectrometer is shown in figure 1.

As the aircraft flies over the test area, the ground surface is scanned in overlapping strips by successive sweeps as a mirror is rotated at about 3,600 rpm. The radiant energy reflected (or, in the case of thermal infrared, emitted) from the earth's surface is reflected off the rotating mirror and focused, by other mirrors (M), onto the slit of a prism spectrometer, thus refracting the rays into a spectrum.

Fiber optics placed at appropriate places lead to photomultiplier tubes which measure the amount of radiant energy received in each of 12 overlapping bands or channels of this spectrum from 0.4 to 1.0 μ m (visible violet to reflective infrared). This energy, which is now a voltage, is fed to a multitrack tape recorder where each of the 12 channels is recorded as a separate synchronized signal on magnetic tape. Similar, separate scanners recorded the infrared part of the spectrum from 1 to 14 μ m (see table 1).

Table 1.--Wavelength bands of University of Michigan multispectral system.

Channel number	Wavelength band, in micrometers (μ m)
SCANNER NO. 1	
1	0.40-0.44
2	.44- .46
3	.46- .48
4	.48- .50
5	.50- .52
6	.52- .55
7	.55- .58
8	.58- .62
9	.62- .66
10	.66- .72
11	.72- .80
12	.80-1.00
SCANNER NO. 2	
1	1.0 -1.4
2	2.0 -2.6
3	3.0 -4.1
4	<u>1/</u> 4.5 -5.5
SCANNER NO. 3	
----	<u>1/</u> 8.0-14.0

1/ Denotes thermal infrared channels; others are reflective.

Photographs taken at the same time the scanner data were acquired provide important supplements to the control data--commonly referred to as ground-truth data^{1/}. These photographs consist of color, color

^{1/}Control data or "ground-truth data" refers to all that is known about the site conditions, including types and distribution of materials, (determined from conventional field mapping and examination supplemented by study of photographs taken from the air and ground, and measurements of such parameters as temperature, relative humidity), porosity, moisture content, and spectral reflectance of surface materials. Collectively, these constitute the control data with which the test data can be compared.

infrared, black and white panchromatic, and black and white infrared film on board the aircraft, and color film from stations on the ground.

DATA PROCESSING

Any given channel of magnetic tape data can be reproduced by photographing a cathode ray tube video (C-scope) presentation of the tape data (fig. 2). In contrast to processing the data in analog form such as that in figure 2, they can be processed in digital form by making a digitized copy of the original magnetic tape. This is the procedure used by the Laboratory for Agricultural Remote Sensing (LARS), Purdue University. The remainder of this report will discuss the LARS method of handling multispectral scanner data, and preliminary results obtained on a section of one flight-line of the Yellowstone Park data.

This particular run was digitized in such a manner that, on the average, there was neither overlap nor underlap of adjacent scan lines (fig. 1). The scanner resolution is 3 milliradians, and the aircraft altitude was about 6,000 feet above terrain. This required that every 10th scan line be digitized. Also, each scan line contains 220 ground resolution cells. The scanner mirror rotates at constant angular rate whereas the digitizing was done at equal linear rate. This, plus the effects of topographic relief, changes the size and shape of the ground resolution cell from the midpoint to both ends of the scan line. Even so, the average dimensions of the ground resolution cell are approximately 20 by 20 feet. There is a gap of about 20 feet between cells along each scan line.

The analog data were quantized to 8-bit accuracy. Therefore, each resolution element of each spectral band has one of 256 possible values.

A computer printout of the data from any given channel is made to simulate the analog video display by breaking the continuous tones of the gray scale into a finite number of discrete gray levels by assigning a letter or symbol to each level in accordance with the relative amount of ink each symbol imprints onto the paper. An example is given in figure 3. Each of the 15 reflective and 2 thermal channels could be printed as video and/or digital printout images, constituting 17-channel multiband imagery (for an example, see Lowe, 1968, fig. 12a and 12b, p. 94 and 95).

It is virtually hopeless to attempt to integrate and evaluate data for each spot on the ground on all 17 images by visual inspection. However, now that the data are recorded as electrical signals on magnetic tape, they can easily be processed electronically in several ways to enhance selected features and to determine the statistical parameters of the spectral radiance (reflectance or emittance) of each category of material in the scene.

In the pattern-recognition method being used by LARS-Purdue, specific, known, target areas in the scene are selected as training areas. The gray-scale printout (fig. 3) serves as a base for locating these areas. The area coordinates are fed to a computer system^{2/}, which

^{2/} An IBM 360 model 44 computer with 64K bytes (8 bits per byte) of core storage was used. The principal computer language used was FORTRAN, with ASSEMBLY used for some of the support programs.

then computes the statistical parameters of each category of material. These statistics are calculated from the relative response in each channel (figs. 4 and 5). Relative response can be considered as an uncalibrated reflectance measurement, where the lack of calibration between channels allows only relative comparisons of the various categories of materials within each channel. The statistical parameters calculated are based on an assumed Gaussian distribution of the data, and include the mean, standard deviation, covariance, and divergence (i.e., the statistical measure of the separability of classes). These statistics are stored by the computer, and are used to represent the multispectral characteristics of each designated category of material. These statistics constitute the multispectral pattern or "fingerprint" of each terrain category, and are used in the computer program to 1) determine which channels are most useful for recognition of all object categories studied, and 2) actually classify the unknown data points into the known categories using a Gaussian maximum-likelihood decision scheme.

Four channels were used in this study. This decision was based on experience at LARS-Purdue which has shown that the use of only 4 of the 12 channels in the 0.4 to 1.0 μ m range results in approximately as good a classification as does the use of more channels. Computer time, which increases in a geometric fashion with the number of channels used in the classification, is costly; therefore, some optimum for the number of channels used, the quality of results, and funds expended must be achieved.

The channel-selection part of the computer program provides the capability of measuring the degree of separability of Gaussian distributed categories and determining the optimum set of channels for doing so. This is done by calculating the statistical distance in N-dimensional space between the classes, N being 12 in this case.

The classification part of the computer program involves the actual classification (mapping) of an arbitrary number of classes using an arbitrary number of channels and a Gaussian maximum-likelihood scheme.

The display part of the program displays the results in line-printer form, and analyzes the recognition performance in each training area

A thresholding capability is provided in the display process. If the resolution element does not exceed a pre-set threshold--that is, if the element does not look sufficiently like a member of the class to which it has tentatively been assigned even though that is the most likely class--then final classification of that element is declined and that element is assigned to a null category (rejected) and displayed as a blank. Different thresholds may be assigned to each of the classes individually.

When coordinates of other known areas (test areas) are fed to the computer, the computer determines the classification of those areas and computes the accuracy of classification. Appraisal of numerous test areas gives a more complete and meaningful evaluation of the overall recognition performance of the computer program.

RESULTS OF DIGITAL COMPUTER PROCESSING

Computer-selected best set of four data channels

A test of automatic recognition and mapping of terrain by digital computer is currently underway at Purdue University. Data from a 12-square-mile area in Yellowstone Park are being used in this analysis. This area (figs. 6, 7, and 8) has a relief of about 1,800 feet. A segment of the digital computer terrain map is shown in figure 9. This map was generated by the digital computer on the basis of 4 channels selected from 12-channel scanner data and the statistical definition of classes provided by the training areas.

The part shown is composed of 127,600 data points--about 47 percent of the full map. The full map covers an area of about 2 by 6 miles and is composed of 269,060 data points. The eight terrain categories discussed on the following pages were selected arbitrarily during field study and the early part of computer processing. They were selected not on the basis of composition or genesis, as we traditionally do in the course of geologic mapping, but on the basis of their overall surface color and brightness inasmuch as that is what the sensor was recording.

For example, geologists are more interested in the areal distribution of a sand and gravel unit, such as glacial till, than in the distribution of forest. Conventional maps would show the extent of till regardless of whether it was the site of a meadow or was covered with dense forest. The terrain units of this study necessarily show the unforested till as one unit (till) and the forested till as a different unit. In fact, all forested terrain, regardless of underlying rock or soil unit, is shown as a single unit.

Initial processing disclosed that at least 13 categories could be separated. Several of these were subunits which have been combined to make the display shown in figure 9. The following is a brief description of the 9 categories (including shadows) mapped, and the accuracy of the computer classification as compared with the control data

1. BEDROCK EXPOSURES (red on fig. 9)

This unit (fig. 10) consists of bare bedrock exposed by glacial and stream erosion and mantled by minor amounts of loose rubble. These are unvegetated except for lichens and sparse tufts of dry grass, and have high reflectance in nearly all channels. This category is present mainly in the western part of the test area, along the banks of the Yellowstone River, and in a quarry where it was moderately well classified. Where misidentified, it generally was classified as vegetated rock rubble--a closely similar unit into which it grades.

2. TALUS (purple on fig. 9)

This category includes blockfields, talus, and talus flows of basalt lava flows, volcanic tuff, and gneiss, formed by frost-riving and solifluction from outcrops. These are blocky and well-drained deposits; trees are widely spaced or absent (fig. 11). Blocks generally are covered with dark-gray lichens (fig. 12). The blocks range from a few inches to a few feet in diameter; most are larger than 3 inches. The slopes range widely, from 35°-45° at the head, to 5° or less at the toe. In places, a basin or trough lies just inside the distal margin of talus flows.

All of the known areas of this unit and a few previously undetected are clearly delineated.

3. VEGETATED ROCK RUBBLE (dark brown in fig. 9)

This unit consists of locally derived angular rubble, frost-riven from basalt lavas, volcanic tuff and breccia and gneiss. Grasses, lichens, evergreen seedlings and mosses now cover more than three-fourths of surface underlain by this debris (fig. 13). Blocks range in diameter from less than 1 inch to several feet and occur on slopes of from 0° to about 25°.

The general areas classified are realistic, but in detail this unit is the least well classified. Because of the small size of the individual areas occupied by this unit, it is not possible to locate precisely a homogeneous training area. In the western part of the test area there are many small areas classified as this unit which are rock rubble frost riven from ice-scoured outcrops which are surrounded by glacial till.

4. GLACIAL KAME (light brown on fig. 9)

These are meadows underlain by sand and gravel, and mantled by sandy silt (fig. 14). The deposits are well-drained and are vegetated by grass and sagebrush. About one-fourth of the area of this unit is exposed mineral soil. Deer and elk manure locally cover as much as one-fourth the surface area.

Areas of kame meadows are accurately depicted. Areas of forested kame sand and gravel between open meadows of kame were erratically classified by the computer, mostly as other units. Control data show that in some places this unit occurs as small scattered patches surrounded by till, in those places it was misidentified by the computer

5. GLACIAL TILL (yellow)

This category consists of meadow areas underlain by glacial till. These are grassland and sagebrush areas (largely dormant at time of flight) with mineral soil exposed over about one-fifth of the area (fig. 15). Mineral soil consists of mixtures of silty to bouldery debris. Deer and elk manure locally is abundant in these meadows. This unit was first classified as four separate subunits on the basis of change in illumination across the flight path, but the four were later combined into one unit for the map printout. Classification is estimated as about 95 percent accurate over the entire flight strip. The other classification symbols scattered throughout areas of this unit generally are correct, for there are small areas of vegetated rubble and of bogs in meadow areas underlain by till.

Although both the till and kame deposits are the sites of meadows, the differences in amount of soil exposed and the subtle differences in soil composition and texture apparently permit these two categories to be accurately distinguished by the computer

6. FOREST (dark green)

Depicted here are Douglas Fir and lodgepole forest (see fig. 11). Local clusters of deciduous trees were recognized separately, but combined with evergreens in this display. This forest unit generally is well recognized in large almost uniformly colored blocks. All forest areas seem to be consistently recognized.

7. BOG (light green)

These are moist areas supporting tall lush growth of sedges and grasses. Bogs are rather abundant because of glacial scour and derangement of drainages. This is one of the best recognized units. All known bogs and many previously unknown small bogs were correctly mapped.

8. SURFACE WATER (blue)

The Yellowstone River and Floating Island Lake (see fig. 11) were clearly recognized. Phantom Lake (not on this segment of map) was dry at the time of flight, and so was correctly classified as bog rather than water. Parts of the Yellowstone River were omitted or generalized, principally because the width of the river is near the threshold of resolution, and because some data

points were integrated values of river plus some other category or categories. Stretches of white-water rapids were thresholded out. In places, the shaded north edges of patches of forest were printed as scattered points of water or talus.

9. SHADOWS (black)

Cloud shadows are near west and south-central margins of the test area (fig. 7), and deep shade occurs at base of north-facing cliffs and along north edge of forest areas. All were recognized well. Those along the south-central margin are shown in figure 9.

10. OTHER (white)

All data points whose reflectance did not closely fit the statistical data for any of the above nine categories were rejected, and shown as blank regions on the map. A few of these are very light and bright areas of shallow water where bottom deposits show through, or are white-water rapids and gravel bars.

A blacktop road can be detected in places as a line of anomalous mixed colors, but is not consistently recognized as any particular category. The road is about as wide as a single data point and hence is at the threshold of resolution.

Although all bedrock types were classified as a single unit, the spectral reflectance histograms, spectrograms, and the divergence data indicate good possibility of distinguishing among several of the rock types present. Further testing over areas of larger rock exposure seems justified.

Thermal overlay

Another aspect of the work underway is a terrain classification made by substituting one or more data channels from the infrared scanners (1.0-14 μm) for those of the 12-channel scanner (0.4-1.0 μm)

For this test, channels 1, 3, 5, 7, 9, 10, 11, and 12 of the 12-channel scanner were combined with the 1.0-14 μm , 2.0-2.6 μm , 4.5-5.5 μm , and 8-14 μm channels. A computer program recently developed at LARS-Purdue made it possible to overlay the data from these two separate scanner systems. The computer selected the best set of four of these channels (table 2) for classification of the terrain in the same manner as before. The maximum mismatch of registry is no more than three ground resolution cells, and probably is mostly no more than one cell.

The "map" on the right side of figure 9 is the result of overlaying one thermal and three reflective channels (0.66-0.72, 0.80-1.0, 2.0-2.6, and 8-14 μm). Only one of these channels is in the visible range. Because the scan angle of the thermal scanner was much narrower than the reflective, this display covers only the middle east-west strip of those shown to the left of it. The close correspondence of this display with the others indicates the accuracy of classification.

Table 2.--Channels used in the terrain classification and mapping, and to simulate the ERTS data channels.

	Wavelength band used	Color or Spectral region	Michigan scanner channel number
Best 4 channels	0.44-0.46 μ m	Blue-----	2
	.62- .66	Orange-----	9
	.66- .72	Red-----	10
	.80-1.0	Infrared-----	12
	.66- .72	Red-----	10
	.80-1.0	Infrared-----	12
	2.0 -2.6	Infrared-----	--
	8 -14	Thermal infrared-----	--

ERTS scanner channels:

0.5-0.6 μ m-----	.52- .55	Green-----	6
.6- .7 -----	.62- .66	Orange-----	9
.7- .8 -----	.72- .8	Infrared-----	11
.8-1.2 -----	.8 -1.0	Infrared-----	12

ERTS RBV cameras *

0.535 μ m peak---	.52- .55	Green-----	6
.680 ---	.66- .72	Red-----	10
.760 ---	.72- .8	Infrared-----	11

These studies should enable us to further extend the range of potential diagnostic spectra for existing categories and may point out some additional terrain categories. In addition, they will be useful tests of how well computer programs can take data from different scanner systems and automatically overlay them to produce a single set of multispectral data

Simulation of ERTS data channels

Along with the studies of evaluating the accuracy of performance, we are studying how well data in wavelength bands tentatively designated for the proposed Earth Resources Technology Satellite (ERTS) might serve for automatic mapping of the same ten terrain categories in the same area

The midpoints of the channels of the proposed ERTS 4-channel scanner, and the peak transmissions of the three Return Beam Vidicom (RBV) cameras were matched with the closest channels of the University of Michigan 12-channel scanner. These data are summarized in table 2 and figure 16.

The classification using the simulated ERTS 3-RBV cameras is shown in the middle display in figure 9. Note the close agreement with the top display--that based on the computer-selected best set of four channels. The display of the simulated ERTS 4-channel scanner data has not been colored yet. A segment of the uncolored classification is shown in figure 17, with the RBV camera simulation and the computer-selected 4-channel display, for comparison (figs 18-20).

ACCURACY

In general, the products are highly satisfactory terrain maps which portray PHYSIOGRAPHIC UNITS or ROCK-SOIL-VEGETATION ASSOCIATION UNITS. Accuracy is determined by comparing the computer-generated maps with the ground control data

Where terrain categories were areally extensive, they were correctly identified by the computer. Most inaccuracies occurred where the units were small and where some were below the threshold of resolution, accordingly, the radiance for a given resolution cell was a complex combination of several categories. Presumably, the computer usually selected the dominant terrain unit or, by thresholding, indicated that the spectral properties did not clearly fit any of the classes.

For comparison of the performance of classification using the ERTS simulations with the best sets of 4 channels, the computer rated itself in the training areas only. For example, of the total of 5,418 data points used in training the computer, less than 20 of those were subsequently classified (using the best set of 4 channels) as something

other than what they were called during the training. The ratings are as follows:

Best set of 4 channels-----	99.6 percent
Thermal overlay-----	98.8
ERTS 4-channel scanner-----	97.7
ERTS 3-RBV cameras-----	93.8

The figures are a good measure of the relative accuracy of each test. They are misleading in part because the computer assumes that each training area is homogeneous and completely what it was labeled. The 0.4 percent error probably is a close measure of the degree of inhomogeneity of the material in the training areas.

Preliminary results of computer studies which rate the accuracy of classification of test areas give the following overall performance (data from unpublished report by Marc G. Tanguay):

Best set of 4 channels-----	86 percent
Simulated ERTS 4 channels-----	83
Simulated ERTS 3-RBV cameras---	82
Thermal overlay-----	81

These figures should be taken as approximations only. They agree with a preliminary visual estimate that the overall accuracy of all displays is more than 80 percent, and indicate that the best set of 4 channels gives slightly better results than the other 3 displays, all of which are about equally good.

The drop in accuracy from 99 to 86 percent, etc., from the training to the test areas, is understandable, because we would expect the computer to perform well in the areas where it was trained, (by circular reasoning) unless the reflectance of two or more categories were closely similar in all channels used.

For the training areas, the classification made using the overlay of thermal and reflective channels was virtually as accurate as the best classification--that using the computer-selected best set of 4 reflective channels (98.8 vs 99.6 percent, respectively). However, for the test areas, the thermal overlay was least accurate (about 81 vs 86 percent). The slight mismatch of registry in parts of the thermal overlay test undoubtedly results in a less accurate classification than if all channels were in complete registry, as would occur if a single scanner system could cover the range of 0.4 to 14 μ m or more.

Nevertheless, these studies indicate that the infrared region is promising in the classification of some terrain units. For example, in the test areas the thermal overlay classification was better than the computer-selected best four channel classification for glacial till (95 vs 93 percent), glacial kame (82 vs 74 percent), and bog (81 vs 80 percent). The accuracy of classification of talus in the test areas was only about 49 percent; however, most of the error was due to talus being misclassified as vegetated rock rubble--a unit which actually is quite

similar to talus. If talus and rock rubble are combined as a single unit, the accuracy jumps to about 83 percent, whereas the same combination was classified only about 76 percent when using the best set of 4 channels in the test areas.

In geologic applications it is more desirable to know what kind of material the forest is growing on than simply to know where the forest is. The thermal overlay classification has some potential in this regard, it has been shown (Waldrop, 1969) that thermal infrared in forest areas can in places indicate the sites of thick, unconsolidated, well-drained gravels vs bare or thinly mantled bedrock.

An obvious advantage of infrared data channels for space applications is the haze penetration ability. Further investigations are needed to adequately assess the potential of these channels, particularly over areas of extensive rock outcrops.

Studies presently underway also include careful evaluation of the overall accuracy by point-to-point comparison with control maps. It is important to recall the recognition of previously undetected areas of occurrence of some terrain units. This means that errors in the control maps are being detected at the same time errors in the computer printout are being sought.

In general, the ERTS simulations differed from the computer-selected best 4 channels as follows:

1. For areas correctly shown as FOREST on the classification using the best 4 channels, the ERTS 4-channel classification showed small to moderate amounts of TALUS and WATER, whereas the RBV 3-channel classification showed greater amounts.
2. In places, both ERTS classifications showed considerably more BOGS than are present in areas that were correctly classified by the best 4 channels.
3. Slightly poorer classification of water was performed in the ERTS classification. However, few of the bodies or areas of water in the test area are of sufficient size to serve as good training areas, so we do not view this part of the classification as a good test of the ability of the ERTS data channels to permit automatic identification of water.

We wish to point out that these are not complete simulations of the ERTS data channels, but are only first approximations, because we have not attempted to simulate 1) the poorer resolution of the satellite sensors due to vast difference in scale, 2) the effects of atmospheric attenuation, or 3) the broader wavelength bands of most of the ERTS sensors (see table 2). Studies underway at the University of Michigan are aimed at more closely simulating the actual wavelength bands of the ERTS sensors

We further emphasize that all of the experiments, including the simulations, are based on only one set of data along 6 miles of traverse. However, the fact that these data were not gathered under optimum conditions^{3/} means that the accuracy of detection and the number of

^{3/} The data were gathered at about 2 p.m., September 19, 1967, along a nearly east-west traverse at about 6,000 feet above mean terrain elevation. No appreciable rain had fallen for several weeks; therefore the ground was very dry. To minimize shadows and illumination-angle variations, it would have been better to fly at midday along traverses directly toward or away from the sun's nadir (roughly north-south). Flights at higher elevations above terrain would also reduce in reduction of variations in illumination-angle and scale; however, there probably is some altitude (not yet determined) above which the advantages gained in more-uniform illumination angle and scale might tend to be canceled by the adverse effects of the thicker column of atmosphere between the ground and the sensors. Flights made shortly after a rain would have been better to emphasize or detect differences in soils on the basis of their porosity and permeability as manifested by relative content of moisture. Flights earlier in the summer would have been better to emphasize differences in vegetation and, probably, in soil moisture.

detectable terrain categories are apt to increase for data gathered under conditions closer to optimum.

The results of these limited experiments on a single set of data, taken together with the vast store of accumulated data from studies of agricultural crops, demonstrate clearly that multispectral terrain analysis can separate a wide variety of categories encompassing a broad range of spectral radiance, and that the data channels selected for ERTS are likely to be about as successful for terrain analysis as any other combination of channels that might have been selected.

APPLICATION

In spite of how well the computer was able to classify and map this test area, an experienced interpreter could have done as well or better with stereopairs of color and color infrared aerial photographs, for (among other things) he has the ability to distinguish objects on the basis of spatial in addition to spectral patterns.

For several years now there have been discussions and expressions of concern about the need to examine vast areas of the earth's surface, the desirability of satellite-borne remote sensors to gather the needed data, and at the same time concern for the appallingly vast quantity of data that are needed and that would become available from satellites. Handling these data will require automatic processing by computer--not to make the final and only decisions of classification, but to perform the first rough culling and reconnaissance interpreting, calling attention to special places that warrant examination by a human interpreter. For, although in general a human can do a better job of interpreting, the computer can do it much faster. It's simply a matter of data compression.

It is with this need in mind that we have engaged in this study of automatic data processing by computer, that includes:

1. Testing the suitability of existing sensors and computer software.
2. Determining how many and what kinds of natural and manmade terrain elements can be satisfactorily classified in this particular climatic region,
3. Simulating the spectral response of the proposed ERTS sensors.

The existing scanners of the University of Michigan are basically well suited for these studies. Satellite application will, of course, require miniaturization, including combining the present three separate scanner systems into one that covers the range 0.4-14 μ m or more

The existing capabilities of classification programs developed at IARS-Purdue are equally well suited for these studies of automatic data processing. Their programs were established for agricultural purposes to work with the University of Michigan multispectral scanner data. Our present studies principally involve an extension of their work into another kind of terrain--one that presents something other than row crops in flat fields.

All four of the experiments (three of which are displayed in fig. 9) produced good results. They are good classifications. We don't wish to set any specific limits on how good "good" is. Obviously some are better than others, and none is perfect--but neither is the manmade control map. We are convinced, however, that all can be considered as more than adequate for the reconnaissance first-approximation kind of interpreting and mapping which we expect to accomplish with the satellite data.

If we examine the spectral range spanned for each of the displays (table 2 and fig. 16), we see that they vary by a factor of nearly 50 from 0.28 μ m for the 3-camera ERTS system to 13 3/4 μ m for the thermal overlay classification. This implies that, for a broad range of terrain categories, many combinations of 3 or 4 channels of data in the 0.4-14 μ m range would be satisfactory. More complete simulations, in which the effects of the atmosphere are considered, undoubtedly will require identification as to what channels would be more suitable. For example, the haze penetration ability of some reflective infrared channels, mentioned earlier, is an obvious advantage for satellite applications, whereas the blue part of the spectrum is apt to have low signal-to-noise ratio and therefore be of limited use except for oceanography. We need worry about careful selection of specific wavelength bands only if a specific category is being sought. Inasmuch as the ERTS program is aimed at covering many scientific disciplines and user groups--hence involving many terrain categories--the highly specific requirements are not now pertinent to tests of the suitability of the proposed satellite sensors.

We believe that the concept rather than the specific immediate results of these studies, is the most important product. Admittedly it is not

really important to find that talus occurs on the shore of a lake here or that a narrow bog lies there--we already know most of that for this particular area. The important point is that eight or more widely different terrain units could be accurately mapped automatically. For the moment it doesn't really matter what the units are or where they occur--they could as easily have been orchards, barns, landing strips, municipal parks surrounded by streets and buildings, beaches, polluted or clean water, marchland, etc.

In fact, we believe that these particular maps (fig. 9) are over-classified in comparison with what we will want to attempt from space--at least for our first attempts. It may well suffice to map out such features as WATER, VEGETATION, BARE SOIL, and ROCKS, and to interpret other things, such as geologic structure, from the resulting patterns and their relation to topography.

Especially significant applications in geology and other fields will be for those features that are time-dependent--changing with the seasons or with a few years' time. Once an area has been mapped by computer, the areas of change can be periodically mapped automatically in terms of material, location, and the amount of area changed.

We suggest that economically feasible geologic applications will include those that contribute to regional mapping, engineering geology, hydrology, and volcanology. Other applications may be in the fields of agriculture, cartography, land-use and land-management studies, and in still other fields in which seasonal and other changes are more rapid than in most geologic applications. In many fields, these data will become more useful by combining them with other (nonspectral) data--for example, the engineering or military application to trafficability studies--by combining these terrain data with slope (from radar images or topographic maps).

The fact that we are sensing surface material emphasizes the need for multidisciplinary approach to terrain mapping because the surface involves the complex interplay of at least bedrock and surficial geology, hydrology, soils, vegetation, and meteorology. Traditionally, in mapping many regions of the earth, we interpret the geology secondarily from the patterns of other materials and features.

We hope that, in the preceding reviews of the steps involved in acquiring and processing the data, other workers can see in the results some applications to their own fields of interest.

COST STATEMENT

The cost of computer time and for digitizing of analog data was about \$7,400. The cost of the entire multispectral survey, of which the present test site is a small part, was about \$26,000. Salaries of research personnel are not included in these cost estimates. In view of the fact that these studies are research- and development-oriented, it is impractical to attempt to establish costs for man-hours involved. Years

of work and research are represented in the developing and continual refining of the scanner systems used in gathering the data and the computer programs used in processing the data.

Now that the geologists and the computer specialists have experience in working together as a team, with this kind of data, it is likely that the costs would be somewhat less for such a study of similar terrain, elsewhere.

ACKNOWLEDGMENTS

The data which form the subject of this preliminary report were derived from work done on contract by the following university research groups and persons: (1) Institute of Science and Technology, Willow Run Laboratories, University of Michigan; airborne multispectral survey and analog processing of data. Phil Hasell, Frederick Thompson, and Leo Larsen; (2) Laboratory for Agricultural Remote Sensing, Purdue University; digitizing the magnetic tapes, computer generation of statistical data, and recognition processing. Robert MacDonald, David Landgrebe, Terry Phillips, and Paul Anuta.

The following U.S. Geological Survey personnel assisted in gathering ground-truth data: Harold Prostka furnished a bedrock geologic map and helped lay out navigation aids along the flight path; and Douglas Carter, David Daniels, Jules Friedman, Stephen Gawarecki, and Philip Philbin furnished ground measurements of radiation and ground and air temperatures during the time of overflight.

REFERENCES

More detailed information on optical/mechanical scanners and the various techniques and computer programs described in this report can be found in the following:

- Cardillo, G. P., and Landgrebe, D. A., 1966, On pattern recognition: Purdue Univ. Laboratory for Agricultural Remote Sensing Inf. Note 010866, 18 p. mimeographed.
- Landgrebe, D. A., and Staff, 1968, LARSYAA, A processing system for airborne earth resources data: Purdue Univ. Laboratory for Agricultural Remote Sensing Inf. Note 091968, 34 p. mimeographed.
- Lowe, D. S., 1968, Line scan devices and why use them, in Proceedings of the Fifth Symposium on Remote Sensing of Environment. Ann Arbor, Michigan Univ. Inst. of Science and Technology, p. 77-100.
- Swain, P. H., and Germann, D. A., On the application of man-machine computing systems to problems in remote-sensing: Purdue Univ. Laboratory for Agricultural Remote Sensing Inf. Note 051368, 10 p. mimeographed.



Waldrop, H. A., 1969, Detection of thick surficial deposits on 8-14/4
infrared imagery of the Madison Plateau, Yellowstone National Park:
U.S. Geol. Survey open-file report, 7 p., 2 figs.

Willow Run Laboratories Staff, 1968, Investigations of spectrum-matching
techniques for remote sensing in agriculture; final report,
January 1968 through September 1968. Ann Arbor, Michigan Univ.
Inst. of Science and Technology Infrared and Optical Sensor Laboratory
report no. 1674-10-F, 48 p. This report contains numerous pertinent
references.

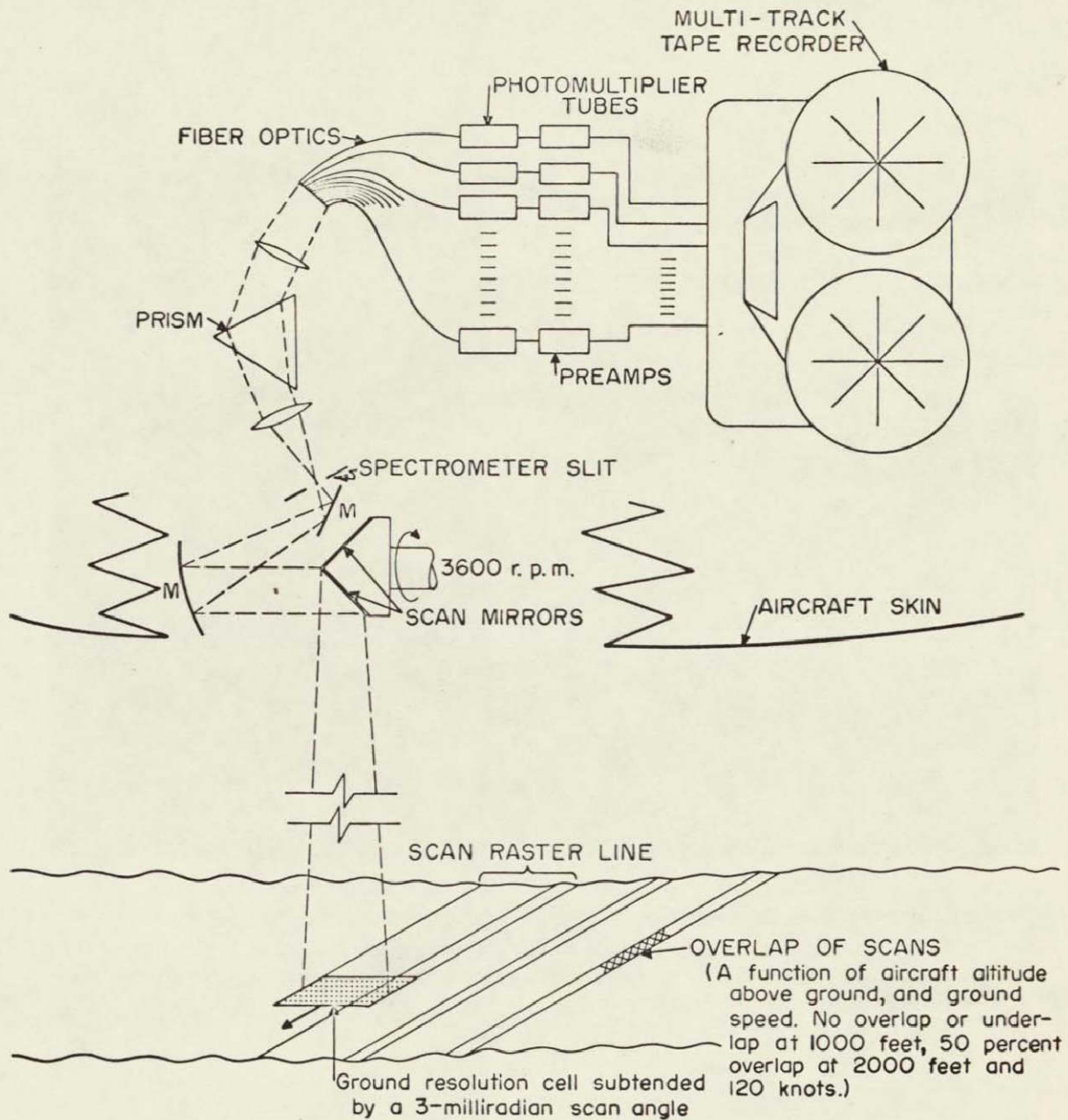


Figure 3-1.- Diagram of optical-mechanical scanner and spectrometer used by University of Michigan in gathering data for this study.



Figure 3-2.- Gray-scale video display of reflectance from channel 9 (0.62-.66 μm). Area is same as shown in eastern parts of figures 7 and 9. Enlarged from data generated by the Institute of Science and Technology, University of Michigan.

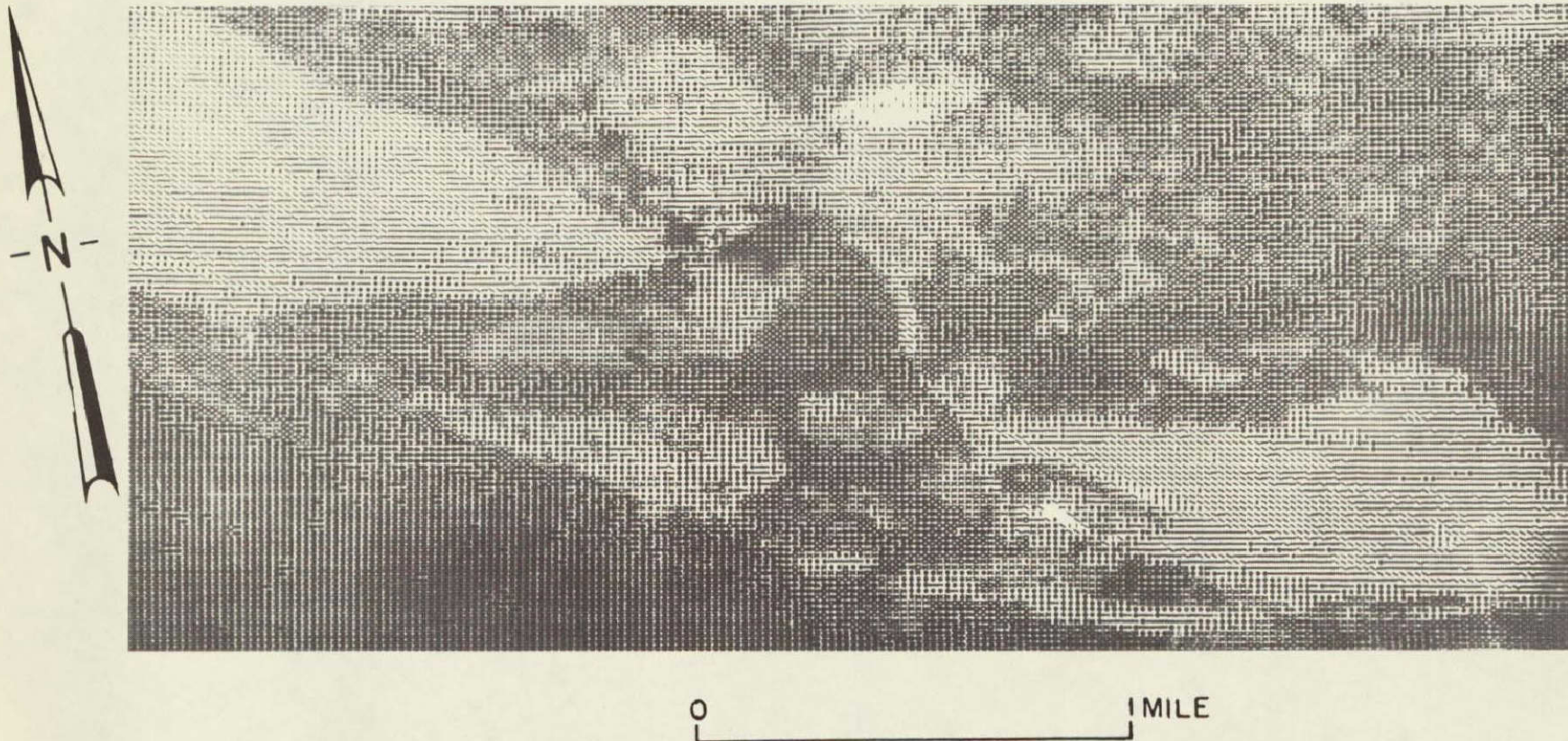


Figure 3-3.- Ten-level gray-scale digital computer display of reflectance from channel 9 (0.62-.66 μm), as obtained by LARS-Purdue. Area shown is bottom (south) half of that shown in figure 2.

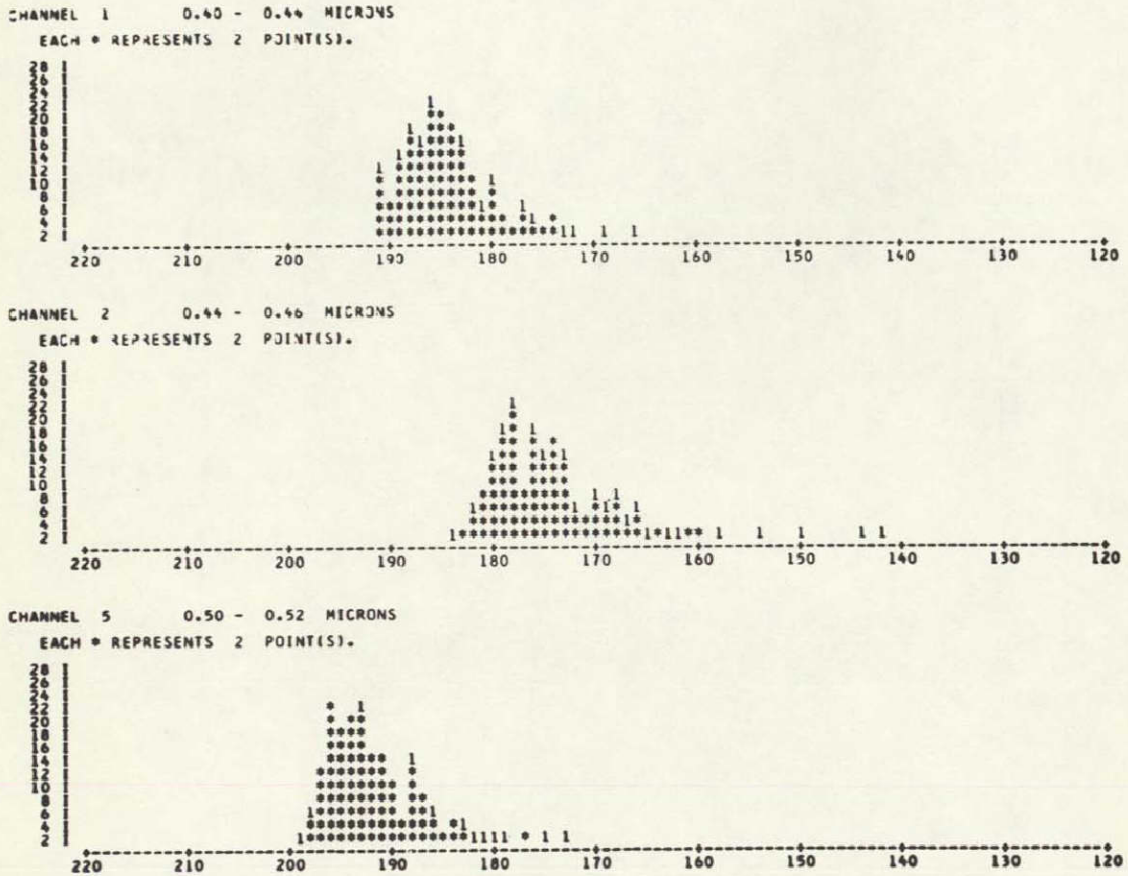


Figure 3-4.- Histograms of reflectance of talus in channels 1, 2, and 5. The abscissa is relative radiance (brightness), increasing to the right. On this direct copy of the computer printout, the numerical abscissa values decrease for increasing radiance because the scanner output signal is inverted. The ordinate gives the number of resolution elements with a given relative radiance.

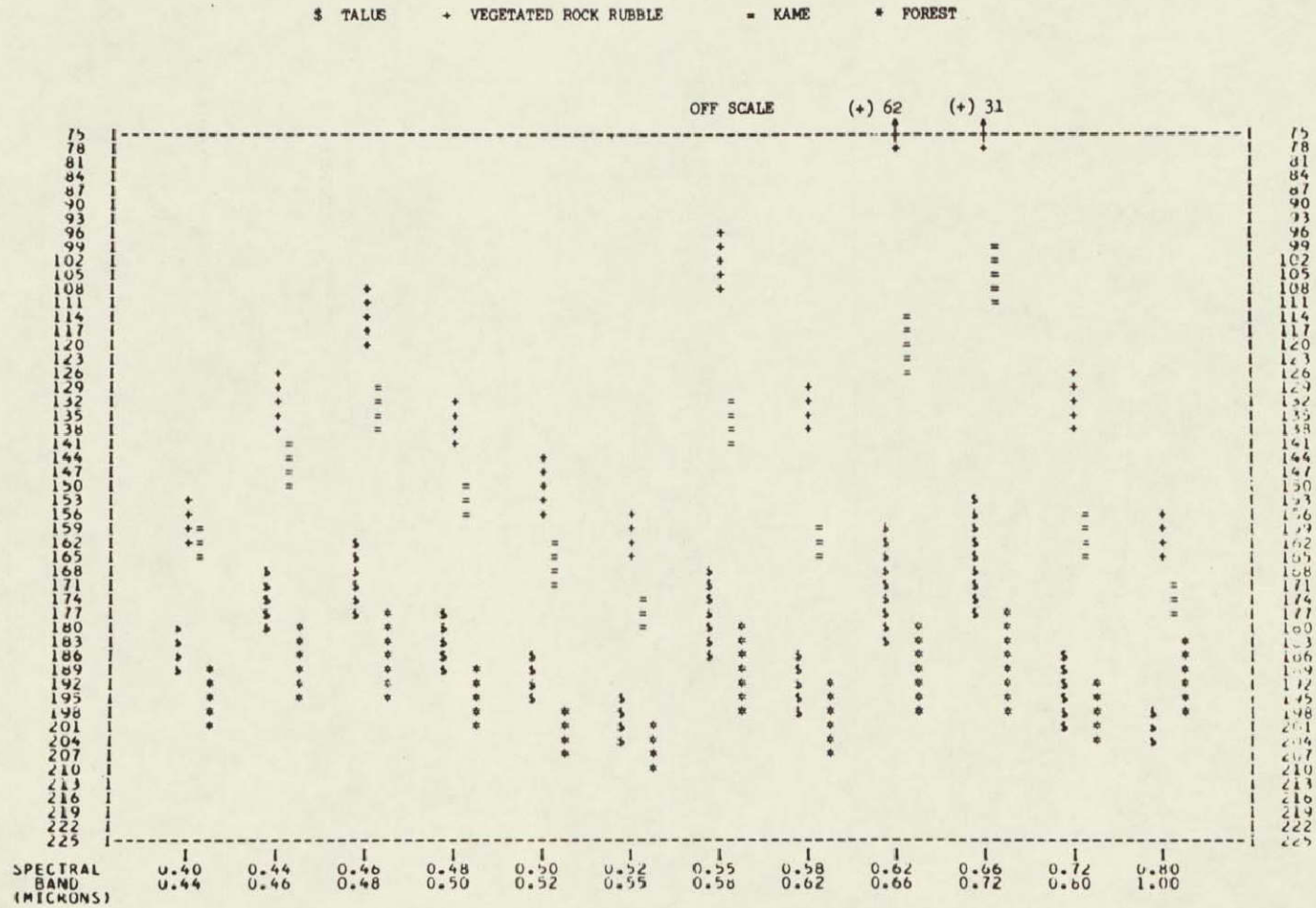


Figure 3-5.- Comparisons of spectral reflectance of training areas of four classes of material. Reflectance or radiance, increasing upward, is shown for each of the 12 channels of the Michigan scanner data. A vertical line two standard deviations long, centered about the mean radiance, is drawn using alphanumeric symbols.

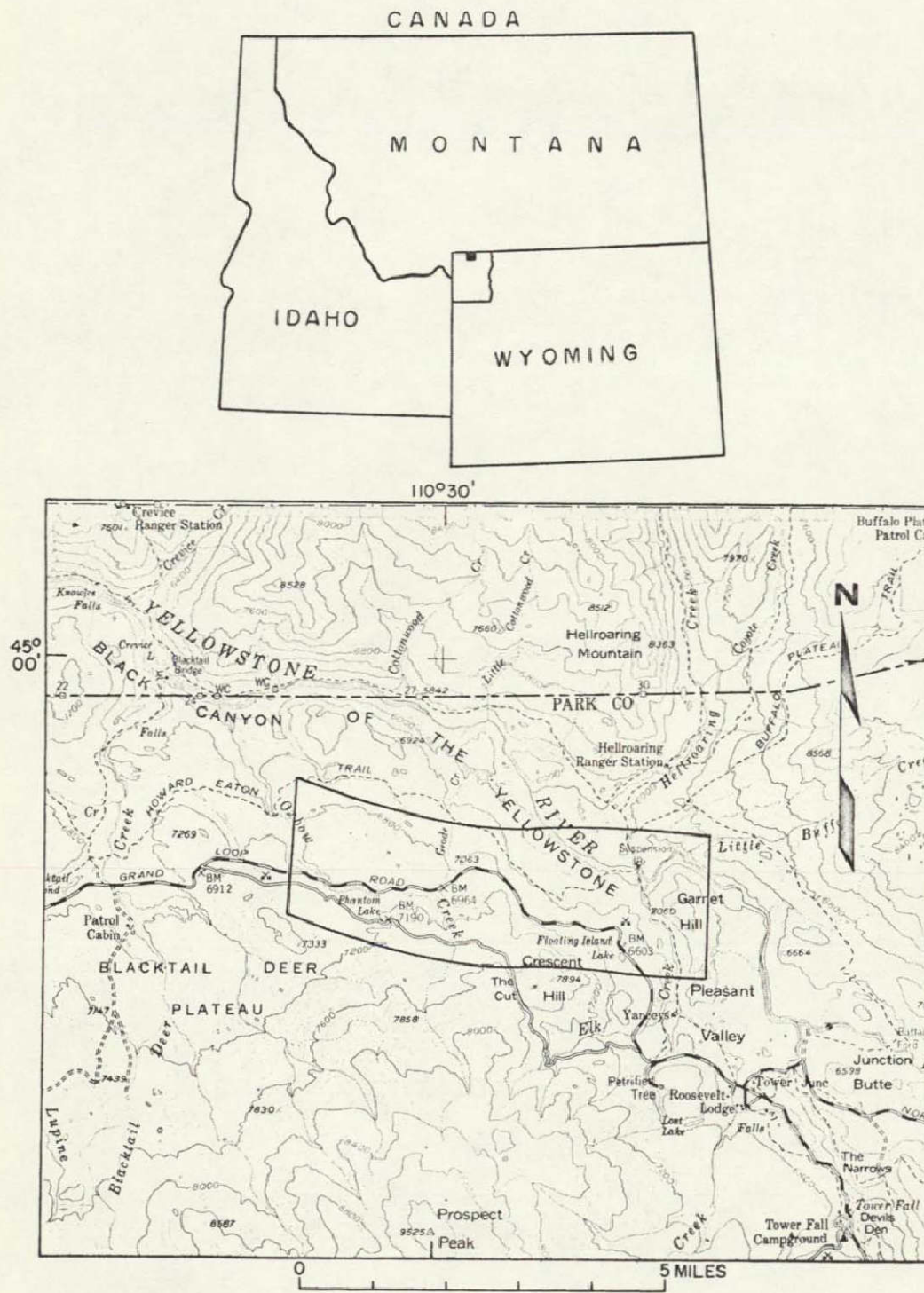


Figure 3-6.- Index map of test area.



Figure 3-7.- Aerial photograph of test area. Tick marks indicate approximate limits of area shown on figure 2-9.



Figure 3-8.- Panorama of test area, looking west. Yellowstone River is near right edge, Crescent Hill is at the left edge.



Figure 3-9.- Photograph of part of hand-colored computer printout of terrain maps, north-central Yellowstone Park. Area is same as shown between tick marks on figure 7.

Left display: based on the computer-selected best set of four data channels.

Middle display: based on the simulation of the ERTS RBV camera data channels.

Right display: based on the overlay of data from the reflective and the infrared scanner systems. Because the scan angle of the thermal scanner was much narrower than that of the reflective, this display covers only the middle strip of those shown to the left of it.



Figure 3-10.- Bedrock exposures. Volcanic tuff breccia is shown in upper photograph, basalt lava flows in lower.



Figure 3-11.- Talus of rhyolite tuff near Floating Island Lake. Crescent Hill is in the background.



Figure 3-12.- Blocks of rhyolite tuff in talus, showing contrast between fresh surfaces (below hammer head) and surfaces coated with dark lichens.



Figure 3-13.- Vegetated rock rubble. These are mixtures of angular blocks of basalt (top photograph), bedrock slabs and blocks of gneiss (foreground of lower photograph), lichens, soil, dry grass, sagebrush, weeds, evergreen seedlings, and twigs.



Figure 3-14.- Glacial kame, showing grass, mineral soil, weeds, dead vegetation, elk manure (top photograph), and sagebrush debris (bottom photograph).



Figure 3-15.- Glacial till, showing sand, rock chips, and boulders in mineral soil, grass, sagebrush, weeds, and twigs. Wild range in texture is shown, from fine grained (top) to coarse grained (bottom).

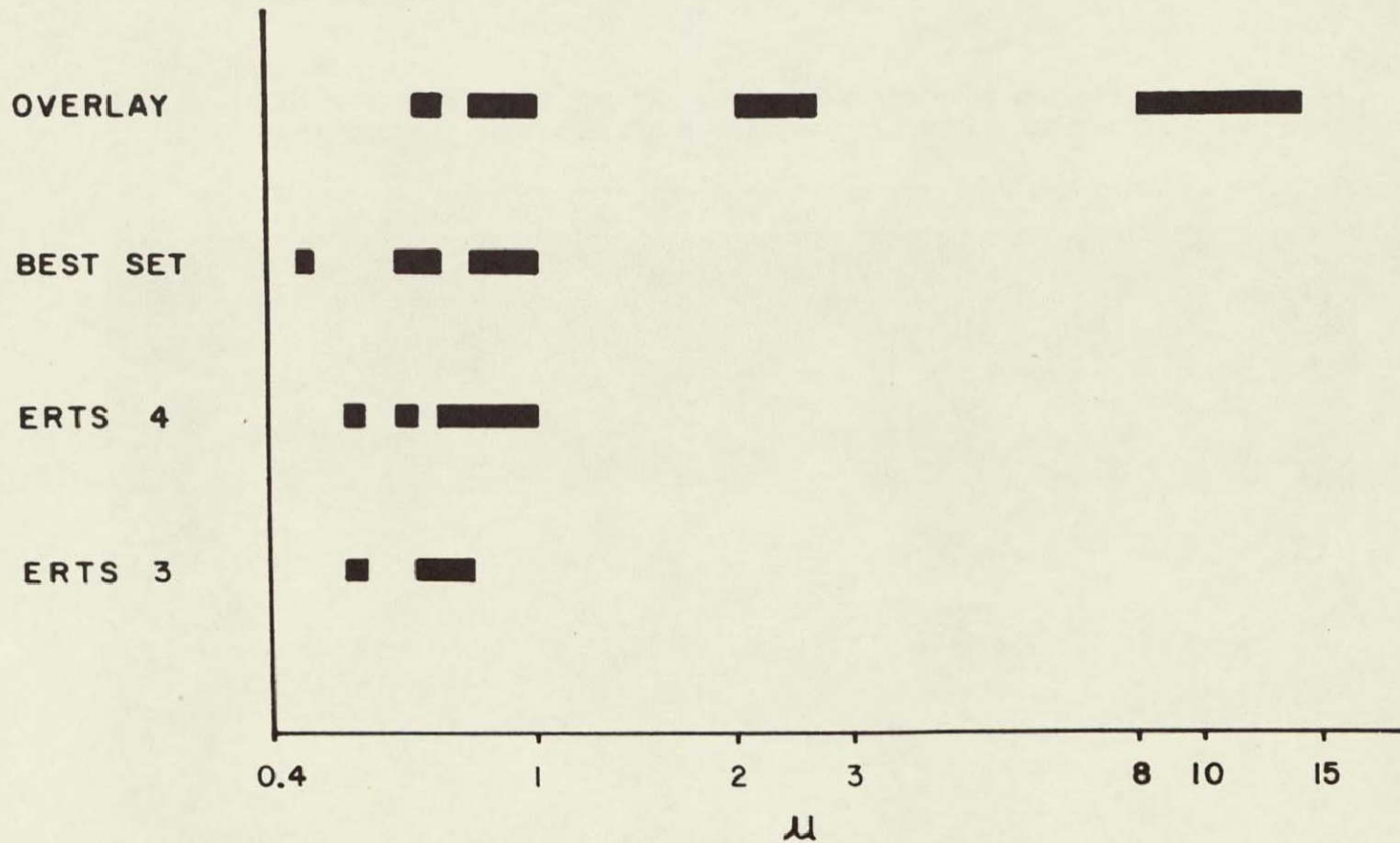


Figure 3-16.- Comparison of wavelength bands used in this computer study.

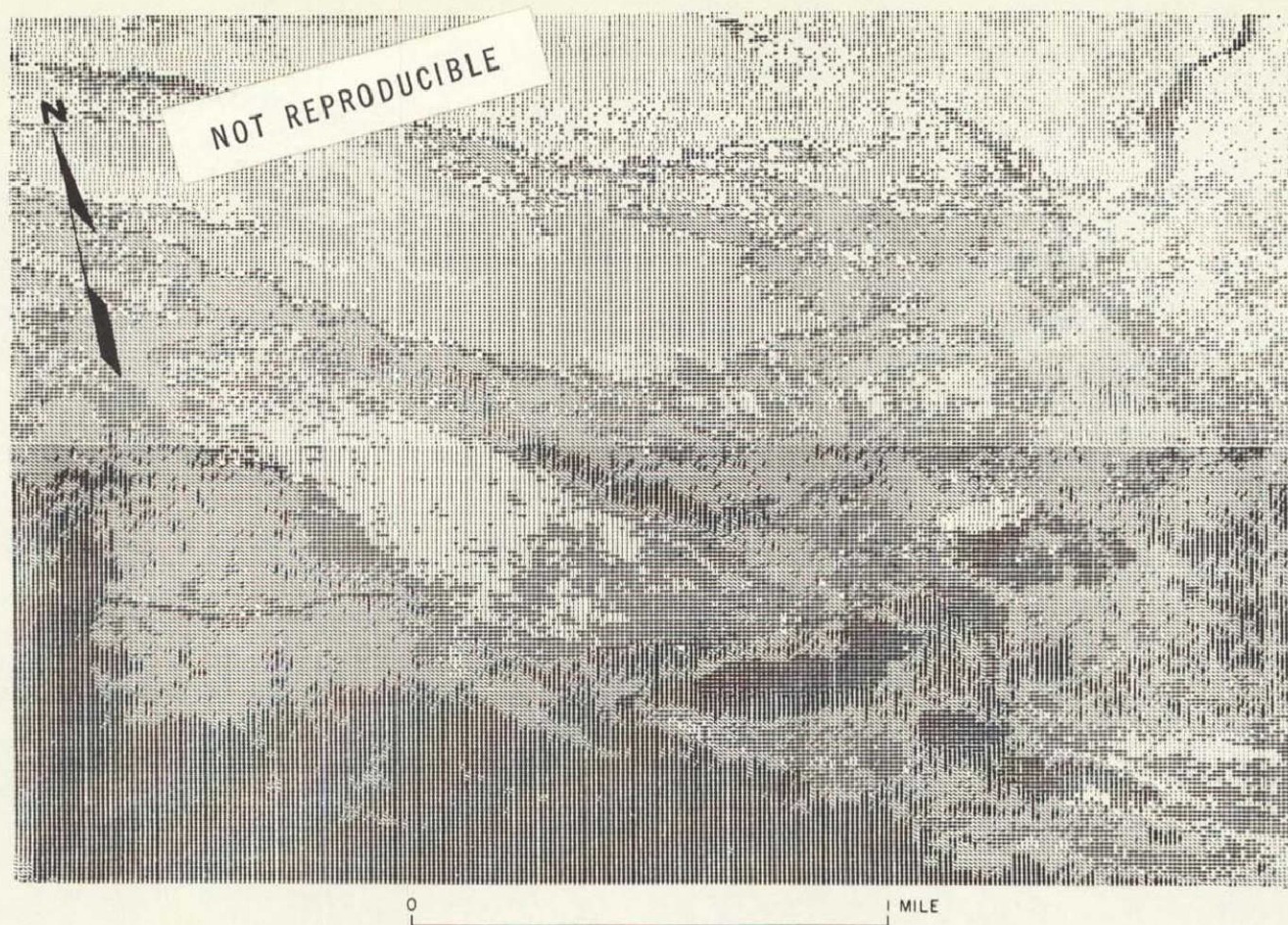


Figure 3-17.- Segment of terrain map obtained by using computer-selected best set of four channels of reflective data. Symbols used to designate the terrain units are:

•	bedrock exposures	=	glacial kame	W	surface water
8	talus	-	glacial till	H	shadows
\$	vegetated rock rubble	/	forest	(blank)	thresholded
		'	bog		

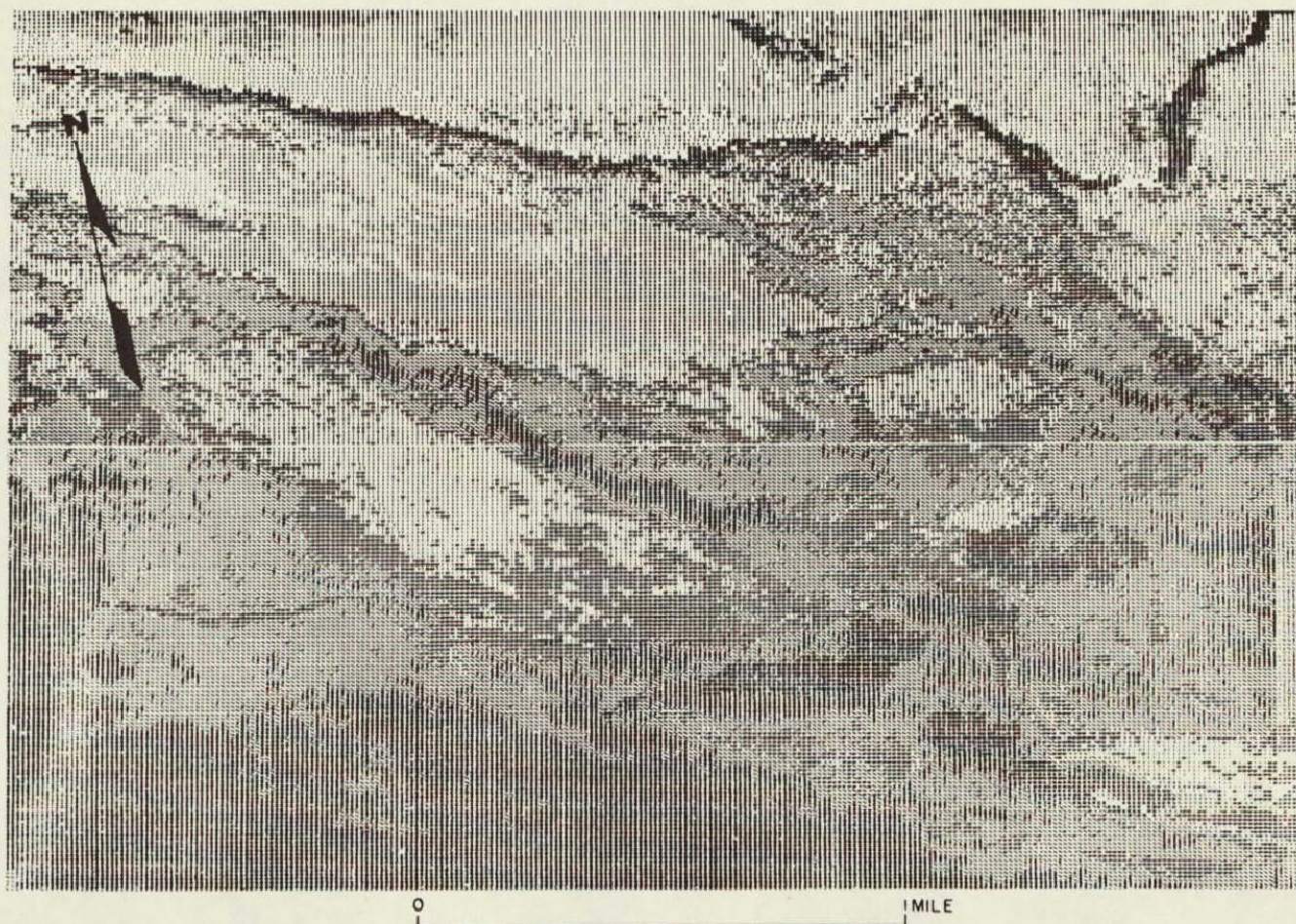


Figure 3-18.- Segment of terrain map obtained by using simulations of ERTS 4-channel scanner data. Symbols used to designate the terrain units are:

•	bedrock exposures	=	glacial kame	W	surface water
8	talus	-	glacial till	H	shadows
\$	vegetated rock rubble	/	forest	(blank)	thresholded
		,	bog		

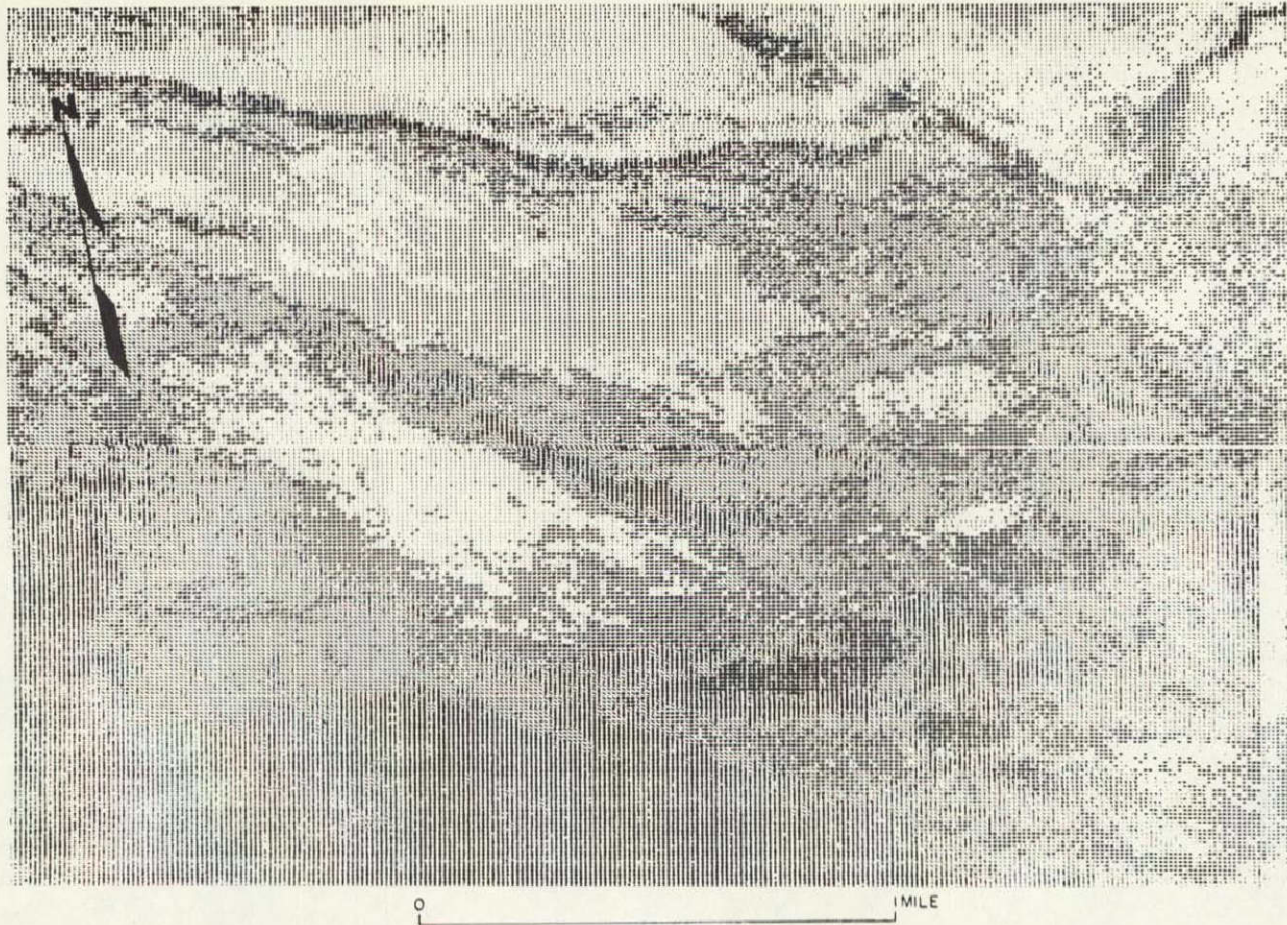


Figure 3-19.- Segment of terrain map obtained by using simulations of ERTS 3-RBV camera data. Symbols used to designate the terrain units are:

•	bedrock exposures	=	glacial kame	W	surface water
8	talus	-	glacial till	H	shadows
\$	vegetated rock rubble	/	forest	(blank)	thresholded
		'	bog		

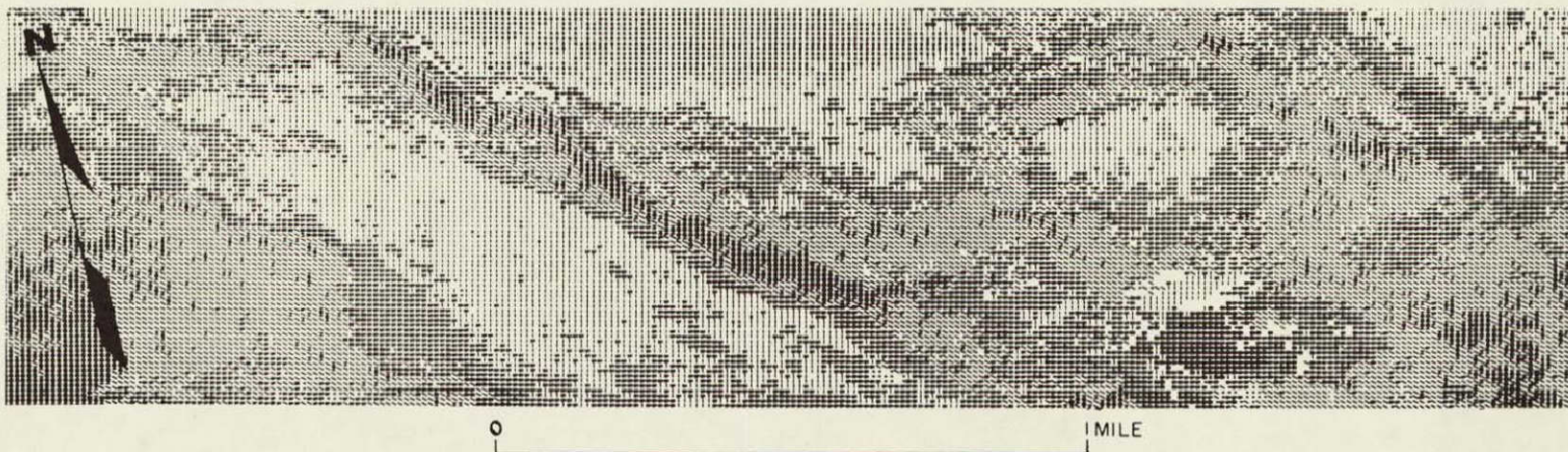


Figure 3-20.- Segment of terrain map obtained by combining one thermal infrared and three reflective channels of data. Symbols used to designate the terrain units are:

8	talus	-	glacial till	H	shadows
\$	vegetated rock rubble	/	forest	(blank)	thresholded
=	glacial kame	'	bog		

SECTION 4
GEOLOGIC ANALYSIS OF THE X-BAND RADAR
MOSAICS OF MASSACHUSETTS*

by
Lincoln R. Page
U. S. Geological Survey

N71-19255

ABSTRACT

The X-band radar mosaic of Massachusetts, at a scale of 1:500,000 made by the Grumman Aircraft Engineering Corporation under contract for the U. S. Geological Survey in cooperation with the U. S. Army and National Aeronautics and Space Administration, presents an overall view of the geologic and geographic features of the state.

Lineament patterns allow recognition of major structural features that can be related by geologists familiar with local areas to faults, joints, folds, and stratigraphy of the bedrock and drumlins, fans, and channels of Pleistocene deposits.

More refinement of the method is needed to obtain uniform quality of imagery, correctness of scale, and appropriate orientation of flight lines for maximum use in unknown terrain.

INTRODUCTION

The X-band radar mosaics of Massachusetts have been analyzed in part and used by several persons in the cooperative geologic mapping projects of the State of Massachusetts and the U. S. Geological Survey. The topographic lineaments emphasized on the radar mosaics have been related to the geology of the areas in which the individuals currently are, or have been, working. The purpose of this paper is to report on some of the results that have been obtained by them in interpreting the geology on the basis of their analysis of the X-band data.

Both an east-looking and a west-looking mosaic were made in 1968 by the Grumman Aircraft Engineering Corporation with the cooperation of the U. S. Army for the U. S. Geological Survey as a project under the National Aeronautics and Space Administration (NASA) program. They were assembled by Hans Behm of Grumman under the direction of William Coulborne (figs. 1 and 2). Later the radar film was sent to the Autometric Operation of the Raytheon Company where it was enlarged 2 times on a Log-E-Tonic printer and assembled into two mosaics which have a much better tonal match between strips but are less sharp (figs. 3 and 4). Prints of these mosaics were made available for sale to the public through the U. S. Geological Survey.

*Publication authorized by the Director, U. S. Geological Survey.

Maurice Pease, Jr. analyzed the lineaments of the entire state (figs. 5 and 6). The south-central part of Massachusetts and north-central Connecticut was studied in detail by Maurice Pease, Jr. and John Peper (figs. 7, 8 and 9) and the western part of Massachusetts was interpreted by David Harwood with the assistance of Norman Hatch (fig. 10).

Robert Schnabel used the mosaics for interpretation of structures in central Massachusetts west of the Connecticut River and related them to aeromagnetic surveys (fig. 11). Donald Alvord, Kenneth Bell, and Richard Volckmann contributed data on areas in eastern Massachusetts. Carl Koteff, Fred Pessl, Jr., and J. Philip Schafer analyzed the mosaics for data relating to Pleistocene materials and drainage systems.

We are deeply indebted to the personnel of Grumman Aircraft Engineering Corporation for their extreme interest and cooperation in this project.

Procedure

Planning for this project was carried out on July 1, 1968, and nine missions were flown in July and August with a Motorola AN/APS 94 system in a Grumman-built OV-1B Mohawk aircraft with on-board processing of the radar film. The imagery, however, was not of a desired quality so changes were made to laboratory controlled printing of the film. Data gathering missions were then flown from September 13 to October 1. The planned nineteen lines were flown to obtain overlapping coverage; however, it eventually took 27 flight lines to produce the mosaics. Seven of the missions were flown from Long Island and one, a double mission, required a re-fueling stop in Massachusetts. Commonly four lines were flown on a four hour mission at nominal aircraft speed of 180 knots and a normal flight altitude of 8,000 feet. This covered a 25 kilometer swath imaged in both directions. The flights were flown along the north-northeast structural trend of the Berkshires parallel to the western border of the state. Later additional missions were flown using stabilized antennae which produced the imagery shown in figure 7. The original imagery was at a scale of 1:500,000. As can be seen in figures 1 and 2, there was much tonal contrast between the flight strips and considerable striping resulting from antennae instability. All flying had to be done on clear days because it was necessary to have visual navigation to fly straight, drift-free paths over the target areas for best results. Calm weather is also desirable because turbulence degrades the imagery. Stabilized antennae that were used later appear to, in part, overcome this difficulty. The original contract from Grumman called for a single mosaic; however, because of the initiative and interest of those working on the project at Grumman, mosaics of both east and west-looking radar were made.

Results and Discussion

The main value of a radar mosaic is that it provides a clear picture over a broad area of the topographic lineaments resulting from deposition of materials or erosion along bedding planes, fracture zones, faults, and other bedrock structures. Superimposed on these main bedrock lineaments of Massachusetts are finer grained lineaments resulting from the deposition of materials formed in Pleistocene time by moving ice or meltwater streams.

In order to get maximum information from the radar mosaics, it is necessary to turn the radar map so that one looks down the structures, or along the lineaments, at a vertical angle of approximately 30°. Many of the lineaments are less noticeable when viewed directly downward. The detail of lineaments on the radar mosaics could be matched by appropriate aerial photography, but in general a mosaic of existing photographs is not as useful for geologic purposes. Figure 12 shows an aerial photomosaic of southeastern New England made by the Army Map Service for NASA at the same scale as the radar mosaics (figs. 1 and 2).

The geologist familiar with the geology of an individual area can sort the lineaments into groups, based on characteristic patterns and trends, and can recognize those formed parallel to bedding, those which follow fractures, those which represent Pleistocene deposits, and so forth. However, there are numerous lineaments on the Massachusetts radar mosaic for which we have no satisfactory explanation at this time and they require observation on the ground before they can be discussed.

Newly recognized features shown on the mosaic include a series of northwest-trending lineaments in the Berkshire area and in the area north of the corner of Rhode Island, Connecticut, and Massachusetts. Another distinctive feature is a large area just west of this corner where very pronounced lineaments with a north-south trend are abruptly truncated on the north and south by a lineament trending northeast. These truncations are probably extensions of faults that have been recognized farther east in Massachusetts.

Maurice Pease, Jr., has made an incomplete analysis of the Massachusetts mosaics and has traced various lineaments on both the east- and west-looking views (figs. 5 and 6). He has attempted to be objective and these are his work sheets. By contrasting figures 5 and 6 it is possible to see those lineaments which are accentuated or subdued depending on look direction; many are visible on only one mosaic. As can be seen from these figures, there are innumerable lineaments with all directions of trend, but within any

one area there are recognizable patterns. More interpretive results may be obtained by connecting many of the lines with a resulting separation of areas of lineaments parallel to bedding or layering surrounded, or bounded in part, by lineaments formed by faults and fracture zones. Such analyses have been done for the specific areas described below.

Figure 10 shows an area in western Massachusetts where David Harwood and Norman Hatch have been able to delineate the boundary of Precambrian and Paleozoic rocks. This figure is essentially a simplified and crude geologic map in which the curved lines outline areas of remarkably different radar reflectivity and topographic relief. The short lineaments conform in general to the trend of the different rock units as mapped by the geologists and the darker lines show lineaments that appear to cross and locally offset the trend of known lithologic units. The western part of the area is a flat valley floor with featureless topography and the uniformly dull gray radar reflection is caused by the underlying carbonate rocks of Cambrian and Ordovician age. Patches of non-carbonate rock stand out well in the floor of the valley. These rocks represent a striking contrast to the Precambrian rocks to the east and the Taconic rocks to the west.

In parts of the area thin lithologic units can be recognized by thin, but very bright reflections. This is shown on the southwest slope of Beartown Mountain by the step-like bright and dull reflections on the east-looking mosaic. The pronounced northwest grain in the Precambrian rocks and their northwestern termination by enlarged lobate fold noses are strikingly shown around Beartown Mountain and to the east northeast. Also, the difference in trend of the Precambrian and Paleozoic rocks to the east is clearly shown, but the unconformity between the two groups of rocks is not clearly visible. It is marked by the dark curved north-south trending boundary on figure 10.

A fairly accurate map of this region can be made from a composite of the east- and west-looking radar mosaic. If either east- or west-looking mosaics are used separately, the lee side of more rugged topography is lost in the shadow. In the same way, those lineaments that trend parallel to the flight line and thus perpendicular to the radar beam are enhanced, while the lineaments parallel to the radar beam are reduced in intensity.

A compilation of aeromagnetic data of the Geological Survey for the same general area was made by Robert Schnabel (fig. 11). The different levels of intensity have been shaded and it is interesting to note that the patterns produced are not unlike the lineament patterns on the radar mosaic.

After the two state mosaics had been compiled, an additional mission was flown by Grumman of an area in central Massachusetts and Connecticut east of the Connecticut River valley using stabilized antennae (fig. 7). Using two strips as a pseudo-stereo pair, Maurice Pease, Jr., developed figure 8, which shows recognizable lineaments and separates them as to type. John Peper analyzed a portion of this area, the Hampden-Monson area which he had mapped (fig. 9a) as a doctoral thesis (1). He made another map (fig. 9b) showing fault or fracture lineaments recognized from the radar data. This appears to explain some of the curves in the contacts of the earlier map and suggests areas most favorable for field checking.

Conclusions

The side looking radar mosaics of Massachusetts (figs. 1 and 2), when compared to the geologic map (fig. 13) of Emerson (2) and to more recent geologic maps which have been published, indicate that the mosaics have great usefulness in enabling geologists to better understand the structure in the area. If the radar maps had been available at the start of the current mapping program, it would have been possible to select the best areas to start structural studies and perhaps a great deal of time and money would have been saved simply by directing the work into the areas where the most critical problems exist. Without this information, mapping was started at numerous places and as yet has not progressed sufficiently to get the overall picture. The radar maps are currently aiding the understanding and tying together of local areas with the overall geologic picture. They indicate many of the complex units and patterns on the geological maps are best explained on the basis of fault rather than fold patterns.

Our limited analysis of the X-band radar mosaics has pointed out several problems related to side looking radar that need more research. The scale should be more accurate for mapping purposes, more knowledge is needed concerning the cause of variations in reflectivity, and we need to learn how to recognize lineaments at right angles to the flight lines before this technique will have its maximum usefulness in unknown areas such as Africa, South America, and Alaska. There needs to be much more research on the relation of reflectivity of the various types of rock units to learn what is causing the apparent tonal differences that seem to be related to rock rather than to any particular type of vegetation. In many parts of Alaska and elsewhere it is going to be impossible to make a systematic survey with radar and have the flight lines parallel to the structure because the structure is relatively unknown and of variable trend. One excellent advantage of radar is its ability to scan through areas which normally have adverse weather conditions such as heavy cloud cover or haze, but to do this more research is needed on the appropriate navigational systems to be used.

With good radar maps available the geologist could use his interpretation of lineaments and overall ground knowledge of the geology to select areas most favorable to prospect for metals or oil or to designate areas needing ground mapping. This use of radar will be very important when more experience has been obtained and techniques have been perfected.

References Cited

1. Peper, J. D., 1966, Stratigraphy and structure of the Monson area, Massachusetts-Connecticut: Univ. Rochester Ph.D. thesis, available on microfilm from University Microfilms, Inc., Ann Arbor, Mich., 127 p.
2. Emerson, B. K., 1917, Geology of Massachusetts and Rhode Island: U. S. Geol. Survey Bull. 597, 289 p.



Figure 4-1.- Side looking radar mosaic of Massachusetts (east looking, uncontrolled, raw imagery, no enhancement).

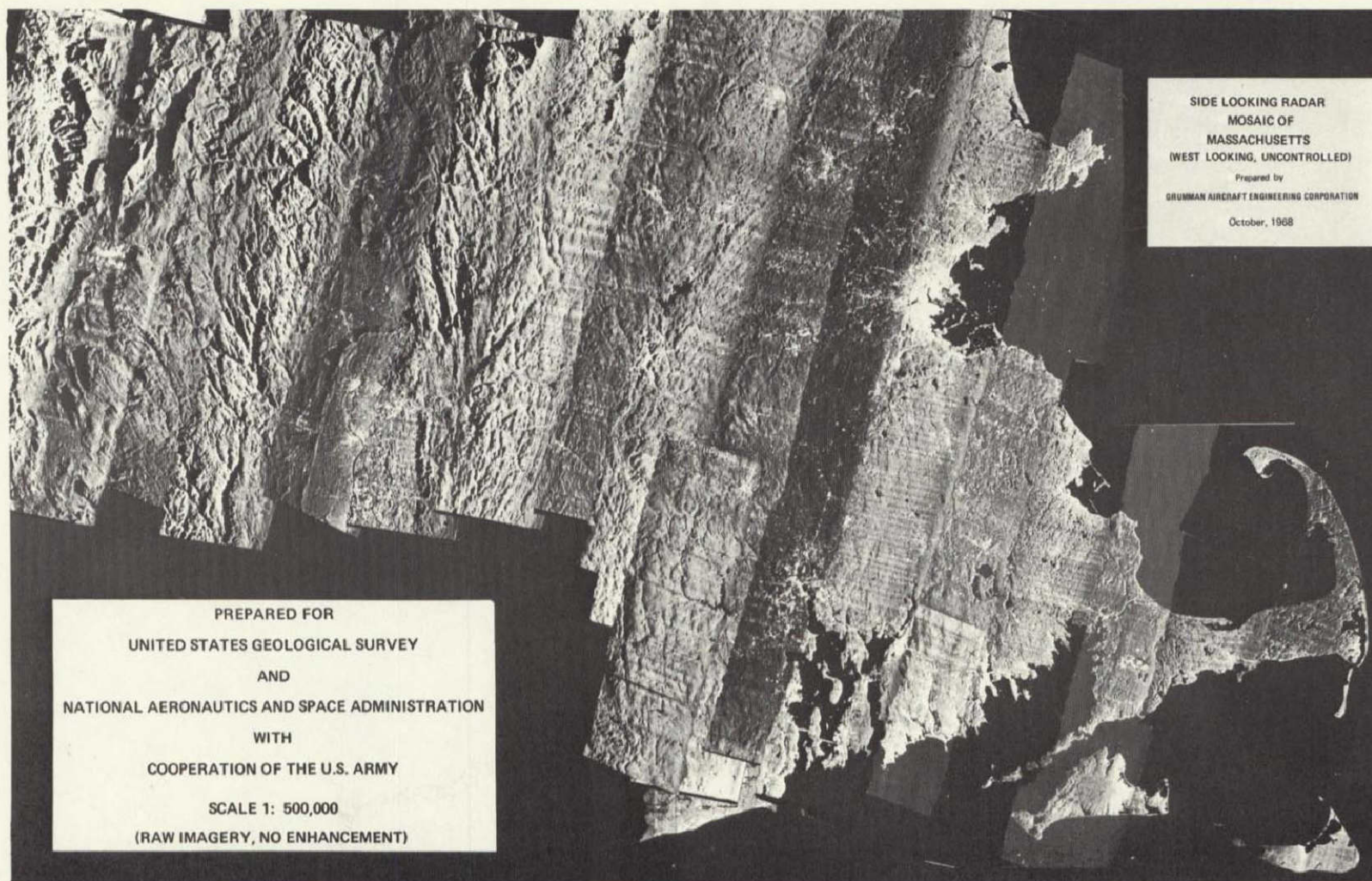


Figure 4-2.- Side looking radar mosaic of Massachusetts (west looking, uncontrolled - raw imagery, no enhancement).

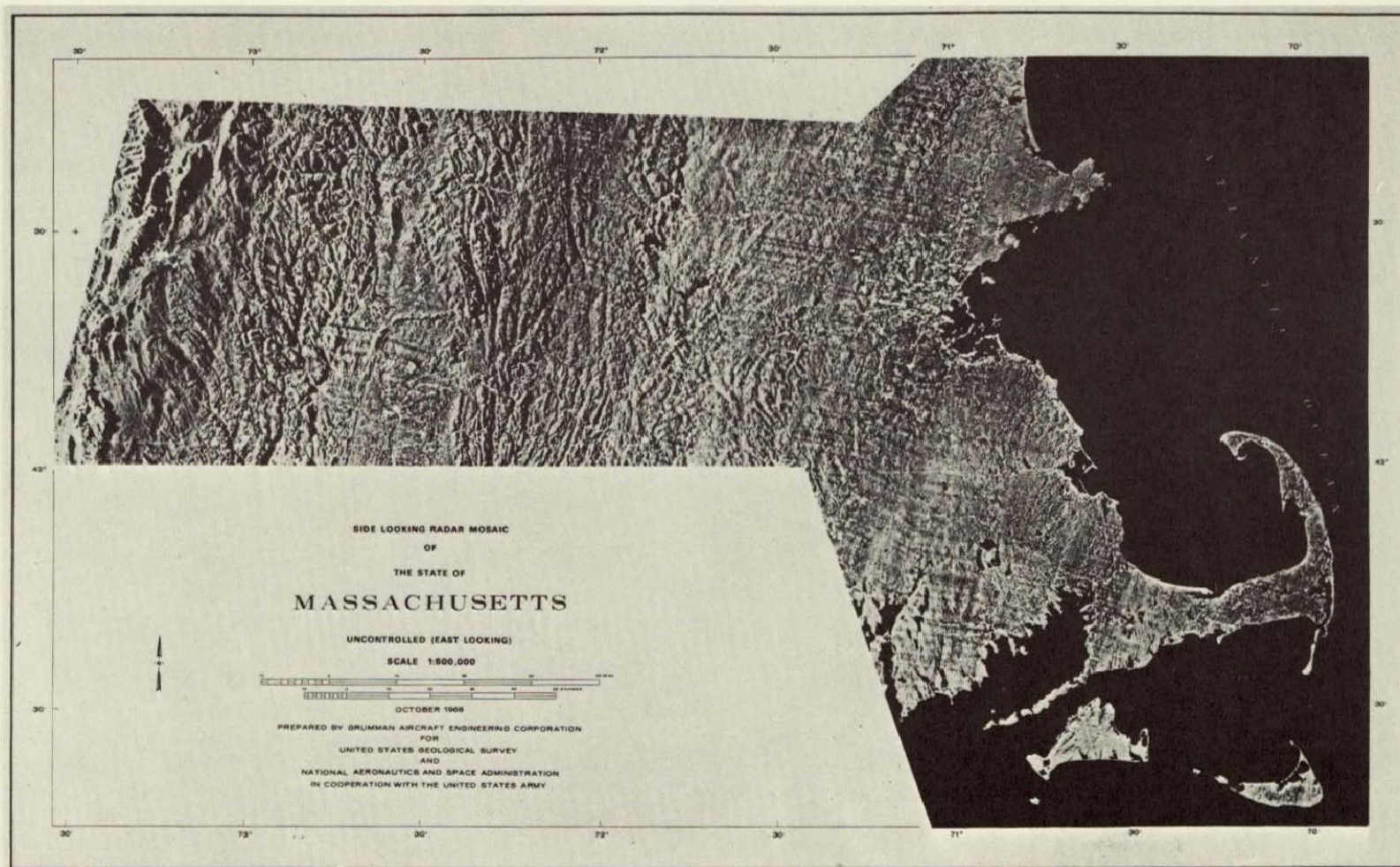


Figure 4-3.- Side looking radar mosaic of Massachusetts (east looking, uncontrolled - enhanced).

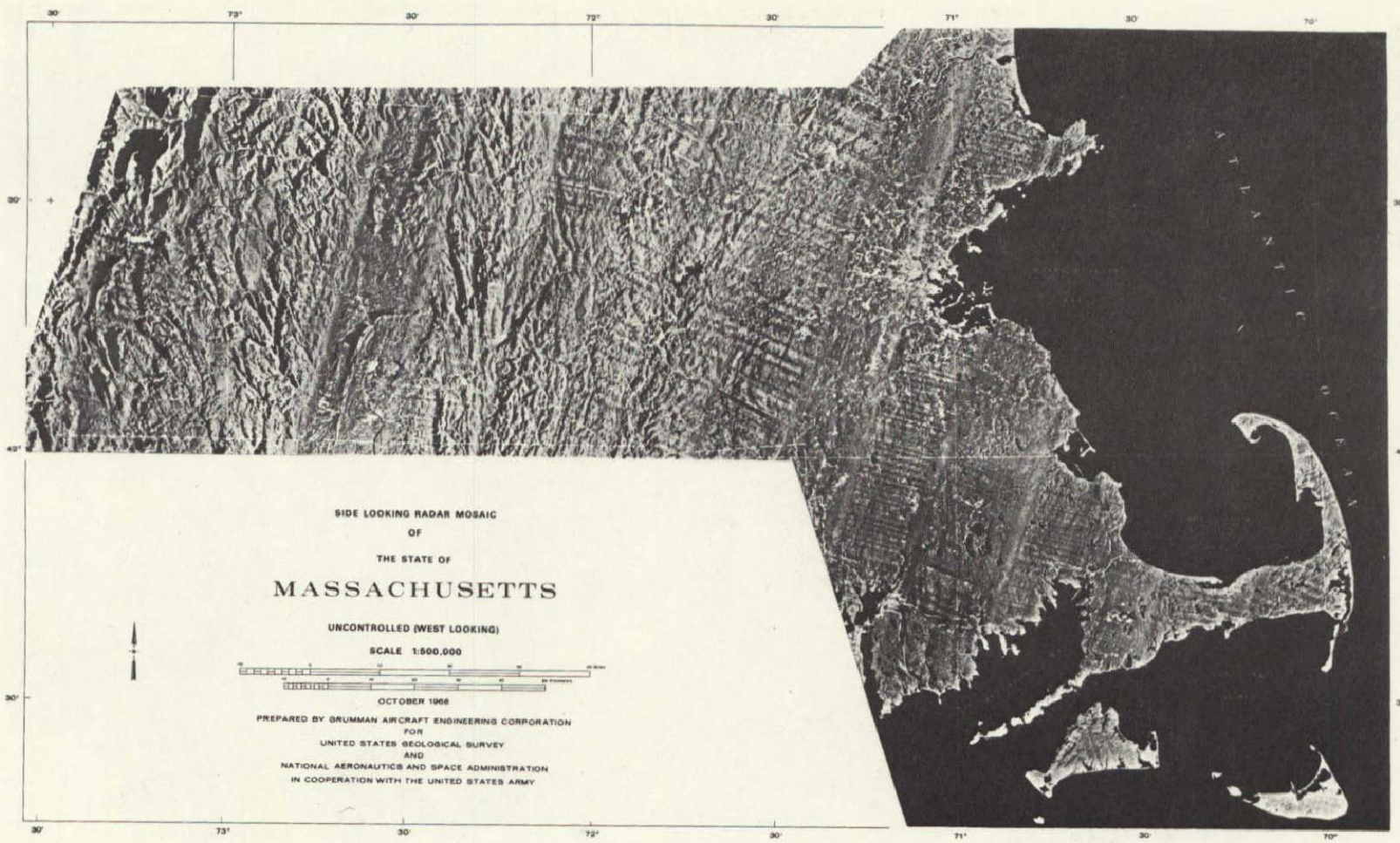


Figure 4-4.- Side looking radar mosaic of Massachusetts (west looking, uncontrolled - enhanced).

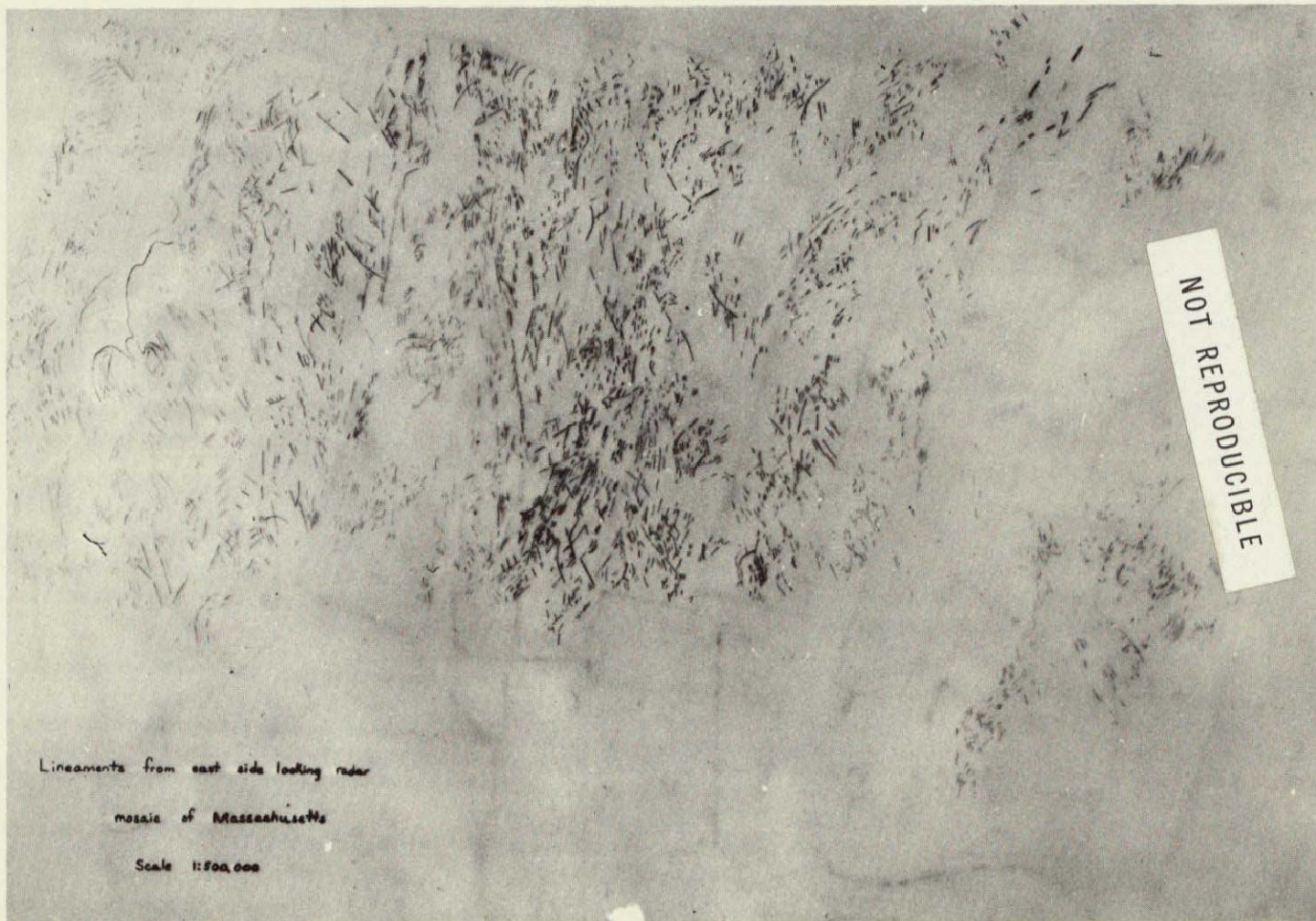


Figure 4-5.- Lineaments traced from side looking radar mosaic of Massachusetts (east looking).

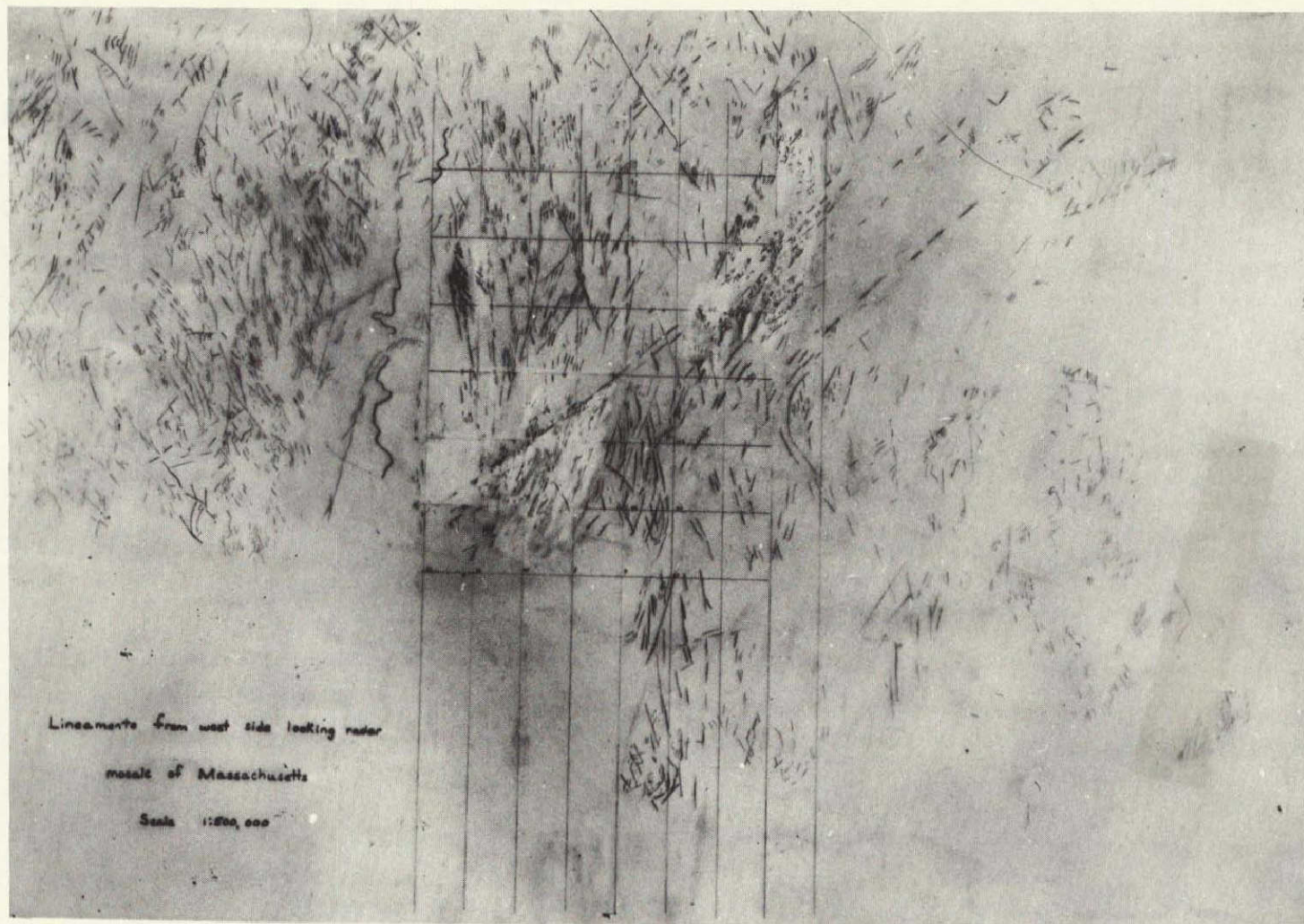


Figure 4-6.- Lineaments traced from side looking radar mosaic of Massachusetts (west looking).

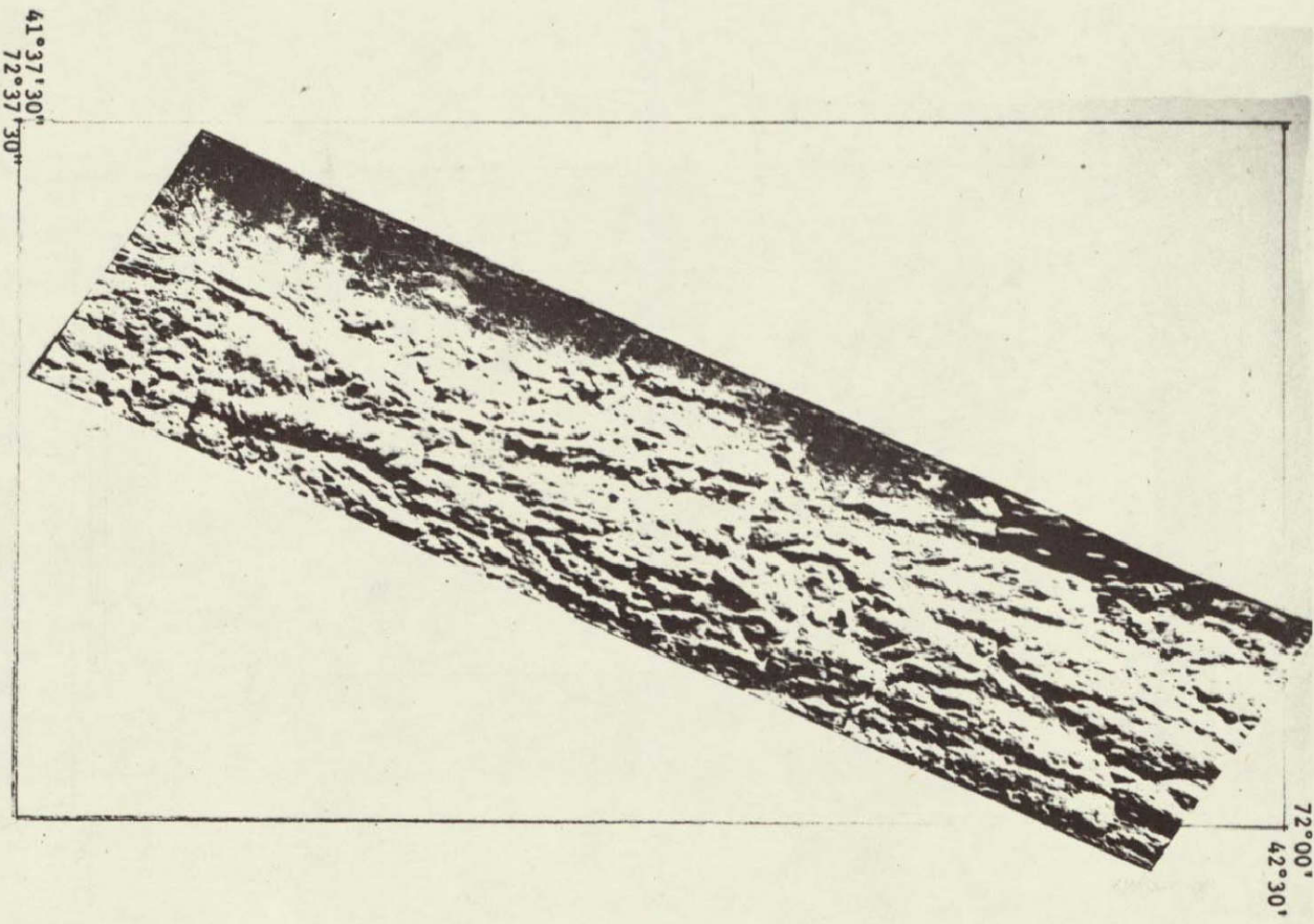


Figure 4-7.- SLAR imagery - central Massachusetts and Connecticut.

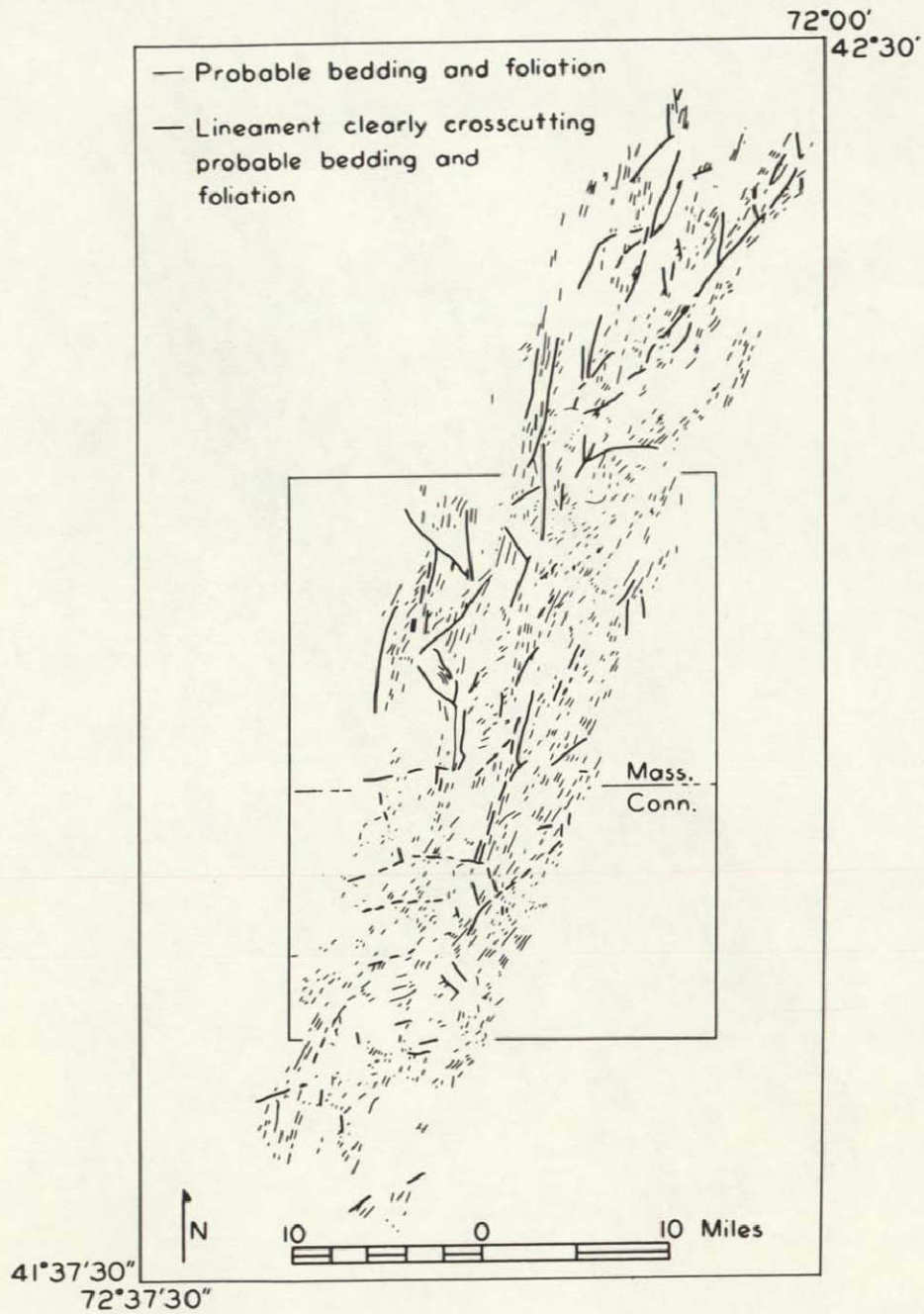
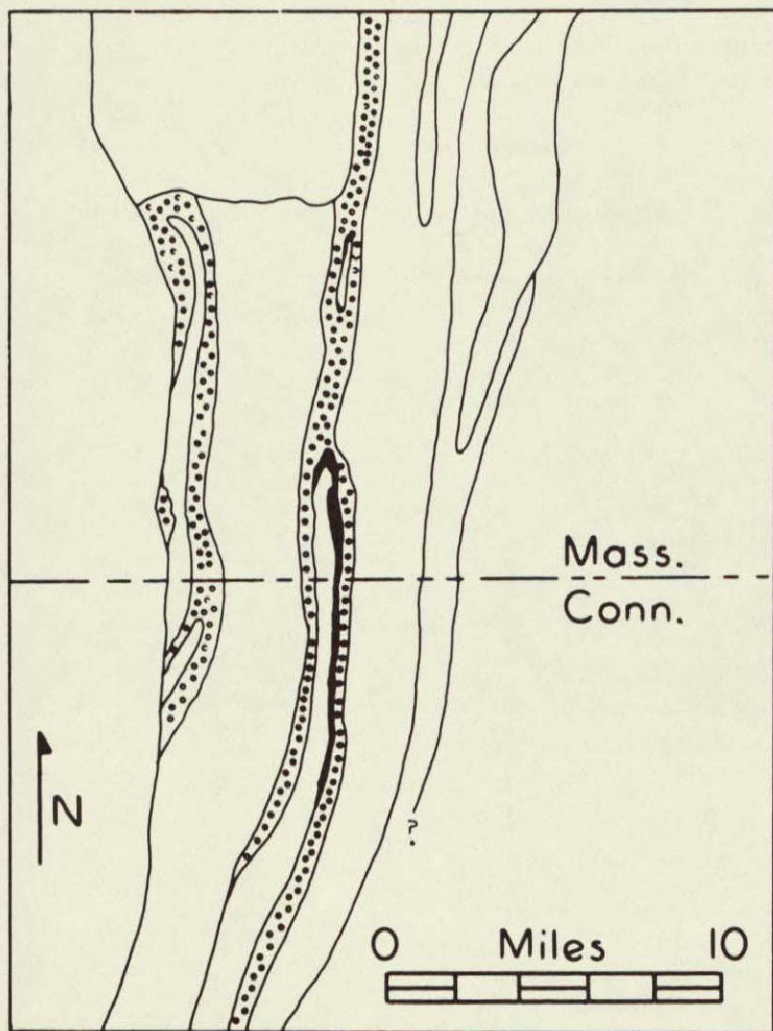
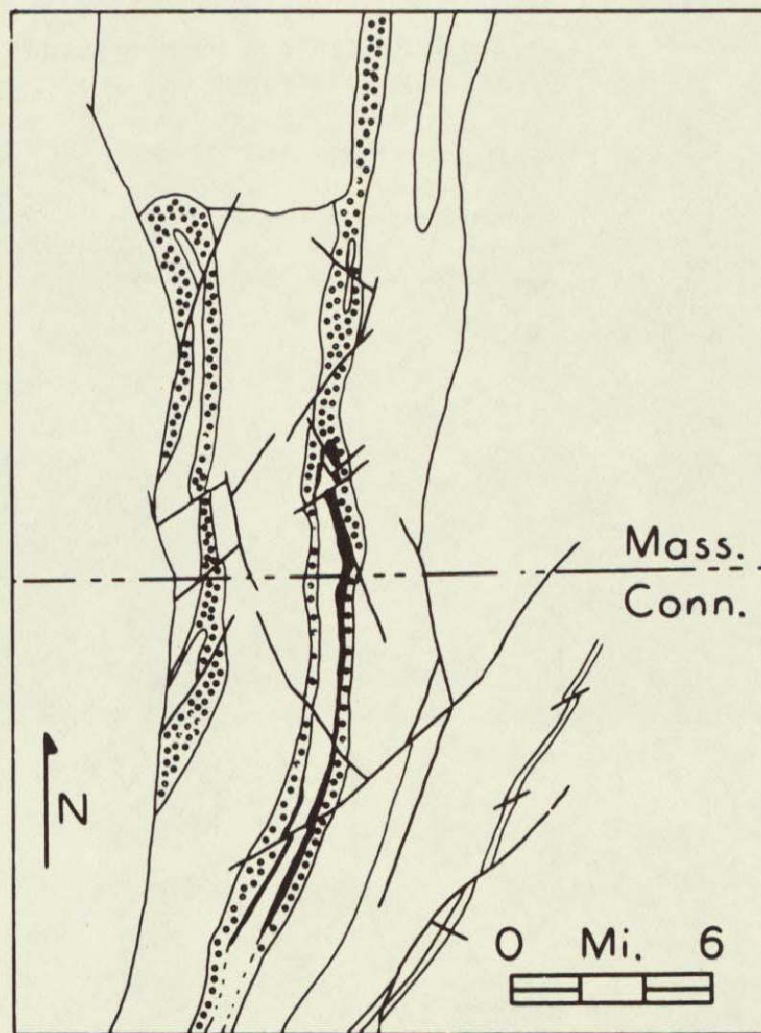


Figure 4-8.- Lineaments from SLAR imagery - central Massachusetts and Connecticut.



a. Geologic map of south-central part of Massachusetts and north-central Connecticut.



b. Reinterpretation of geologic map using SLAR imagery.

Figure 4-9.- Massachusetts/Connecticut maps.

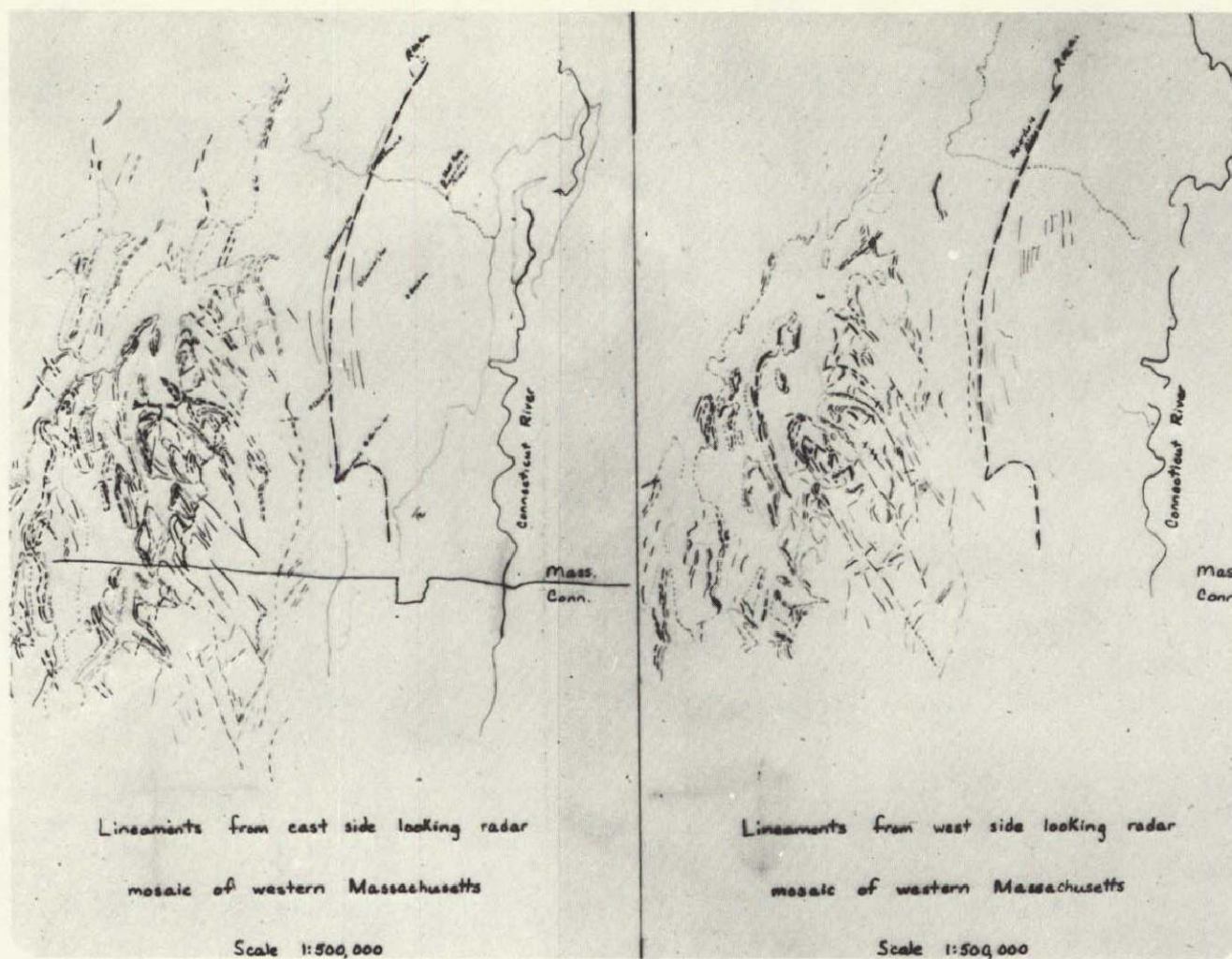


Figure 4-10.- Lineaments interpreted from two side looking radar mosaics of western Massachusetts (east looking and west looking).

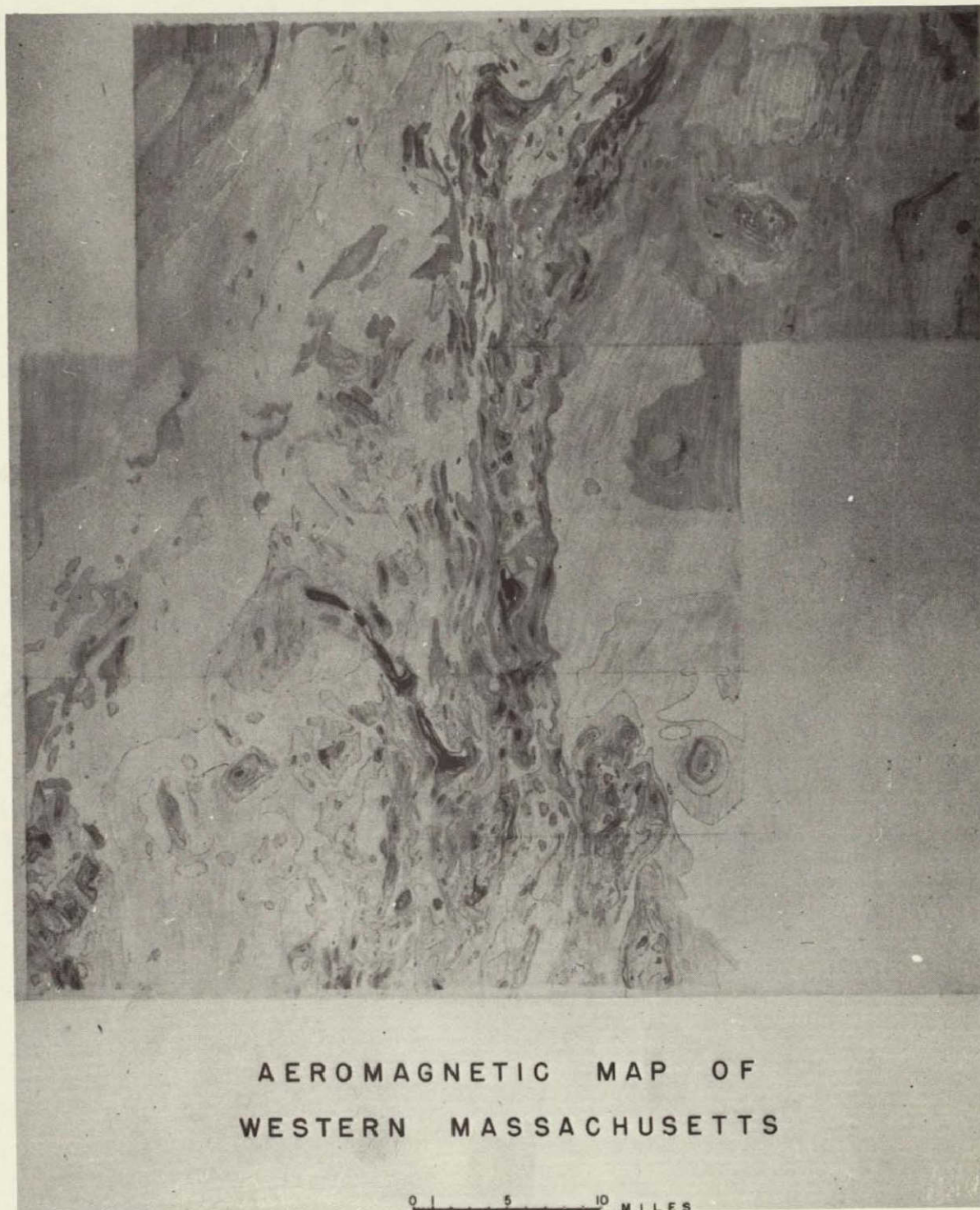


Figure 4-11.- Aeromagnetic map of western Massachusetts.

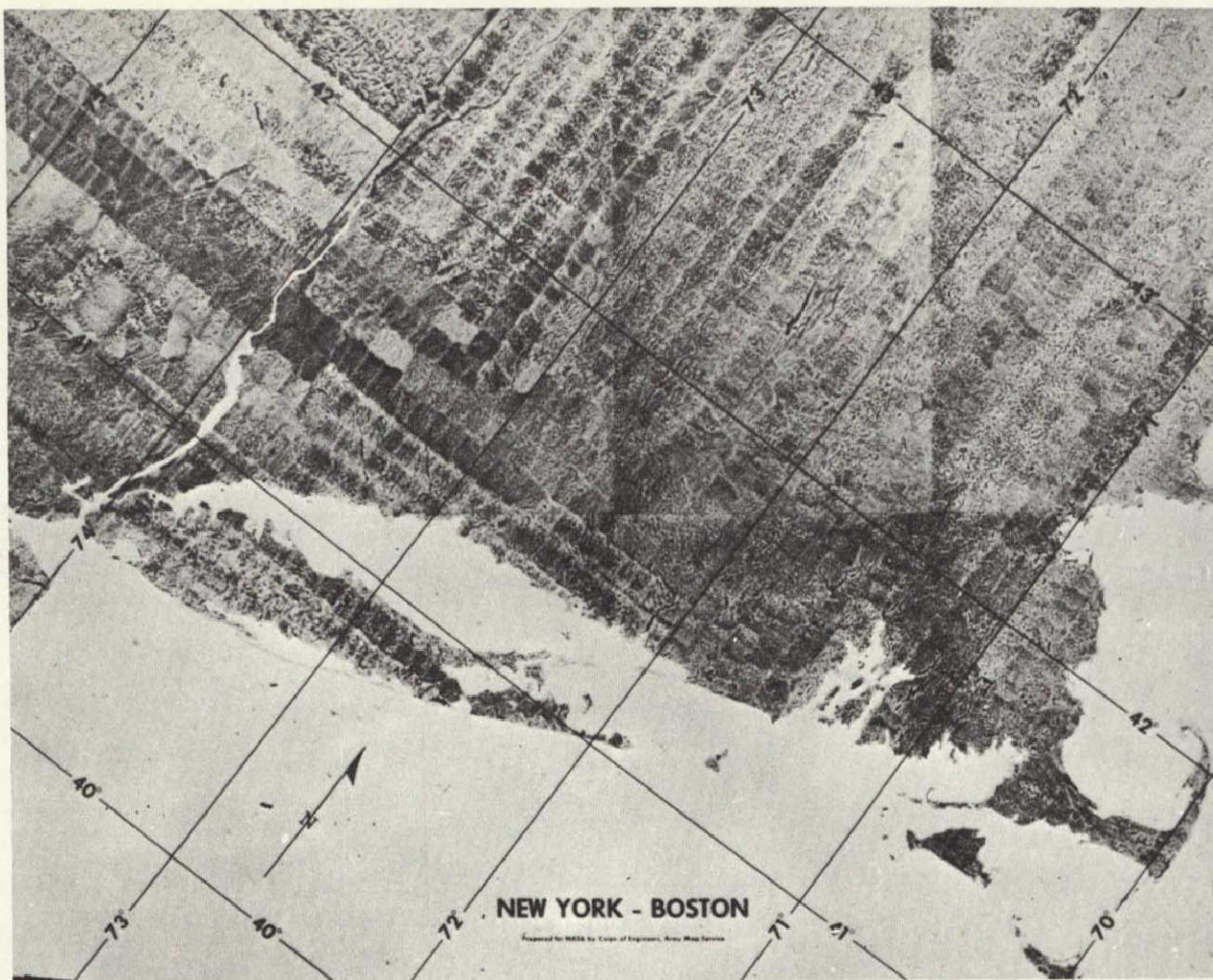


Figure 4-12.- Aerial photomosaic of south-eastern New England.

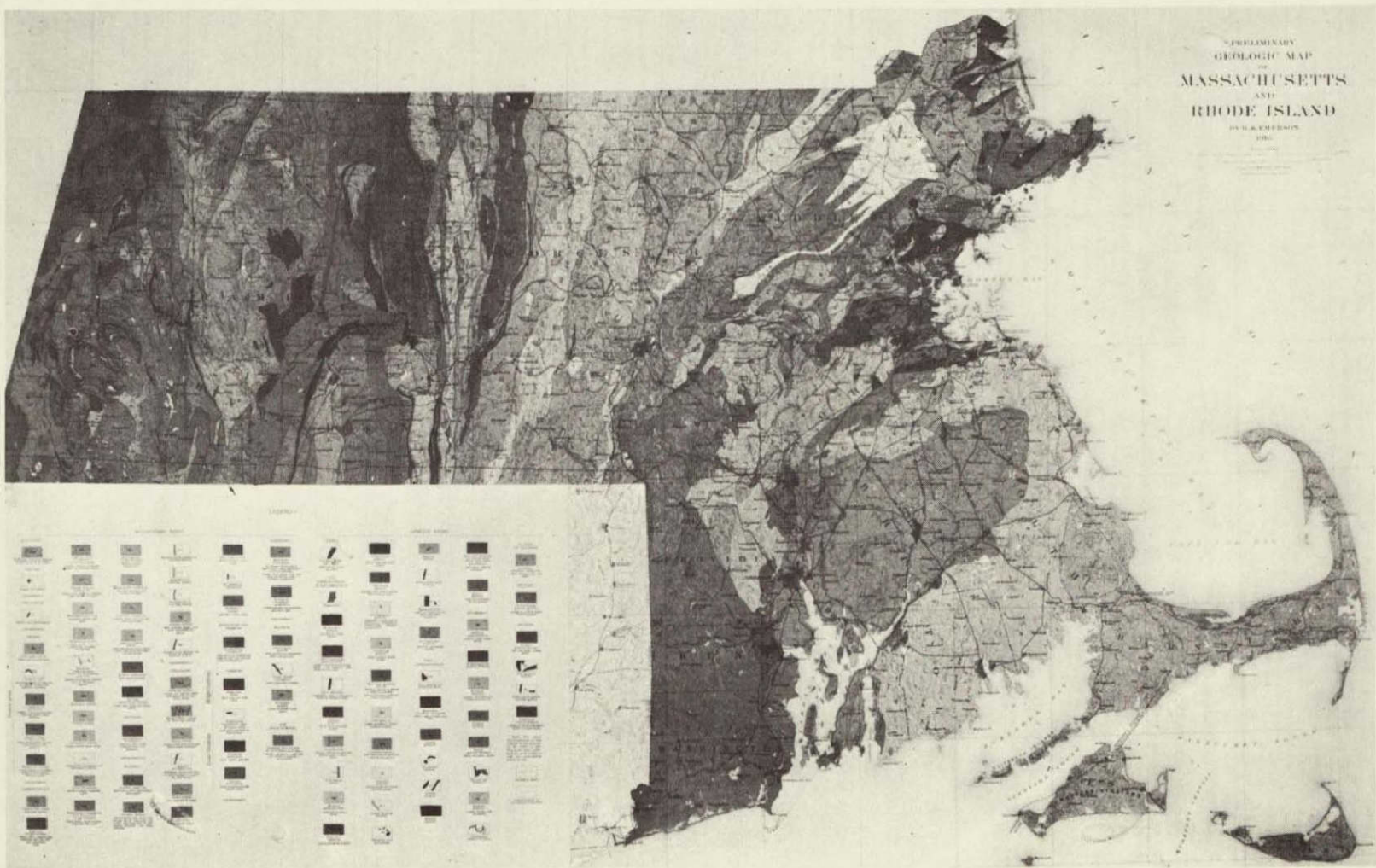


Figure 4-13.- Geologic map of Massachusetts and Rhode Island.

SECTION 5

THERMAL INFRARED INVESTIGATIONS,

MILL CREEK AREA, OKLAHOMA

By L C Rowan, T W Offield, Kenneth Watson, R D Watson
U S Geological Survey, Denver, Colorado

and

P J Cannon
U S Geological Survey, Flagstaff, Arizona

N71-19256

ABSTRACT

Thermal-infrared images obtained on flights over the Tishomingo anticline and South Flank near Mill Creek in the Arbuckle Mountains, Oklahoma, were used to study the possibility of identifying some common rock types from their diagnostic reflection and emission characteristics, and to evaluate the usefulness of infrared images in structural geologic investigations. The areas flown are underlain by folded and faulted Paleozoic dolomite, limestone, sandstone, shale, and Precambrian granite.

Images were obtained at 6 00 a m , 11 00 a m , and 2 00 p m . The predawn (6 00 a m) image is the most useful in distinguishing rock types. Of particular interest is a thermal contrast of dolomite (warm) and limestone (cool), sufficient to distinguish those rock types and to reveal facies changes between them. Theoretical considerations indicate that this thermal contrast arises from a combination of albedo and thermal-inertia characteristics distinctive of dolomites and limestones in many areas.

The daytime images display much stratigraphic and structural detail. Small-scale bedding detail is enhanced in the morning images of low-relief areas, and contrasts of alternating formations that form hogbacks and valleys are enhanced in the afternoon images of higher relief areas. The difference in features displayed in morning and afternoon images appears to be a function of the insolation on sunward and shadowed slopes of differing scale. Fault or fracture zones are best displayed in the predawn image, they appear cooler than surrounding ground, because of greater water content and concomitant evaporation. The abundance and throughgoing nature of lineaments (which coincide for the most part with joint systems) are more obvious in the infrared images than in aerial photographs. Lineaments striking northwest are preferentially enhanced in the morning images and lineaments striking northeast are preferentially shown in the after-

noon images This enhancement cannot be ascribed to the effects of topography, insolation, or wind, it may relate to a combination of ground-water and vegetation effects

INTRODUCTION

As part of the U S Geological Survey's Remote Sensor Application Studies program, infrared images (8-14 μ) were obtained on reconnaissance flights over two areas in the Arbuckle Mountains near Mill Creek, Oklahoma (Fig 1a) These data were used in a preliminary investigation (1) to determine the diagnostic reflection and emission characteristics of various rock types, and (2) to evaluate the usefulness of infrared images in structural geologic investigations In the evaluation of image character and quality, the effects of such features as rock texture, surface reflectivity, topography, and atmospheric conditions were examined These test areas provide good exposures of several mineralogically simple rock types in different structural and topographic settings Preliminary analysis of the reconnaissance data has yielded considerable insight into the numerous factors affecting the reflection and emission characteristics of rocks

The data were acquired on December 19-20, 1968, by instruments aboard the NASA Earth Resources Program Convair 240A aircraft The flights were part of NASA Mission 84, under NASA contract 160-75-01-43-10

GEOLOGY

The areas studied are located on the south flank of the Arbuckle Mountains uplift in south-central Oklahoma Rocks of interest in these areas range in age from Precambrian to Pennsylvanian, they were folded and faulted when the uplift formed in Pennsylvanian time The generalized geology of the areas is shown in figures 1b and c

The two areas are in different physiographic and structural provinces separated by the Washita River The Tishomingo anticline area, east of the river, consists of gently rolling hills where the relative relief is approximately 100 feet and is underlain by gently dipping beds It was selected for study because differences in rock type dominate the infrared images, and the effects of topography and structure are subordinate The South Flank area, west of the river, is underlain partly by the same rock units as well as formations higher in the geologic column which are distinguished by their greater topographic relief of approximately 200 feet Topographic effects in much of the South Flank area dominate the images, differences in rock type are not conspicuous

Rock units of principal interest are the abundant, relatively pure dolomites, limestones, and sandstones in the Cambrian and Ordovician section, and Precambrian biotite granite exposed in the core of the

Tishomingo anticline Other rock types in the areas, but not considered in the present study, include shale, chert, arkose, granitic gneiss and quartz conglomerates, and transitional types such as dolomitic limestone, argillaceous limestone, and sandy dolomite In the South Flank area, the topographic effects of interest reflect differences in strata ranging in age from Cambrian to Pennsylvanian

Cambrian and Ordovician stratigraphic relations in the southern Arbuckle Mountains are complex (Ham, 1950), and only those relations pertinent to the analysis of the remote sensing data will be mentioned here Figure 2 shows the Precambrian, Cambrian, and Ordovician geologic section of the Tishomingo anticline area Some of the stratigraphic units are difficult to recognize not only on photographs and images but in the field as well, because the boundaries were defined mainly on faunal data It is possible, however, to distinguish certain rock types in the photographs and images, and where these rock types characterize geologic map units, stratigraphic determinations can be made through remote sensing techniques

Cambrian dolomites comprise a thick sequence in the Tishomingo anticline area (Fig 2) The Royer Dolomite, which forms the largest part of this sequence, shows only minor variations in its outcrop characteristics, it is dark to very dark gray and has highly pitted ledges or castellated pedestals The Honey Creek Formation is composed of sandy dolomite which commonly forms boulders or rounded pedestals, the Butterfly is composed of dolomitic limestone and is somewhat more thinly bedded and lighter in color than the purer dolomites The dolomite of the Fort Sill Formation is similar in color and texture to the Royer, but show a facies change to limestone

Limestone exposures are abundant in the Middle and Upper Ordovician units of the South Flank area, but are sparse in the Tishomingo anticline area except in the Upper Cambrian and Lower Ordovician units (Fig 2) The limestone of the Tishomingo anticline area is commonly relatively impure, with argillaceous material, chert, and dolomite comprising the main impurities, in places, thin sandstone beds occur In both areas most of the limestone is light gray to light bluish gray and forms rubbly, platy outcrops, however, a massive, moderately dark gray limestone marks the top of the Bromide Formation, and some dark gray limestone is present in the McKenzie Hill Formation

In the Tishomingo anticline area both dolomite and limestone form flat to gently rolling prairies bearing a sparse growth of grass, but in the South Flank area the steeply dipping beds of limestone form hogbacks between valleys underlain by shale

In contrast to the limestone and dolomite of the Tishomingo anticline area, the sandstones of the Reagan Sandstone and of the Simpson Group and the Tishomingo Granite are tree covered, and 50 to 75 percent of their outcrop surfaces are coated by lichen and moss. Prominent lineaments and somewhat greater topographic expression distinguish granite outcrops from sandstone outcrops.

The two areas cover parts of major anticlines which trend west-northwest and dominate the structural pattern of the region. In the Tishomingo anticline area, poorly developed fracture systems which show well only on infrared images are parallel to the major anticline axis and to cross faults noted on the geologic map (Fig 1b). In the South Flank area, fracture systems are well developed parallel and perpendicular to the axis of the Arbuckle anticline and are associated with cross folds and cross faults which distort the south flank of the anticline.

ANALYSIS OF INFRARED IMAGES

Infrared (8-14 microns) images were obtained at 11 00 a m , 2 00 p m , and 6 00 a m in the Tishomingo anticline and South Flank areas in order to relate surface temperatures to the diurnal heating cycle.

The imaging system used, Reconofax IV (HRB Singer RX-IV), has an instantaneous field of view of 3 milliradians and an angular scanning width of 120° perpendicular to the flight path. The flight altitude was 5,000 feet above mean ground surface, identification resolution is estimated to be 30 feet near the nadir. The thermal resolution of the Reconofax IV system is 0.25°C.

The principal difficulties in analyzing the images arise from calibration problems and image geometry distortions. External calibration of the images is complicated both by an apparent limited dynamic range in the film-recorded images and by lack of internal drift correction. For example, the temperatures of the north and south lakes at the Mill Creek sand quarry as obtained with a Barnes radiometer show differences of 4° to 5° at the time of the 11 00 a m overflight on December 19 and the 6 00 a m overflight on December 20. Yet no apparent difference in the radiative flux from the two lakes is detectable on the images. This lack of sensitivity due to limited dynamic range can be rectified by recording future data on magnetic tape and at a variety of gain settings to take advantage of the full range of small variations in infrared intensity. The geometric distortions on the edges of the images reduce the useful width of the image which can be analyzed, this problem can be alleviated by obtaining flights with large side lap.

Tishomingo Anticline Area

The part of the Tishomingo anticline area that was selected for detailed analysis lies south and southwest of the town of Mill Creek.

(Figs 1b and 3) Although the stratigraphic sequence detailed in Figure 1 can be fully recognized in the field, some of the formations are, as previously mentioned, difficult to delineate on photographs and images. In particular, the Honey Creek Formation is difficult to distinguish from the overlying Fort Sill Limestone, and the Butterly Dolomite is in transitional contact with limestones of the McKenzie Hill Formation above and the Royer Dolomite below.

Shown in Figure 3 are the major rock-type variations in part of the Tishomingo anticline area, from east to west the sequence is from oldest to youngest rocks as shown in Figure 2. Formations in the area of the black-and-white photomosaic (Fig 3) are the Tishomingo, the Reagan, the alternating dolomites and limestones of the Honey Creek and Fort Sill, the Royer and Butterly, and limestones of the Butterly and the McKenzie Hill. Also in the area shown on the photomosaic are limestones of the upper formations of the Arbuckle Group, but these rocks were not imaged by the Reconofax IV system, equivalent rocks are covered by infrared data of the South Flank area but have not yet been examined in the field for comparative purpose. It must be emphasized that although identification of the granite is not difficult on the photomosaic, differentiation of the limestone and dolomite is either very difficult or impossible even after considerable familiarity with the area has been attained.

Of the three times during which the infrared images were obtained, the predawn (6 00 a m) images appear to be most useful in distinguishing rock types, particularly limestone and dolomite. Shown in Figure 4 are the predawn and the two daytime infrared images of the south-southwestern part of the Tishomingo area. Most striking is the predawn image (Fig 4a) which shows an anomalously bright (warm) area near the center of the image. The rocks of this area are mainly dolomite and biotite granite, whereas the adjacent, relatively dark area (cool) is underlain chiefly by limestone in the Fort Sill and McKenzie Hill Formations. Considerable detail can be discerned in these areas. For example, sedimentary layering in the limestone is conspicuous as alternating light and dark tones, it is less obvious in the dolomite except where dolomite and limestone alternate in the Fort Sill Limestone. At point A in Figure 4a, dolomite changes to limestone through a facies transition or a fault as shown by Ham (1950, p1 2) in the Fort Sill, an observation of considerable geologic significance. This transition is clearly defined on the image by the thermal contrast of the dolomite and the limestone along strike. This type of warm-cool contrast should not be confused with other prominent dark areas which are stream channels, particularly in the dolomites, and in areas of dense foliage, such as the areas underlain by the Reagan Sandstone and the Tishomingo Granite. The distinction between limestone and dolomite by radiometric character is similar to the distinction between sandstone and siltstone noted by Sabins (1967) and between various other rock types by Friedman (1968). Stratigraphic units have been distinguished elsewhere by radiometric

differences, but these differences are generally ascribed to vegetative cover on different rock types rather than to inherent rock properties (e g , Lattman, 1963)

In order to evaluate the radiometric differences between the limestone and dolomite, film-density measurements of the nighttime image were made using a Joyce-Loebl recording microdensitometer. Figure 5 shows one of the density profiles prepared (line F-F', Fig 4a). Although there is considerable variation in film density within the limestone and the dolomite areas, it is clear that the dolomite has characteristically (up to 15 percent) lower film density and therefore higher total emission. Notable features on the profile are a small pond and the high frequency and large amplitude of film-density variations in areas of relatively dense foliage and small, cool stream channels. Although the granite is not included in this particular density profile, it also shows a film density approximately equivalent to the dolomites but with higher amplitude film-density variations indicating larger total emission contrast.

Within the limestone and the dolomite sequences are relatively dark (cool) areas on the predawn image (Fig 4a). Most of these correspond to drainage channels in a dendritic pattern or to areas of dense foliage (point B, Fig 4a). In the south-central part of this image, however, are several prominent intersecting dark bands. Three of these indicated by C, D, and E on Figure 4a, are strikingly linear and were examined in the field, on the topographic map (Fig 6), and on all available photographs. These are saturated with ground water and are fracture or fault zones; significantly, they are not everywhere topographically lower than the surrounding terrain, and are not readily detectable on conventional photographs. For example, in Figure 6 the northwest-trending feature is a topographic depression northwest of point C, but transects topographic highs southeast of point C. Of the two north-trending fracture zones (points D and E, Fig 4a), only the one with the two ponds (E) occupies a topographic low for a significant distance along its trend, the other band transects the east side of a rounded hill (Fig 6) for most of its extent.

Because water saturates these fracture zones, the most adequate explanation for the relatively low emission appears to be that these areas have cooled by evaporation. This explanation may also be sufficient to explain the low emission in the drainage channels. Settling of cold air in the topographic lows also contributes to heat loss in these areas.

The daytime infrared images of the Tishomingo anticline area show, in some places, excellent definition of sedimentary layering and fracture zones (Fig 4b and 4c). On the 11 00 a m image (Fig 4b), sedimentary layering, which generally trends north to northwest, is conspicuous on sunward (southeast) slopes. Although fracture and joint traces are not well displayed on the 11 00 a m image, traces trending west-northwest extend from the granite near the southeast

border of the image into the Cambrian sandstone and carbonate rocks and into the northern part of the area. Northeast-trending joint and fracture traces are detectable in a few areas near the center of the image. Unlike the areas of prominent bedding, these features appear to be virtually independent of local topography.

The infrared image of the Tishomingo anticline area obtained at approximately 2 00 p m (Fig 4c) shows only a few areas of bedding (in which the thermal contrast probably reflects the total integrated effect of insolation as the sun azimuth changed through the morning). Structural information shown is mainly restricted to fracture traces, trending east-northeast, which are prominent in the southern part of the area shown in Figure 4c. The occurrence of these traces does not appear to be significantly affected by the topography inasmuch as topographic highs and lows with variable orientations to the sun are transected. These fractures are not as apparent on any of the available photographs as they are in the infrared image.

South Flank Area

Stratigraphic information displayed in the infrared images of the South Flank area stems mainly from the excellent definition of bedding in the daytime images. The 11 00 a m image (Fig 7a) shows a remarkable bedding "grain" representing fine-scale bright-dark (warm-cold) contrasts. Presumably the bright stripes are groups of beds, as single beds generally are smaller than the ground resolution limit. Formation contacts, however, are poorly defined. In the 2 00 p m image (Fig 7b), the "grain" of bedding is not so conspicuous, and small-scale bright-dark contrast is less than at 11 00 a m. However, several formations are readily distinguishable and their contacts fairly sharply defined. The 6 00 a m image (Fig 7c) does not show most formation contacts well, but shows many conspicuous groups of beds as brighter (warmer) than their surroundings. Included in the brighter areas are such diverse lithologies as white-weathering, fine-grained, impure dolomite and dark-gray, coarse-grained, crystalline limestone, as well as the dark dolomite of the Royer and Butterly Formations (Fig 7c, near "fault") noted as bright in the predawn image of the Tishomingo anticline area. The area marked "A" on Figures 7a, b, and c provides a comparison of stratigraphic formation obtained at the different flight times.

Structural information in the infrared images is derived from the excellent display of bedding so that faults and folds are clearly evident (see Sabins, 1969, for a comparable example), and from the display of lineaments. Many of the lineaments cannot be seen in color or black-and-white photographs. The lineaments (areas of prominent lineaments are indicated by arrows on the three images) are of particular interest because some of them are uniquely visible on infrared images, and because they are important to interpretation of the overall structure of the area. Only northwest-trending lineaments are visible in the 11 00 a m images, only those trending northeast are seen at 2 00 p m, and only

sparse rare east-northeast-trending lineaments show at 6 00 a m. The lineaments appear warmer than adjacent ground. Some can be seen on photographs as grassy low zones along fractures, but most can not be recognized. Field observation shows the three major directions of lineaments to coincide with joint sets, but the extent of single lineaments and their overall abundance are nearly impossible to determine except in infrared images.

Another interesting structure best defined in the infrared images is a fault zone indicated on the 2 00 p m and 6 00 a m images. It is obscured by minor topographic and thermal effects at 11 00 a m. Part of the zone can be traced on photographs, because it shows as a grassy zone between outcrop ridges. On the infrared images, however, and particularly on the predawn image, the exact width of the broken zone along the fault is clear. The width varies considerably in short distances, and is defined by a strip cooler than adjacent ground. Field examination shows that this strip is not consistently a topographic low, and we conclude that the coolness is related to ground water concentrated in the zone of broken rock. This has interesting implications with respect to locating and defining such zones elsewhere for engineering, ground water, and mining purposes.

THEORETICAL CONSIDERATIONS AND INTERPRETATION

Parameters Affecting Infrared Images

The emitted thermal flux which is sensed by the infrared detector of the imaging system is a function of two major classes of parameters: 1) rock or soil parameters (albedo, thermal inertia, emissivity), and 2) insolation parameters (sun's declination, latitude of site, local time, and local topography). Other parameters including transmission, nighttime sky radiation, and evaporative cooling.

Because insolation provides the driving function to heat both ground and atmosphere, the ground surface temperature during the daytime is dominated by the insolation parameters and by the surface albedo. (The absorbed flux is the product of the local insolation, the cosine of the local zenith angle, and the co-albedo.) During the nighttime, the effects of the atmospheric parameters and the rock thermal inertia have a significant effect on the surface temperature, and in general their roles are more pronounced just before sunrise when insolation effects are least important. In general, then, it is expected that daytime infrared images should be most responsive to variations in local topography and co-albedo, and that nighttime infrared images should be most responsive to variations in atmospheric effects and thermal inertia. Variations solely in emissivity of natural surfaces produce a proportionate change in the emitted flux. Exposed rocks are less efficient radiators than soils because, within the precision of imaging systems, all soils behave approximately as

black bodies, independent of their composition

Daytime Infrared Images

The daytime images of the Tishomingo anticline area show that bedding detail is enhanced on sunward topographic slopes, and that lineament sets are preferentially displayed in either the morning or afternoon, depending on the direction in which they trend. In the South Flank area, where hogbacks that formed by dipping formations are numerous, the marked contrast between conspicuous formation delineation in the afternoon image and pronounced "grain" of smaller scale bedding in the morning image is clearly a topographic effect related to time of day. Preferential display of lineaments at the two times is similar to that in the Tishomingo anticline area.

In order to analyze the directional character of insolation parameters that contribute to the observed effects, a mathematical model of the diurnal temperature variation of an inclined planar element was constructed to determine the strike at which the computed temperature changes most rapidly with slope angle (Watson and Pohn, written communication, 1970). This direction (thermal strike) should provide an indicator (1) of optimum daily and seasonal times to enhance (or suppress) topographic lineaments and (2) of the insolation contribution to linear trends observed on daytime infrared images. In addition, the direction for most rapid change in insolation with slope angle (insolation strike) was also computed.

For the Mill Creek areas (lat $34^{\circ} 5'$, sun declination $-23^{\circ} 3'$) thermal and insolation strikes versus times at which the images were obtained are presented in Figure 8. The model predicts thermally enhanced strike direction of $N 25^{\circ} E$ for the morning flight and $N 80^{\circ} E$ for the afternoon flight. The calculations also predict that the insolation strike (best observed in visible and near infrared photographs) should enhance a morning direction of $N 70^{\circ} E$ and an afternoon direction of $N 70^{\circ} W$. Presumably both sets of directions should be present to some degree on the infrared imagery inasmuch as thermal strike should reflect moderate slopes and the insolation strike should reflect steeper slopes which cast shadows. Lineaments are not primarily topographic features and apparently do not owe their prominence on the images to these factors, but the "grain" of bedding and formations is a topographic expression and is enhanced as the model predicts in many places. Images of the Tishomingo anticline area (southern edge, Fig. 4) show the afternoon enhancement of topographically conspicuous formations parallel to the maximum insolation strike. The infrared images of the South Flank area (Fig. 7) illustrate the prominence of features parallel to the afternoon thermal strike and, possibly to a lesser degree, parallel to the morning insolation strike.

The difference in stratigraphic information contained in the two daytime images of the South Flank area appears to result from topo-

graphic scale effects. The morning image shows bedding emphasized by small-scale, but conspicuous bright-dark (warm-cool) contrast due to the preferential heating of the sunward sides of small ridges formed by outcropping bedding edges. The afternoon image shows a significant reduction in this thermal contrast inasmuch as both sides of the bedding ridges have received illumination from the sun which tends to equalize their temperatures. But the opposite faces of hogbacks, which are larger scale features with steeper slopes, retain the thermal contrast because shadowing and hence insolation differences are still present. In summary then, average slope differences at the two topographic scales result in an enhancement of bedding detail in the morning image and of whole formations that form the hogback-valley system in the afternoon image.

Nighttime Infrared Images

Because the nighttime images showed strong thermal contrast between limestone (cool) and dolomite (warm), an attempt was made to interpret the observations in terms of a model that seemed consistent with the field observations and could be tested by later flight measurements. A simplified model of the rock parameters for the limestone and dolomite was used to compute theoretical cooling curves (Watson and Pohn, written communication, 1970). The results (Fig 9) illustrate the mutual enhancement from the lower albedo (due to weathering) and higher thermal inertia of dolomite (a compositional property) in raising its nighttime temperature with respect to that of limestone. During the daytime the two parameters work against each other, the higher thermal inertia tends to reduce the dolomite temperature and the lower albedo tends to increase it. Hence, the daytime temperature differences between limestone and dolomite are less useful as a diagnostic tool. But at nighttime, maximum contrast should be expected between rock types that combine maximum differences in albedo and thermal inertia, provided that a lower albedo is paired with a higher thermal inertia. The converse -- that is, that high (low) albedo paired with high (low) thermal inertia would provide maximum daytime contrast -- should also prove to be true, provided that the effects of the topography do not overwhelm the observed thermal distribution. A more rigorous test, now being planned, will be made by repeatedly taking calibrated images to examine in greater detail the diurnal cooling cycles of the rock types exposed in the Mill Creek site, especially for an intercomparison among the dolomites (low albedo, high thermal inertia), the limestones (high albedo, low thermal inertia), and the impure dolomites (high albedo, high thermal inertia).

Atmospheric Parameters

The preceding discussion has omitted an evaluation of the influence of the atmospheric parameters in order to emphasize the types of geologic information that can be extracted from infrared images. It is clear that at nighttime the dominant features of the images are the thermal cold anomalies in topographic lows or water-saturated fracture zones. The most reasonable explanation is heat loss from the ground

due to evaporation and the conduction of ground heat into cold, water-saturated mists which, being denser, collect in the topographic lows or do not disperse readily from above their water sources. Atmospheric effects (e.g., cloud cover) are also important in modulating the daytime insolation and, especially in wintertime when the insolation is minimal, in introducing various periodicities in the thermal cycle due to the passage of weather fronts. Thus as a more quantitative analysis of infrared data is undertaken, a more careful treatment of atmospheric effects, including ground and air measurements, will be required.

CONCLUSIONS

The infrared data obtained for this reconnaissance study contain significant stratigraphic and structural information. Perhaps the most important conclusion is that relatively pure limestones and dolomites of the test area can be differentiated in nighttime infrared images, and that facies changes between them can be detected along and across strike. Such discrimination of rock type is possible because of a combination of the inherently different albedo and thermal inertia properties of the limestones and dolomites, and doubtless the same distinction can be made in other areas with only a minimal amount of field observation as control.

Topography strongly influences the distribution and scale of stratigraphic information displayed in the infrared images. Sunward slopes display maximum bedding detail, and in some areas show very subtle lineaments preferentially in either morning or afternoon images, depending on the lineament trends. Bedding detail is enhanced in morning images of low-relief areas. Such detail is not prominent in afternoon images, which instead show contrasts at the scale of geologic formations wherever moderate-relief topography is controlled by the bedrock. This effect appears to be a direct function of the amount of sunlight received by sunward and shadowed slopes of differing scale.

Fault or fracture zones are delineated on infrared images as thermal lows, apparently because of water saturation and concomitant evaporation. The images contain information on width and continuity of such zones that cannot be observed by reflected energy recorded in conventional photographs. Lineaments are well displayed on the infrared images, even in areas where no lineaments can be detected on ordinary photographs, but where their presence has been confirmed by field examination. The prominence of lineaments without noticeable topographic expression cannot be ascribed to insolation or wind effects and does not appear to be simply related to ground water or vegetation concentration, this enhancement of linear features is not yet understood, but illustrates the use of the infrared images for structural geologic investigations.

Our study indicates that several flights during a diurnal cycle are needed to maximize the stratigraphic and structural information.

obtained Data on rock surface characteristics and thermal properties, and on topographic and insolation effects are necessary for detailed analysis of rock responses in the thermal infrared part of the spectrum

REFERENCES CITED

- Clark, S P , Jr , ed , 1966, Handbook of physical constants Geol Soc America Mem 97, 587 p
- Friedman, J D , 1968, Thermal anomalies and geologic features of the Mono Lake Area, California, as revealed by infrared imagery U S Geol Survey Open-File Rept
- Ham, W E , 1950, Geology and petrology of the Arbuckle Limestone Yale Univ , Ph D dissert , 162 p
- Ham, W E , and McKinley, M E , and others, 1954, Geologic map and sections of the Arbuckle Mountains, Oklahoma Scale 1 72,000 (1 in to 6,000 ft), Okla Geol Survey
- Lattman, L H , 1963, Geologic interpretation of airborne infrared imagery Photogram Eng , v 29, no 1, p 83-87
- Sabins, F F , Jr , 1967, Infrared imagery and geologic aspects Photogram Eng , v 33, no 7, p 743-750
- Sabins, F F , Jr , 1969, Thermal infrared imagery and its application to structural mapping in southern California Geol Soc America Bull , v 80, no 3, p 397-404

		<u>EXPLANATION</u>	
		Qal Alluvium	Quaternary
	Lower Cretaceous	Kt Trinity Group	Cretaceous
	Upper Mississippian and Lower Pennsylvanian	Pv Vanoss Formation	Pennsylvanian
	Upper Mississippian	Pms Springer Formation	Mississippian
		Mc Caney Shale	Mississippian
		MDsw Sycamore and Welden Limestones, and Woodford Shale	Devonian and Mississippian
	Middle and Upper Ordovician	DSh Hunton Group	Silurian and Devonian
		Osv Sylvan Shale, Fernvale and Viola Limestones	Ordovician
	Middle Ordovician	Obm Bromide, Tulip Creek, and McLish Formations	Ordovician
		Ooj Oil Creek and Joins Formations	Ordovician
	Lower Ordovician	Owk West Spring Creek and Kindblade Formations	Ordovician
	Lower Ordovician	Ocm Cool Creek and McKenzie Hill Formations	Ordovician
	Upper Cambrian	Cbf Butterly Dolomite, Signal Mountain Formation, Royer Dolomite, and Fort Hill Limestone	Cambrian
		Chr Honey Creek Formation and Reagan Sandstone	Precambrian
		pCt Tishomingo Granite	Precambrian

Arbuckle Group

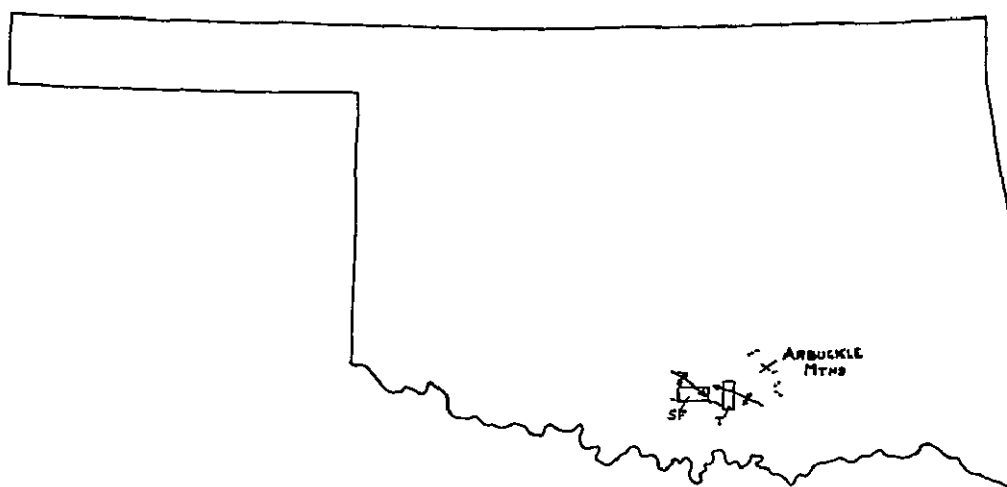


Figure 1a - Index map of Oklahoma showing Tishomingo anticline area (T) and South Flank area (SF) in the Arbuckle Mountains Trends of major anticlines are also shown

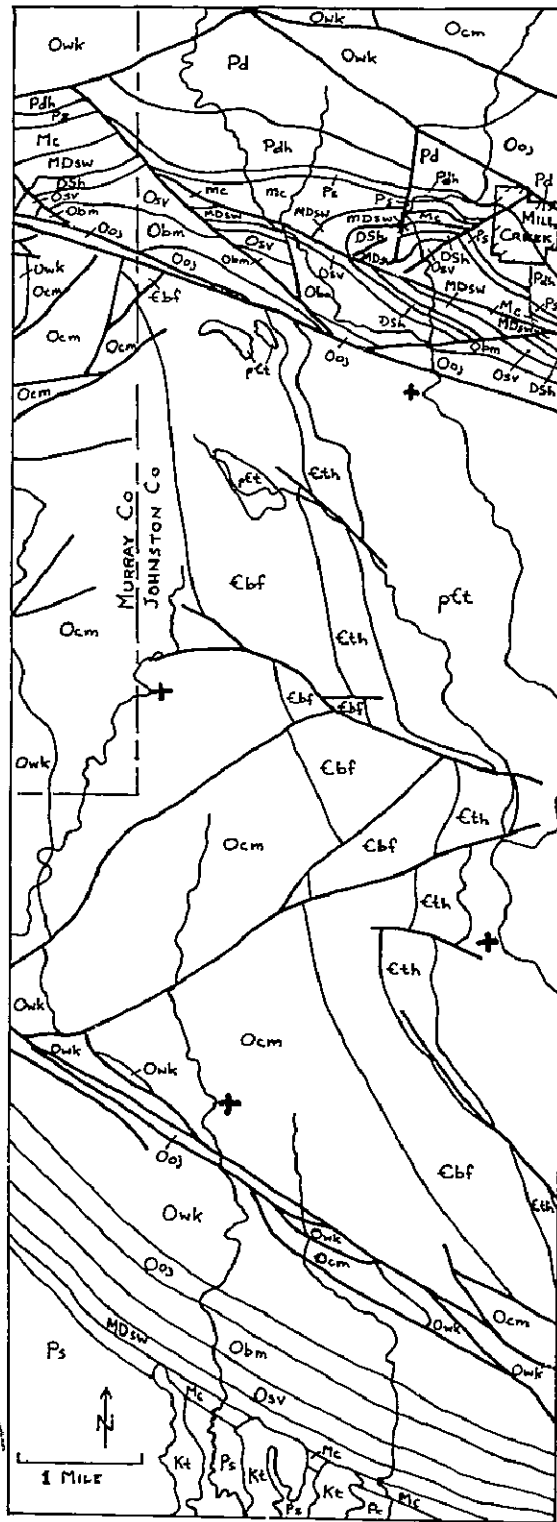


Figure 1b - Geologic map of Tishomingo anticline area (after Ham and McKinley, 1954) Reseau marks shown for matching with Figures 3 and 4

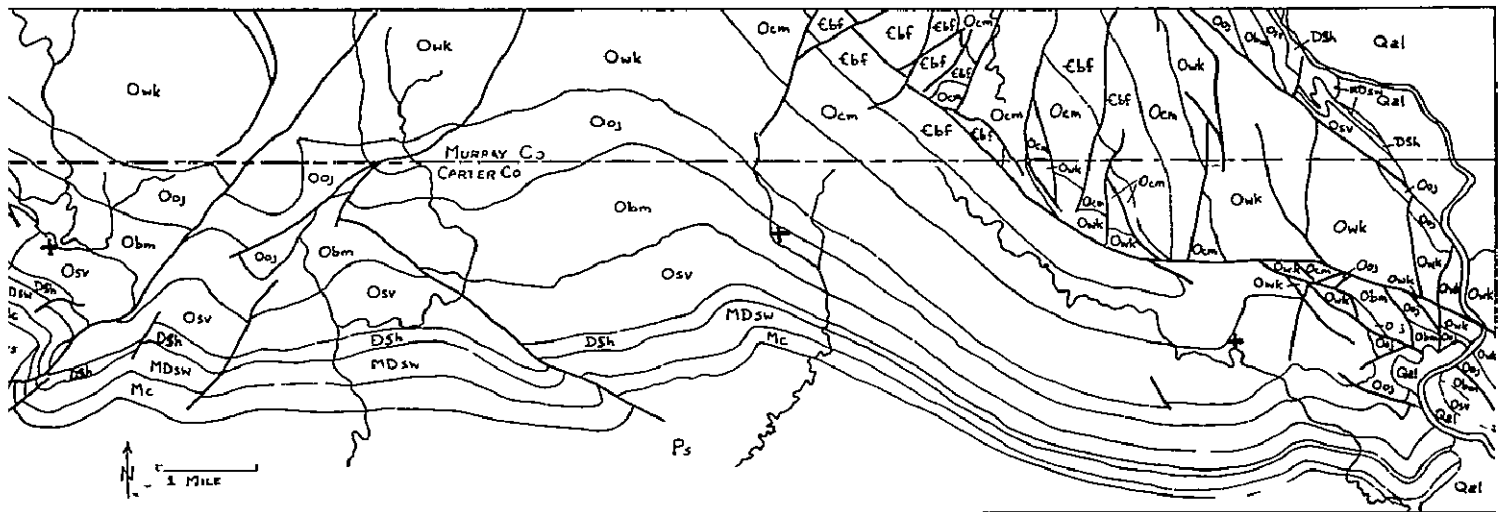


Figure 1c - Geologic map of South Flank area (after Ham and McKinley, 1954) Reseau marks shown for matching with Figure 7

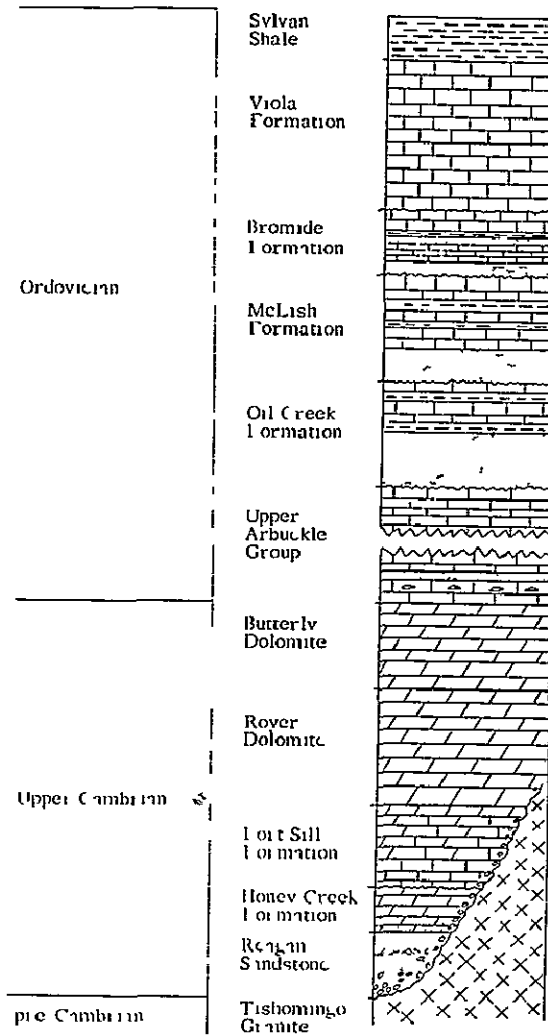


Figure 2 - Precambrian-Ordovician stratigraphic section, Tishomingo anticline area (modified from Ham, 1950)

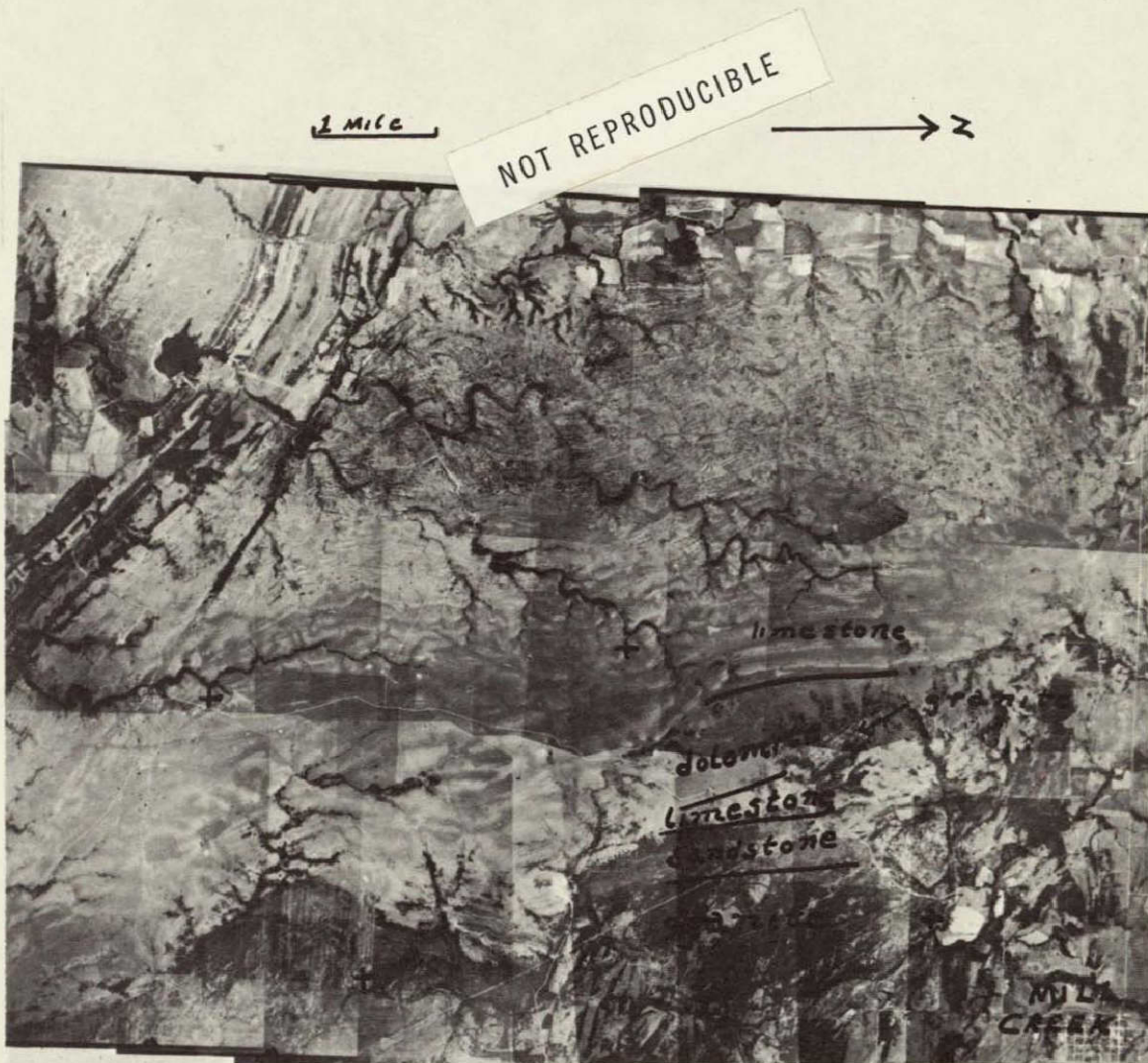
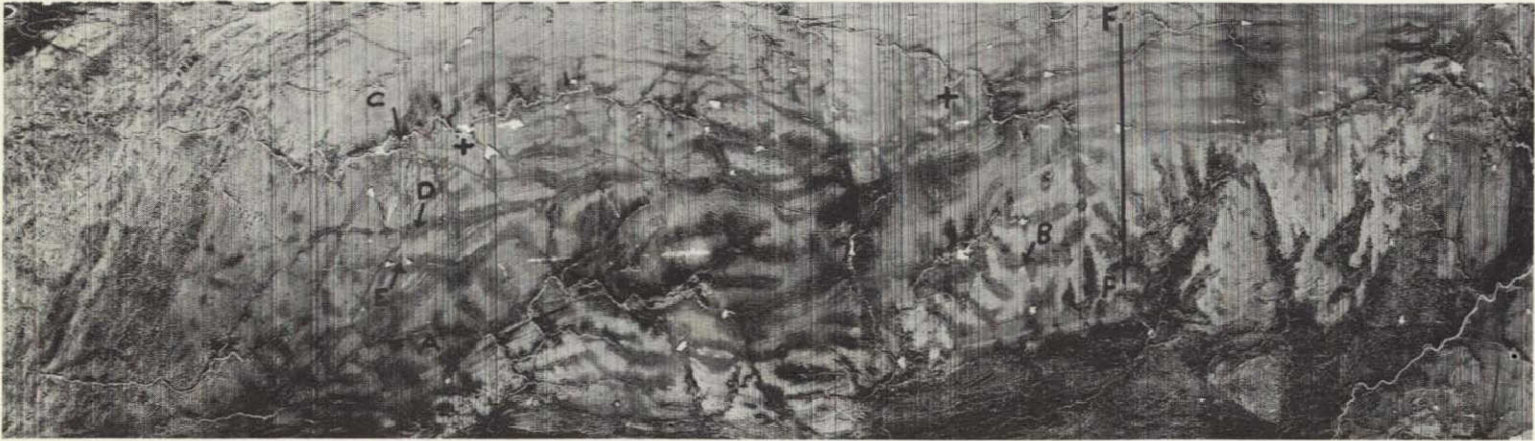
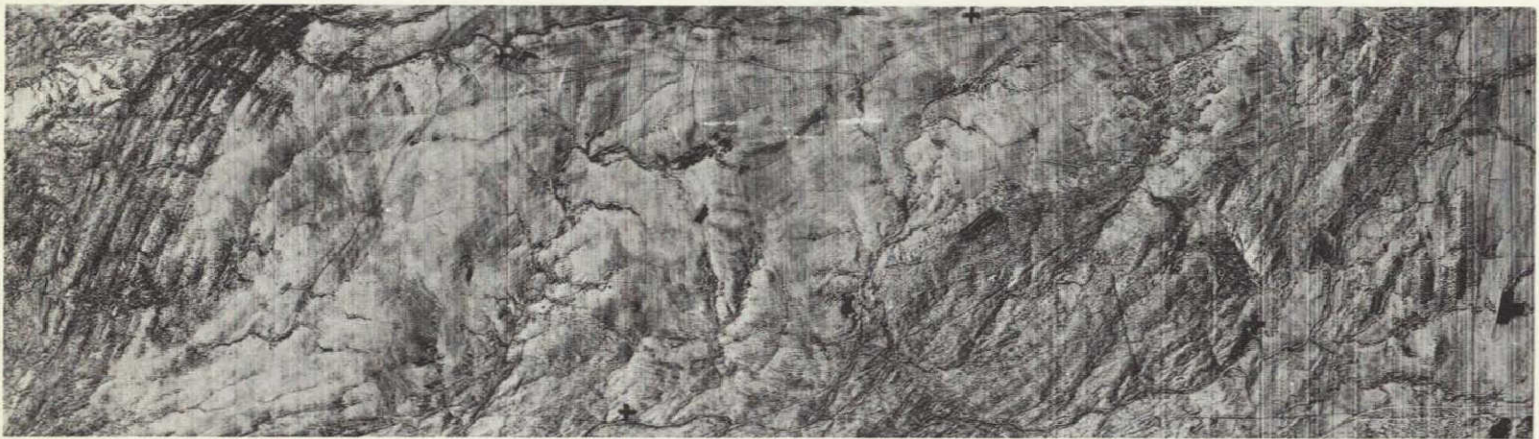


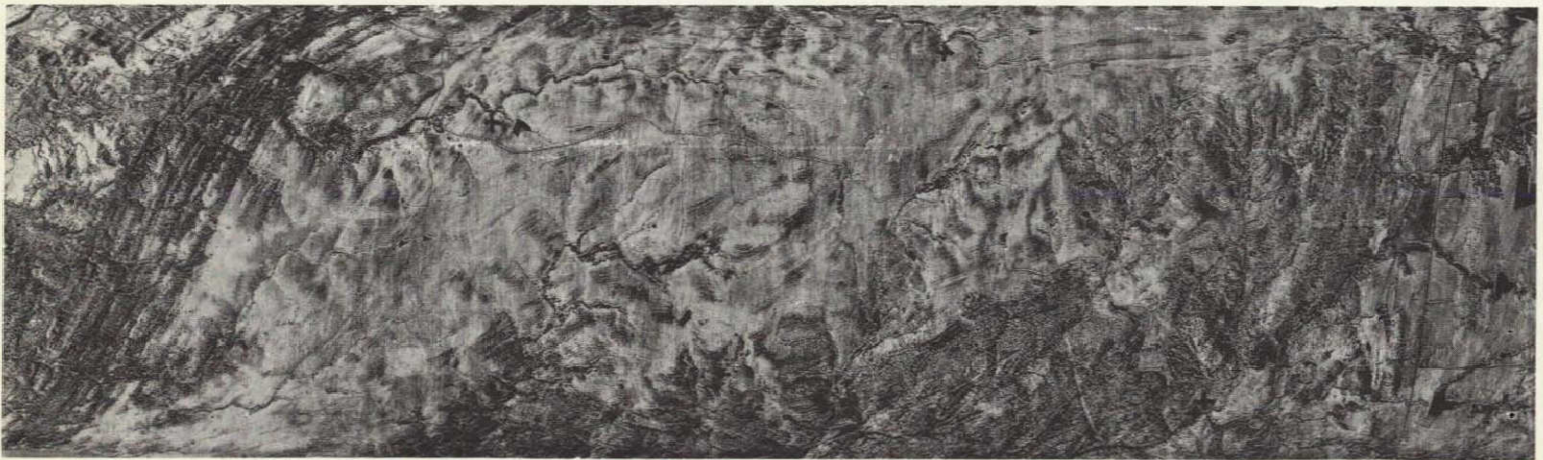
Figure 3. - Photomosaic showing rock-type occurrence, Tishomingo anticline area. Reseau marks shown for matching with Figures 1b and 4.



a.



b.



c.

Figure 4. - Infrared images of Tishomingo anticline area.
 a) 6:00 a.m. (CST) image; point A, facies change from limestone to dolomite; B drainage channel; C, D, and E, fracture on fault zones; F-F', line of isodensitracing profile shown in Figure 5.
 b) 11:00 a.m. (CST) image.
 c) 2:00 p.m. (CST) image.
 Reseau marks shown for matching with Figures 1b and 3.
 Scale approximately 1:90,000.

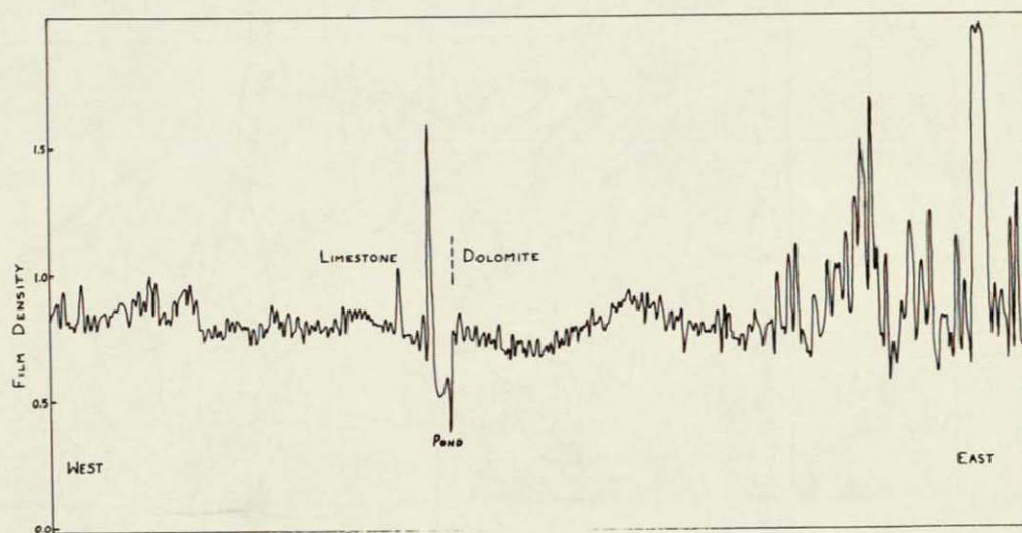


Figure 5. - Isodensitracing of limestone-dolomite area on nighttime infrared image, Tishomingo anticline area (line of profile shown on Figure 4a).

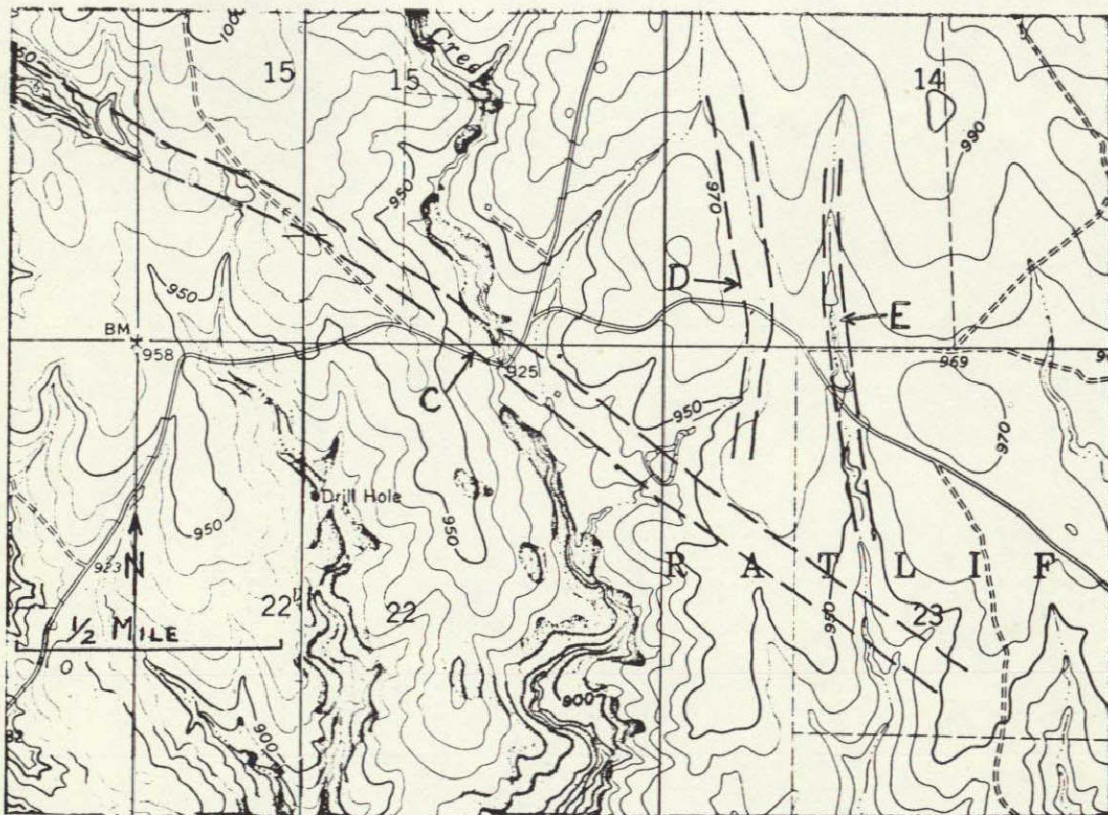


Figure 6. - Topographic map showing cool linear zones shown at C, D, and E on Figure 4a.

N
↑



a



b.



c.

Figure 7. - Infrared images of South Flank area., a) 11:00 a.m. (CST) image, b) 2:00 p.m. (CST) image, c) 6:00 a.m. (CST) image. Area A demonstrates comparison of stratigraphic and structural information displayed at different flight times; areas of prominent lineaments marked by arrows. Reseau marks shown for matching with Figure 1c. Scale approximately 1:120,000.

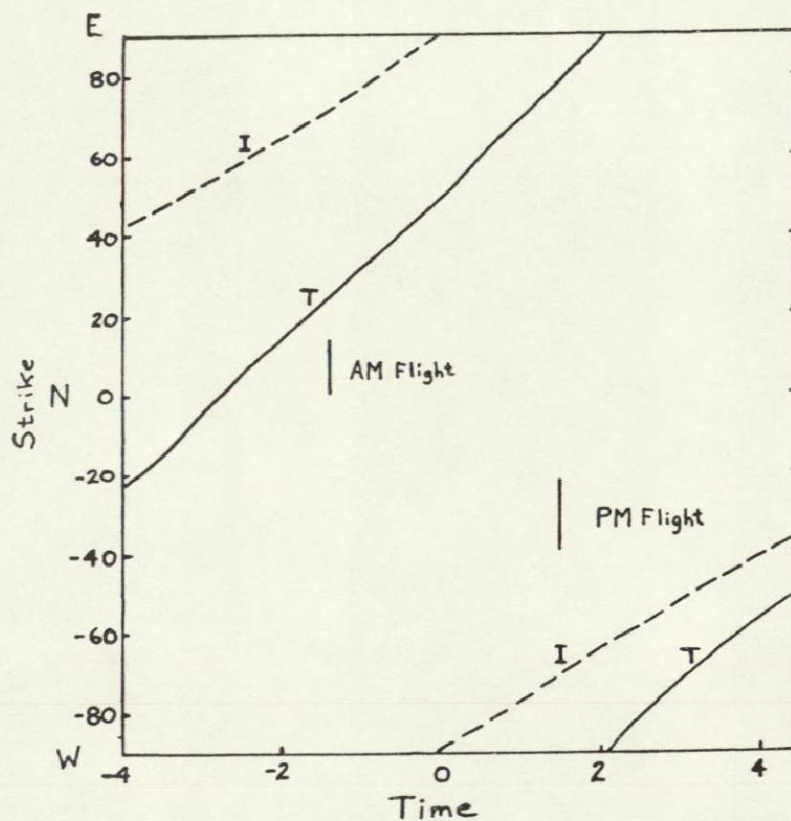


Figure 8. - Strike computed from theoretical models for enhanced thermal contrast (T) and enhanced insolation contrast (I). The times for the morning and afternoon aircraft overflights that provide the infrared images are indicated. Local time is measured in hours from the time of local noon (0hr local mean solar time = 12:30 p.m. CST).

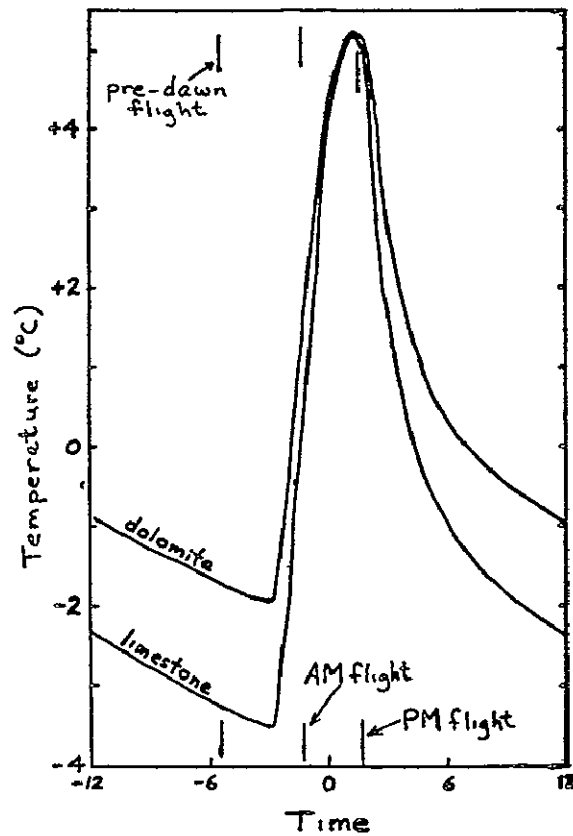


Figure 9 - Theoretical cooling curves constructed using thermal inertias constructed from representative thermal property values in Clark (1966) and albedo values consistent with the observations that (1) the dolomite appeared darker than the limestone and (2) daytime temperature differences are not noticeable on the infrared images (0hr local mean solar time = 12 30 p m CST)

SECTION 6¹
 REMOTE SENSING TECHNIQUES
 AS APPLIED TO COASTAL SEDIMENTATION, SOUTH TEXAS^{1/}

By

Henry L. Berryhill, Jr
 U S Geological Survey
 Corpus Christi, Texas

N 71 - 19257

INTRODUCTION

The barrier coastline of Texas from Corpus Christi Bay south to the Rio Grande consists of Padre Island, the longest barrier island in the world, and the adjacent inshore waters of Laguna Madre (figure 1). This segment of the Gulf of Mexico coastline is marked by differences in patterns of sediment transport and deposition, by differences in lagoonal salinity and turbidity, and by variations in weather, not only geographically but from year to year. Persistent southeast winds during much of the year are an important agent in moving sediment across the barrier island. Furthermore, this is a coastline that is raked from time to time by hurricanes that alter normal sediment patterns by moderate to heavy erosion. Long-shore currents are active in moving sediment along the seaward side of the barrier island, but their patterns on a long-term basis are very poorly known.

The U S Geological Survey is studying processes of sedimentation along the south Texas coast as a part of its Marine Geology Program. The purposes of the study are to develop principles that can be used in studying and comparing coastal processes in general and to establish guidelines that can be used for the efficient management of not only the south Texas coast, but other barrier coastlines of the United States.

Remote-sensing techniques are being applied as a complement to the regular field investigations in order to evaluate the usefulness of remote sensing in several aspects of the study of sedimentation processes: 1) to determine bottom topography in shallow water, 2) to show the morphology of sand bodies in the several environments of deposition: shallow marine, barrier island and lagoon, 3) to determine the movement pattern of sediments in suspension at a given time and under a specific climatic and sea state condition, and 4) to monitor the coastline on a sequential basis as a means of relating rates of sediment movement to current patterns, sea state and atmospheric conditions. Special emphasis is on measuring rates of erosional healing following major storms or hurricanes.

^{1/} Publication authorized by the Director, U S Geological Survey.

Study of the south Texas coast by remote-sensing techniques began in late September 1967. Five days after Hurricane Beulah, the coastline was photographed in Ektachrome regular color by the Geological Survey. Thirteen months later, in October 1968, the area was re flown and again photographed in Ektachrome color. In December 1968 the same coastal strip was photographed from a NASA aircraft. Images obtained were Ektachrome regular color and Ektachrome color infrared by RD-8 cameras and thermal emission by Reconofax IV. All images were obtained from an altitude of 12,000 feet in order to closely approximate the 1:24,000 scale of standard USGS topographic maps. Photographic data have been compiled on selected 1:24,000 quadrangle maps and used as a supplement to field investigations to establish environmental relations to provide a fixed model in time for measuring future changes in coastline features during sequential monitoring.

RESULTS AND DISCUSSION

Aspects of the study discussed are those believed to best show the comparison of the remote-sensing techniques and at the same time demonstrate the value of sequential monitoring in coastal marine geologic investigations. These aspects are sediment movement, current patterns, water penetration and clarity of bottom features, and bay and lagoon flushing as indicated by infrared imagery.

Sediment Movement

A. Coastal erosion and healing -- Major storms and hurricanes are the primary agent in moving large quantities of sand along a barrier coastline. Erosional damage is most common to beaches and the seaward side of the foredune ridges. Breaches or washovers occur in gaps between foredunes. If the barrier is low, storm inlets may be cut all the way through the barrier island by the flood tide. During Hurricane Beulah which passed over the south Texas coast near Brownsville in late September 1967, some 67 storm-tide inlets or storm passes were opened across Padre Island.

Three passes opened by Beulah near the southeast corner of Corpus Christi Bay are shown in figure 2A. These passes had been previously opened by earlier hurricanes, but had been closed for some five years before Beulah. The original of figure 2A is Kodak MS Aerographic Ektachrome film taken with a K-17 camera. Evident are the washover deltas deposited by the flood tide and the greatly increased turbidity in the water that is spilling back into the Gulf following receding of the flood tide. In color, the "lacework" of the sand bodies and the different water masses within the effluents are more effectively displayed than in black and white.

The extent of erosional healing after elapsed time is shown by figures 2B and 2C, photographs taken from a NASA aircraft with an RC-8 camera in the mid-afternoon of December 21, 1968 about 15 months after Beulah. Figure 2B is a print from Ektachrome regular color film, figure 2C a print from Ektachrome infrared color film. In both photographs, the degree of modification of the tidal deltas is readily apparent, as is the extent of healing of the inlets by sedimentation. The orientation of the spit bars at the mouths of the channels clearly shows the predominant southward direction of the longshore drift. By comparing the two photographs, the contrasting quality of certain features also are apparent. Figure 2C, made from color IR film, displays the island features and the sand bodies in sharper image. Conversely, figure 2B, made from Ektachrome color film, better shows the details of the darker areas covered by water in the upper part of the photograph and of sediment in suspension in the surf zone. Depth of water in the lagoon is one to two feet, depth in the Gulf of Mexico water in area shown at the lower edge of the figure is about nine feet.

B. Sediment effluence from bay and lagoon -- The amount of turbidity in coastal waters at a given time gives a direct indication of both the amount of suspended sediment being carried to the sea and the current patterns and velocity of effluence under specific conditions of sea state. Figure 3 includes a photograph of the jetties seaward of the mouth of Corpus Christi ship channel at Port Aransas, Texas, and two pictures of the ship channel through the extreme southern end of Laguna Madre at Port Isabel, Texas. The photographs were taken from a NASA aircraft on December 21, 1968 in mid-afternoon. Figures 3A and 3B are prints from Ektachrome color film, figure 3C a print from Ektachrome infrared film. The pictures were taken within 24 hours after passage of a cold front and wind at the time of the flight was from the northeast at 20 to 25 mph. Both outlets lie at the southeast corner of large bodies of water where the fetch of the northeast winds is creating a hydrostatic head as the water is pushing southward. Source of suspended sediment is in part runoff from land and in part bottom sediments stirred up in the shallow bays and lagoons by wind action following passage of the weather front. Size and strength of sediment and water mass plumes entering the Gulf of Mexico at the two points can be compared from figures 7A and 7C, the complete plumes are not shown in figure 3.

The size and shape of the plumes seaward (see figure 7) is a function of the velocity and volume of water outflow, and the configuration seaward is a measure of the influence of longshore currents. The plume emanating from the Corpus Christi ship channel (figures 3A and 7A) extends well out to sea and its flow pattern is almost circular, with a tendency to diffuse southward, indicating a weak longshore current at this point. In contrast, the plume off the mouth of the Port Isabel channel seems to have less forward momentum and hugs the shoreline closely, indicating stronger longshore current. The difference in size of the two plumes not only

shows the contrasting velocity of outward flow but also suggests that the relatively strong southward longshore current may be confined to a narrow band adjacent to the shoreline, though the difference could be a result of differences in velocity of water outflow at the two sites. The nature of sediment outflow as a function of current patterns is important in determining sedimentation rates and in predicting where sediment accumulation or buildups are likely to occur

C. Sediment patterns, Gulf of Mexico and adjacent Padre Island -- The patterns of sediment deposition along a barrier coastline commonly shift on a seasonal basis or show a cumulative direction of movement that is a vector of forces acting from different or variable directions. The dune fields on Padre Island are an excellent example of this type of pattern. Acted upon by winds that vary from two predominant directions, southeast and northwest, the sand forms ridges or wind rows that are linear to the northwest, as shown in the upper-right quadrant of figure 4B. These same patterns may form in the sand deposited in the shallow water of the Gulf adjacent to Padre Island, although this is yet to be confirmed by bottom studies. The presence of sand ridges oriented similarly to the sand dunes on the land nearby is suggested by the northwestward alignment of the many small southwest-pointing plumes shown in the lower two-thirds of figure 4A. Presumably the sediment is being dragged from linear highs on the sea floor. Sand waves of this type have not been previously described along this coast, yet the pattern shown in figure 4A was evident along much of the south Texas coast when the photographs in figure 4 were taken by NASA on December 21, 1968.

Comparison of the two photographs shows the individual characteristics of the two types of film used. Sediments in suspension are best shown by regular color, patterns of unconsolidated sand on land are shown in much better detail by color IR film. Even the very thin sheet of sand in the top center of figure 4B that marked the recent shift in wind direction is clearly evident. Furthermore, the three dimensional character of sand bodies on color IR film, when viewed under magnification, is a decided asset in estimating thickness and in studying geometric details.

Current Patterns

Although many examples could have been selected from the NASA photographs of December 1968 to demonstrate the wide variation in current patterns along the south Texas coast at the time of the flight, the two photographs of figure 5 seem to best illustrate the value of synoptic sequential coverage in studying current movement. The figure covers a part

of the west end of Corpus Christi Bay and a part of the City of Corpus Christi. The current vortex is formed by water entering the bay from the harbor channel which lies near the lower left hand corner of the photographs. Wind is from the northeast (or left hand upper corner of the figure) at 20 to 25 mph. The turbidity is caused by the wind-agitated water stirring the bottom sediments. Water depth is uniformly about 13 feet in the bay proper except in the ship channel, which runs from the harbor entrance diagonally northeast to the area shown in upper left hand corner of the figure.

In comparing the effectiveness of regular color film and IR film for use in coastal studies, it is obvious that the total mass of water entering the bay is best outlined by the color IR print, as might be expected. Furthermore, briefly stated, the nature of the circulation vortex shown in figure 5 shows that circulation in a semiclosed bay or lagoon is a complex system that can be studied best by synoptic viewing rather than by the time-consuming monitoring of a few randomly placed current buoys.

Water Penetration

Of utmost importance in studying coastal sedimentation is the need to prepare maps that show sediment patterns in considerable detail, in particular the distribution of sand bodies in the shallow waters of the coastline. Maps that show these patterns at a given time are especially necessary for studying quantitatively the movement of sand on a yearly basis and as a result of storms. Thus techniques must be sought that permit preparation of such maps for sizable areas in a relatively short time.

The two photographs of figure 6 represent the relative effectiveness of two types of sensors. Figure 6A is a print from Ektachrome film, figure 6B a print from Ektachrome IR film. The pictures were taken on December 21, 1968, by a NASA aircraft using an RC-8 camera. The superior light penetration through the water of Laguna Madre obtained by the regular color film is readily apparent. Details of the interference sand waves along the inshore side of the lagoon are particularly impressive. Intricacies of sand body morphology in such detail are excellent for deducing long term current and wave patterns in shallow waters. On the other hand, the superiority of color IR in showing detail of sand patterns on land is again well demonstrated by figure 6B. The sand dunes on the back side of Padre Island do not show at all in figure 6A.

Thermal Patterns in Water Movement

Thermal patterns as indicators of fresh-water effluence into the coastline environments are perhaps more directly applicable to studies of water-mass movement than the sedimentation studies. However, the

three infrared images shown in figure 7, when compared with figures 2 and 3, dramatically show the close relationship between suspended sediment and water discharge

The images in figure 7 have been selected from a continuous strip made by NASA on December 21, 1968 in the late afternoon using the Reconofax IV. The plumes in 7A and 7C not only outline the cooler fresher water entering the Gulf of Mexico but also show the close correlation of drainage outflow and water turbidity when compared with regular color photographs.

Seepage of less saline water in the Gulf from the barrier island was detected in several places. One of these is shown at the left hand side of figure 7C, where water is seeping into the surf zone from ponds that are sealed off from the sea by the sand bars. See plumes near left-central edge of the photograph.

Use of Data and Future Plans

In this report, much of the discussion of data and results has been descriptive. However, most of the attention given to the data so far has been to assess its broad usefulness for studies of coastal sedimentation.

Future work will be directed toward image enhancement of data to bring out details of sediment patterns and bottom topography that cannot be qualitatively defined in the present state and to establish principles that have broad application to coastline studies in general. Also, much emphasis will be placed on compiling ground-truth maps of several types that will form bases for comparison with future remote-sensing images. Coastline changes with time can be most accurately measured by comparing images taken at intervals. Furthermore, the remote sensing technique offers an ideal opportunity to study the interrelationship of the multiple aspects that affect processes of sedimentation along regional segments of the coastline. And study of synoptic data over large areas offers the most efficient means of selecting local areas where field investigations would be of greatest benefit.

Preparation of ground-truth maps that show in detail the environments of the south Texas coastline is underway. Figure 8 is a generalized version of one of these maps (South Bird Island Quadrangle) made from color aerial photographs taken in October, 1968.

CONCLUSION

Each of three sensing techniques used in studying sedimentation along the south Texas coast offers features that are directly applicable. The Ektachrome regular color film is best for detecting current patterns as

indicated by water turbidity and for revealing bottom topography in depths up to about 10 feet. Enhancement techniques are expected to improve the water penetration quality of the film. Possibly some improvement can be gained by use of filters and by varying flight times during the day for better reflectivity conditions. Ektachrome IR is superior to regular color in showing details of sand bodies on the land and even in very shallow water. Infrared imagery also offers excellent possibilities for studying water exchanges in coastal areas between bays and lagoons and the sea.

The most significant result of our studies so far is the usefulness of synoptic coverage of a coastal region on a sequential basis. The photographs presented have been selected to demonstrate this fact.

The unique opportunity for coastal studies offered by remote sensing techniques can best be summed up by reference to the photograph, in figure 9, made from Apollo 9 in March 1969. The detail shown is remarkable, even in a B/W print. Notable is a phenomenon not previously commented on by investigators working along the south Texas coast. The long shore current patterns shown by the suspended sediment contain two opposing currents operating in the near-shore zone, as indicated by the fishhook pattern of the suspended sediment. A southward-flowing current is hugging the shoreline, but a northward-flowing current farther out is dragging the suspended sediment northward. This photograph shows the value of continuous monitoring of the coastline from an orbiting satellite using high-resolution cameras.

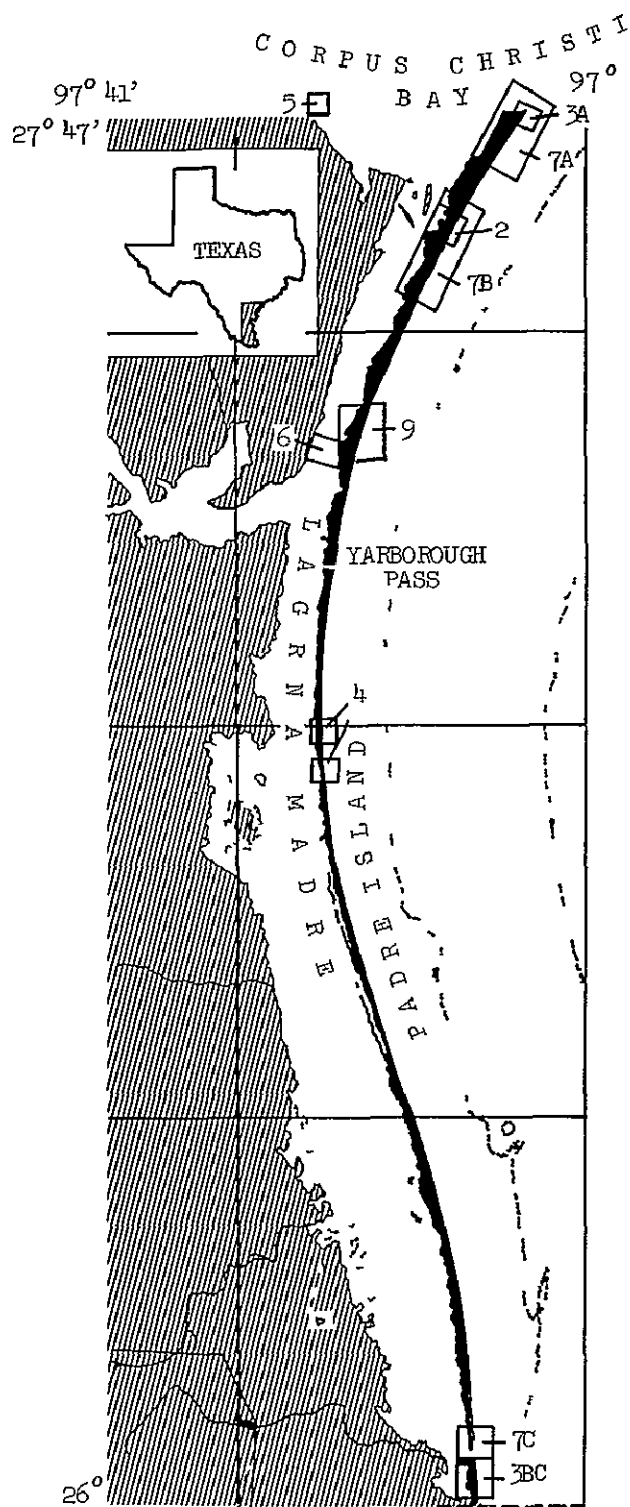
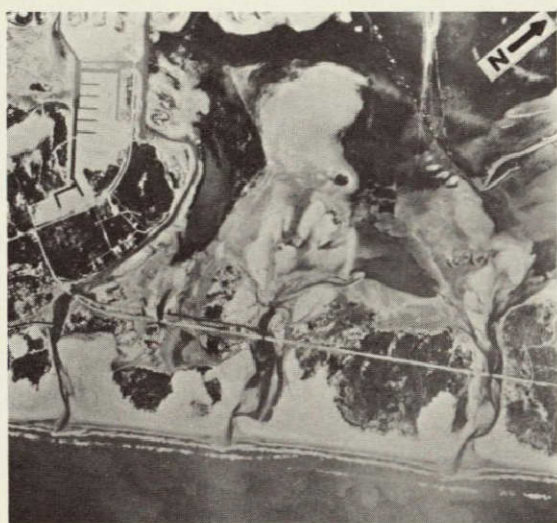


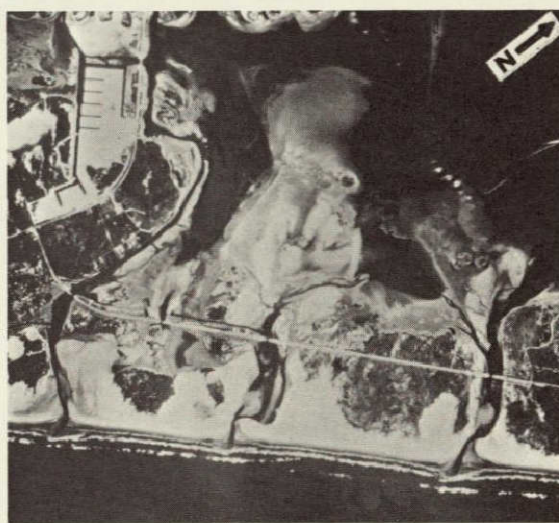
Figure 6-1 - Index map of the south Texas coast and key to figures



a.



b.

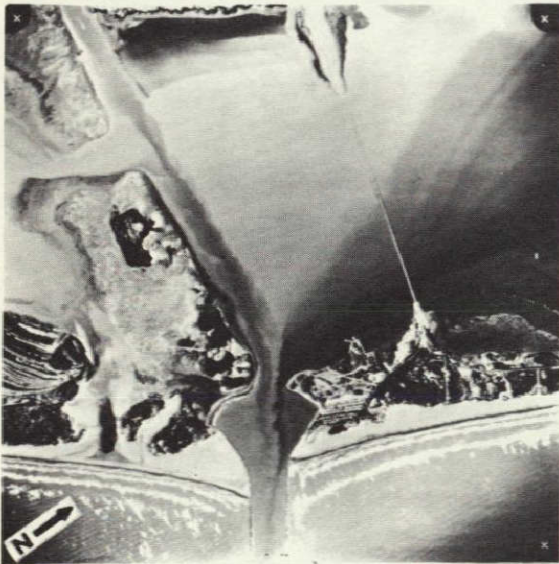


c.

Figure 6-2.- Effects of hurricane erosion and rates of healing.
 (a) Print from Ektachrome film showing inlets opened by Hurricane Beulah, September 1967 and storm tide deltas. (b) Print from Ektachrome film photographed December 1968 showing amount of healing by sedimentation over the 15-month period.
 (c) Print from Ektachrome infrared film taken at same time as (b).



a.

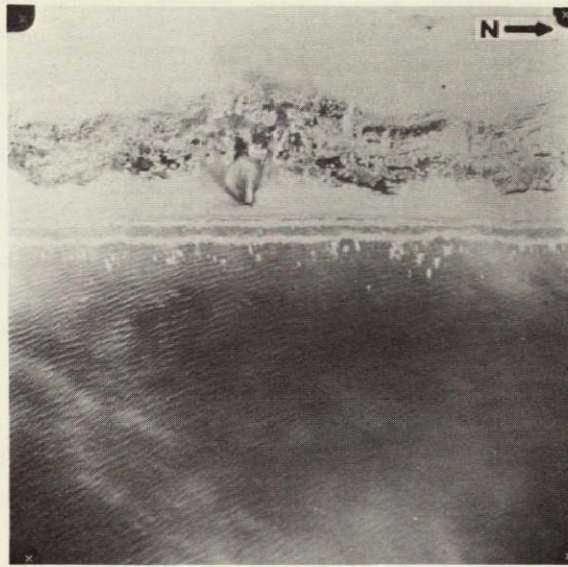


b.



c.

Figure 6-3.- Sediment effluence. (a) Sediment effluence from Corpus Christi ship channel taken on Ektachrome film. (b) Sediment effluence from Port Isabel ship channel taken on Ektachrome film. (c) Same general area as (b) on Ektachrome infrared film.



a.

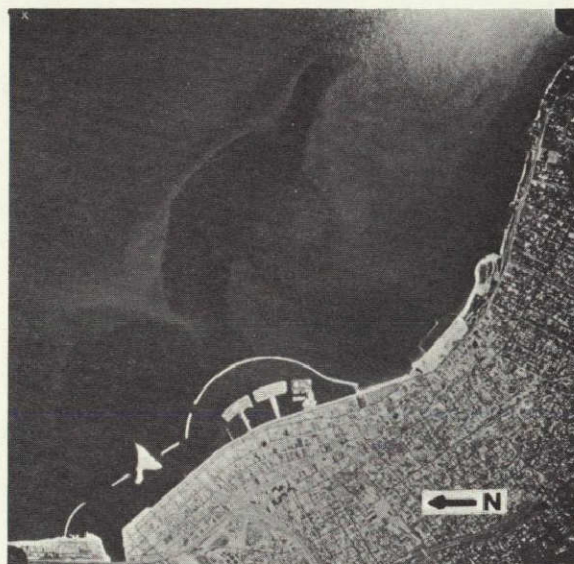


b.

Figure 6-4. Sediment patterns.
 (a) Section of central Padre Island taken on Ektachrome film; note details of sediment patterns both on land and in the Gulf of Mexico. (b) Nearby area taken on Ektachrome infrared film; compare details with (a).

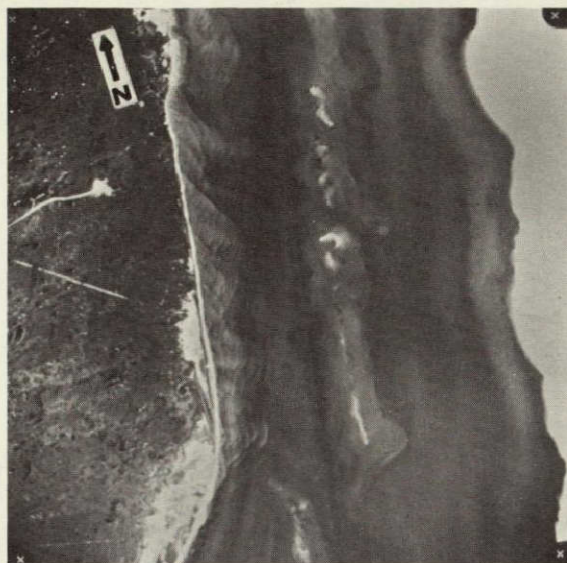


a.

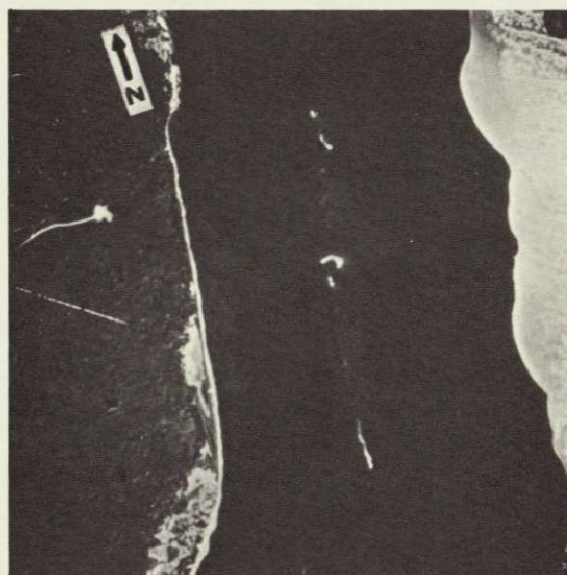


b.

Figure 6-5.- Circulation vortex in western part of Corpus Christi Bay. (a) Print from Ektachrome regular film. (b) Print from Ektachrome infrared film. Compare for details.



a.

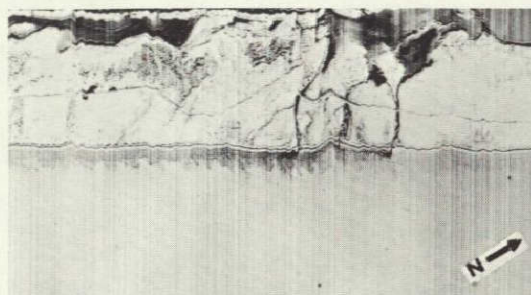


b.

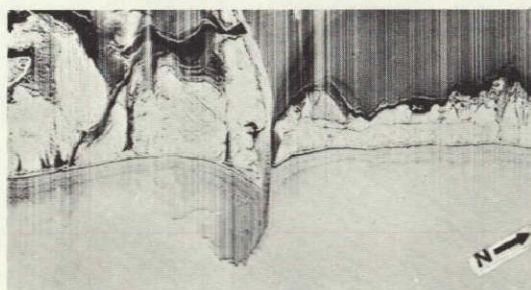
Figure 6-6.- Section of northern Laguna Madre showing comparison of techniques for water penetration. (a) Print from Ektachrome regular color film. (b) Print from Ektachrome infrared film.



a.



b.



c.

Figure 6-7.- Thermal characteristics of bay and lagoonal water entering the Gulf of Mexico. (a) Corpus Christi ship channel. (b) Natural inlets cut by storm erosion at southeast end of Corpus Christi Bay. (c) Port Isabel ship channel. Image taken by Reconofax IV.

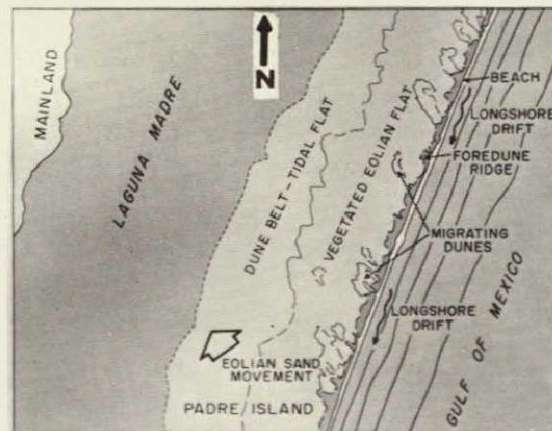


Figure 6-8.- Generalized environmental map of South Bird Island Quadrangle made from color aerial photographs.

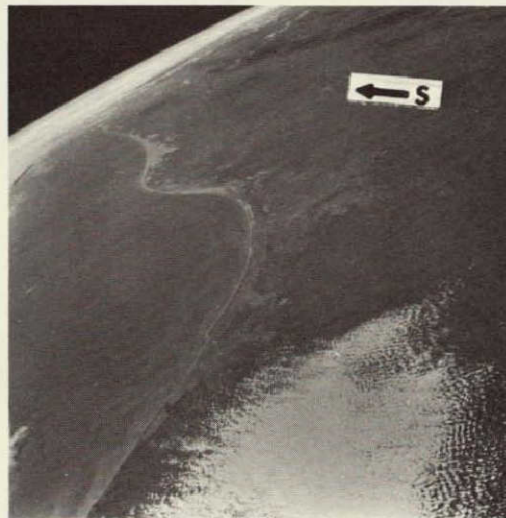


Figure 6-9.- View of Texas coast facing southward, taken by Apollo 9, March 1969. Note how fishhook pattern of suspended sediments shows two opposing longshore currents.

SECTION 7

Remote detection of geochemical soil anomalies *

by

F. C. Canney

U.S. Geological Survey
Denver, Colorado

N71-19258

Introduction

This paper describes a preliminary experiment that was made to compare the spectral reflectance from trees growing in soil over a mineral deposit with reflectance from trees of the same species growing in a nearby unmineralized area. Although the measurements were made on a relatively small number of trees, some significant differences were obtained and the overall results are encouraging enough to warrant additional studies. Preliminary results suggest that measurement of spectral reflectance may become a dramatic new way of detecting geochemical soil anomalies by remote means in tree-covered areas.

Traditional prospecting methods, wherein rocks are examined directly for valuable minerals, can no longer be expected to produce many important mineral discoveries, except possibly for those deposits of minerals that were of little or no economic interest until recently. Most areas of the world amenable to this type of prospecting have been examined repeatedly by several generations of prospectors. However, in large areas, rocks and geologic structures favorable for the occurrence of ore are concealed beneath soil and alluvium. In such areas many important ore discoveries have been made in recent years by utilizing the newer geochemical and geophysical prospecting methods. And, it is reasonable to assume that in such areas many future mineral discoveries will be made as we refine existing exploration methods as well as develop new ones.

In the past 20 years, geochemical prospecting has progressed from a little-used and often-scorned technique to one that is widely used in most modern-day exploration programs. At present, geochemical soil sampling methods have been perfected to a higher degree than most other geochemical techniques. In areas of residual soils, the identification of an area of soils having abnormally high amounts of certain metals furnishes a strong clue as to the possible presence of a nearby concealed mineral deposit. To locate and delineate many metal anomalies in soil requires that large numbers, often many thousands, of closely spaced soil samples be collected and analyzed for one or more trace constituents. In most parts of the world such soil-sampling programs are becoming increasingly expensive. Developing

* Publication authorized by the Director, U.S. Geological Survey.

a method of detecting such anomalous areas by appropriate sensors mounted in aircraft, or even in orbiting satellites, would constitute an important breakthrough in mineral exploration and might dramatically reduce exploration costs.

In considering ways of sensing abnormal chemical conditions in the soil by remote means, the possible use of vegetation is, for two reasons, a natural avenue to explore. First, data from many biogeochemical surveys performed during the past few decades have shown that plants growing in a geochemically anomalous soil generally reflect this in their trace element content; and, sometimes, these plants show characteristic variations in their form, color, size, or rate of growth. Second, the forest canopy is easily visible to a sensor in a plane or satellite.

Interrelationships between a tree and its environment are complex, and many nongeological parameters, of course, affect plant health, growth, distribution, and composition; nevertheless, the geologic environment is one of the more important environmental parameters. Chlorosis is a common diseased condition of chlorophyll-bearing plants characterized by absence of or deficiency in green pigment and manifested typically by a yellowing of the leaf which in turn causes the green veins to stand out prominently. Chlorosis can be caused by the presence, in excessive amounts, of elements that are antagonistic to iron in plant metabolism and that interfere in the production of chlorophyll. Although other causes of chlorosis are fairly common, prospectors and geologists have long known that a chlorotic patch of vegetation may indicate an area of metal-rich soils or rocks and therefore merits their attention.

Actually, mineral-deposit-related chlorosis is rather rare in virgin environments. While different plants seem to vary greatly in their ability to tolerate excesses of various elements in their nutrient solutions, the concentrations of most elements required in the supporting soil to produce symptoms visible to the unaided eye are often fairly high. Further, in areas of many geochemical soil anomalies that are genetically related to important mineralization, the vegetative canopy is apparently healthy, no toxic symptoms being visible to the eye. It is possible, however, that the abnormal chemical environment causes subtle--but nevertheless definite--changes in some physical or chemical aspect of one or more plant organs. These changes, if detected and quantitatively measured, can then serve as an indicator of an abnormal chemical environment at the tree roots. Because many common ores contain elements known to be antagonistic to iron in plant metabolism, it appears reasonable to assume that such excess metal content might induce incipient chlorosis, a condition identifiable from measurements of the spectral reflectance. Other variables, of course, affect spectral reflectance but if their effect can be accounted for satisfactorily, trees should be useful as sensors of geochemical soil anomalies.

Published spectra of vegetation are scarce and no data are known in the literature that would indicate whether the spectral reflectance of apparently healthy trees in a geochemically anomalous area differs significantly from the spectral reflectance of trees growing in areas of normal elemental content. Therefore, an experimental plan was designed to measure spectral reflectance of trees growing in anomalous and in background areas under natural conditions, wherein tree targets would be viewed and measured much as an aerial camera or other type of airborne spectrometer would view them.

The work on which this report was based was supported by the National Aeronautics and Space Administration (NASA). The Geological Survey contributed the chemical analyses of the soils and vegetation. The overall direction of the project was by F. C. Canney, who was also responsible for the selection of the site, the trees to be measured, and the geologic and geochemical ground control analyses. The reflectance measurements in the field, the reduction of the data, and the statistical study were done by the Science Engineering Research Group of Long Island University under the direction of Prof. Edward Yost.

Previous work

An appreciable amount of research is currently underway on the applications of remote sensing to problems in forestry and agriculture and has been reported in the literature. By comparison, very few experiments specifically directed to the mineral exploration field appear to have been done. In the highly competitive mineral industry, industry-sponsored experiments of this nature would very rarely be reported anyway in the scientific literature, especially if results were encouraging enough to suggest that a new exploration tool might be forthcoming. The concept that spectral signatures of vegetation might be useful in the detection of biogeochemical anomalies genetically related to mineralization has apparently occurred independently to various individuals. During the past 6-8 years several aerial reconnaissance surveys were flown by several organizations over mineralized structures in forested areas; the sensor used was false-color infrared film. Available information suggests the results were not generally felt to be encouraging. This was certainly my appraisal after making several experimental aerial surveys in 1966 and 1967. Admittedly, most of these surveys, including my own, were not made under closely controlled conditions.

The experiment closest in scope to the one described herein was executed by C. E. Olson, Jr., of the University of Michigan, and H. T. Shacklette of the U.S. Geological Survey, in 1962. They collected leaves from a variety of deciduous trees rooted in both geochemically anomalous and background areas in the southwestern Wisconsin lead-zinc district, and then they measured their spectral reflectance. Although the experiment unfortunately had to be recessed, reduction of the data has been resumed by Olson and the data are expected to be available in the near future.

Selection of test site

The test site selected was Catheart Mountain in west-central Maine, where a large but low-grade copper-molybdenum deposit was discovered a few years ago by private investigators. It seemed to be an appropriate test site for the following reasons:

1. The area is still largely undisturbed by man.
2. It is completely forested with both deciduous and coniferous trees.
3. Detailed and extensive geochemical ground control is available.
4. Large areas of soil contain highly anomalous amounts of copper and molybdenum, which are also anomalously concentrated in the trees.
5. The major geochemical soil anomaly encompasses an area about 1 mile square, a target large enough for possible later experiments from orbital altitudes.

The area is slightly more complex, both botanically and geologically, than was desirable for a first test, but that disadvantage was far outweighed by the advantages.

Field procedure

For the initial experiment balsam fir (Abies balsamea (L) Mill) and red spruce (Picea rubens Sarg.) were selected as the species to be examined. Five specimens of each species growing in the anomalous area of metal-rich soils were measured and compared with similar specimens growing in a nearby unmineralized area. So far as possible, other factors--such as soil type, soil moisture, and exposure--that might affect reflectance were kept constant between the two groups. A sample of the foliage of each tree and a sample of the supporting soil in which it grew were collected for chemical analysis.

Each tree spectra consisted of 27 measurements of reflected radiation, and 27 measurements of simultaneously incident solar radiation, made at each wavelength. The wavelengths were spaced at 25-nanometer intervals in the 350- to 750-nanometer region and at 50-nanometer intervals in the 750- to 1100-nanometer region. Reflected radiation greater than 1100 nanometers could not be recorded because overcast conditions prevailed during much of the test period. Each tree was scanned three times and the average values of reflected and incident radiation were used to compute the percent directional reflectance.

To make the reflectance spectroradiometric measurements meaningful for possible future experiments using an aerial sensor, the spectroradiometer was placed above the tree so the measurements were obtained in a downward-looking orientation. This was accomplished by placing the instrument in the bucket of a "cherry picker." Figure 1 shows the method used to obtain reflectance spectra. Extreme care was taken to ensure that the field of view of the tree being measured was completely full so unwanted radiation from the background would not leak into the optical system.

Results

The spectral reflectance curves for red spruce and balsam fir are shown in figures 2 and 3 and the chemical data in tables 1 and 2. The vegetation samples collected for analysis were of 1- and 2-year-old needles and twigs composited from the general area of the tree imaged by the spectroradiometer. Copper and molybdenum analyses are expressed as parts per million (ppm) in the vegetation ash. The amount of ash of the dried plant material ranges from 2.5 to 3.5 percent.

The curves for both anomalous and background groups of red spruce (fig. 2) are essentially the same in the visible region of the spectrum. In the near infrared, from 750 to 1100 nanometers, the anomalous group shows a uniform pattern of decreased reflectance. This was, of course, the result we had hoped to find. Actually though, while the spectral differences are highly encouraging, the values are not significantly different at the 95-percent confidence level.

The chemical data for red spruce, shown in table 1, reveal that, unfortunately, the trees selected for measurement were growing, for the most part, in soil only slightly anomalous in copper and molybdenum. And though all spruce trees of the anomalous group were weakly anomalous in molybdenum, only one tree (no. 5) was anomalous in copper. In this preliminary study, however, the selection of trees was severely hampered by the restricted mobility of the cherry picker on a rough mountainside.

The reflectance curves for balsam fir (fig. 3) show a marked contrast with those of spruce. At every wavelength the anomalous fir group had a higher reflectance than the background group. The statistical analysis of these data showed that in the 525-750 nanometer region the difference was significant at the 95-percent confidence level. From 750 to 1100 nanometers, the difference would have been significant if the spectra of one tree (no. 15) had been deleted from the data set. The balsam fir group (table 2), on the whole, were rooted in soils that contain distinctly more copper and molybdenum than the spruce-group soils.

The inferences to be drawn from these data are limited by the small sample size and by the relatively large variance of the data, especially in the 750- to 1100-nanometer region of the spectrum. There is a strong suggestion, however, that the effect of metal-rich soils on the spectral signatures of trees may be quite variable between species. As judged from the described experiment though, multispectral photographic techniques could probably be used to separate balsam fir trees with anomalous metal contents from the other tree groups sampled. The present results are encouraging enough to warrant additional studies. The continuation of this research should ultimately lead to a new way of detecting mineral deposits by remote means.

Table 1

METAL CONTENT OF RED SPRUCE (AND SUPPORTING SOIL)
USED FOR REFLECTANCE MEASUREMENTS

	SAMPLE NO.	PARTS PER MILLION			
		COPPER		MOLYBDENUM	
		VEG. ASH	SOIL	VEG. ASH	SOIL
ANOMALOUS GROUP	1	120	115	8	10
	2	120	115	8	10
	3	150	225	8	20
	5	230	60	20	75
	6	120	60	8	40
BACKGROUND GROUP	13	150	5	3	3
	16	150	5	3	5
	17	150	5	3	5
	18	120	5	5	<3
	19	120	<5	5	<3

Table 2

METAL CONTENT OF BALSAM FIR (AND SUPPORTING SOIL)
USED FOR REFLECTANCE MEASUREMENTS

	SAMPLE NO.	PARTS PER MILLION			
		COPPER		MOLYBDENUM	
		VEG. ASH	SOIL	VEG. ASH	SOIL
ANOMALOUS GROUP	4	150	115	60	150
	7	450	2250	225	150
	8	450	2250	225	225
	9	300	15000	150	75
	10	450	9000	60	80
BACKGROUND GROUP	11	150	30	5	8
	12	120	5	3	3
	14	120	<5	3	3
	15	150	5	3	3



Figure 7-1.- Photograph showing method of obtaining reflectance data in a downward-looking orientation.

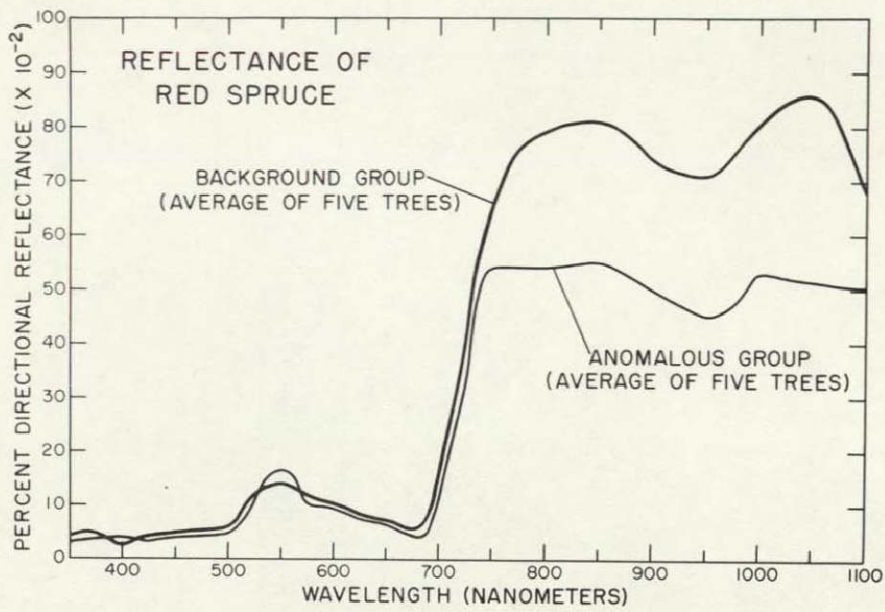


Figure 7-2.- Reflectance of Red Spruce.

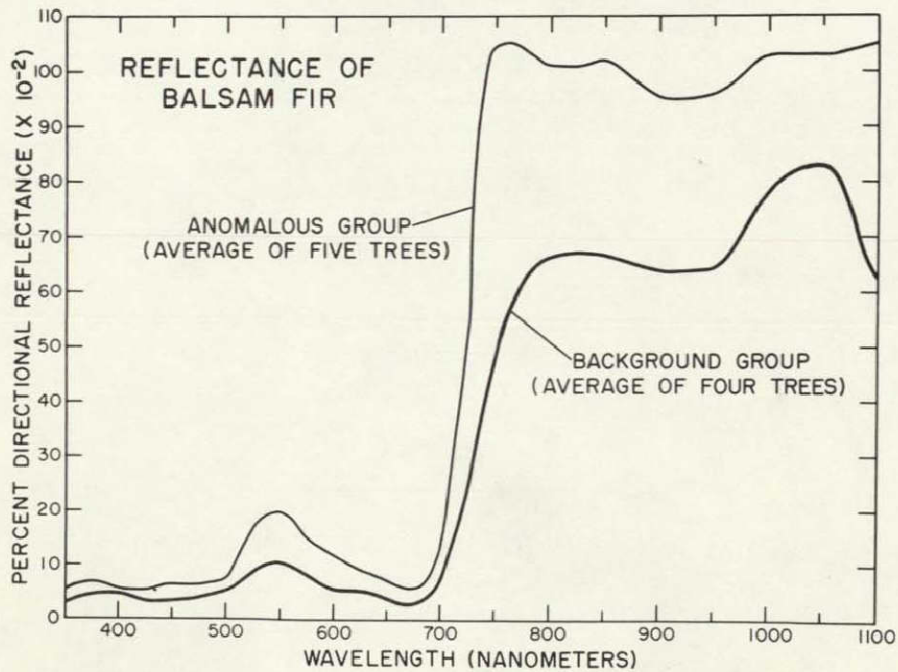


Figure 7-3.- Reflectance of Balsam Fir.

GEOLOGIC UTILITY OF SMALL-SCALE AIRPHOTOS¹

By Malcolm M. Clark, Menlo Park, Calif.

N71-19259

ABSTRACT

This report emphasizes the geologic value of small-scale airphotos by describing the application of high-altitude oblique and 1:120,000 to 1:145,000 scale vertical airphotos to several geologic problems in California. These examples show that small-scale airphotos can be of use to geologists in the following ways:

1. High-altitude, high-oblique airphotos show vast areas in one view, introducing a geologist or his audience to the salient geographic and topographic attributes and many geologic features of an area.
2. Vertical airphotos
 - a. Offer the most efficient method of discovering the major topographic features and commonly, important structural and lithologic characteristics of new or unfamiliar terrain.
 - b. In stereo, show a broad region in one three-dimensional view that may reveal relations or suggest geologic hypotheses not otherwise apparent
 - c. May reveal features of such extent, subtlety, or discontinuity that a broad view is necessary to recognize them.
 - d. Instantaneously record rapidly changing conditions over large areas, such as tidal flow and surface wind patterns

Small-scale airphotos do not replace large-scale airphotos or field investigations. They make the geologist more effective by saving time or revealing relations he might otherwise miss because of lack of experience or astuteness. Geologists would be helped in most projects by using airphotos at several scales that are smaller by successive factors of 3 than the largest scale used.

¹Publication authorized by the Director, U.S. Geological Survey.

Color and black and white airphotos at scales as small as 1:175,000 are within the capability of present commercial airphoto aircraft using cameras equipped with short focal length lenses. Small-scale airphotos also have potential use now in cartography, forestry, agriculture and geography, both in current programs and those contemplated for earth resource satellites. Moreover, several years, if not decades, are likely to pass before photos from orbit replace small-scale airphotos.

INTRODUCTION

Small-scale vertical air photographs covering large areas of the earth will become available in the immediate future, both from imminent earth resources satellites (Report for the Committee on NASA Oversight, 1968) and from increased use of high altitude aircraft (e.g., Bock, 1968) and short focal length cameras in aerial photography. To take full advantage of these photos, geologists should become aware of their potential usefulness in solving geologic problems.

Hemphill (1958), using 1:60,000 scale airphotos, pointed out that the chief benefit from such photos is that they permit continuity of observation over large areas. This broad view leads to easier recognition of geologic features such as rock strata, tectonic lineaments or lithologic units characterized by subtle but persistent topographic or tonal differences. The purpose of this report is to support and add to Hemphill's work by illustrating the geologic utility of airphotos that range in scale from 1:120,000 to 1:145,000. These airphotos are of significantly smaller scale and contain information that is not obvious on present "small-scale" airphotos, either the widely available 1:60,000 USGS photos or photos taken for special projects, such as a series of 1:90,000 photos that cover the western portion of California. Furthermore, the scales of the photos in this report are attainable by present commercial aircraft and cameras.

The photos to be described were taken in 1967 and 1968 for this investigation of geologic uses of small-scale airphotos by U.S. Air Force aircraft flying between 60,000 and 70 000 feet. Cameras were equipped with 6-inch focal length lenses and used 9 1/2-inch black-and-white roll film. Flight lines covered geologic features of interest in the Far West, principally active faults in California. The project thus far has yielded about 1300 overlapping vertical photographs, covering many swaths 16 to 18 miles wide and up to several hundred miles long. Figure 1 shows locations and approximate ground coverage of the airphotos of Figures and Plates

EXAMPLES OF GEOLOGIC USE OF 1:120,000-1:145,000 SCALE AIRPHOTOS

Garlock Fault

Figure 2 is a high oblique airphoto looking east across the northern boundary of the Mojave Desert from about 60,000 feet. In a single view this photo shows much of the geographic and geologic character of an immense region. Such photos afford an excellent and often spectacular

way to introduce, display or summarize the geologic relations of a large region. They can be very useful to a geologist in the first steps or the reconnaissance part of a field study or in areas which lack vertical airphotos. Moreover, they can serve the geologist later when he communicates his findings to an audience.

Some of the small-scale vertical photographs described in this report are being used in a project to locate the most recent breaks along the Garlock fault throughout its 150-mile length. Figure 3 (scale 1:120,000) shows part of the fault (A-A') near Searles Valley. The linear aspect of the fault, expressed mainly by scarps, valleys, and ridges shows clearly in this photo, as well as on large scale (1:20,000) photos, which have been the primary tool for locating and recording the position of recently active traces of the fault. However, in places where surface evidence of the fault is missing for several miles, the large-scale photos are much less useful than small-scale photos, which reveal the continuity of the fault throughout its length.

Plate 1 (scale 1:120,000) shows the course of the Garlock fault at Koehn Lake, a playa about 40 miles west-southwest of the area shown in Figure 3. Here most of the surface continuity of the fault disappears as it changes trend by two poorly defined en echelon steps. Large-scale photos are of little use at Koehn Lake, for the features that mark the location of the surface traces are scarps 5 or more miles apart or a few subtle tonal lineaments among many tonal boundaries not necessarily of tectonic origin. In this area the value of the small-scale airphoto becomes clear. From an inspection of Plate 1, one can discover features that line up with existing scarps or that are aligned with projections of the fault from either side of this area. For example, scarp A and lineament B on Plate 1 are aligned with the prominent scarp C. C, in turn, is almost continuous with the trace shown in Figure 1. A line up with the projected trace from the southwest (Pl. 2). Subsequent field checks showed the lineament at B to be a drainage channel across the playa and the one at E to be the southern boundary of a zone of light-colored modern channels. In both places the channels, and hence the resulting lineaments, appear to be controlled by subtle topographic trends of probable tectonic origin, in view of their position in line with prominent fault scarps.

Squares on Plate 1 represent the size of available photos at scales of 1:20,000 and 1:32,000 in the same area. Presumably these photos could be used to locate the traces shown in Plate 1 by assembling them into a mosaic or by using them to locate many linear features, transferring the features to a map and then looking for alignments. Inspecting a single photo is obviously easier and probably more accurate.

A photo scale of 1:250,000 would perhaps be even better for working on the problem at Koehn Lake. The 1:120,000 photo shown in Plate 1

had to be joined to the overlapping photos on either side in order to project the prominent traces from the northeast and southwest on to Plate I. One photo at a smaller scale would eliminate this extra step, provided the lineaments were still visible.

It could be argued that a high oblique photo similar to Figure 1, but with Koehn Lake somewhere in the foreground and with a direction of view within about 10° of the bearing of the fault traces, would also reveal the location of the faults in the vicinity of the playa. Such a photo, however, would require careful positioning of the aircraft and some foreknowledge of the features of interest. One vertical airphoto, in contrast, can be inspected from any direction, in a sense simulating many oblique photos. Vertical photos, in further contrast to obliques, present the geometric relations of surface features in a form that is more easily studied and understood. In my experience with high oblique and vertical photos taken from low, high, and even orbital altitudes, I have yet to see a high oblique that was more useful for general geologic interpretation than a vertical photo, at suitable scale, of the same area.

Although the use of 1:120,000 scale airphotos described above was part of an investigation to locate the most recent breaks along the Garlock fault, the general position of the fault had earlier been known throughout its length (Jennings et al., 1962; Smith, 1965, Dibblee, 1967). Had the Garlock fault and the geology of its surroundings been completely unknown, a geologist would have been able to easily discover it and determine most of its extent from a cursory inspection of a few 1:120,000-scale photos, if not from orbital photos at 1:600,000 scale or so.

ANZA-BORREGO DESERT AREA

Coyote Creek Fault

Plate 3 (scale 1:145,000) shows an area along the eastern edge of the Peninsular Ranges of southern California about 50 miles north of the Mexican border. Traversing the photo from right to left (A-A') is the surface rupture along the Coyote Creek fault that accompanied the Borrego Mountain earthquake of April 8, 1968. This earthquake, which was of Richter Magnitude 6.5, was the strongest to occur in California since 1952. The 1968 break extended the known position of the fault roughly 12 miles beyond its previously mapped southeastern end near Highway 78 (B), at the lower right corner of Plate 3 (Rogers, 1965). However, a casual inspection of these photos when they were received in December 1967, 4 months before the earthquake, revealed the fault at C

and its probable extension along the faint lineament out to D. Thus, study of a few photographs that were obtained for the purpose of investigating the San Jacinto fault system (of which the Coyote Creek fault is a branch) quickly suggested an extension of the fault beyond its recorded location, an inference dramatically verified a few months later by the earthquake.

Without the photos shown on Plates 3 and 4, the search for extensions of the fault beyond its mapped extent at this location would involve use of existing airphotos: those of the California Division of Highways at 1:90,000 scale, U.S. Geological Survey at 1:25,000, or U.S. Department of Agriculture at 1:20,000. Assuming the search to be restricted to a zone 5 miles wide, extending for 17 miles beyond the then known end of the fault (roughly the width of Pl. 3), stereo coverage of that area by the three available types of photos would require, respectively, 5, 20 and 33 photos. Obviously at least the first part of such a search is most efficient using three 1:145,000 scale photos.

During the subsequent investigation and mapping of the new break formed April 8, all these other photos were used, but only after reconnaissance by aircraft, with the help of the 1:90,000 and 1:145,000 scale photos (which showed the traces resulting from previous earthquakes), revealed the general extent and location of new breakage. The surface ruptures were plotted on 1:20,000 and 1:25,000 photos, but the smaller scale photos were indispensable for establishing continuity of breaks, indicating locations that should be investigated for breaks, and organizing such logistic problems as access to different parts of the break.

SMALL-SCALE STEREO

The advantage of small-scale airphotos are greatly extended by stereo use, which yields a 3-dimensional view of a very large area. Although topographically expressed features such as lineaments are generally obvious on a single photo, particularly if illumination is favorable, the addition of stereo may reveal otherwise obscure topographic lineaments or topographically expressed differences between lithologic units.

Moreover, problems dealing with the analyses of surfaces and their relations to each other and surrounding terrain may be more quickly and easily recognized and analyzed with stereo photos than with a topographic map. Plate 4 forms a stereo pair with Plate 3. The strikingly dissected region of folded sediments in the vicinity of Fish Creek Wash 5 to 10 miles west of the Coyote Creek fault preserves fragments of

several levels of older alluviated surfaces, as at E, F, and G. These different levels may represent episodes in the tectonic history of these mountains and the adjacent Imperial Trough. Analogous surfaces exist in many other drainages of the region. Any attempt to understand the history of the older surfaces requires, among other efforts, correlation of the existing fragments, visualization of their probably former extent, and identification of sources and direction of distributary channels on those alluvial surfaces. A single stereo view of the entire drainage containing the surfaces makes such tasks much easier, and may reveal relations or lead to hypotheses that could not be gained by other methods.

For example, the stereo view leads directly to such questions as the following: What is the relation of surfaces H, I, and J (Pl.3) to the two major surfaces E and F? When during the history of these surfaces did the canyon at K become part of the drainage system? Do the different surfaces represent distinct episodes of equilibrium throughout the drainage during its erosional history, or do they represent preserved remnants of local equilibrium during a continuing process of erosion whose intensity switches from place to place throughout the basin as the major channels move laterally across the basin?

The single stereo view at small scale helps the investigator form the questions that must be asked and helps him organize the task of answering them by presenting a single, detailed three-dimensional view of a large part of the system being studied.

A problem commonly arises whenever airphotos must provide a single stereo view of a specific region. As ordinarily obtained, airphotos of a region yield individual stereo models that overlap each other by about 10 to 30 percent, in contrast to roughly 60 percent overlap of the individual photographs. Thus a geologic feature of interest such as a basin might not coincide with a single stereo view, even though its dimensions are small enough, because the photo centers fall in the wrong places.

The most practical way to overcome this problem is to use photos at a scale sufficiently small that the region of interest is small compared to the area covered in a single stereo model. The smaller the target area with respect to the coverage of the stereo model, the lower the probability that it will be split between two stereo models. If necessary, the feature can be enlarged for study in stereo, and photos of larger scale can be used for investigating details of critical parts of the basin.

Study of the dissected surfaces shown by Plates 3 and 4 would probably be further helped if areas outside of the stereo model shown here, but still in the same immediate drainage basin, could be included

in a single view. Photos at 1:200,000 to 1:400,000 scale would probably cover the necessary area, moreover, photos at even smaller scales would show relations between several adjoining basins, if they retained the necessary detail.

In the above example, the use of small-scale stereo models broadly illustrates the general relations between photos of different scales and indicates how a problem in a relatively small area might benefit from the availability of both high altitude and orbital photographs, in addition to ordinary large-scale photos.

Sierra Nevada

Glacial Deposits

Another type of geologic study in which a single stereo view of a large region is valuable, is illustrated by Plates 5 and 6 (1:125,000), which show the abundant Pleistocene glacial deposits near Virginia and Green Creeks on the east slope of the Sierra Nevada Just north of Mono Lake. Figure 4 is a geologic map of part of this area. These two drainages contain prominent lateral and terminal moraines of the Tahoe and Tioga Glaciations (early and late Wisconsin, respectively) and large areas of older till (Sharp, 1965, p. 75; Blackwelder, 1931, p. 898) and moraines that may represent deposits of more than one pre-Tahoe glaciation (Clark, 1967, p. 57).

A single stereo view reveals a possible relation between some of the older till masses (moraines?) that lie beyond the Tahoe moraines of Virginia Creek. The bodies of till at A and B on Plate 5 are evidently remnants of a pre-Tahoe right-lateral moraine from Virginia Creek. From the photo, the till body at C appears to be a remnant of the same lateral moraine. This relation was not obvious to me or several others, even after spending several days in the field equipped with 1:16,000 and 1:60,000 airphotos. We considered it as a possibility, yet it did not seem mechanically likely. In particular, the canyon immediately west of the till, leading south to Mono Lake, would appear to complicate the flow of any glacier in Virginia Canyon, if not divert it away from the till at C. Yet the small-scale stereo view reveals a degree of continuity between the till masses at A, B, and C that strongly suggests they are remnants of the same lateral moraine. By this explanation the canyon west of the till at C would have been shallower when the till was deposited, and was presumably filled with till of the lateral moraine, subsequently eroded out. This hypothesis receives strong support from the broad stereo view afforded by the small-scale photographs.

In Green Creek, the next drainage north, the small-scale stereo view reveals what appear to be remnants of lateral and terminal moraines (D) left by a large pre-Tahoe glacier. These presumed moraines were first detected on a 1:60,000 photo (Plate 7) (Clark, 1967, p. 57), and, if interpreted correctly, represent the best example yet known in the Sierra Nevada of the preservation of moraines of a glaciation older and more extensive than Tahoe. As far as I know, the possible morainal nature of the till at D was not earlier recognized on the ground or on large-scale air photographs.

Additional information, not obvious on photos of larger scale, can be seen on Plates 5 and 6. The crests of the older assumed moraines (D) are distinctly lower than the enclosed Tahoe-Tioga crests, implying relative down-faulting of the older till with respect to the mountain front and subsequent alluviation east of the resulting scarp. This caused the later Tahoe glacier to emerge from the mountain front relatively higher than the older, more extensive moraines, as evidently happened also in Mono Basin, 20 miles to the south (Clark, 1967, p. 41-42). In both areas this relation was not recognized until a single stereo view on small-scale airphotos became available of the entire morainal assemblage of each drainage.

Faults

Plate 5 reveals faults heretofore unrecognized in this area. Two gently curving discontinuous tonal and topographic lineations, probably related to faults bounding the eastern margin of the Sierra Nevada, are quite noticeable between E and E' on Plate 5. The upper lineation is distinctly less apparent on 1:60,000 airphotos. Both are difficult to recognize on large-scale airphotos, and their continuity is not evident on the ground. Their position is proper for range front faults, and they are aligned with the major range front scarps to the north and south. The lower, more prominent of the two lineations at E-E' is composed of vegetation contrasts (presumably in part controlled by ground water), a few subdued and short topographic scarps, and irregularities in the otherwise continuous moraine crests above Robinson Creek at the northern end of the lineament. Considered individually, such features are of little note. Vegetation contrasts and small scarps abound in this area, created by lithologic boundaries, joints, and minor structural irregularities. Indeed, in the field, the interrupted crests of the moraines (representing three different ages, Sharp, 1965, p. 74-76) appear to be a result of local sliding. However, the remarkable alignment of so many features along E-E' strongly suggests a fault. A parallel, more continuous lineament, almost certainly a fault, is at F-F'. This feature is also prominent on 1:60,000 scale photos (see Plate 7). None of these features, however, were detected during geologic mapping of this area until the small-scale airphotos became available.

ADVANTAGES OF USING SEVERAL PHOTO SCALES IN A SINGLE AREA

During a reconnaissance field check of the glacial deposits, three scales of vertical airphotos were used: 1:16,000 (Plate 8), 1:60,000 (Plate 7), and 1:105,000 (flown by USAF, but not shown). The photos of Plates 5 and 6 (1:125,000) were obtained after field work was finished. The 1:16,000 photos were the base for recording field information and investigating differences between adjacent lateral moraines of the same drainage. Plate 8 shows the Tioga terminal moraine (latest Wisconsin) of Green Creek and surrounding older moraines. 1:60,000 photos (Plate 7) proved valuable for comparing some of the moraines of adjacent canyons; for example, the Tahoe and Tioga moraines of Virginia Creek to those of Green Creek. They were also valuable for discovering some of the faults (e.g., F, Plate 7) and checking detail of structures seen on the smaller scale photos. However, the 1:60,000 photos did not extend far enough to show obviously the continuity of the main range-front fault system, or permit convenient comparisons between the moraines of Green Creek and those of the next drainage north, Robinson Creek. These regional structures and relations show best on the 1:125,000 photos (Plates 5 and 6) (The 1:105,000-scale photos mentioned above divided the moraines of both Virginia and Green Creeks between two adjacent flight lines, hence were much less satisfactory than the 1:125,000 photos). Photos at scales of 1:200,000 to 1:400,000 would be very valuable to any study of the structural setting of the Virginia-Green-Robinson Creek area. Such photos would show the orientation and continuity of faults and joints of this region in relation to the structure of adjoining parts of the Sierra Nevada and the ranges immediately to the east.

San Andreas Fault

Carrizo Plain

Small-scale airphotos have proven useful in the study of the tectonic settings along faults. R. E. Wallace (1968, written commun.) has evaluated small-scale photos of the San Andreas fault where it traverses the Carrizo Plain in central California (A-A', Plates 9 and 10, 1:133,000 scale). He had previously made a detailed study of the fault in this region, aided by airphotos at scales of 1:6,000 and 1:24,000. Subsequently, using the small-scale photos, Wallace discovered several lineaments (parallel to B-B', Plate 9) that he had not earlier recognized near the fault; although once located, he could identify them on the larger scale photos. He also noted that features more than one mile long were more easily identified on the small-scale photos than on large-scale photos and suggested that a distinctive feature is enhanced by a certain amount of nondistinctive or random

background pattern. For example, a lineament becomes more apparent when it is obviously longer than the randomly oriented linear elements of the local terrain. Such recognition requires a single view significantly larger than the size of the random elements. Thus, Wallace was more easily able to recognize landslide scars 1 to 1-1/2 miles across at (C) and vague but persistent folds at (D) on the 1:133,000-scale photos than at larger scales.

The detailed field studies completed by Wallace prior to receiving the small-scale photos included examination of stream channels offset were obvious during a rapid scan of contact prints of the small-scale photos, and offsets as small as 50 feet were apparent with 2 to 3X magnification. On the photo, these distances are roughly 0.03 to 0.05 inch and 0.005 inch, respectively. Hence, at this location, the practical limit of resolution on a contact print for an offset linear topographic feature is about 0.05 inch (roughly 0.1 mm), or 50 feet on the ground. Somewhat smaller offsets are probably evident on the film negative. Significantly better resolution is presumably attainable with other cameras and films.

Moreover, for the recognition of linear patterns, 9-inch contact prints at a scale of about 1:130,000, offer a minimum length of 11-miles of terrain in stereo and 18 miles in a single photo. Whether a geologist can recognize a given feature in these distances depends on the characteristics of the feature and the surrounding terrain and the skill and experience of the user.

Cholame Valley

Plates 11 and 12 (scale 1:133,000) show the San Andreas fault in Cholame Valley, about 50 miles northwest of the Carrizo Plain shown on Plates 9 and 10. This segment of the fault ruptured with several inches of right-lateral offset at the surface during the earthquakes of June - August, 1966 (Brown et al., 1967), however, the part of the fault on the right half of Plate 12 is difficult or impossible to detect at this scale. (Plates 11 and 12 were taken in November 1967, after the earthquake.) The recently active traces are evident on large-scale photos, on which they were located by both Dickinson (1966) and Brown before the 1966 movement. The active traces were mapped in more detail after the earthquake, again using large-scale photos (Brown et al., 1967, p. 10).

R. D. Brown, Jr. (written communication, 1968) has inspected Plates 11 and 12. He pointed out that scarps and mounds 1 to 2 feet high, small contrasts in vegetation and depressions mark the active trace in the places where it is not visible on these Plates. Apparently these features or their linear nature are too small to be evident

at 1 133,000 scale. Thus, although the San Andreas fault is a thoroughgoing linear feature in this region, plainly visible on large-scale airphotos, it does not show locally on the high altitude photos if the elements that mark its position are too small to be resolved or recognized.

However, Brown found other characteristics of the high altitude airphotos that made them valuable to a study of the fault in the Cholame Valley area. One feature the photos show, as a result of their broad but relatively detailed view, is the systematic deflection of many northeast-trending channels at B (Plate 12). The deflection is apparently the result of right-lateral deformation of downstream reaches of the channels. This relationship was not obvious either on the limited coverage of large-scale airphotos or the generalized topography of a 1 62,500-scale map.

Another characteristic Brown noted is that the large stereo view of the high altitude photos reveals a broad but discontinuous alluvial surface northeast of the fault (C) that is now being dissected, apparently as a result of recent fault movement. As has been pointed out elsewhere in this report, this relation can be gleaned from topographic maps or a mosaic of larger scale airphotos, but not nearly as easily nor are the relations as obvious as on small-scale stereo airphotos.

Flow Patterns in Water

Small-scale photos have proven useful in the study of patterns of tidal currents. Cameron (1961) described the use of 1 80,000 photos in such studies near New Brunswick. The U S Geological Survey has employed the small-scale photos described in this report to record the distribution and flow patterns of suspended particles in San Francisco Bay. Plate 13 (1 140,000) shows the southern part of the bay. Three such pictures, taken within about 5 minutes of each other, cover the entire bay, effectively recording flow patterns and relative sediment distribution during that time interval. A series of these pictures, taken at different times during a tidal cycle, at different seasons and during periods of unusual runoff, would record a wide range of current and sediment conditions.

If it had sufficient resolution, a single photo at a scale of about 1 400,000, covering the entire bay, would be the most efficient way of making this particular study. Perhaps suitable photos will be available in a few years from satellites. However, at present, high altitude photos offer the best way of accomplishing this work.

Moreover, an instantaneous view of a large area might be useful in studies of the waxing and waning of floods, waver patterns, eolian transport, of any other phenomenon characterized by rapid changes over a large area.

SUMMARY OF GEOLOGIC USEFULNESS

The foregoing examples of geologic uses of small-scale airphotos are limited in scope and application, yet, hopefully, they illustrate the general utility of these photos in work on geologic problems. Unfortunately, none show clearly an important attribute of small-scale photos illustrated and emphasized by Hemphill (1958, fig 6), that a broad view may reveal subtle but pervasive regional differences between lithologic units in topography, reflectivity or vegetation (expressed as photographic texture or tone)

Summarizing the uses illustrated above

- 1 High-altitude, high-oblique airphotos show vast areas in one view, introducing a geologist or his audience to the salient geographic and topographic attributes and many geologic features of an area
- 2 Small-scale vertical airphotos
 - a Offer the most efficient method of discovering the major topographic features and, commonly, important structural and lithologic characteristics of new or unfamiliar terrain
 - b Show a broad region in one 3-dimensional view that may reveal relations or suggest geologic hypotheses not otherwise apparent
 - c May reveal features of such extent, subtlety, or discontinuity that a broad view is necessary to recognize them
 - d Instantaneously record rapidly changing conditions over large areas, such as tidal flow and surface wind patterns

Anyone can correctly argue that nearly any feature displayed by or "discovered" on small-scale airphotos, can be recognized by an experienced and astute geologist using a topographic map and large-scale photos or field investigation. The major claim made in this report is that small-scale photographs furnish the geologist with another tool, that helps make geologic features evident to him and thereby makes him more effective, either by saving time or by revealing relations he might otherwise miss because of lack of experience or astuteness.

RESOLUTION AND SCALE

High resolution appears to be an important aspect of the usefulness of small-scale photos, particularly if a feature is expressed by small, discontinuous elements that require such resolution for detection.

Furthermore, an observer nearly always wants a closer look at any feature of interest. Magnifying a high resolution, small-scale image is nearly always more convenient than switching to another air photograph taken at larger scale.

Conceivably, in a few situations the detail resulting from high resolution of small features might obscure more subtle, larger elements of a photograph. It is always possible to degrade resolution or change tonal contrast of prints in order to search for things thus hidden, rather than to specify or accept inferior resolution in the original photos.

Thus, the most versatile airphoto would be one taken at the smallest useful scale and capable of magnification to the largest practical scale for a given project. Such an ideal is most closely approached by using very fine-grain films that yield transparencies, which in turn are analyzed on light tables equipped with high magnification stereoscopes. A far more practical solution for most geologists, however, is to translate this ideal into terms compatible with his equipment and methods.

For most geologists a major advantage of airphotos is their ease of use in the office and in the field. Convenient use of the information on airphotos in such locations virtually demands prints rather than transparencies and light tables, and simple 2X to 4X magnifying stereoscopes rather than bulkier stereoscopes of higher magnification. Prints and simple stereoscopes can be and are used almost anywhere by geologists. Faced with the option of using high resolution transparencies plus a high magnification stereoscope as opposed to prints at two scales yielding the same information with a low magnification stereoscope, I suspect most geologists would pick the latter as being more convenient for their type of use. Such an attitude will prevail until transparencies become as easy to view, annotate, and carry, along with the necessary stereoscopes, as are prints and common stereoscopes.

The useful limit of magnification for ordinary paper prints of most airphotos is about 3X, based on my comparisons between magnified small-scale photos and unmagnified photos of larger scale (e.g., Plates 5, 7 and 8). Hence, the most effective use of small-scale photographs for geologic field work dictates that they be available in scales differing by roughly a factor of 3. The geologist should pick the large-scale photos best suited to his project and then attempt to secure smaller scale photos according to the above guide. Thus, in the project described earlier at Green Creek, photo scales of 1:16,000, 1:60,000 and 1:125,000 are reasonably close to the 1:16,000-1:50,000-1:150,000-1:450,000 scales suggested as most suitable. Hopefully, such a spread in scales permits the most efficient transition from one scale to the next larger and allows small-scale views of features of a wide range of sizes.

With scale ratios of 3:1, each photo of one scale covers 9 times as much area as those of the next larger scale. Once coverage is obtained of an area at the largest, "working", scale, additional coverage at 1/3, 1/9, and 1/27 of that scale means an increase in the total number of photos for the project of 11, 12, and 14 percent, respectively. These are quite small increases in view of the potential benefits to be gained, assuming the small-scale photos already exist, and do not have to be flown for the project.

MOSAICS

Various types of assembled large-scale photos, from photo indexes to carefully matched and controlled mosaics, yield a single view of large areas, and are commonly reduced to scales of 1:100,000 or smaller. Such mosaics may be very useful in the absence of single small-scale photos, but in comparison to the latter, mosaics have two major disadvantages

- 1 Line and tone discontinuities between adjacent photos greatly reduce the usefulness of assembled photos. Minimizing or eliminating these discontinuities is difficult and expensive
- 2 A mosaic of photos cannot be viewed stereoscopically. Most of the applications of small-scale photos described in this report would have been more difficult, and some would have been impossible without stereo. Hence, mosaics would have been a poor substitute in these applications.

Of course, mosaics of small-scale photos will be valuable in certain regions until orbital photos that cover the same area become available. Once aircraft and satellite photos at all scales become available for the entire earth, mosaics will likely become obsolete except for such uses as world photomaps or cloud-free images of an entire hemisphere.

AVAILABILITY OF SMALL-SCALE AIRPHOTOS

The 1:60,000-scale airphoto covers most of the U.S. They were flown in the 1950's with 6-inch lenses and are sold by the Map Information Office of the U.S. Geological Survey in Washington, D.C. Airphotos of smaller scale, such as the California 1:90,000 photos, are available for a few areas. As far as I know, all are larger than 1:100,000 scale. The series of 1:125,000 to 1:145,000-scale vertical and corresponding high obliques described in this report are available for research purposes from the U.S. Geological Survey in Menlo Park, California.

Although present nonmilitary jet aircraft cannot attain the altitudes from which the photos in this report were taken (ca. 70,000 feet), operational commercial jet photographic aircraft equipped with "superwide-angle" cameras will yield comparable scales. These aircraft can operate near 50,000 feet (Bock, 1968). "Superwide-angle" lenses have a focal length of about 3-1/2 inches that produces a 9-inch image, and have been used for years. The 190,000 California photos were made with such a camera in 1964. At 50,000 feet above the surface a superwide angle lens yields an image scale near 1:175,000. Thus, operational commercial air photographic equipment can presently produce scales smaller than those of the photos in this report.

Such a system, in essence, has been in use since mid-1968 by the Phoenix Research Unit of Water Resources Division of the U.S. Geological Survey. Members of that group modified a T-33 jet trainer to accept a KA-50A superwide-angle camera loaned by the U.S. Navy. The camera uses 5-inch roll film and has a 1-3/4 inch focal length lens, yielding the same ground coverage as does a 3-1/2 inch lens on 9-1/2 inch roll film from the same altitude.

The camera was obtained from the Navy specifically for this evaluation of small-scale airphotos and a related study of small-scale, low sun angle airphotos. However, the Phoenix Research Unit has since used the camera and aircraft for many other projects involving collection of hydrologic and geologic data. Virtually all the photos are taken from about 35,000 feet, yielding scales of roughly 1:120,000 on 9-by-9-inch enlargements. The Phoenix Unit finds that the small-scale photos commonly offer the best way of studying such hydrologic phenomena as water flow, wave patterns, flooding and pollution.

Plate 14 shows a 2X enlargement of a portion of the Garlock fault taken with this camera from about 32,000 feet. The picture was one of a series obtained in early morning to study small-scale photos taken with a 6-inch lens ("normal" wide-angle) on 9-1/2-inch film from roughly twice the altitude. The flight lines and ground coverage were nearly the same for the two flights, but the sun angle is quite different.

The purpose of Plates 14 and 15 is to compare the effectiveness, for geologic purposes, of the photographs taken by cameras with superwide- and wide-angle lenses. Unfortunately, the great difference in illumination between the pairs prevents any meaningful comparisons of tonal differences. However, there is little reason to believe that focal length should significantly affect the rendition of tone contrasts. Furthermore, a careful comparison of sharpness is difficult, because no control existed over such factors as type of film, camera vibration, film processing and printing. Resolution should, however, deteriorate more rapidly towards the sides of the image of the shorter focal length camera, other things being equal (Gruner and others in Thompson, 1966, p. 86).

As far as geologic interpretation is concerned, the primary difference between the images is the greater parallax in those made with the shorter focal length lens. Greater parallax leads to greater apparent stereo relief and increased relief distortion (Ray, 1964, p. 14). In most of the examples cited in this report, exaggerated relief would make interpretation easier. Certainly this is so when the problem includes identification of geologic features that are expressed topographically. Exaggeration also helps in the study of old erosion surfaces by more clearly separating those at different elevations. On the other hand, exaggeration and distortion of relief would be detrimental when features marked on airphotos are transferred to maps with a reflecting projector rather than by inspection or with a plotter.

A potential disadvantage of short focal length lenses arises in areas of rugged topography because some parts of the surface may be hidden from the camera. With respect to a 9-inch square image size, a camera with 6-inch lens has a 90° field of view between opposite corners and about 74° between opposite sides, whereas a $3\frac{1}{2}$ inch lens (or $1\frac{3}{4}$ inch lens with a $4\frac{1}{2}$ inch image) includes about 120° between corners and 104° between sides (Fig. 5). This means that a camera with $3\frac{1}{2}$ inch lens will not "see" slopes steeper than 38° that are facing away from the camera along the sides of the flight path, whereas a camera with 6 inch lens will miss only those slopes steeper than 53° along the edges of the flight path. Of course, the amount of terrain thus hidden from the camera will be reduced if there are adjacent, overlapping flight lines. Thus, in general, the amount of terrain hidden from a $3\frac{1}{2}$ inch lens is small except in very steep terrain.

Some of the remarks about relief and hidden slopes are illustrated by Plates 14 and 15. Tops and bottoms of both pairs of images extend fully to the edges of the original photos. The increased relief and relief distortion and poorer resolution in 14 is obvious. But also notice that little information is missing in Plate 14 from the slopes along the edges as compared to Plate 15, because of the low angle of view.

Thus, a camera with a short focal length lens appears to be generally suitable for geologic interpretation except in areas of particularly steep terrain or for problems in which relief distortion must be minimized. Even then, however, such disadvantages can be removed, by using sufficient side lap between adjacent flight lines to eliminate the need to use the edges of the photos.

Although all of the photographs evaluated for this report were taken in black and white, color should be entirely suitable for small-scale airphotos, either from high altitude (ca. 70,000 feet) or from medium altitude with superwide-angle lenses. Certainly the excellent quality of color pictures from Gemini and Apollo spacecraft indicates

that high altitude does not significantly diminish the usefulness of color photographs for the study of the surface of the earth. Moreover, given proper anti-vignetting filters, superwide angle lenses should also be able to produce good color pictures (e.g., Duddek, 1968, p. 158-160). Indeed, the Phoenix Research Unit of the U.S. Geological Survey has routinely and successfully used Eastman type 2448 Ektachrome and 8443 Infrared Ektachrome with the superwide angle camera described above, at altitudes up to 35,000 feet.

Hence airphotos in both black and white and color, at scales as small as 1:175,000 are within the present capability of commercial aerial photographers. Smaller scales from aircraft await the routine and unclassified use of superwide angle cameras in high-altitude military aircraft, or the availability of this type of aircraft to private firms. At 70,000 feet a superwide angle camera with a 9" square image yields a scale of 1:240,000. Such photos could be useful in many projects today, if they were available.

OTHER USES OF SMALL-SCALE AIRPHOTOS

Disciplines other than geology may find small-scale airphotos useful. Surveys of large regions for cartography, forestry, agriculture, land and resource management, and urban planning could use small-scale airphotos if resolution is sufficient to the task. For example, the U.S. Geological Survey selected the 1:140,000 high-altitude photos described in this report as the most rapid, economical and accurate method of revising 1:250,000 scale maps in the San Francisco Bay area to show shorelines changed by landfill operations, and new highways. The high-altitude photos were chosen because they contained the necessary information in the smallest number of photos, and offered a more efficient source of the information than alternatives such as large-scale maps or other types of records.

Moreover, it is likely that many of the photographic projects contemplated for earth resources satellites (e.g., Badgley and others, 1967), could be effectively carried out now by the systems described in this report. Certainly if small-scale orbital photos are claimed to be a more effective or efficient way to do some tasks presently accomplished by large-scale airphotos, then currently available small-scale airphotos will also be more effective and efficient for such tasks. Moreover, projects of a regional nature which are contemplated or proposed for satellites because they cannot be reasonably or practically carried out now by large-scale air photographs, might effectively be done now by airphotos of the scale described in this report.

The first earth resources satellites will probably secure photos at small scales, perhaps 1 500,000 to 1 1,000,000 (for a 9-inch image size) and televise them to earth (Report for the committee on NASA oversight, 1968, p 24-25). As explained elsewhere in this report, these photos will be most useful if studied along with photos at 3 to 4 times their scales. Presumably, earth satellites will eventually be able to produce vertical photos which range in scales from a single view of an entire hemisphere to the larger scales commonly used now in aerial photography. Furthermore, increases in resolution of the image transmission system of the use of film recovery will likely make photos from orbit as good as those obtainable from aircraft.

Eventually a resources satellite will probably be capable of producing all the photographs necessary for detailed geologic studies of any region. However, this does not mean that a satellite will be the most economical or efficient way of obtaining all the necessary photographs. Certainly, during the development of orbiting photographic systems there will always be a scale larger than which aircraft systems are most economical. This "boundary scale", separating practical aircraft and orbital photographic systems, will doubtless become larger as satellite photographic systems develop. However, it will probably be at some value large enough to require general use of aircraft-mounted cameras for at least a decade or several decades, assuming we employ aircraft and satellite camera systems as they are presently conceived.

The small-scale photographic systems described in this report are not in immediate danger of being replaced for earth resource studies, by cameras in orbit. Earth resource satellites are not yet operating, and when they do, early models are not likely to produce images with the scales or resolution of the photos described in this report.

Thus, the small-scale airphotos have a definite use now and perhaps for years to come in earth resource work. Hopefully, this report will stimulate users to either obtain and use available small-scale aerial photos or order such photos flown for their projects, using available aircraft and cameras.

REFERENCES

- Badgley, P C , Childs, W. L. Vest, 1967, The application of remote sensing instruments in earth resources surveys Geophysics, v. 32, no 4, p. 583-601.
- Blackwelder, Eliot, 1931, Pleistocene glaciation in the Sierra Nevada and Basin Ranges Geol Soc America Bull , v. 42, p 865-922
- Bock, A. C., 1968, A breakthrough in high-altitude photographs from jet aircraft Photogrammetric Eng , v. 34, no. 7, p 634.
- Brown, R D , Jr , J G Vedder, R. E Wallace, E F Roth, R. F Yerkes, R. O. Castle, A. O. Waananen, R W. Page and J. P. Eaton, 1967. The Parkfield-Cholame, Calif., earthquakes of June-August 1966, surface geologic effects, water resources aspects, and preliminary seismic data U.S. Geol. Survey Prof. Paper 579, 66 p
- Cameron, H. L , 1961, Interpretation of high-altitude, small-scale photography Canadian Surveyor, v. 15, p 567-573.
- Clark, M. M., 1967, Pleistocene glaciation of the drainage of the West Walker River, Sierra Nevada, California Unpublished Ph.D. thesis, Stanford University, 130 p
- Dibblee, T. W , 1967, Aerial geology of the western Mojave Desert, California U.S. Geol. Survey Prof. Paper 522, 153 p.
- Dickinson, W. R., 1966, Structural relationships of San Andreas fault system, Cholame Valley and Castle Mountain Range, California Geol Soc. America Bull , v. 77, p 707-726.
- Duddek, M , 1968, Wild mapping cameras for color, in Smith, J T., Jr., ed. Manual of color aerial photography, Falls Church, Va., Am. Soc Photogrammetry, 550 p
- Hemphill, W R., 1958, Small-scale photographs in photogeologic interpretation Photogrammetric Eng., v 24, no. 4, p. 562-567.
- Jennings, C W , J. L. Burnett and B W Troxel, 1963, Geologic Map of California, Olaf P Jenkins Edition, Trona Sheet California Div. Mines and Geology, 1 250,000
- Ray, R. G., 1960, Aerial photographs in geologic interpretation and mapping U.S. Geol Survey Prof. Paper 373, 230 p

- Report for the subcommittee on NASA oversight, 1968, Earth resources satellite system Committee on Science and Astronautics, U S House of Representatives, 90th Congress, 2nd Session, Serial W, December 31, 1968, Washington, D C , 1968
- Rogers, T H , 1966, Geologic Map of California, Olaf P. Jenkins, ed., Santa Ana Sheet California Div Mines and Geology, 1 250,000
- Sharp, R P., 1965, in Wahrhaftig, C. A., and R P Sharp, Sonora Pass Junction to Bloody Canyon, in Guidebook for field conference 1, Northern Great Basin and California Internat. Assoc. for Quaternary Res , 7th Cong., 1965, p 74-84
- Smith, A. R , 1965, Geologic Map of California, Olaf P Jenkins edition, Bakersfield Sheet California Div. Mines and Geology, 1 250,000.
- Thompson, M. M , ed., 1966, Manual of Photogrammetry, v. 1, 3d ed., Falls Church, Va , Am. Soc. Photogrammetry, 535 p
- Wallace, R. W , 1968, Notes on stream channels offset by the San Andreas fault, southern Coast Ranges, California, p 6-21, in W R Dickinson San Andreas fault system School of Earth Sciences, Stanford Univ.

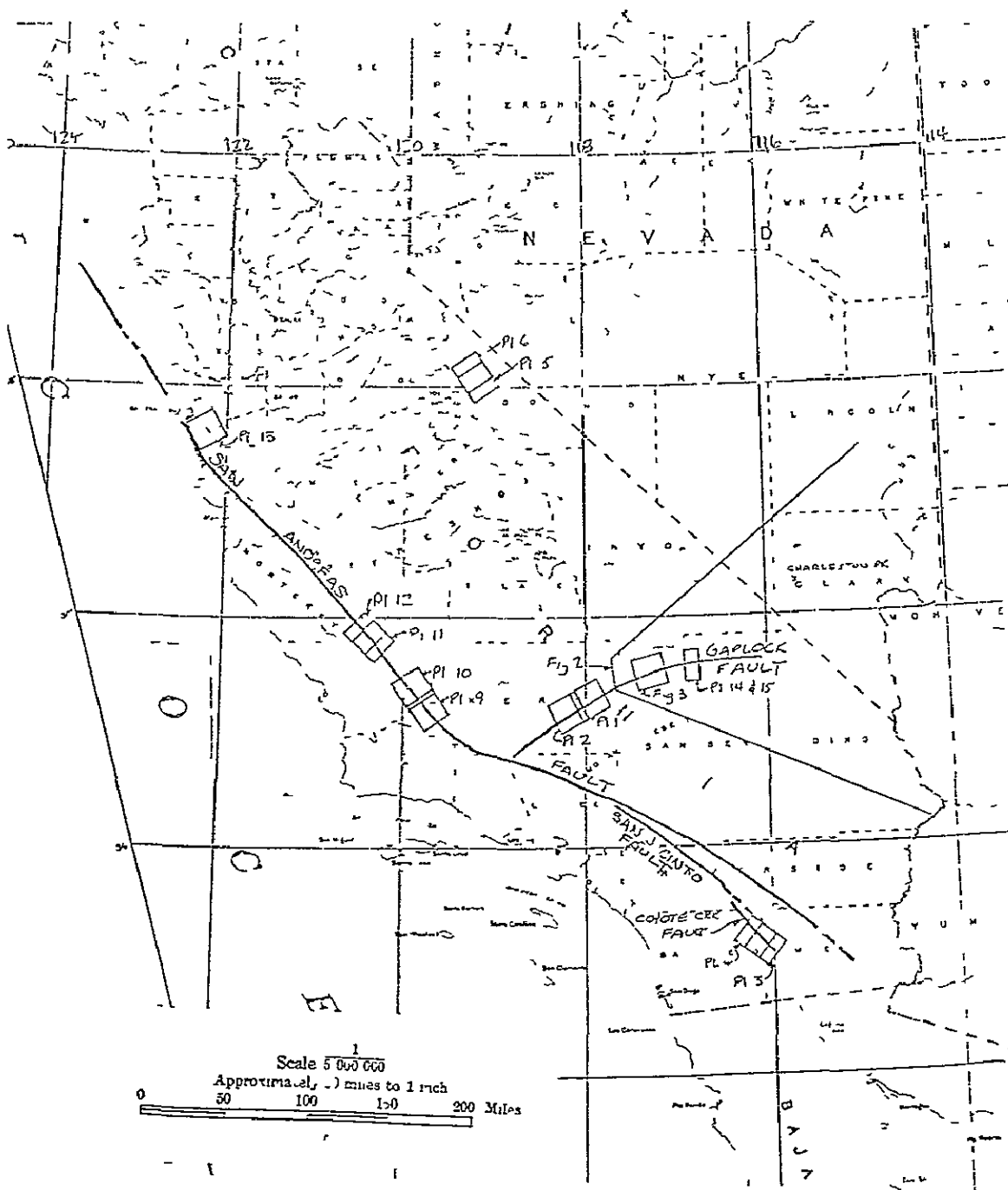


Figure 8-1 - Locations and approximate coverage of high altitude photographs shown in figures and plates



Figure 8-2.- Oblique photo taken from 60,000 feet. View is eastward along the Garlock fault (A-A'), which separates the Mojave Desert to the south from the Great Basin region to the north (see also Fig. 8-3). Although not active in historic time, the Garlock fault exhibits many of the same surface features as the active San Andreas fault, including offset stream channels and aligned scarps, valleys, trenches and depressions, all of which make it conspicuous in Figures 8-2 and 8-3. Over this large area the photo shows the positions and varied relations between eroded hills and mountains, their surrounding alluvial aprons and the playas at the lowest points of many closed drainage systems. Details of tone and erosional texture permit discrimination and tentative identification of lithologic units such as the dark volcanic rocks at B. (Locations of figures and plates are shown in figure 8-1.)

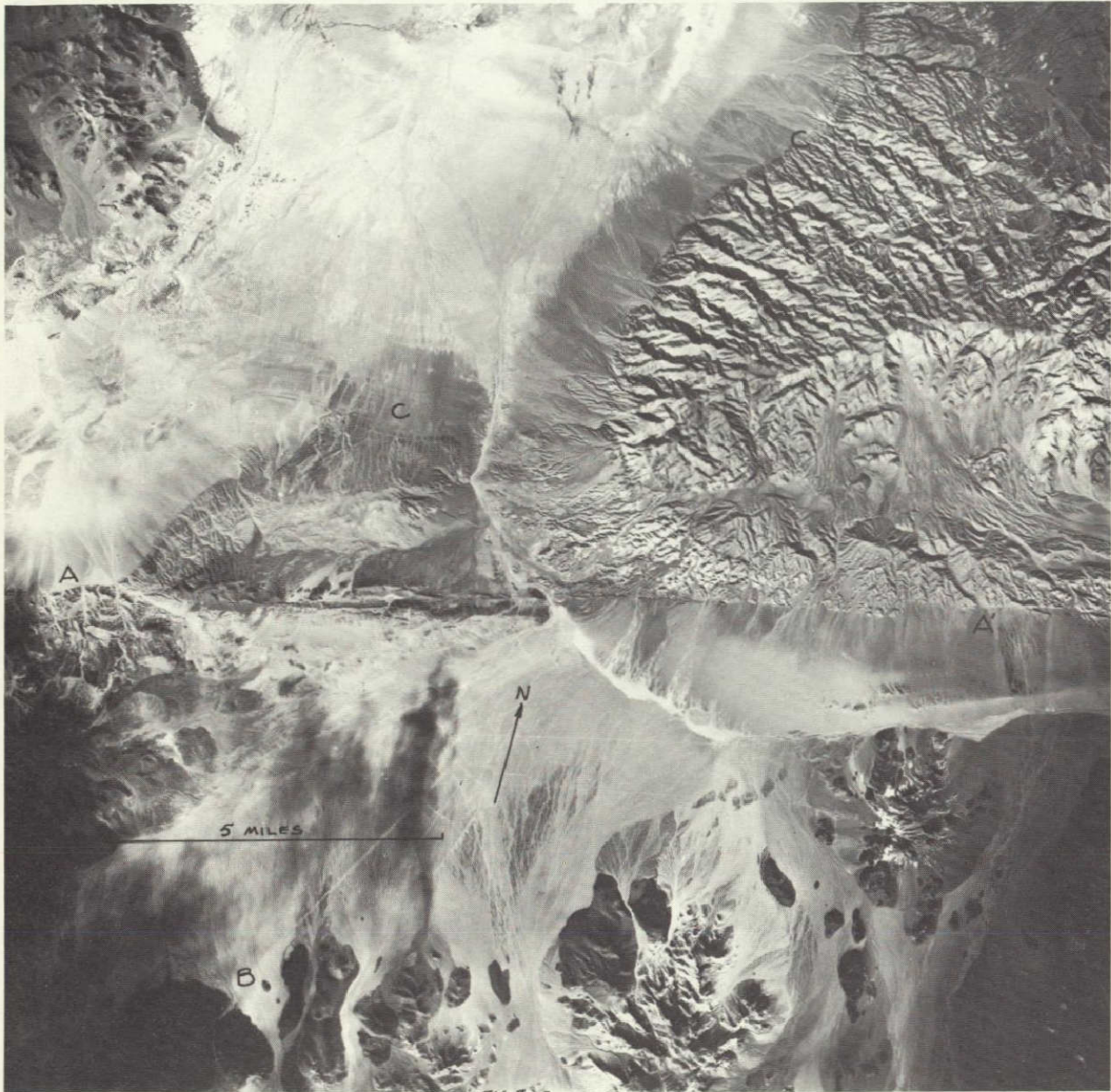


Figure 8-3.- (1:120,000). Small-scale view of the Garlock fault (A-A') near Searles Valley. Cloud shadows obscure detail of volcanic rocks in the southwest corner at B. Shorelines of Pleistocene Lake Searles are evident at C; the modern playa is just beyond the north edge of the photo.

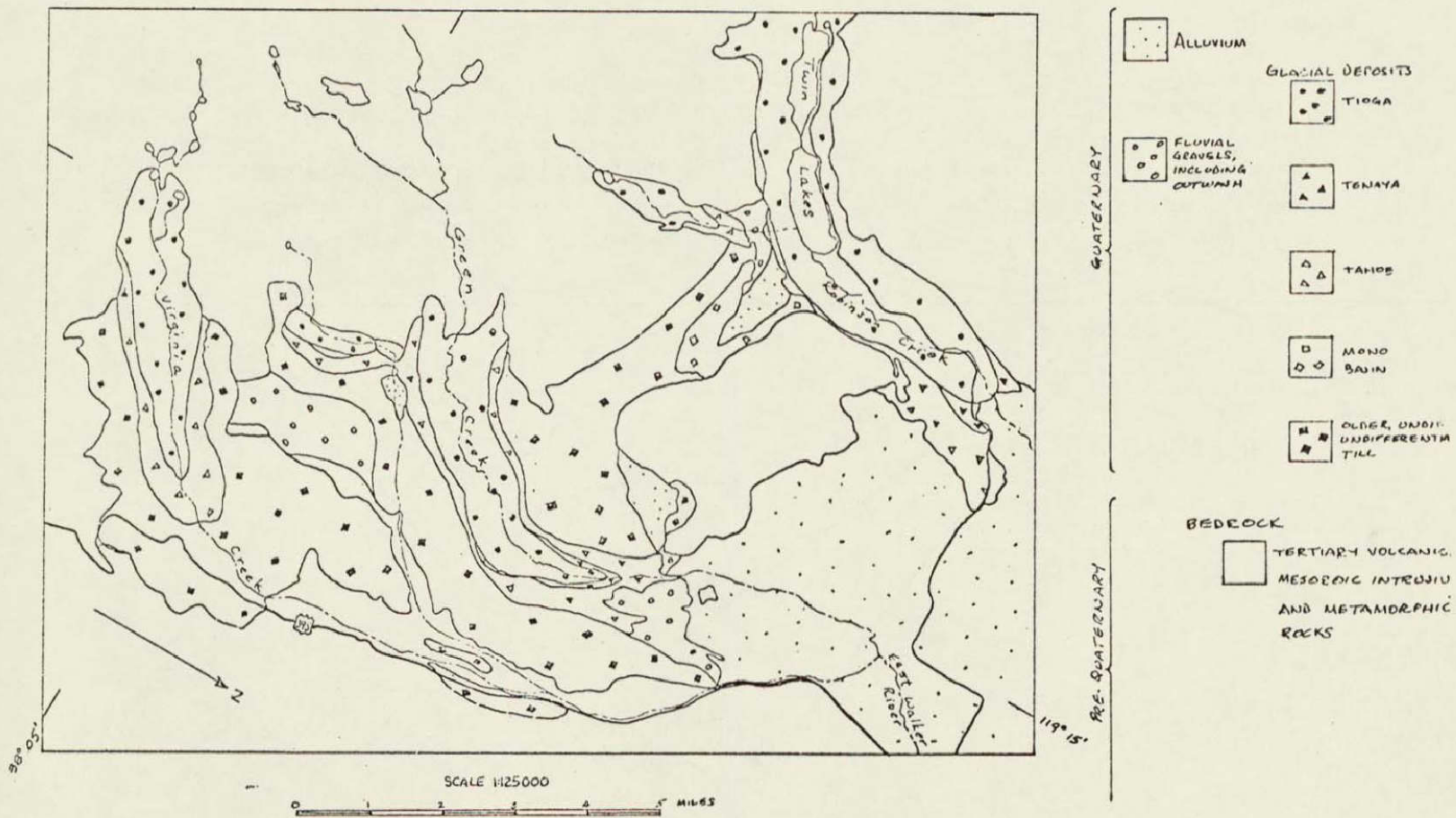


Figure 8-4.- Geologic map of Pleistocene glacial deposits near Virginia and Green Creeks. This region is located on the east slope of the Sierra Nevada range, just north of Mono Lake.

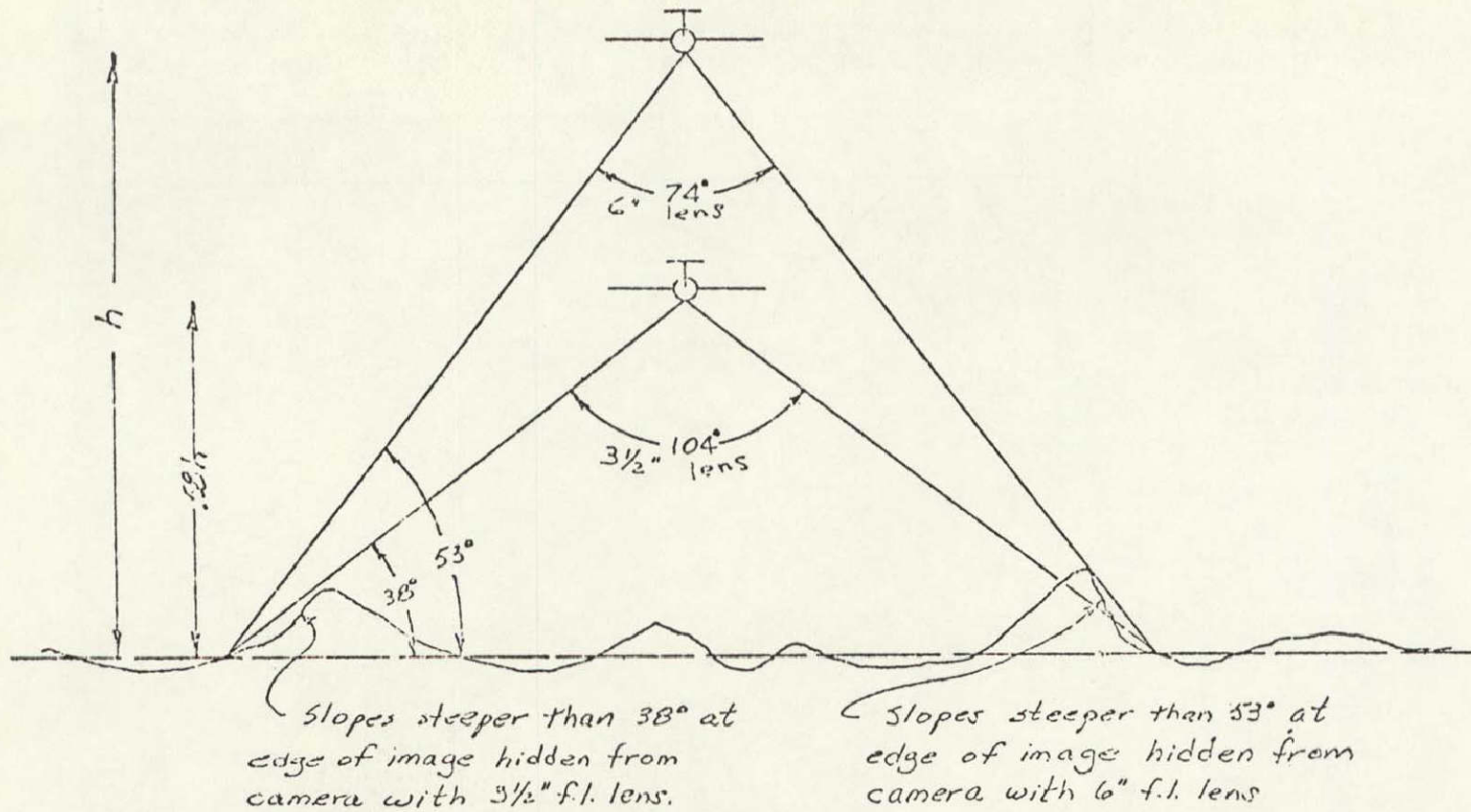


Figure 8-5.- Relations between flying height, h , angular field of view and terrain hidden from view of aerial cameras equipped with 6-inch and 3-1/2 inch focal length lenses and 9-1/2-inch roll film.



Plate 8-1.- (Scale 1:120,000). Koehn Lake, a playa crossed by the Garlock fault. Scarp A and lineament B are aligned with the prominent scarp of the fault at C. Scarp at D and tonal lineament at E are aligned with the portion of the fault that extends to the southwest beyond the photo (see Plate 8-2). Squares show coverage of existing 1:32,000 and 1:20,000 photos.



Plate 8-2.- (1:120,000). Portion of the Garlock fault (A-A') southwest of that shown in Plate 8-1 .



Plate 8-3.- (1:145,000). Southeast end of Coyote Creek fault. Southeast part of the surface rupture of April 9, 1968 earthquake is at A-A' (northwest portion of the rupture is on Plate 8-4). Previously known southeast extent of fault is at B. Lineations at C and D were identified on this photograph as probable extensions of the fault before the earthquake. E through J are old erosion surfaces. K is the canyon of Fish Creek Wash.

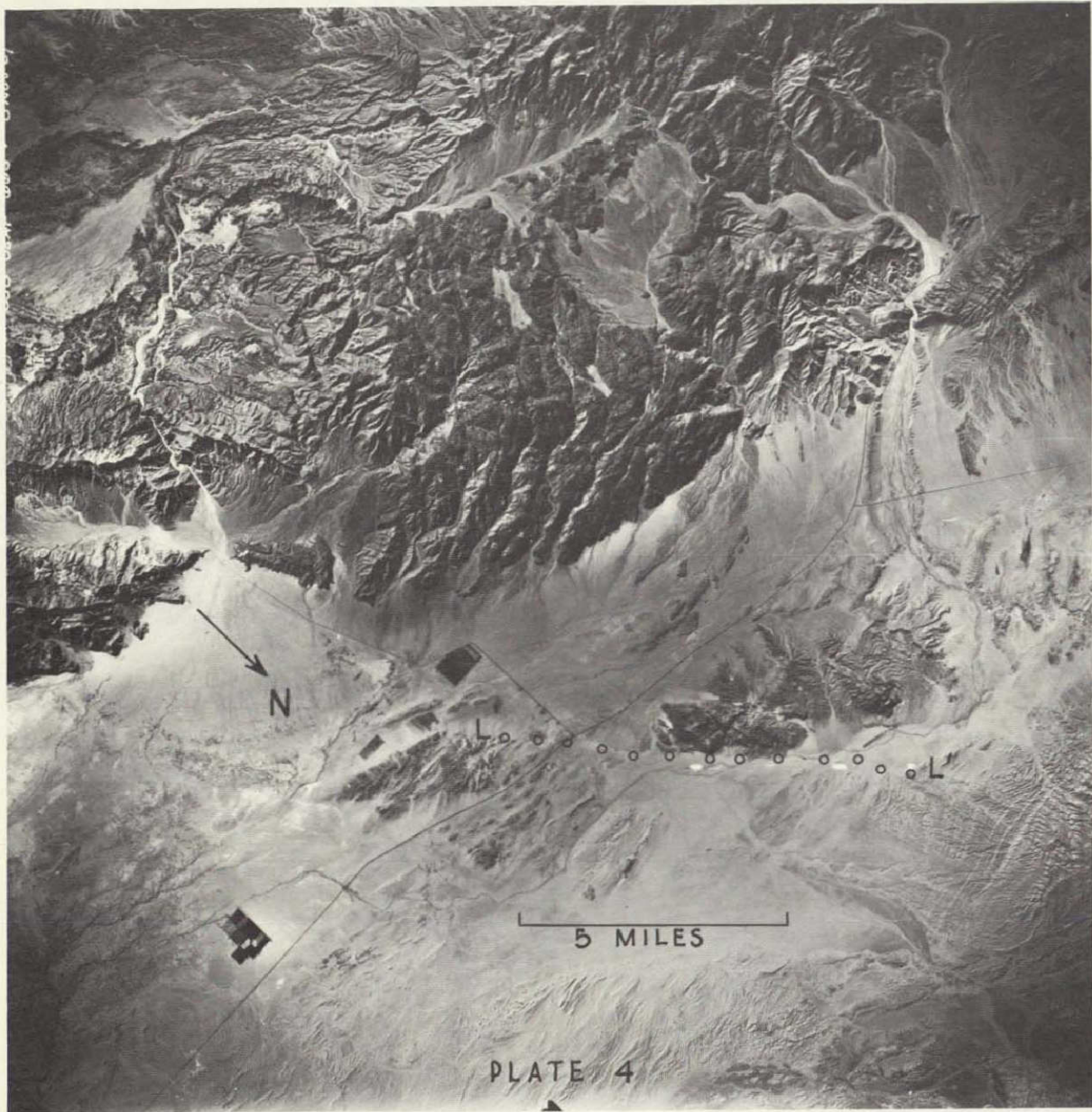


Plate 8-4.- (1:145,000). Southeast portion of Coyote Creek fault. Plate 8-4 forms a stereo pair with Plate 8-3. Line L-L' is the northwest branch of the main surface rupture of the Borrego Mountain earthquake of April 9, 1968.



Plate 8-5.- (1:125,000. See Figure 8-4 for map of this location.) Mono Lake and drainages of Virginia and Green Creeks. A, B and C are remnants of a postulated pre-Tahoe moraine of Virginia Creek. Curved ridges at D appear to be lateral and terminal moraines of an extensive pre-Tahoe glacier. Lineations at E-E' and F-F' are probably part of the range-front fault system of the Sierra Nevada.



Plate 8-6.- (1:125,000). Bridgeport Basin. Plate 8-6 forms stereo pair with Plate 8-5.



Plate 8-7.- (1:60,000). Green and Virginia Creeks. Location shown on Plate 8-5. Lineaments at E-E' and F-F' may be part of the Sierra Nevada range front fault system.

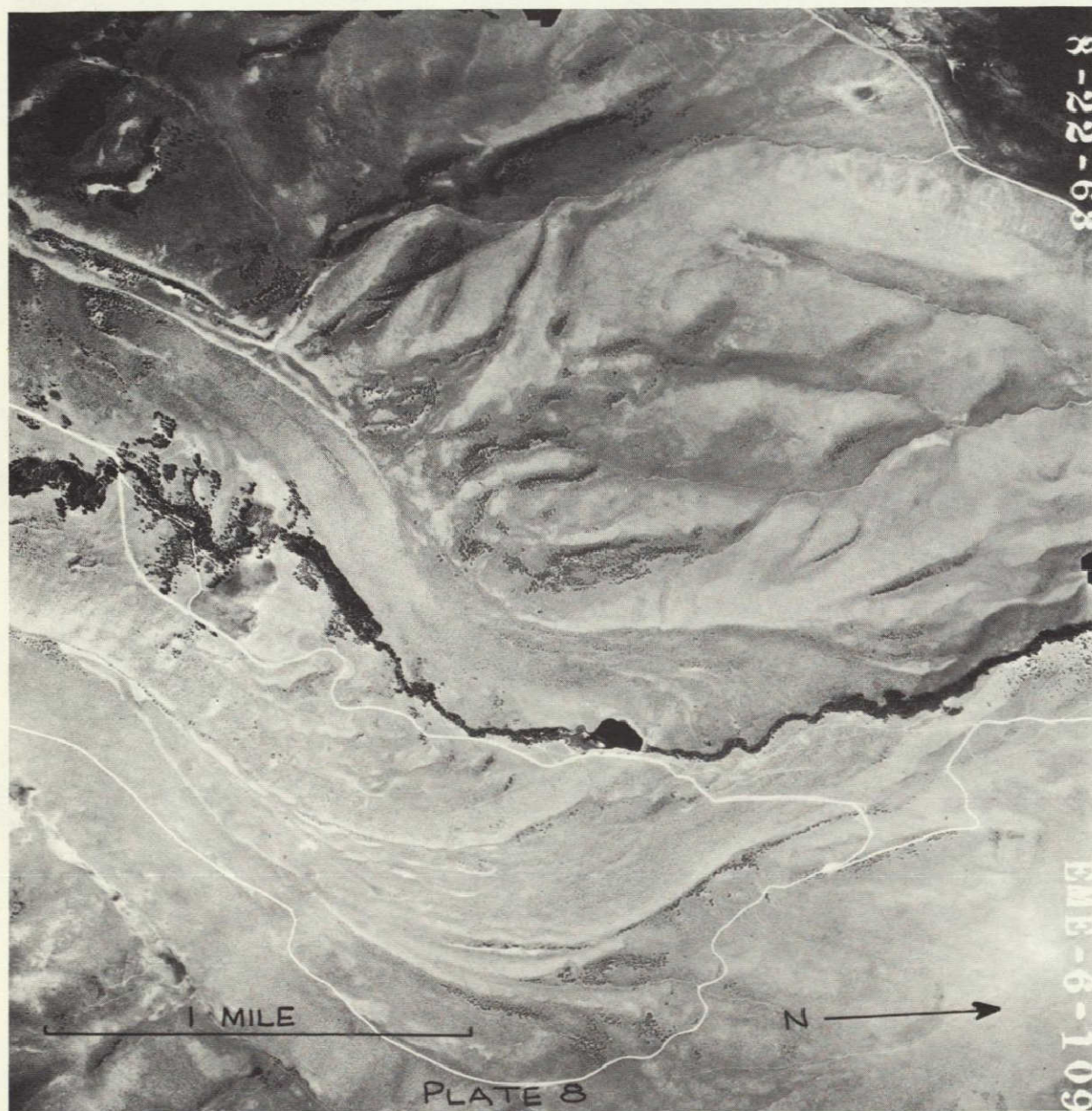
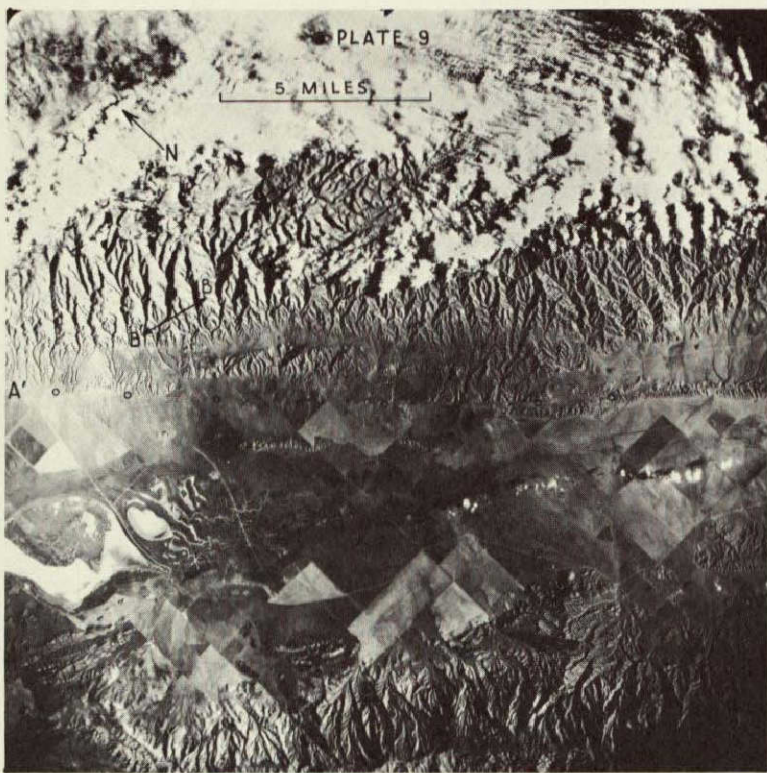


Plate 8-8.- (1:16,000). Wisconsin moraines near Green Creek.
Location shown on Plate 8-5.



Plates 8-9 and 8-10.- (1:133,000). San Andreas fault (A) at Carrizo Plain. Both plates show several stream channels offset by the fault.



Plates 8-11 and 8-12.- (1:133,000). San Andreas fault (A-A') at Cholame Valley. A group of deflected stream courses is at B. C is an old erosion surface, now being dissected.



Plate 8-13.- (1:140,000). Southern part of San Francisco Bay. San Mateo Bridge is at left center, and San Francisco Airport at top right. Three photos of this series record major surface water flow patterns of the entire bay.

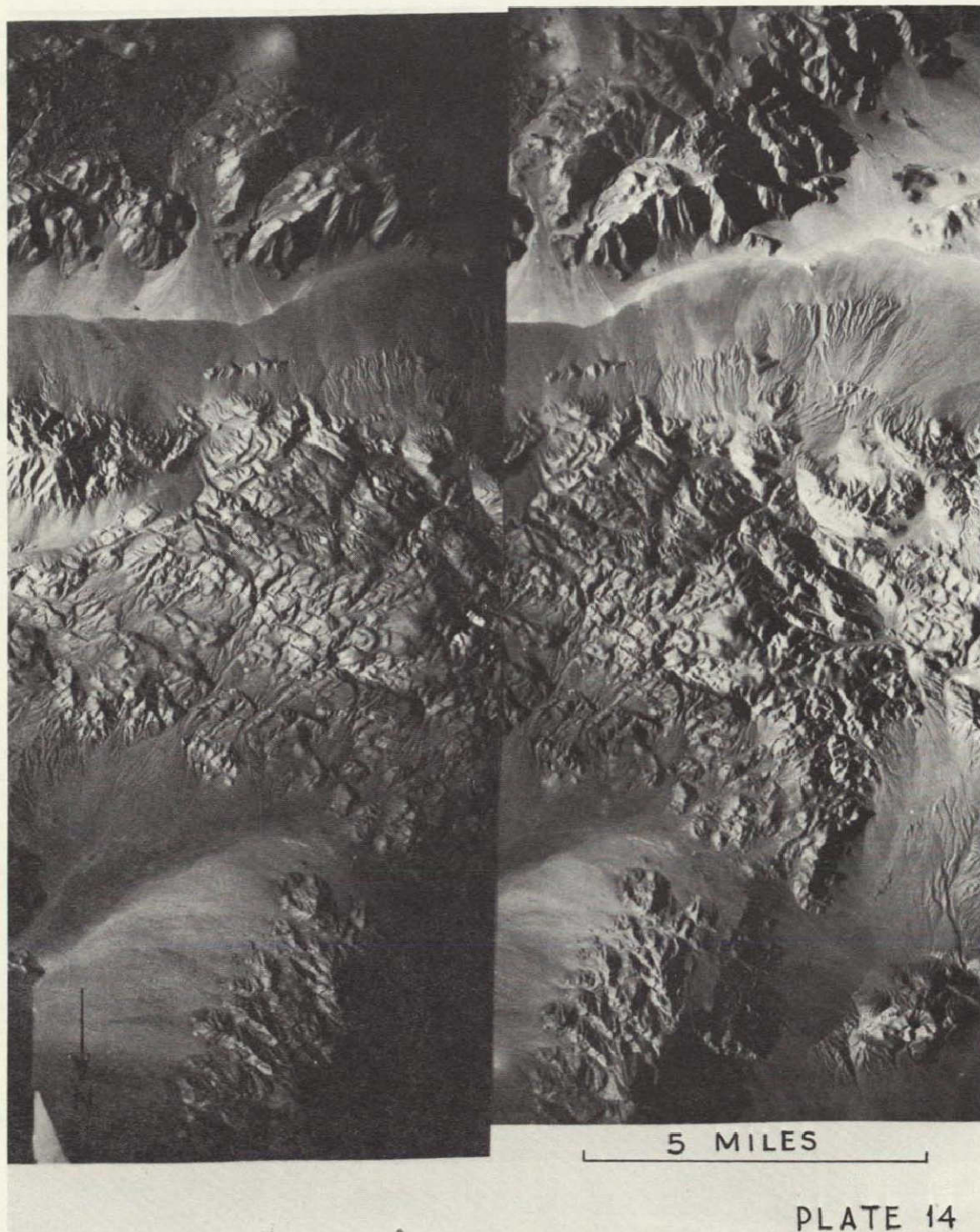
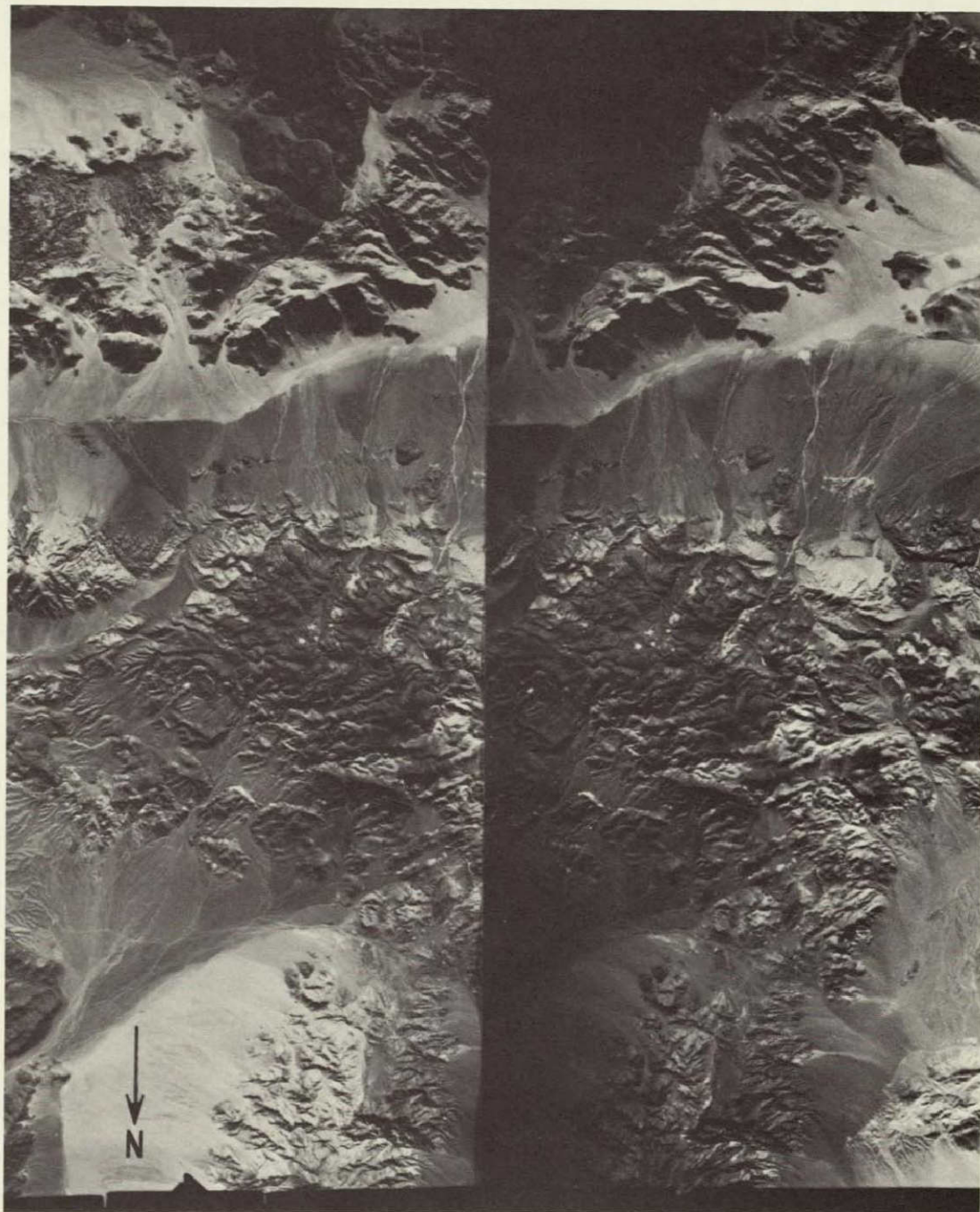


Plate 8-14.- (1:120,000). Stereo pair of Garlock fault zone taken with superwide-angle lens (1-3/4" focal length on 5" film; enlarged X2) from 35,000 feet.



5 MILES

PLATE 15

Plate 8-15.- (1:120,000). Stereo pair of Garlock fault zone taken with normal wide-angle lens (6" focal length 9 1/2" film) from 60,000 feet.

SECTION 9

EFFECTIVE RADAR LOOK-DIRECTIONS FOR GEOLOGIC INTERPRETATION

N71 - 19260

H. C. MacDonald

Center for Research in Engineering Science, Remote Sensing Laboratory
University of Kansas

ABSTRACT

The synoptic presentation of side-looking radar systems in combination with an oblique angle of incident "illumination" has provided enhancement of certain topographically expressed geologic features (such as faults and lineaments) which were neither obvious, nor interpretable on conventional aerial photography. Multiple imagery passes were not available for most areas previously studied, therefore, the capability for repeatedly recognizing these anomalous geologic features on multiple imaging passes, and the influence of a preferred look-direction (direction orthogonal to the ground track of the aircraft) could not be investigated. The recent availability of multiple flight coverage from eastern Panama and northwestern Colombia, however, has provided sufficient data for a semi-quantitative look-direction analysis in which the detection of certain geologic features under a variety of terrain conditions has been examined. The geologic features selected for this study are faults, joint systems, and dip slopes.

Specific examples from those areas of the United States (NASA imagery) with multiple pass coverage are compared with the data obtained from the Panama imagery, and it is apparent that look-direction does influence the detectability of certain geologic features. Depending on the relative topographic relief, effective incidence angle, and look-direction, geologic features can be advantageously enhanced or can be completely suppressed. Geological reconnaissance in poorly mapped areas will necessitate imaging from four orthogonal look-directions to provide maximum terrain information. However, where the terrain configuration or structural grain has already been determined, trade-offs between depression angle, range position, and look-direction will provide near optimum data retrieval with only two imaging passes.

INTRODUCTION

During the past year, because the University of Kansas has not received radar imagery generated for the NASA-ERS Program, our geological studies have been concerned primarily with the analysis of previously obtained K-band and a limited amount of C-P and L-band imagery. These investigations have concentrated on determining the value and effect of polarization, look-direction, depression angle, and frequency in the geological interpretation of radar images. The University of Kansas technical reports, which were submitted to NASA within the past year have generally emphasized the use of imaging radars for structural analysis, (Dellwig, et. al , 1968, Jefferis, 1969a, Jefferis, 1969b, Gillerman, 1969) however, one study (Dellwig, 1968) was concerned with an evaluation of long-wavelength imagery, and it appears there will be a real value in multifrequency imaging for geological reconnaissance studies. In previous studies, polarization has been shown (Gillerman, 1967) to be useful in some cases as a lithologic discriminant, but comparison of results in different geologic environments shows that a unique signature is not usually available from multipolarized K-band imagery.

The goal of future research will be to demonstrate the necessity and relevance of controlled experiments in which specific radar parameters are varied over selected geological test sites. These experiments will be conducted in different terrain environments where detailed geologic ground studies have already been completed. The importance of such controlled experiments can be readily realized when the results of a recent look-direction analysis (conducted during the last year at the University of Kansas) are examined (MacDonald, 1969).

Most investigators involved with radar imagery analysis are familiar with the fact that the synoptic presentation of side-looking radar systems in combination with an oblique angle of incident "illumination" has provided enhancement of certain topographically expressed geologic features (such as faults and lineaments) which were neither obvious, nor interpretable on conventional aerial photography. Multiple imagery passes were not available for most areas previously studied; therefore, the capability for repeatedly recognizing these anomalous geologic features on multiple imaging passes, and the influence of a preferred look-direction (direction orthogonal to the ground track of an aircraft) could not be investigated. The recent availability of multiple flight coverage from eastern Panama and northwestern Colombia, however, has provided sufficient data for a semi-quantitative look-direction analysis in which the detection of certain geologic features under a variety of terrain conditions has been examined. Although the bulk of the imagery used for this study was not gathered specifically for the NASA-ERS Program, the results of the experiment are directly applicable for future mission planning. It is the purpose of this presentation to relate both the conclusions derived from this look-direction study and to emphasize the pertinence of similar experiments for future NASA-ERS radar studies. Hopefully, these studies will permit specification of spacecraft imaging radars for geologic purposes.

RADAR PARAMETERS

Radar imagery provides terrain data in a format approximating a three-dimensional strip map. Because of the areal coverage generally supplied by radar imagery, the geologist can integrate subtle terrain features over large areas to extract useful information. The characteristics of side-looking radar suggest that look-direction¹ plays an important part in the detection of geologic features. The recent availability of multiple flight coverage of eastern Panama and northwestern Colombia has provided the first significant amount of radar imagery for an effective study of the influence of look-direction. A semi-quantitative analysis of the data will be presented later, but first, in order to understand why certain geologic features may be either enhanced or suppressed on radar imagery, specific fundamentals of radar operation and imagery interpretation must be understood.

The basic system operation of a typical side-looking airborne radar system (SLAR) is illustrated in Figure 1. The antenna (A) is repositioned laterally at the velocity of the aircraft (V_a). Each radar pulse transmitted (B) returns signals from the targets within the beamwidth. These signals are converted to a time/amplitude video signal (C) which is imaged as a single line (E) on photographic film (F). Returns from subsequently transmitted pulses are displayed on the CRT at the same position (D) as the previous scan lines. By moving the photographic film past the CRT display line at a velocity (V_f) proportional to the velocity of the aircraft (V_a), an image of the terrain is recorded on the film (F) as a continuous strip map.

Radar provides its own "illumination," and when the criteria for radar shadowing are met,² shadows are always created on that side of the terrain feature most distant from the transmitter. When terrain features are enhanced on radar imagery, the enhancement can usually be attributed to radar shadowing. Analogous examples of shadow enhanced terrain features have been observed on satellite photography taken at times of low sun angle. From orbital altitudes, particularly with the analysis of oblique images, shadowing from low angles of solar illumination has proven useful for accentuating otherwise subtle relief features. The geometric parameters of SLAR imaging systems are such that along the swath width of an area imaged (near to far range), there is a continuous change in the angle of incidence³ (Figure 2). SLAR systems which image the terrain at comparatively low incident angles provide shadows analogous to those formed on aerial photographs taken at comparatively low-sun

¹ Direction orthogonal to ground track of the aircraft

² When terrain back slope exceeds depression angle (see Figure 2)

³ The angle of incidence, θ , is that angle formed by an impinging beam of radar energy and a perpendicular to the incident surface at the point of incidence. The angle between a line from the transmitter to a point on the terrain, and a horizontal line passing through the transmitter is the depression angle

angles, however, on radar imagery, the shadowing of terrain features (of equal height and equal terrain back slope) increases from near to far ranges (Figure 2). Thus, a terrain feature exhibiting extensive shadowing in the far range, may be completely "illuminated" in the near range

SLAR systems use either a slant range or ground range presentation on their image recording CRT indicators. For this study, slant range imagery was used exclusively for analysis, and consequently the spacing between return signals on the image were directly proportional to the time interval between the terrain features being recorded. SLAR systems are designed to produce imagery with minimal scale distortions, however, aside from certain flight parameters which may influence image geometry, the most obvious distortion on slant range imagery is the continuous scale change in the range direction (orthogonal to ground track). Figure 3 illustrates the geometry of a square grid pattern that is crossed by two diagonal features, in one case showing the ground range geometry, and in another example the slant range geometry. In the far range, on the slant range display, the distance between adjacent points varies only slightly, whereas in the near range, large scale changes occur. Of particular importance to the geologist is the realization that linear terrain features (such as faults, joint systems and lineaments) which are oriented either parallel or normal to the flight path would normally show no distortion in orientation, whereas those features oriented obliquely to the flight path will have considerable orientation distortion in the near range. The near range compression and its resultant effect on the portrayal of geometric shape is illustrated in Figure 4, where the outlines of several islands in the San Miguel Bay area of Darien Province, Panama have been sketched directly from the radar imagery. Using imagery from six different flights, the outline of the islands show great distortion in the extreme near range (flights A, F), moderate distortion in the near range (flight E), and somewhat uniform outline in the mid-range (flights B, C, D). The apparent elongation of these islands parallel to ground track (flights A and F) is of particular significance to the geologist concerned with delineating linear landforms which might be indicative of structure.

Evaluation of radar-derived terrain parameters presents a multi-variable problem. Even when the inherent distortions of radar imagery are ignored, the quantification of radar-derived, geological parameters is complicated by 1) the divergent terrain environments in which these parameters are expressed, 2) the intricate relationship between terrain parameters and the radar return signal recorded on the imagery, and 3) the highly subjective approach necessary for the initial selection and identification of any geologic parameter interpreted from radar imagery. Noting these qualifications, an evaluation of multiple flight coverage from eastern Panama and northwestern Colombia has provided sufficient data for a semi-quantitative look-direction analysis in which the detection of geologic features under a variety of terrain conditions was examined.

LOOK-DIRECTION ANALYSIS

Many examples have been cited in the literature where radar has actually defined structural features such as lineaments and faults which had not been previously detected using normal geological reconnaissance methods (Dellwig, et al., 1968, Kirk and Walters, 1968, Hackman, 1966, MacDonald, et al., 1967, Snavely and Wagner, 1966, Levine, et al., 1966, Dellwig, et al., 1966, and Cameron, 1965). Unfortunately, multiple imaging passes were not available for these studies, because most areas were covered by only a single strip of imagery, the aspect of repeatedly recognizing anomalous terrain features with multiple flight coverage from different look-directions could not be documented.

The recently obtained (1967) radar imagery of eastern Panama and northwestern Colombia provided multiple imagery passes (in most cases four orthogonal look-directions and in all cases, at least two) over the entire region. Fortunately, the imagery was also collected during a three week time period which eliminates any speculation about seasonal changes which might have influenced the rain forest canopy, and thus affect the return signal on the radar imagery.

The Panama imagery includes both extensive areal coverage and multiple passes which provide a sufficiently large sample of data for a semi-quantitative analysis. Unfortunately, due to the classified nature of this imagery, specific examples illustrating different look-directions can not be shown. However, several examples of NASA imagery (in the United States) in locales familiar to most geologists are cited which illustrate the influence of look-direction on geologic interpretation.

Spanish Peaks, Colorado

The Spanish Peaks region, comprising approximately 5200 square km, is located mainly in Las Animas and Huerfano Counties in south-central Colorado (Figure 5). This region is well known to geologists for its diverse igneous rocks and structures, and topography is dominated by intrusive and extrusive igneous rocks, stocks, plugs, dikes, and sills which have invaded the sedimentary rocks over the entire region (Johnson, 1968). Although large igneous masses are characteristic of the areas of maximum local relief (2,375 meters), dike protuberances ranging up to 30 meters in both width and height dominate the terrain of flat lying sedimentary rocks. Most dikes are members of an extensive radial dike system associated with the main igneous mass of the Spanish Peaks.

Radar imagery of this region is ideally suited for evaluating look-direction, first because of the numerous rectilinear features which are topographically expressed, and second because of the availability of two separate strips of imagery, flown from opposing look-directions. When comparing the two radar images of the Spanish Peaks (Figure 5), the differences in shadowing by the dominant terrain features imaged from opposite directions is especially striking. West Spanish Peak and East Spanish Peak (B) and (C) respectively of Figure 5 are "illuminated" in both the near and far ranges. On image A the

two peaks (B) (C) cast a large distinctive shadow in the far range, whereas the same two features have minimal shadowing in the near range (image B). Similarly, dikes (A)-(A'), (D)-(D'), and (J) are accentuated by shadowing in the far range of image B, whereas these same features are less pronounced in the near range. On image A, dike (D)-(D') is subdued to such an extent that it is almost undetectable. This same distinction between the appearance of terrain features in the near and far ranges is illustrated east of area (H) where a subparallel dike system is much better defined in the far range of image A than in the near range of image B.

The imagery of Spanish Peaks also reveals the influence of look-direction on the delineation of stream drainage patterns. In the far range of image A the channel of the Apishapa River (G) can be easily traced, however, the same stream channel in the near range of image B is poorly defined. The perimeter of the drainage basin west of location (I) can be easily outlined on image A, but this same distinction is much more difficult on image B (near range).

Near range compression, a characteristic of all slant range systems (and previously illustrated in Figure 3) is disadvantageous when attempting to delineate topographic features which are oblique to the flight path. The presentation of the linear valleys of Figure 5 in area (E) on image A (far range) can be contrasted with area (E) of image B (near range).

Central Humboldt Range, Nevada

The Humboldt Range of western Nevada characterizes Basin and Range fault-block mountains, i.e., subparallel block-faulted mountain ranges separated by alluvial valleys of approximately equal size. The core of the central range illustrated in Figure 6 is composed predominantly of Triassic volcanics, whereas limestones comprise the younger strata flanking the mountain range on the west. The limestone-alluvium front-fault along the western front of the range is particularly pronounced on image A between (b) and (c). The northward-trending, westward dipping, high angle normal fault is conspicuous because of the triangular faceted, truncated spur ends, and steep, V-shaped canyons. On image B, taken from the opposite look-direction, the fault scarp is not as conspicuous.

Analysis of both images reveals that the accentuation of the fault scarp on image A is caused by the northwesterly orientation of the triangular slope facets bounding the fault scarp. These slope facets, oriented toward the look-direction, result in an extremely high return as compared with the lower return observed on image B. This preferred orientation highlights the alluvial-fault contact when imaged from one direction, however, it is not as well defined from an opposite look-direction.

The effect of shadowing in the delineation of minor streams is illustrated at location (D). In the far-range of image B the delicate dissection of topography resulting in numerous distributaries in the alluvial apron is well defined, but the same pattern cannot be detected in the near range of image A. The delineation of distributaries in the far range is totally attributable to alternate

highlighting and shadowing which is completely absent in the near range.

Boston Mountains, Arkansas

Multiple flight coverage over the southern portion of the Boston Mountains, Arkansas, has provided radar imagery over a geographic area that has received considerable attention by geologists involved in remote sensor studies (Dellwig, et al., 1968, Kirk and Walters, 1968, Dellwig, et al., 1966, and Kirk, et al., 1968). The detection of a pronounced system of north-south trending lineaments on radar imagery was the primary reason for concentration of effort in this particular area (Dellwig, et al., 1966). Initial field investigations provide evidence that the lineaments, originally delineated on low-resolution radar imagery are, in fact, structurally controlled stream valleys which appear to have the same general trend as one of the dominant joint-sets which are recorded at the outcrop.

A portion of this area is shown, and the north-south linearity of several stream valleys is well illustrated, in Figure 7. Three different directions have been provided, 1) look-direction perpendicular to the linear stream valleys (image A), 2) look-direction oblique to the stream valleys (image C) and 3) look-direction parallel to the trend of the stream valleys (image B). On the imagery of the flight perpendicular to these linear trends (image A) the enhancement of valleys (A)-(A'), (D)-(D') is particularly striking. These same valleys, however, do not express the distinctive linear parallelism on image B. Similarly, the linearity of (F)-(F') is well defined on image B (look-direction orthogonal to stream valley), whereas on image A, no such distinction can be made. Numerous other examples can be isolated when comparing images A and B, especially when the minor tributaries are examined (see for example, Area (C)).

Image C provides us with an intermediate look-direction, i.e., between the look-directions of A and B. The imagery produced at this intermediate look-direction appears to have compromising qualities for the detection of linear topographic features. This is to say that image C displays most of the linear features discussed above at an intermediate stage of definition between suppression and accentuation.

The question naturally arises, does look-direction influence the detection of lineaments in the terrain environment of the Boston Mountains (i.e., heavily wooded) even though most of the lineaments are expressed as stream valleys having a local relief up to 270 meters. Obviously, if the linearity of the stream valleys in this area had not been previously recognized on other imagery passes, and if only image B were available for analysis, the north-south linearity and parallelism of (A)-(A') and (D)-(D') would probably not have been interpreted except by an experienced interpreter.

Panama Imagery

Evaluation of multiple flight coverage from eastern Panama and northwestern Colombia has provided sufficient data for a semi-quantitative look direction analysis in which the detection of geologic features under a variety

of terrain conditions could be examined. The detectability of faults, joint-fracture systems, and dip slopes was selected for look-direction analysis because 1) they are significant to geologic reconnaissance studies, 2) in the tropical terrain environment these features are usually reflected in the topographic configuration which is recorded on the radar imagery, and 3) regardless of the rock type involved, these are ubiquitous features. The distinction between faulting and jointing on radar imagery, as with air photo interpretation, is often very difficult. As pointed out by Lueder (Lueder, 1959) when discussing photogeologic interpretive methods in areas in which there is absence of conclusive fault evidence, it is common to consider the longer, stronger linears as faults, whereas the shorter criss-crossing linears are interpreted as joints or joint systems⁴

In previous studies (Dellwig, et al., 1968, Kirk and Walters, 1968, and MacDonald, et al., 1967) concerned with the geologic interpretation of radar imagery, it had been observed that the relative topographic relief was one of the determining factors for the radar enhancement of certain geological features. For the present study, it was determined that two subcategories (based on local relief) would be applicable for the look-direction analysis, one subcategory less than 50 meters relief, and the other subcategory greater than 50 meters relief. These two topographic subdivisions are extremely subjective, at least in the Darien area of Panama, because of the limited topographic field data available. It is extremely important to emphasize that the boundary (i.e., 50 meters) between subdivisions of local relief is not a critical factor other than distinguishing between "high" and "low" relief areas. When sufficient multiple flight coverage becomes available in the United States, or any other country where adequate topographic data are available (contour interval 6 meters or less) a more definitive subdivision between "high" and "low" relief can be ascertained. Before examining the data from Table I, which is a summary of the data from a study by MacDonald (1969), it is necessary to define some of the terms used in this look-direction analysis.

Azimuth Azimuth is the angular relationship between the look-direction and the geologic feature imaged. For example, a geologic feature such as a fault, oriented perpendicular to look-direction would have an azimuth of 90 degrees, whereas a fault, reflected in a terrain configuration parallel to the look-direction would have an azimuth of 0 degrees.

Detectability A particular terrain configuration is sufficiently distinctive on at least one imaging pass to be interpreted as a specific geologic feature.

Non-Detectability The interpretive evidence on any single imaging flight will not support identification of a specific geologic feature, even though the precise geographic position of this feature has been established on a previous imaging pass.

⁴ A group of joints with a characteristic pattern

Matrix The term total matrix as used in this study refers to the number of imaging passes over a defined geologic category. For example, for any specific geologic feature, a maximum of four different look-directions were included in the matrix, however, in those cases where four different passes were not available, at least two passes were always included in the matrix. Thus, the matrix for faults comprise the total number of different imaging passes over a certain number of faults, where the maximum number of different look-directions for every fault is not more than four nor less than two.

As previously discussed, the detectability of certain geologic features is influenced by radar shadowing, and this shadowing increases from the near to far range as a function of increasing incidence angle. In order to be cognizant of the primary factors which might significantly influence a look-direction analysis, the following units have been arbitrarily selected which subdivide the imagery format into three (approximately equal) range segments

- Near Range - incidence angles less than 55 degrees
- Mid Range - incidence angles between 55 and 69 degrees
- Far Range - incidence angles greater than 69 degrees

Significance of Data (Table I)

Faults are normally recognized on radar imagery as persistent linears which cut across lithologic or structural trends as well as the other interpretive criteria such as erosional scarps, and off-setting linears or stream patterns, etc. Regardless of the topographic relief (i.e., less or greater than 50 meters) it is obvious that as the azimuthal orientation of a fault approaches parallelism to look-direction, the detectability of this particular geologic feature decreases (75% of the non-detectable matrix have an azimuthal direction of 30° or less). Where the local relief exceeds 50 meters, shadowing in the far range is also a significant contributor to the non-detectability of faults. When the azimuthal direction of any fault approaches orthogonality to look-direction (greater than 60° azimuth), the detectability of such a geologic feature increases.

Joint Systems

When considering radar imaging systems, it is important to stress that joint systems rather than individual joints, are recorded on the radar imagery. Basically, this is a function of the resolution of the particular sensor involved, and not at all dissimilar to the reduced resolution encountered when utilizing high altitude or orbital photography for geologic interpretation. A significantly higher percentage of the joint system matrix was detectable where the terrain relief exceeded 50 meters. Obviously, because such geologic features are usually expressed as short terrain linears, their detectability on radar imagery would be significantly increased if the terrain configuration were sufficient to produce topographic enhancement. The non-detectability of joint systems was influenced by both topographic relief and look-direction, however, look-direction plays a dominant role in non-detectability where 58% of the non-detectable joint-fracture systems were recorded in the azimuthal range of 30° or less.

Dip Slopes

Analysis of the data summarized in Table I reveals that the detection of dip slopes is obviously influenced by both the look-direction of the imaging systems and the topographic relief of the terrain involved. When the strike of the strata is perpendicular to look-direction (and the dip slope parallel to look-direction) the strata can either dip toward or away from the radar. Where the topographic relief was less than 50 meters, 63% of the non-detectable category of dip slopes had a slope toward the radar, and where topographic relief exceeded 50 meters, all of the non-detectable category had a slope toward the radar. It can therefore be seen that the influence of radar foreshortening⁵ as dictated by look-direction, is inherently related to the non-detectability of dip slopes.

DATA APPLICATION

The results of this experiment can be immediately applied to future mission planning of radar-geologic studies. For example, if only high relief areas (such as the mountains in the Spanish Peaks area) were to be imaged, depression angles of 35 to 55 degrees from two opposing look-directions would provide near optimum terrain information.

In regions of moderate relief (such as the Boston Mountains), two orthogonal look-directions utilizing depression angles between 20 and 40 degrees would provide near maximum terrain shadowing coincident with minimal data loss. If the structural grain of the area was already known, a single look-direction with these intermediate depression angles might provide near optimum data retrieval.

For low relief areas such as those illustrated in the alluvial apron of the Central Humboldt Range, Nevada, depression angles less than 25 degrees would obviously be the most satisfactory for geological interpretation.

SUMMARY

Depending on the relative topographic relief, depression angle (or effective incidence angle), and look-direction, geologic features can be advantageously enhanced or can be completely suppressed. The data derived from this study suggests that flexibility in determining a specific range of depression angles would be advantageous for geologic interpretation. For radar geology studies in areas of a known terrain configuration, trade-offs between depression angle, range position, and look-direction will provide near optimum data.

⁵ Radar foreshortening, a distortion inherent to all radars when imaging irregular terrain surfaces, is the variation in the measurement of equal terrain slopes when the slope measurements are taken at different incidence angles.

retrieval with only two imaging passes. For geological reconnaissance in poorly mapped areas, however, imaging from four orthogonal look-directions will be required for maximum terrain information.

Certainly experiments of this type should be carried out in other terrain environments to further document the advantages and constraints of radar look-direction and other radar parameters which affect geologic interpretation. This is, in fact, the ultimate goal of our radar geologic research at the University of Kansas.

REFERENCES

- 1 Dellwig, L F , H C MacDonald, and J N Kirk, 1968, The Potential of Radar in Geological Exploration Proc. Fifth Symp Remote Sensing of Environment, University of Michigan, Ann Arbor, p 747-764
2. Jefferys, L H , 1969a, An Evaluation of Radar Imagery for Structural Analysis in Gently Deformed Strata, A Study in Northeast Kansas. CRES Tech Rept 118-16, 36 pp
- 3 _____, 1969b, Lineaments in the Grand Canyon Area, Northern Arizona, A Radar Analysis CRES Rept. 118-9, 15 pp
- 4 Gillerman, E , 1969, Major Lineaments and Possible Calderas Defined by Side-Looking Airborne Radar Imagery, St Francois Mountains, Missouri. CRES Tech Rept 118-12, 28 pp
- 5 Dellwig, L. F , 1968, A Geoscience Evaluation of Multifrequency Radar Imagery of the Pisgah Crater Area, California CRES Tech Rept 118-6, 18 pp.
- 6 Gillerman, E , 1967, Investigation of Cross-Polarized Radar on Volcanic Rocks CRES Tech. Rept 61-25, 11 pp.
- 7 MacDonald, H C , 1969, Geologic Evaluation of Radar Imagery from Darien Province, Panama, Unpublished Ph D. Dissertation, University of Kansas, Accepted for publication, Modern Geology
8. Westinghouse Electric Corp , 1967, Side-Look Radar, Westinghouse Electric Corp , Aerospace Division , Baltimore, Maryland, (limited distribution) 45 pp
9. Innes, R. B., 1968, An Interpreter's Perspective on Modern Airborne-Radar Imagery, Proc 5th Symp Remote Sensing of Environment, (April 1968) University of Michigan, Ann Arbor, pp. 107-122
- 10 Kirk, J N and R L. Walters, 1968, Preliminary Report on Radar Lineaments in the Boston Mountains of Arkansas, Compass of Sigma Gamma Epsilon, vol 45, no 2, pp 122-127
- 11 Hackman, R J , 1966, Geologic Evaluation of Radar Imagery in Southern Utah, U S Geological Survey Prof Paper 527-D, pp D135-D142
12. MacDonald, H C., P A. Brennan, and L F Dellwig, 1967, Geologic Evaluation by Radar of NASA Sedimentary Test Site, IEEE Trans Geoscience Electronics, vol GE-5, no 3, pp 72-78

- 13 Snavely, P D , Jr , and H C Wagner, 1966, Geologic Evaluation of Radar Imagery, Oregon Coast, U S Geological Survey Unpublished Report, 13 pp
- 14 Levine, D C Colbert, L C Graham, P Crane, and B B Scheps, 1966, Combinations of Photogrammetric and Radargrammetric Techniques, Manual of Photogrammetry, Published by Amer Soc Photogrammetry (3rd Edition) Banta Publ Co , Menasha, Wisconsin, pp 1003-1048
- 15 Dellwig, L F , J N Kirk, and R L Walters, 1966, The Potential of Low Resolution Radar Imagery in Regional Geologic Studies, Journal of Geophysical Research, vol 71, no 20, pp 4995-4998
- 16 Cameron, H L , 1965, Radar as a Surveying Instrument in Hydrology and Geology, Proc 3rd Symp Remote Sensing of Environment, (October 1964), University of Michigan, Ann Arbor, pp 441-452
17. Johnson R B , 1968, Geology of the Igneous Rocks of the Spanish Peaks Region, Colorado, U S Geological Survey Prof Paper 594-G, 47 pp
- 18 Kirk, J N , L F Dellwig and L F Jefferis, 1968, The Influence of Radar Look-Direction on the Recording of Geologic Lineaments-- A Study in the Boston Mountains, Arkansas, Unpublished manuscript, University of Kansas, Lawrence, 10 pp
- 19 Lueder, D R , 1959, Gray Tones in Aerial Photographic Interpretation, McGraw-Hill Book Company, Inc , New York, pp 76-101

TABLE I

ANALYSIS OF LOOK-DIRECTION
PANAMA IMAGERY

Geologic Feature	Total Matrix*	Topographic Relief (meters)	Matrix Sub-Categories	Percent Matrix Detected	Percent Matrix Not Detected	Dominant Azimuth [†] Direction
Faults	96	<50m	54	70%		55% $\geq 60^\circ$
					30%	75% $\leq 30^\circ$
		>50m	42	83%		46% $\geq 60^\circ$
					17%	71% $\leq 30^\circ$
Joint Systems	78	<50m	47	60%		36% $\leq 30^\circ$, 32% $\geq 60^\circ$
					40%	58% $\leq 30^\circ$
		>50m	31	90%		40% $\geq 60^\circ$, 35% $\leq 30^\circ$
					10%	65% $\leq 30^\circ$
Dip Slopes	65	<50m	28	71%		50% $\leq 30^\circ$
					29%	63% - dip slope toward radar
		>50m	37	87%		47% $\geq 60^\circ$
					13%	100% - dip slope toward radar

* The term total matrix as used in this study refers to the number of imaging passes over a defined geologic feature.

[†] Azimuth direction refers to the angle between the look-direction (orthogonal to ground track) and the geologic feature imaged.

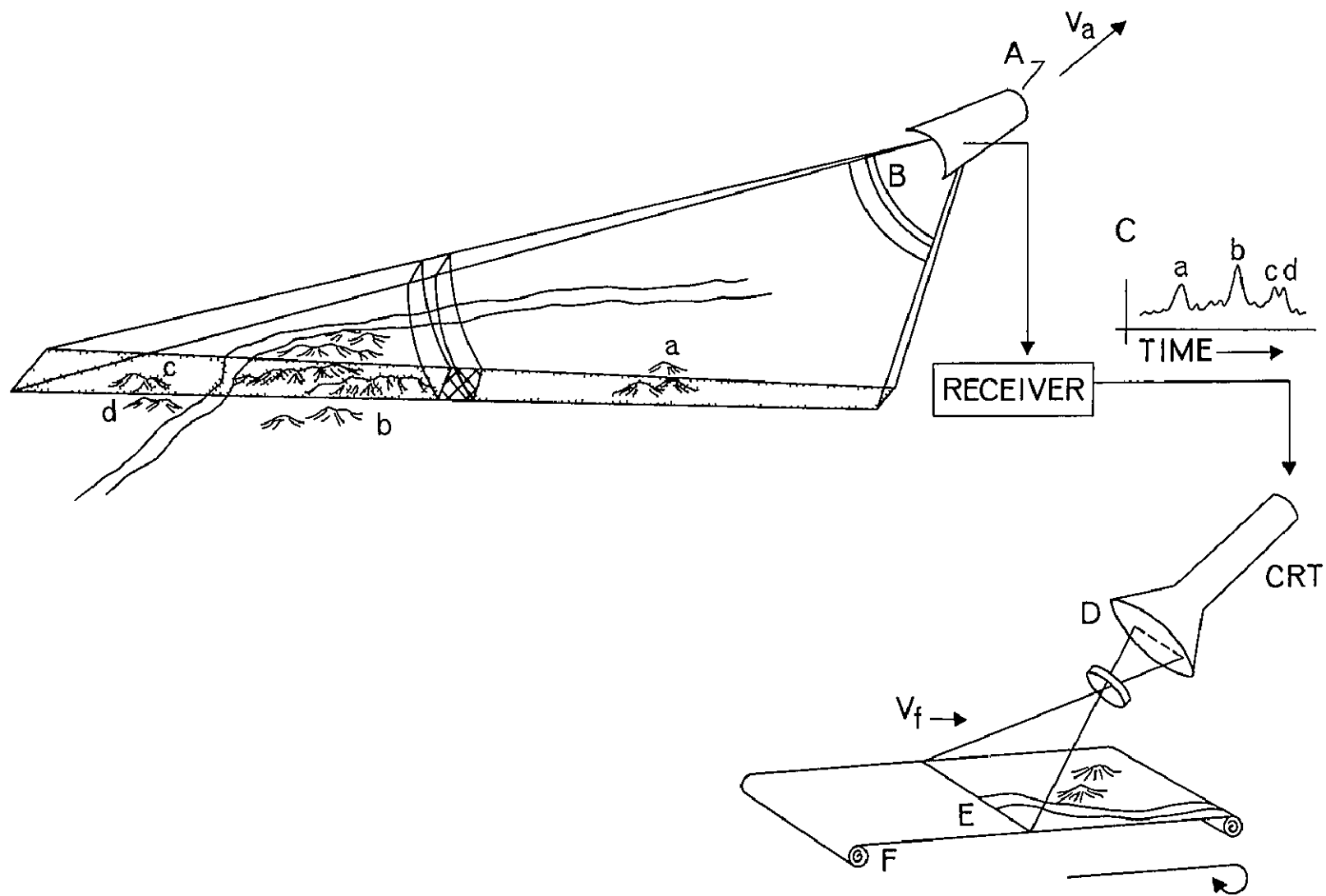
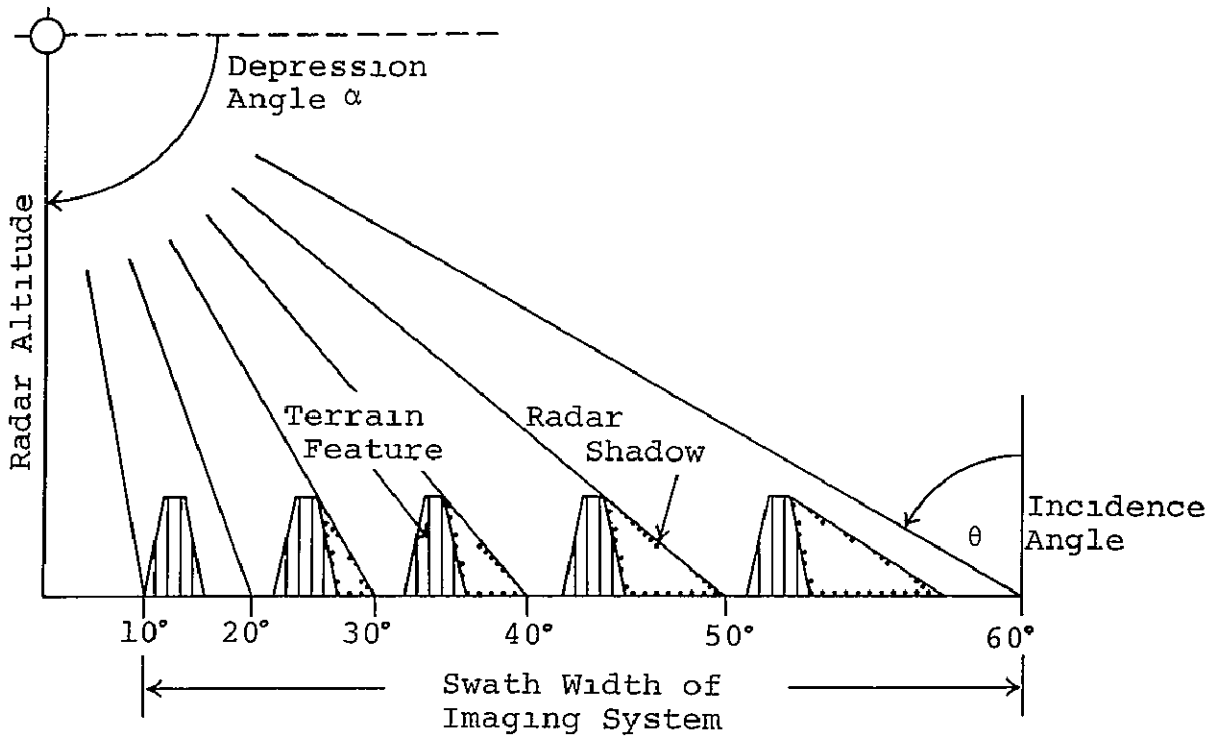


Figure 9-1 - Sketch diagram Typical side-looking airborne radar system
 (Modified from Westinghouse, 1967)



Plan View SLAR Imagery Simulation

Figure 9-2.- Shadowing characteristics associated with SLAR imaging systems

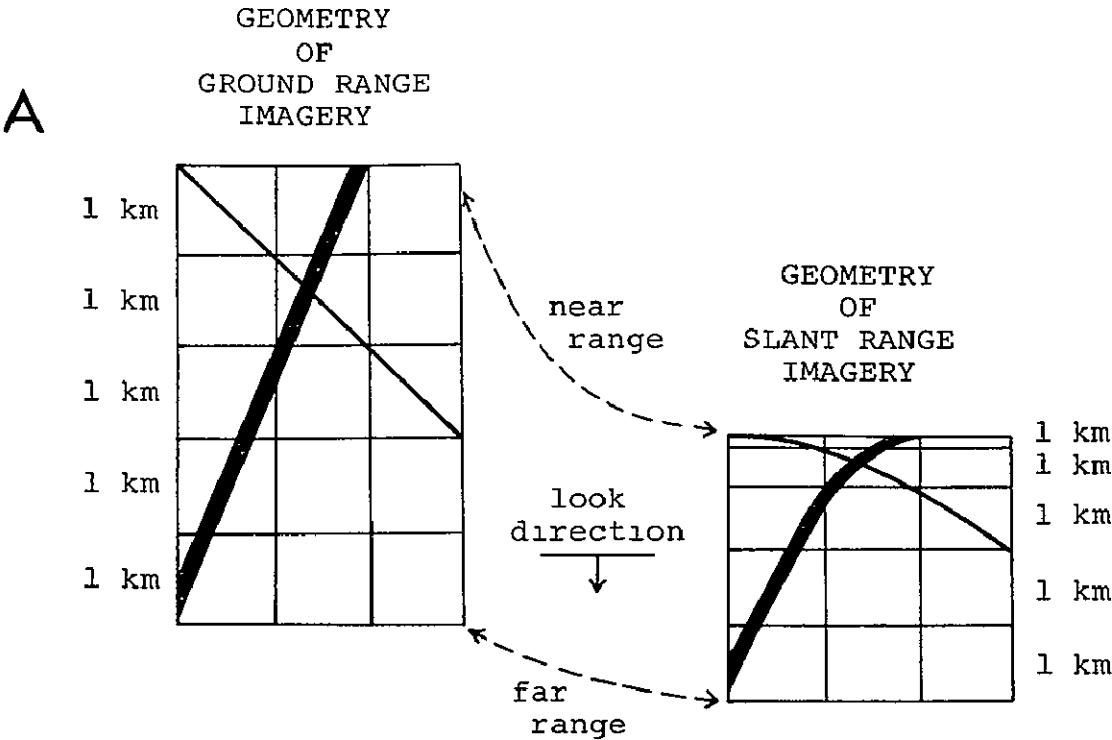


Figure 9-3 - Geometry of slant range and ground presentation (after Innes, 1968)

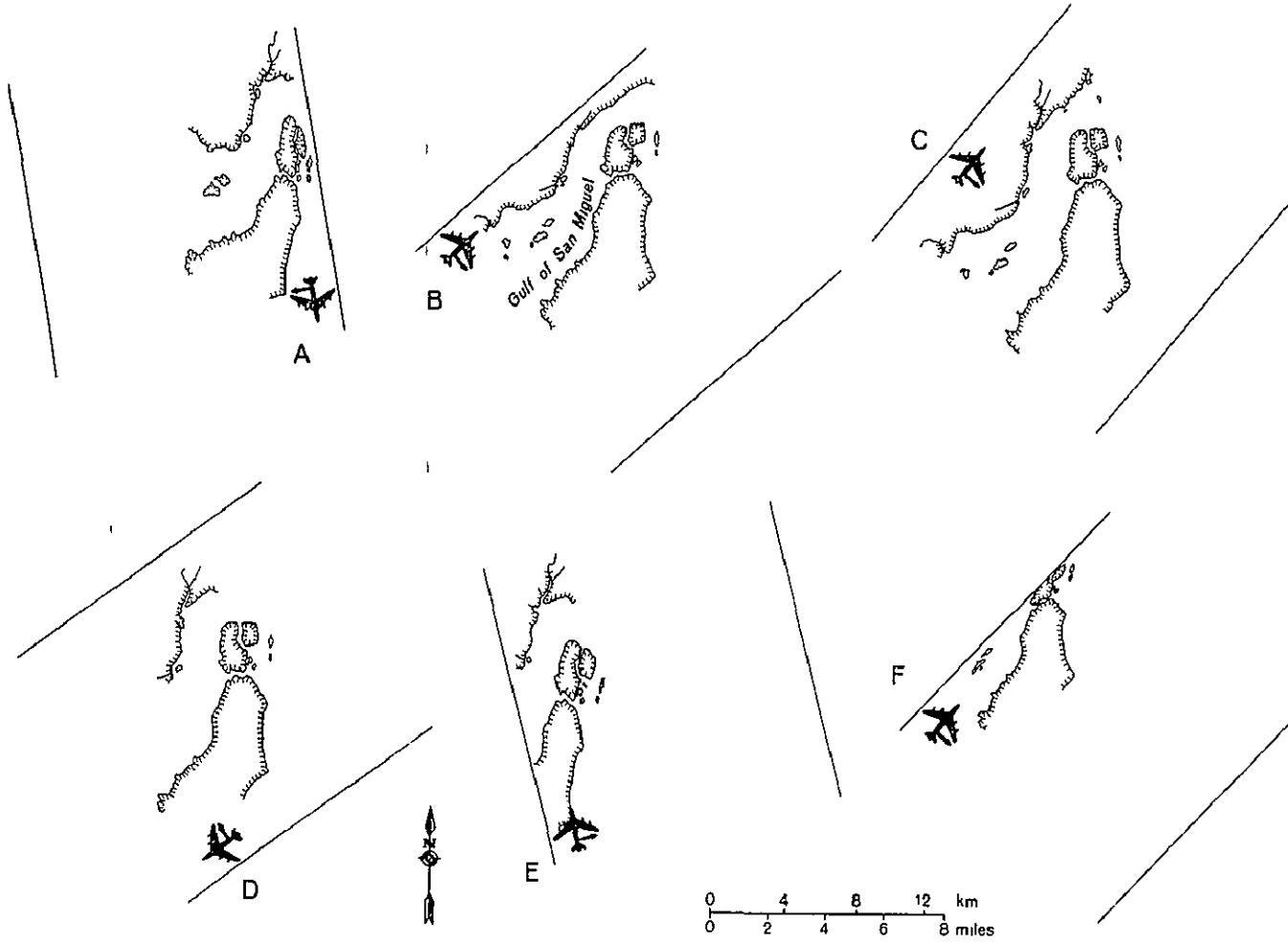
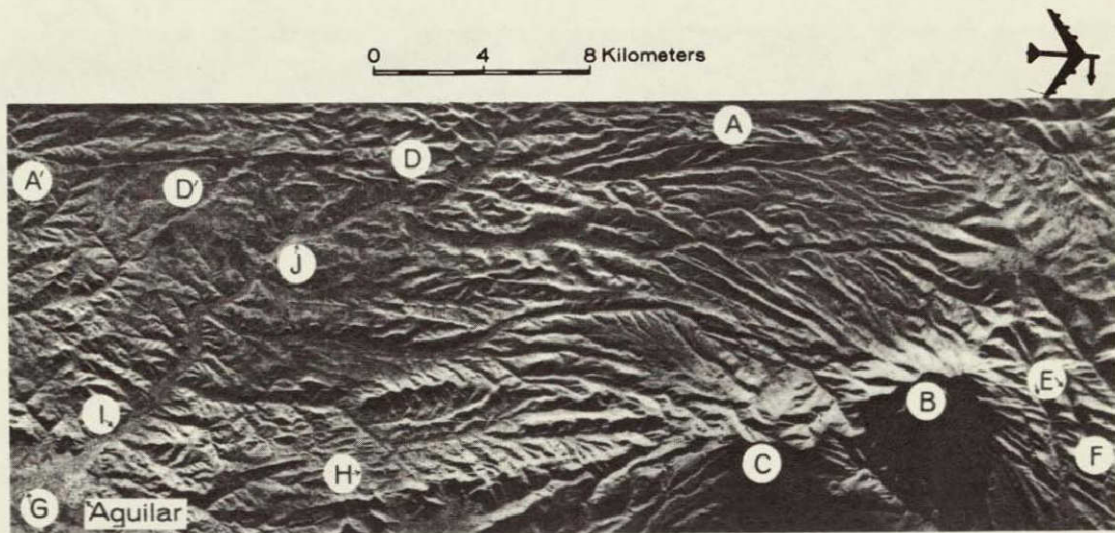
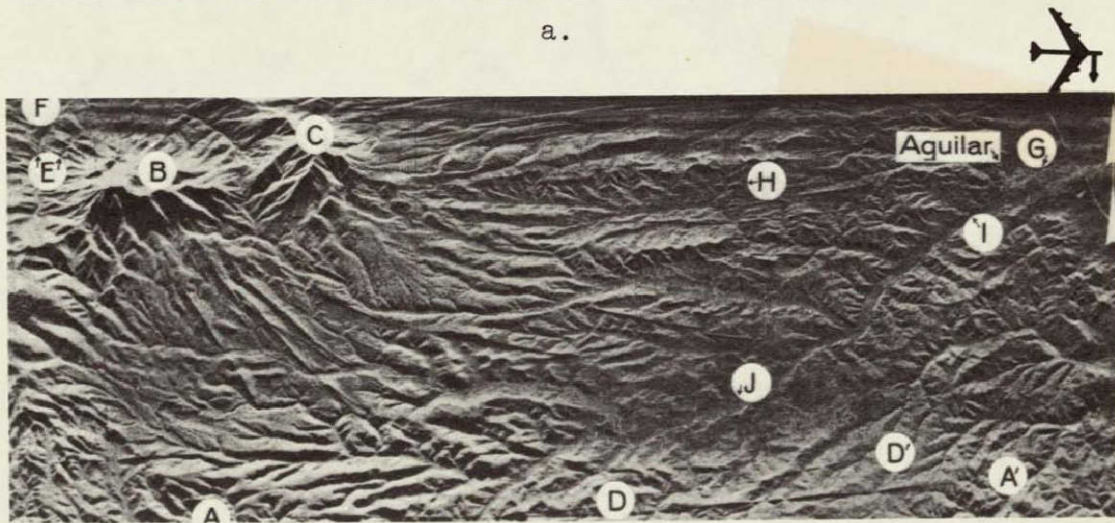


Figure 9-4 - Effect of near-range compression on geometric shape,
La Palma Peninsula, Darien Province, Panama



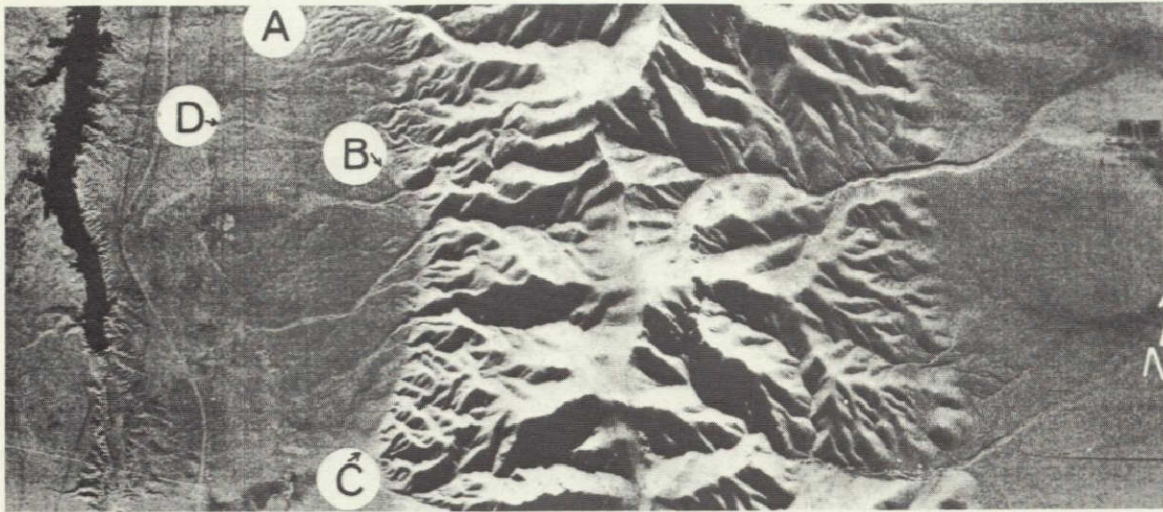
a.



b.

Figure 9-5.- Spanish Peaks, Colorado. (a) Look-direction, north.
(b) Look-direction, south.

0 4 8 Kilometers



a.

NOT REPRODUCIBLE



b.

Figure 9-6.- Central Humboldt Range, Nevada. (a) Look-direction, south. (b) Look-direction, north.

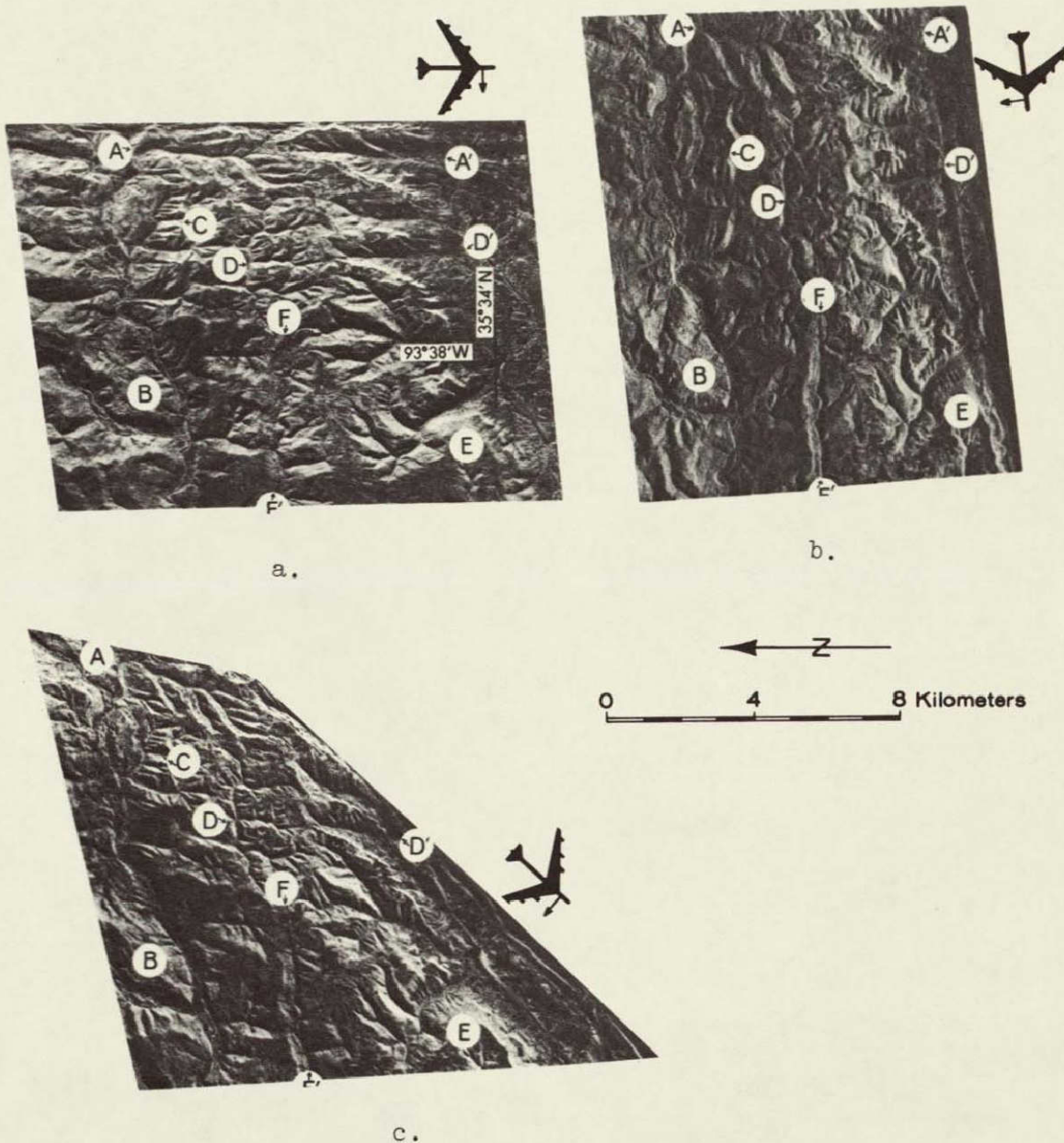


Figure 9-7.- Multiple flight coverage, Boston Mountains, Arkansas. (a) Look-direction, west. (b) Look-direction, north. (c) Look-direction, northwest.

SECTION 10

CARTOGRAPHY

BY

N71-19261

Alden P. Colvocoresses
U.S. Geological Survey

INTRODUCTION

This paper reviews the earth-resources cartographic applications program as currently being implemented within the Topographic Division of the U.S. Geological Survey (USGS). Five subjects are covered as follows:

1. Goals of the program
2. Development of in-house capabilities
3. Relationship to NASA (MSC) aircraft program
4. Current work on space imagery
5. Conclusion

GOALS

Listed below are the goals of the program as now envisaged. In-house and/or contract tasks have been defined in support of each listed item.

1. Develop procedures to accurately relate space imagery and other unconventional remote sensor products to the Earth's reference surface and maps thereof.
2. Utilizing the above-defined relationships, develop the following products in graphic and/or statistical form:
 - New and revised topographic maps
 - Thematic maps in near real time of

water

snow

Presented at the Second Annual Earth Resources Program Review at NASA Manned Spacecraft Center, Houston, Texas, September 1969.

Publication authorized by the Director, U.S. Geological Survey.

vegetation (IR reflective)

massed cultural features of high relative reflectance

- Bases for other thematic maps, including maps of temporal phenomena

3. Develop concepts and methods for storage, retrieval, and dissemination of cartographic products.

CAPABILITIES

Since 1965 the USGS has had a moderate cooperative research program with NASA to investigate cartographic applications of earth-resources data obtained from cameras and other sensors in aircraft and spacecraft. Recent emphasis on the use of earth-oriented space sensors has resulted in an expansion of this program and a corresponding increase in the professional staff to support it.

The Topographic Division is taking appropriate steps to develop capabilities in the cartographic applications program. Two engineers, Robert H. Nugent and Carl F. Kirsch, have been working in the program for several years and remain on the staff.

The following space-oriented personnel have been added to the research staff in January through July, 1969:

Frederick J. Doyle	Scientist/Mapping Systems
Alden P. Colvocoresses	Geodesist/Cartographer
Warren T. Borgeson	Photogrammetrist
Robert B. McEwen	Photogrammetrist
Roy A. Welch	Photogrammetrist (Postdoctoral associateship)
Anthony E. Salerno	Chemical (Photographic) Scientist

Additional specific support comes from John D. McLaurin who is working for a doctorate at the University of Michigan and is studying the geometry of optical scanner systems.

Part-time effort and technical guidance is available from more than 100 specialized professional personnel in the Topographic Division.

RELATIONSHIP TO NASA AIRCRAFT PROGRAM

The USGS has a limited capability with respect to aircraft as remote sensor platforms. There are at least three types of projects where aircraft support, such as that being developed at the Manned Spacecraft Center, is needed. They are:

1. High-altitude simultaneous metric and panoramic photography of a mapping project. Specifications have been submitted for photographic coverage of the Eagle Pass, Texas, area which is needed in developing small-scale mapping procedures. The frame photographs provide the geometry, and the panoramic photographs provide the resolution needed to identify and classify detail.
2. High-altitude photographs on various film types taken with a calibrated mapping camera of 12-inch focal length. These photographs are needed in developing optimum line map, photomap, and orthophotomap products. The USGS has acquired a 12-inch Kelsh-type plotter to support this kind of effort.
3. Imagery to support the development of rapid "mapping" of temporal phenomena. The destruction caused by hurricane Camille is an example of the type of phenomenon which probably warrants recording and rapid dissemination on a fairly wide basis. The various types of imagery of the devastated areas are being examined, and methods of rapidly converting the imagery into cartographic products suitable for dissemination are being developed. If a high-quality mosaic of this area had been laid, printed, and distributed within a week after the storm, it would be interesting to know what the value (and response) would have been. Probably the only way to evaluate such a product is to go ahead and produce one when the next appropriate occasion arises. Of course, a space image of suitable resolution would be much easier than aircraft photography to convert into a useable photomap.

Procedures for graphically documenting such disaster areas should be jointly developed by the concerned agencies before the next need arises.

CURRENT WORK ON SPACE IMAGERY

The past year's work of the cartography program will be documented in the annual report to NASA which is now in preparation. A few projects dealing with space imagery are worth mentioning here. By next March, experimental maps in standard format at 1:250,000, 1:500,000 and 1:1,000,000 scales are expected to be prepared from Apollo and Gemini space imagery. The 1:1,000,000-scale map will have about half space imagery and half line detail, the other maps will have full space imagery. Apollo 6 imagery has already been laid as a strip mosaic at 1:500,000- and 1:1,000,000-scales. These sheets will soon be available in photocopy form through the Map Information Office, USGS, Washington, D.C. 20242. All sheets are in the Southwest U.S.

Another item of current interest is the experiment with the SO65 imagery recorded on Apollo 9. In this experiment, steps towards automated mapping of snow and vegetation are in progress with the help of Philco-Ford Corporation. Figures 1 and 2 are examples of this work. By using

optical density slicing techniques, both the geometry and resolution of the imagery have been maintained. Automated water mapping experiments are also being conducted. As figure 3 indicates, a great deal of information on water areas can be extracted from color IR photography.

Another active project is the analysis of the external geometric effects on space imagery, particularly ERTS imagery. Figure 4 illustrates the five effects involved. A report on this matter is available and is being published in Photogrammetric Engineering.

Although not funded by NASA, considerable work on image correlation is underway within the USGS. A Giannini three-channel additive color viewer has been obtained from the U.S. Air Force and is installed at the Branch of Special Maps in Silver Springs, Maryland. Investigators are invited to use this instrument, which is designed for 70-mm roll film.

A new Bolsey optical image correlator is currently being installed at the Topographic Division's research center in McLean, Virginia. This machine can correlate non-metric imagery, a step which is critical in optical image processing.

CONCLUSION

The goals of the cartography program cannot be achieved easily. Current effort must and will be stepped up so that when the first earth resources satellite flies (ERTS-A), appropriate cartographic procedures and suitable map bases will be available to reference the imagery to the Earth's surface and to provide cartographic support for the various disciplines.

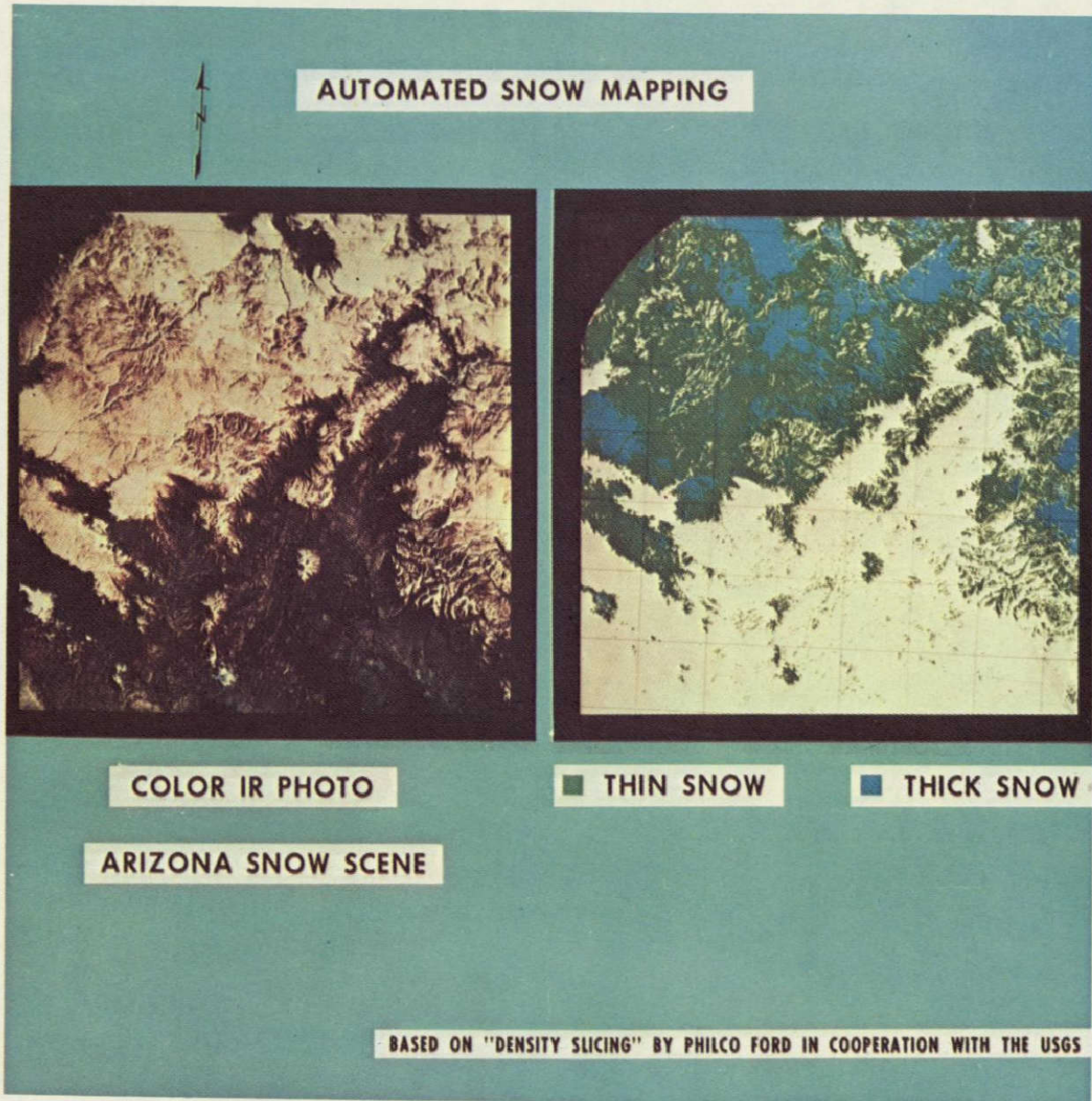


Figure 10-1.- An example of automatic snow mapping.

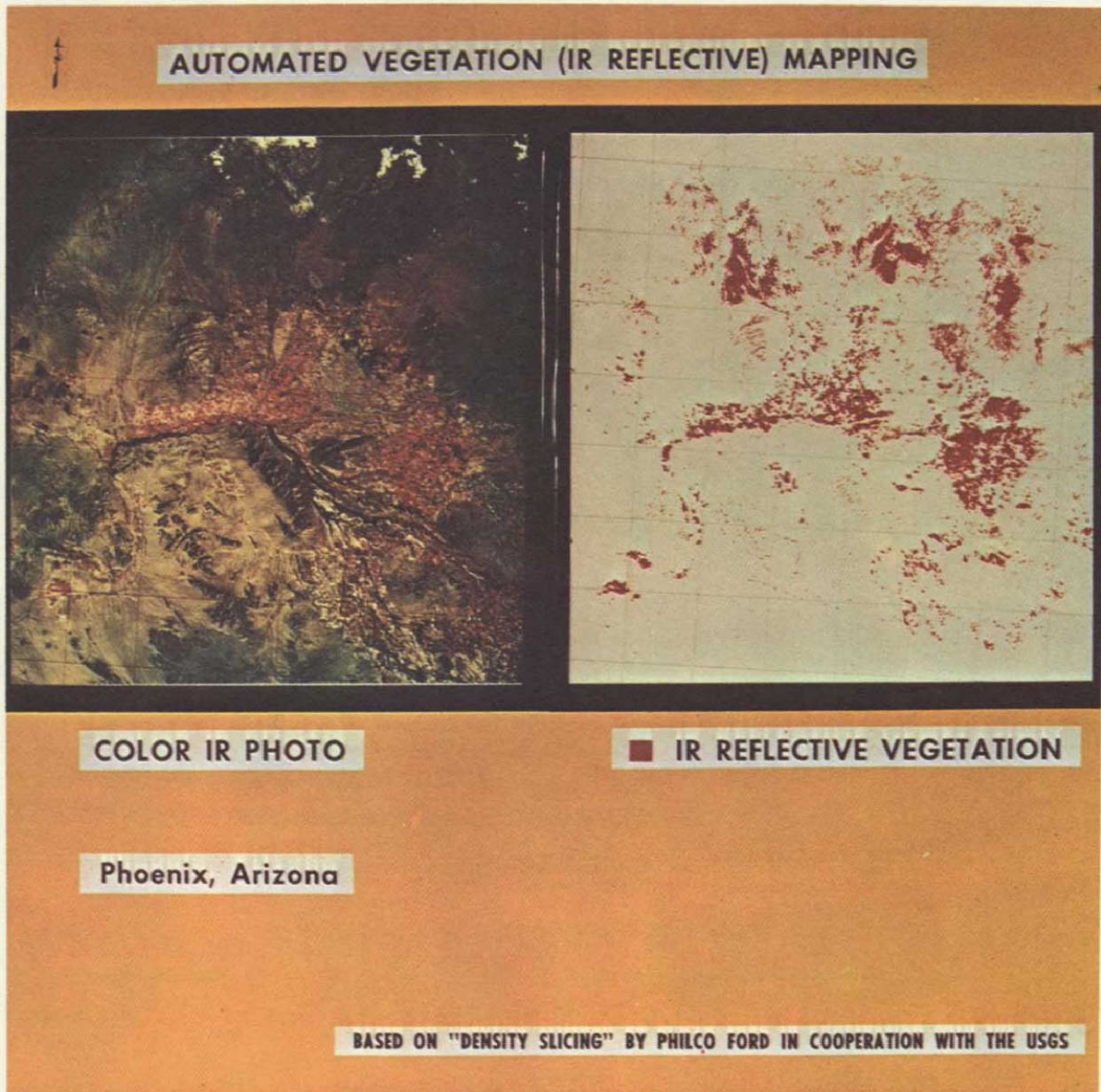
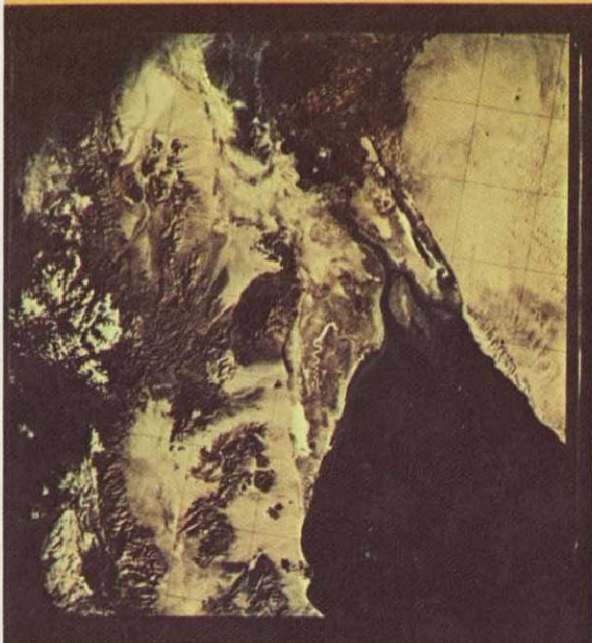


Figure 10-2.- An example of automated vegetation mapping.

MOUTH OF THE COLORADO RIVER



COLOR IR PHOTO



**ENHANCED B&W PRINT
OF COLOR IR PHOTO**

**Enhancement of water detail using
conventional photolab procedures**

APOLLO 9 PHOTOGRAPH

Figure 10-3.- An example of underwater detail enhanced by photolab procedures.

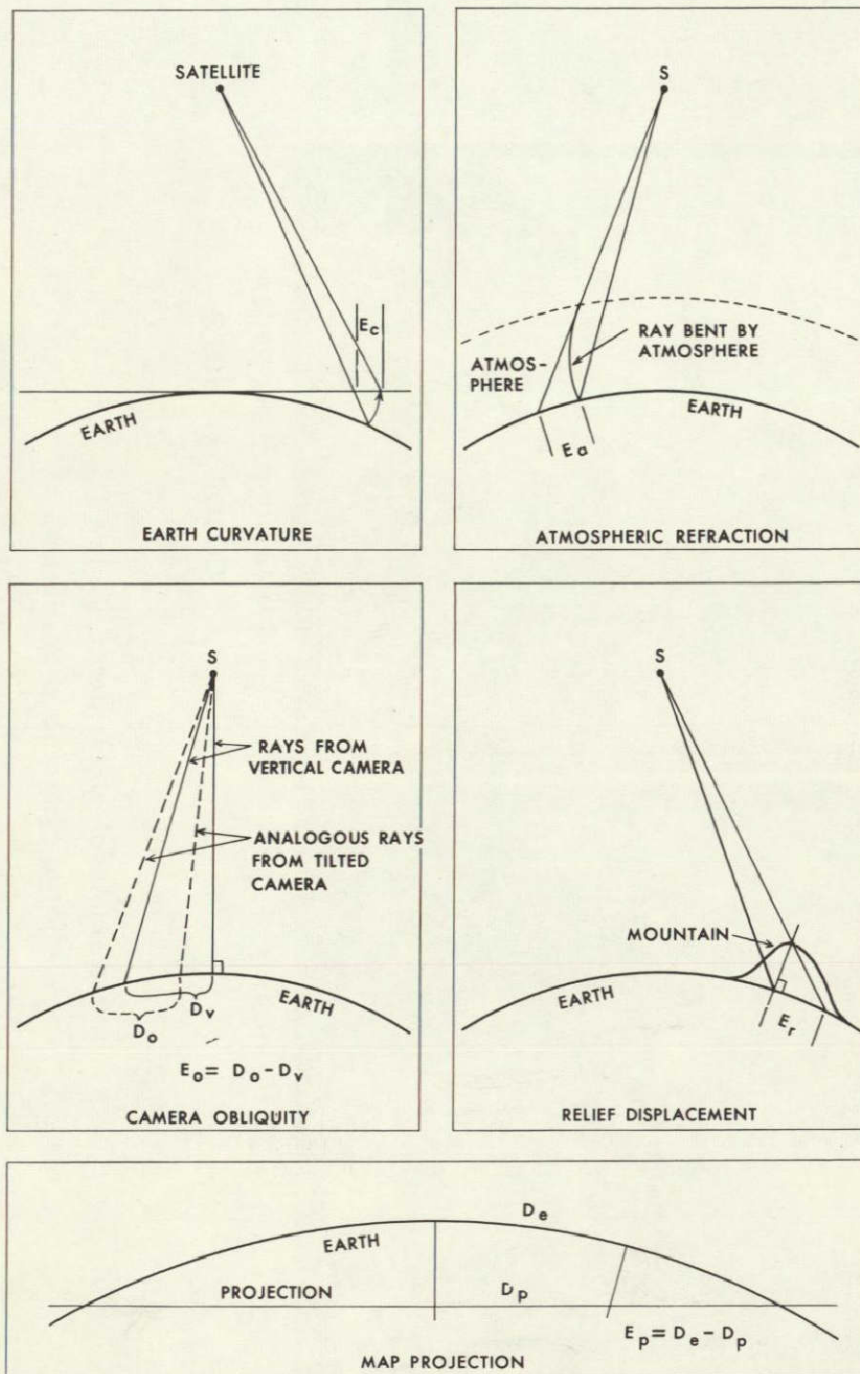


Figure 10-4.- Simplified drawings illustrating displacements in satellite imagery.

SECTION 11
Summary of Objectives and Progress in the
Geographic Applications Program

Arch C. Gerlach
Discipline Coordinator
Geographic Applications Program
U. S. Geological Survey

N71 - 19262

Introduction

Within four task areas funded by NASA in FY 1969, the Geographic Applications Program of the Geological Survey undertook or maintained more than a dozen specific projects, five of which will be discussed in detail by the respective Principal Investigators. The others are reviewed briefly by the Discipline Coordinator with respect to their objectives, achievements to date, publications prepared since September 1968, and an analysis of the quality and utility of information and equipment available to the Investigators.

The primary purpose of this presentation is to identify what has been learned during the past year from materials and equipment funded by NASA, with a view toward selecting types of data, instrumentation, and techniques that have proved to be most effective in geographical research and its applications to user problems. Deficiencies in the data and voids in the scope of the program that should be rectified to relate past achievements to the ERTS program are given special attention.

Mr. Chairman, with your permission, I would like to make the following changes in the sequence of papers for this review of the Geographic Applications Program:

1. After my introduction, Professor Frank Horton will report on urban research under a contract with Northwestern University, instead of speaking at 10:45 a.m. as scheduled. The papers by Prunty and Simonett will then follow as programmed before the coffee break.
2. After the coffee break, the Imperial Valley land use study which was to have been presented by Dr. Bowden will be given by his colleague, Claude Johnson, due to the illness of Dr. Bowden. The papers by Pease and Alexander will then follow in scheduled sequence, to conclude our session this forenoon.

Discussion

In my own presentation, I am pleased to begin by reporting the successful achievement of a goal that was fundamental to the establishment of the Geographic Applications Program in the U.S. Geological Survey.

The whole geographic profession has been made aware of, and significant segments of it are participating in, the use of remote sensing techniques and data returns developed by, or in cooperation with NASA. For example:

1. The Association of American Geographers, under contracts with my office, has created a Commission on Remote Sensing, organized summer courses on remote sensing that were subsequently financed and administered by the National Science Foundation, and involved geography staff members in more than a score of universities in remote sensing research.

2. The International Geographical Union has devoted plenary sessions to the subject at its regional meeting in 1966 at Mexico City, and at its world Congress in 1968 at New Delhi, and has converted its Commission on Interpretation of Aerial Photographs to a Commission on Geographical Data Sensing and Processing.

3. The Secretary General and several Department Directors in the Organization of American States have repeatedly expressed a desire for that organization to serve as a channel through which other American nations might participate effectively in the U.S. space program for earth resources surveys and development. A specialized agency of the OAS for scientific and technical work in the fields of cartography, geography, the geophysical sciences, and history (Pan American Institute of Geography and History) established two years ago a Committee on Remote Sensing and devoted to that subject an evening plenary session at its General Assembly in Washington last June. Dr. Tepper made a very well received presentation and James Morrison took part in that meeting, as did also representatives of Interior, Agriculture, and the Department of State.

4. Geography Departments in more than 20 universities have submitted unsolicited research proposals, about half of which have been endorsed by an Advisory Committee in the National Academy of Sciences, and integrated into the general program plan and objectives agreed upon between the Geological Survey and NASA.

Having awakened and involved the profession at both national and international levels, we have been considering ways to improve the effectiveness of their efforts. We recognize that, in accordance with recommendations of advisory groups in the National Academy of Sciences, the Association of American Geographers, and the U.S. Geological Survey, it is now time for some restructuring of the Geographic Applications Program. To date our program has been largely oriented toward, and influenced by, academic institutions and professional organizations. The utilization of the initiative and scientific capability of university groups and professional organizations has yielded commendable results that appear in some 138 reports, papers, and publications listed in the

USGS/NASA Interagency Report No. 154, which is now in the channels for reproduction. We have here a few copies of the typescript for those who may wish to pick them up at the coffee break.

Through involvement of the academic research community, we have been successful in identifying a number of areas in which direct applications of space data and subsequent pay-offs will be greatest. Armed with these results, we can now more positively work toward the solution of more specific critical and resource management problems of real concern to both Government and industry. A thorough review and assessment of the Geographic Applications Program has, therefore, been undertaken, supplementing our Advisory Committee in the National Academy of Sciences with the Association of American Geographer's Commission on Remote Sensing, and some special groups, recognized by both the Academy and the AAG for their eminence in the NASA Task Areas of land use analysis, urban studies, environmental impact research, and information systems. These groups have prepared for submission to the Academy Committee and the AAG Commission, recommendations on the types of experiments that are most likely to yield important returns and meet significant user needs. The special groups clearly favored a more closely integrated program, structured along problem lines such as those which arise where urbanized areas are impinging on the surrounding country, where restructuring of urban functional areas interacts with the whole complex of their environmental factors, and where developmental alternatives for regional growth need testing by predictive models. Concern was expressed also about the need for more research in the field of urban climatology.

Such an orientation of the program would have direct relevance to Interior Department programs dealing with use of the Nation's lands, and definitions of environmental systems affecting urban development. In addition, the geographically analyzed data would provide valuable information to other agencies. To be most effective, however, we must understand their needs and operational objectives, so that both data acquisition and processing requirements can be met. Potential interdepartmental uses of geographically interpreted data appear to include:

1. Marketing studies for commercial developments and industrial location sites, of use to the Department of Commerce.
2. Studies of highway and road networks and traffic flows, of interest to the Department of Transportation.
3. Studies of settlement patterns, population growth, and movements in relation to more efficient land use, of use to both the Departments of Interior and of Housing and Urban Development.
4. Better management of disaster areas, of use to Interior, Commerce, and the Office of Emergency Preparedness.
5. Integrated resource inventories, of interest to Interior, Commerce, and in foreign areas to AID.

6. Studies yielding data on which to base tax revisions by State and local governments.

7. Changes in functional structure as well as rates and directions of growth, of use to HUD and Commerce.

8. Development of techniques for supplementing traditional census methods and data.

9. Studies of urban and regional development in relation to resource needs, such as construction materials, industrial components, recreation facilities, etc.

10. Analysis of climatic interactions, particularly in urban areas, for use by planners and decision makers throughout government hierarchies.

One way to achieve reorientation of the Geographic Applications Program would be to give more attention to geographers in Government, who can effectively promote, within their respective agencies, more awareness of, and interest in the utilization of remote sensor data and techniques for agency operations. A survey completed last month by a Committee in the National Academy of Sciences revealed that more than 600 professionally trained geographers are employed in Federal agencies, that their average grade falls between GS-12 and 13, (which should be adequate to exert some policy influence), and that geographers hold supergrade positions (GS 16-18) in eight Executive agencies and the Library of Congress. In addition, more than 100 geographers hold positions of responsibility in State and local planning agencies.

To achieve a more balanced program, with more emphasis on Government and industrial applications, our Academy Advisory Committee has recommended an increase of in-house research capabilities, which have been limited to about 15% of NASA funding during the past two years. We hope, therefore, to increase the in-house control and research to approximately 30%.

Since the time for our program review is very limited, I shall turn now from general accomplishments and program plans to the activities, achievements, and needs of participants in the Geographic Applications Program during the past year. Five of our Principal Investigators, or their chief associates, will review their own programs. Of the nine other research projects in the Geographic Applications Program, four are in the completion phase, and three are too new to take a significant part in this review. Projects which have been, or soon will be brought to conclusion are:

1. The Rudd/Aldrich project, at Oregon State University, to locate and map the forest-tundra ecotone in Canada, used weather satellite data, which is somewhat analogous in scale and character to anticipated returns from ERTS-A. The research, begun in April and completed during the first week of September, resulted in a well

illustrated report and map which is now enroute for reproduction as an interagency document. The experiment was to interpret a major vegetation boundary from the low resolution but broad coverage returns from weather satellites. The technique was successful, and a map was made to show for the first time the forest-tundra ecotone across Canada.

2. A similarly concise, but only partly successful project was completed this summer by Dr. Paul Alexander of the Geography Department at the University of Montana. Using data from the Forest Service Firescan Project, which provided thermal IR coverage of the Bitterroot Region of Western Montana and Eastern Idaho, he sought to map time-lapse changes in land use within forest enclaves, and to identify the distributional and behavioral patterns of air drainage. The small scale of the imagery and the small size of the enclaves made analysis of land use changes impractical, but studies of air drainage resulted in some useful contributions to the broad field of environmental impact that are included in Dr. Alexander's final report.

3. During the past two years, Professor Latham at Florida Atlantic University has completed some 30 interpretation studies of simulated orbital TV imagery, and has conducted numerous experiments with electronic waveform interpretation methods, applied to signature variabilities that appeared to be related to environmental and film type differences. Reports on those investigations are being prepared under a no-cost extension of the contract to December 31. I cannot at this time tell you the specific conclusions of Latham's research, but they will be in his reports, which will be submitted to the USGS and NASA by the end of this calendar year. Dr. Latham has expressed interest in using high altitude flights over Florida for land use and census data analysis, but it is too early to know whether funds and the reorganized Geographic Applications Program will permit acceptance of a new proposal from Florida Atlantic along those lines.

4. Likewise, the autocorrelation and spectral density studies by Professors Curry, MacDougall, and van der Eyk at the University of Toronto are being brought to conclusion, at least in their present form, this year. Completed reports on coherent optical data processing of remotely sensed imagery have been combined into Interagency Report No. 145 which was routed through reproduction channels on September 11, but is not yet available for distribution. Illustration No. 1, and its explanation on the following two pages (for which there was not time to show a slide during the oral presentation at Houston), indicates the type of work that has been done. The objective during the remainder of that contract is to utilize the equipment constructed and results achieved under the first phase of research, to make applications of practical value in the processing of data from TV-equipped satellites. No overflights or special data acquisitions by NASA are contemplated for completion of this contract.

New contracts which supplement other work in the general task

areas funded this year by NASA, require little new data acquisition. These three contracts are:

1. A six-month contract which has been negotiated with Clark University, beginning September 6, to:
 - a. Identify interpretive signatures for scanning and mapping tropical land use systems.
 - b. Develop sampling and scanning strategies for estimating areas covered by various land use categories.
 - c. Develop information systems for summarizing land use change and estimating agricultural commodity flows.

Considerable ground truth information on tropical lands is on file at Clark's Graduate School of Geography for comparison with recent flight data. The principal investigator, Professor Jeremy Anderson, has selected the imagery he will need from the data bank at Houston, and will begin his work as soon as that material is delivered.

2. A contract with the University of Denver to develop remote sensor display modes to satisfy urban planning data input needs is expected to demonstrate the importance and function of remote sensor data as a basic information source for urban planning, preparation of up-to-date land use maps, control of urban and suburban land use, and possibly to provide information of value in forecasting, preventing, or recovering from disasters. An RB-57 overflight has been requested, and was flown in August (Mission 101). When the photography has been reproduced at MSC, the principal investigator, Dr. Griffith, will visit Houston to inspect it and make selections pertinent to his work.

3. The newest contract in the Geographic Applications Program became effective September 5 with the TRACOR Company. The objective is to investigate time variant phenomena by means of color and color IR photography over approximately 50 carefully selected targets along a 400-mile triangular flight route from San Diego to Los Angeles, to Salton Sea and back to San Diego. This is a multi-discipline experiment, with some guidance and financial support from Geology, Hydrology, and MSC/Houston, but the Geographic Applications Program provides the project direction and about 65% of its financing. TRACOR will overfly the targets every three weeks and ground check them every six weeks. Photos will be fully coded for location, time, target/background reflectance, etc. It is hoped that this experiment will lead toward the development of automated techniques for analyzing time-lapse changes recorded on photography.

In the remaining time allocated to me, I shall pass over the Dartmouth College grant under which Professor Simpson is investigating various aspects of urban developments in New England, because his work is

already well known to you, and report briefly on the current work of the Association of American Geographers. The Association has been particularly effective, through its Commission on Remote Sensing, in enlisting participation by top flight members in remote sensing research. The chief objective of its contractual efforts have been:

1. To develop an operational plan for land use mapping from orbital platforms. With that objective in mind, the Association has selected consultants and sub-consultants at centers shown on Illustration No. 2. They are needed in a country of this size because any land use classification which would apply to all of its regions would be too complex for use with low resolution satellite data expected in the near future. Consequently, basic land use classification systems are being developed in the Southwest, Northwest, Rocky Mts., Central, Southeast, and Northeast regions, and a Consultant-at-Large in the Chicago area is responsible for urban land use classification throughout the country. The program Director, Dr. Robert Peplies, is at East Tennessee State University. Professor Thrower and his associates at UCLA have practically completed for reproduction a land use map along the southern boundary of the United States from California to Texas, based on Gemini and Apollo photography. The map, including ten categories of land use, has been compiled at a scale of 1:250,000, but will be reduced for reproduction to 1:500,000, and possibly 1:1,000,000. During July and August, significant progress has been made in thematic mapping of sections of the Southeastern U.S. from Apollo 9 photography, particularly in the Florence, Alabama area. Location of towns, highways, and drainage have been placed on a $7\frac{1}{2}$ -minute grid, and vegetation and land occupation overlays are nearing completion. A text will be prepared to describe the methods, procedures, and results of the project.

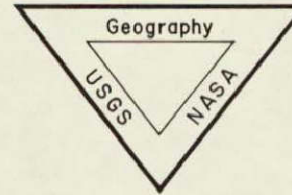
2. To organize and develop educational programs in the techniques and utilization of remote sensor data for geographers. Such courses, financed by the National Science Foundation, have been held in 1968 at the University of Michigan, and in 1969 at the University of Tennessee. Illustration No. 3 shows the distribution of participants from 38 States. These college professors now constitute an important nucleus for training additional scientists that will be required to process and interpret the masses of data they may be expected from ERTS and subsequent satellites.

3. To determine user needs in the area of man-environment interactions, and relate them to space derivable data. Current progress along that line is being made in the TVA area, and through geographers in Federal agencies. Unfortunately, the AAG request for \$86,000 this year was cut by NASA to \$46,000 because the use of RB-57 flights over the Tellico Basin would reduce the amount of data and resultant data handling costs. That may also reduce the results to be achieved, but in any case the reduction overlooked the many other activities being carried out under contract with the Association of American Geographers such as the development of regional classifications for land use, planning of educational programs to be carried out with NSF or Office

od Education funds, thematic mapping from satellite photography in the Southwestern and Southeastern United States, experimental applications of regional land use classifications to simulated base maps of high latitude regions such as the Northwest and New England, and up-dating MacPhail's analysis of Gemini photos of El Paso with data from Apollo 6 and 9.

I want now to introduce in sequence those who will present summaries of their own contractual research. The first speaker will be Dr. Frank Horton, who was formerly at Northwestern University and continues to work closely with Duane Marble under that contract, although Dr. Horton is now a Professor at the University of Iowa. Dr. Marble cannot be present due to critical illness of his father in Seattle, Washington. The second speaker will be Dr. Merle Prunty, Chairman of the Geography Department at the University of Georgia, where experiments have been focused on identifying, mainly through color IR, the chronology and effects of fire in tropical grasslands. Dr. Prunty has encountered some interesting results, such as seeing from overflight data burns that cannot be seen on the ground by experienced field teams, and some problems connected with data processing that he will share with us. The last speaker before the coffee break will be Professor David Simonett from the Geography Department at the University of Kansas. He has been engaged in a wide variety of experiments with remote sensing instruments and data, but his recent efforts have been concentrated on problems of thematic mapping from satellite photography.

Following the coffee break, Claude Johnson of the University of California at Riverside will substitute for his colleague, Leonard Bowden, who is ill, in summarizing the land use analysis, automated data storage, and small scale mapping from Apollo photography of the Imperial Valley. The resultant map of land use in approximately 1,000 plots, some of them as small as 10 acres, needs considerable explanation of the process by which it was made to be fully understood. Professor Robert Pease, also of Riverside, will then continue with a description of his work in peeling dye layers from color IR for analysis, as a substitute for using three black-and-white multispectral films that are subsequently combined, with some registration difficulty, to create a composite color image. He will also report on his instrumentation and research in the field of energy budget (environmental impact) studies. Robert Alexander, the senior scientist of our Geographic Applications Program in the Geological Survey, will explain how these projects fit together, and illustrate their integration through a rather elaborate and sophisticated form, originally suggested to us by Robert Porter, and now referenced appropriately as a Portergram.



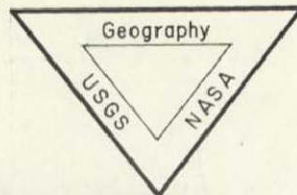
Geography Test Site 46
Asheville Basin, N.C.



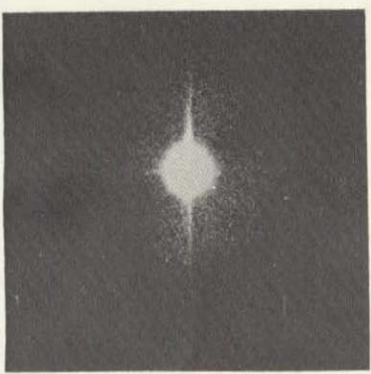
By analyzing power spectra produced by passing coherent light from a laser through conventional aerial photographs, it was found that unique signatures (spectral density patterns) exist for such general land use types as urban, orchard, and forest. Power spectra signatures for a forested area and an urban area in the Asheville Basin test site are shown here.

Power spectra signatures may provide an early step toward eventual automated photo interpretation. The spectral density patterns may also reveal lineaments in the photos too subtle to be detected with the unaided eye. The diagonal dark smears on the power spectra from the forested mountains represent some such subtle lineament, probably in landforms. Some measurement of change gradient is possible.

The potential for several possible forms of image enhancement, filtering, and identification appears to be inherent in this tool for geographic research. Optical processing is more efficient than digital processing for automated storage of imagery.



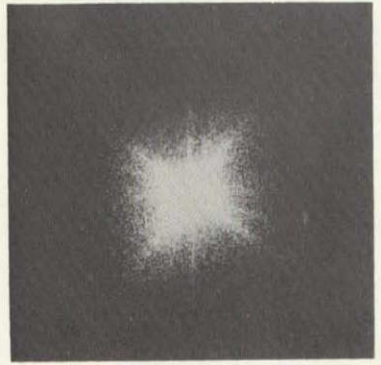
NOT REPRODUCIBLE



Power spectra signature of forested area in photo below



Power spectra signature of Asheville, N.C. in photo above



Based on research at the University of Toronto ...

...as part of the USGS / NASA Geographic Applications Program

b.

Figure 11-1.- Concluded.

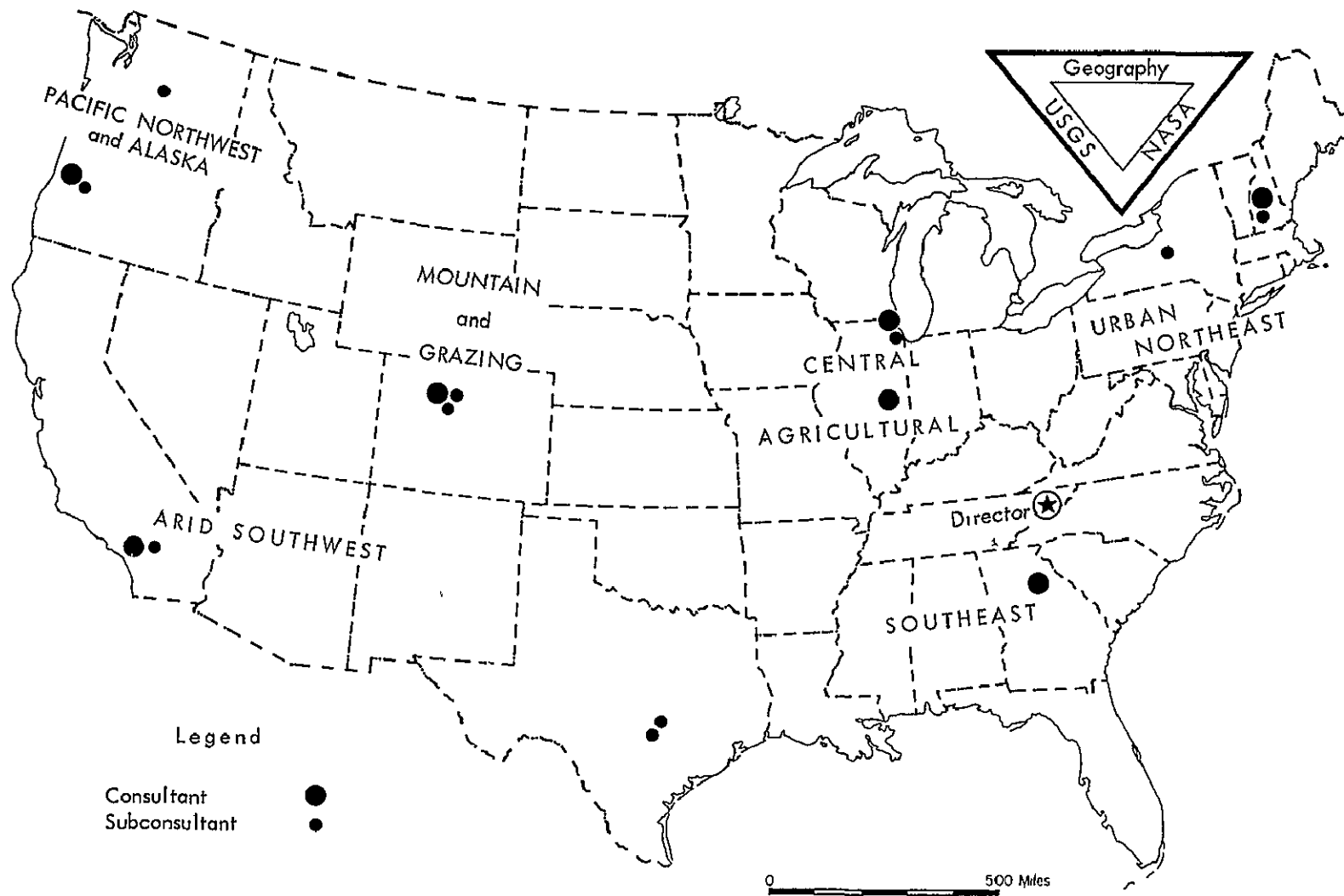


Figure 11-2.- Geographer consultants in remote sensing, by regions

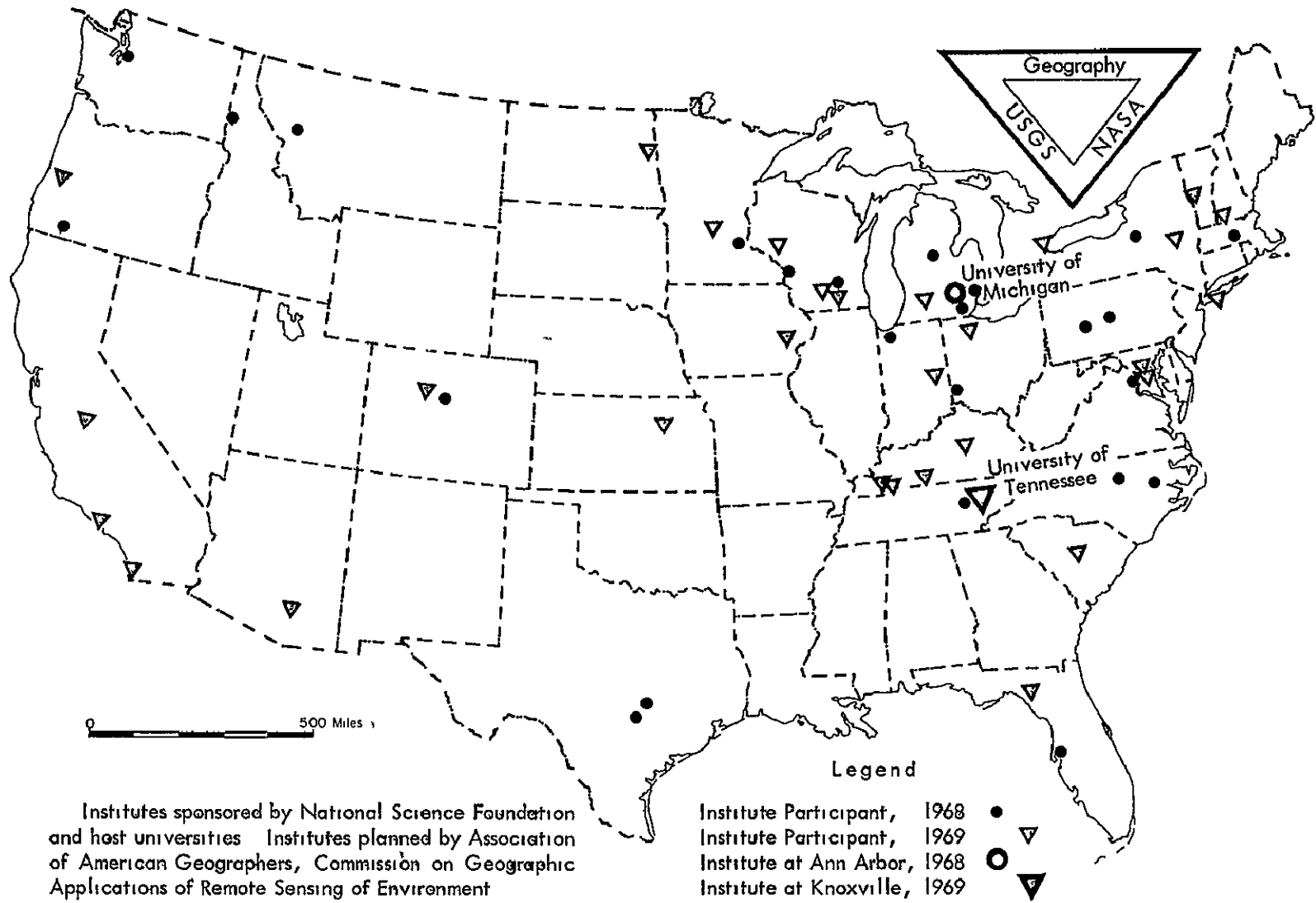


Figure 11-3.- Geographer participants in remote sensing institutes

Aircraft Program Review
MSC/Houston
Sept. 17, 1969
Geography Session

Geography

SECTION 12

REMOTE SENSING ANALYSIS OF GRASSLAND FIRE
PHENOMENA THE FLORIDA TEST SITES, 1968 - 69.

Merle C Prunty
University of Georgia

The long-range objectives of this project are to develop data for the analysis of the occurrence, areally and temporally, of grassland or ground fires in tropical savannas. As indicated in the Aircraft Program Review a year ago, the maintenance of the savanna vegetation type is believed to be primarily a function of ground fires. Recurrent ground fires are characteristic of savannas everywhere and apparently have been so for thousands of years. Although the role of fires in maintaining the ecology of savannas is known from numerous studies of small savanna areas, conducted by many scholars for different purposes and from many viewpoints, there is little uniformity--hence areal or temporal comparability--among these studies. Remote-sensing of ground fire phenomena from satellite platforms can provide observations that are standardized as to observational procedures, quality and time, and are both areally comprehensive and inclusive. Particularly, such observations can encompass large areas in a uniform manner, the savannas of the tropics are, of course, huge regions. Since the Latin American savannas are now subject to considerable pressure for settlement from the rapidly expanding Latin American populations, knowledge of the temporal and areal traits of the fires that are indigenous to these areas has critical significance for the savannas in terms of their land usages and development in the future.

Since the autumn of 1967, the project has been using test sites in Florida and southwest Georgia as simulation surfaces (Figure I). The sites involved were described at the Aircraft Program Review a year ago. In brief, they encompass simulations of upland, lowland, and marsh or swampland savannas, and wooded as well as "open" savanna conditions. They are subject to recurrent burning by ground fires. Some cropland and fallowland are included. The sites include large amounts of unimproved rangeland, a particularly important criterion since low-grade cattle ranching is the areally dominant land use in Latin American savannas today. Both the Deseret and the Griffith Ranch sites are dominated, areally, by grazing operations

During 1967-68, the hypotheses under test were that modifications in vegetative cover caused by ground fires, 1) could be recorded by remote sensing instruments at levels of accuracy sufficient for the production of relatively large scale maps, 2) that these modifications could be recognized and mapped in the chronological order in which the various fires occurred, and 3) that two or more sensors might reasonably provide collative, or supporting, data on both fire occurrence and chronology. Detailed field mapping of the test sites, to establish the nature of the vegetative cover by phytomorphic classes, supplied the principal ground control elements (Figure II) Two flights, one in January 1968 (Mission 964) and one in March 1968 (Mission 67), provided

this project with imagery from 3,000 feet and 15,000 feet altitudes. The imagery included returns from the Reconofax IV plus Ektachome and color infrared transparencies. The project personnel considered the quality of the infrared imagery to be good and comparability of the returns on the infrared medium from the two flights was superior. It became evident, almost immediately, that the color infrared was the critical sensor for the phenomena upon which the project is focussed. The Ektachome imagery, which was of uneven quality, provided some corroborative returns. Reconofax IV imagery, since it is restricted by its powers of resolution, supplied corroborative returns in an areal sense but was of limited value in boundary determinations of burned areas as altitude increased.

The project established from the two flights of early 1968 that the three hypotheses noted above were valid. Phytomorphic classes of vegetation, which also are ecologic categories, clearly and definitely are identifiable and mappable (Figure III). We established that color infrared imagery could record the distribution of burns and the chronology of burns not only during a given "fire season"--a given year--but also could sense the patterns of two and three year old burned areas that were not recognizable to trained observers on the ground. The ability of color infrared to produce such returns was established for the smaller scale imagery, that from 15,000 feet altitude, as well as from the larger scale imagery. At this stage, the project's personnel did not envision the large number of variables that could be introduced into the analysis if changes in the quality of the infrared imagery were to occur.

For 1968-69, the project focussed upon the following notions: 1) coverage of all possible combinations of vegetation cover relevant to savanna conditions that could be obtained in the central Florida area. The Deseret site was expanded and the Griffith ranch site, north of Lake Okeechobee, was added for this purpose. Thus, full coverage of the rangeland vegetation complex, by phytomorphic classes, in Florida was introduced on a typological basis. 2) During 1967-68, ground control was established by large-scale mapping of phytomorphic classes prior to overflights. The same control procedure was used in 1968-69 with one exception. As a test of the validity of interpretation results, a 15 square mile area--previously untested-- was left unmapped for 1968-69. The purpose was to invert the procedure, e.g. map the area from the imagery, then test results on the ground to see if both distribution and chronology of burns could be established accurately without direct ground control. 3) Interpretation indices based upon the returns from flights during a single season obviously have serious inherent limitations if they are used throughout the entire cycle of plant growth--that is, throughout an entire year. Thus, interpretation indices arranged in "families", i.e. indices of the same phytomorphic category at various stages of growth and regrowth throughout the year, became necessary. Because all vegetation is in a growth stage during spring and summer, the identification of growth occasioned by a recent burn, as distinct from normal seasonal growth, is complex. 4) The identification and analysis problems occasioned by reductions in scale, i.e., imagery from the relatively high altitude platforms, had not been tackled during 1967-68. The project needed some high-altitude returns, particularly in the color infrared medium.

In brief, then, the project expected to concern itself with some new and intriguing variables, variables that appeared to be related to problems in

employment of satellite-derived imagery. These were 1) coverage of all available relevant vegetative categories, 2) imagery analysis without direct ground control, 3) imagery from all seasons, introducing the morphologic changes involved in regrowth, and 4) small-scale imagery derived at a high altitude.

Let us consider last things first. It has not been possible to obtain overflights at altitudes of more than 15,000 feet because of the many demands on the P3-A aircraft. Therefore, the problems associated with imagery scale changes remain essentially untouched.

The other problems which the project hoped to resolve during 1968-69 remain only partially satisfied because several unexpected variables were introduced into the color infrared imagery delivered to the project. Project personnel discovered these variables, and identified them with the assistance of MSC personnel, after the imagery variations had taken place--not before. The project was not prepared to handle another series of variables--from its viewpoint, uncontrolled variables--in addition to those built into its program for analysis.

The uncontrolled variables introduced into the infrared imagery are the following: 1) a change in film type from #8443, used in 1968 mission #964, 67, 81, to film type #S0117, beginning in January 1969 with mission #85 and continuing through #90, 92, 93, and 95, 2) the #S0117 film reportedly contains a fast cyan layer which leads to accentuated red tones and suppression of yellows and magentas, 3) there has been some variation in the laboratory processing of the infrared imagery, comparisons of original infrared imagery with the duplicates delivered the project revealed that several times the duplications were not nearly so good as the originals. This problem emerged on mission #81, flown with #8443 film and continued in mission #85 and 90 (using #S0117 film). Reprocessed and substantially improved imagery was supplied to the project from missions #81 and #85, 4) there is no way for the project to know the age of the infrared film in use and we surmise that MSC has not known its age either. It is clear that the older the infrared film, the less sensitive is the cyan layer. Since a cardinal problem has been excessive reddish tones and virtual absence of green and yellow tones, we presume that film used in flights since mission #85 of January 1969, has been relatively fresh, 5) apparently some of the infrared has been underexposed from one half to one stop. This is especially evident in mission #85 imagery, and 6) the yellow layer in #S0117 has, largely, been eliminated from the imagery.

The resultant problems in imagery analysis are indicated by the accompanying figures, all segments of the infrared imagery for the flights indicated and covering the same area. (When referring to the figures the following areas should be used for reference: 1) the main east-west dirt road ("Pipeline Road") through each frame, 2) the large area of improved pasture north of the road and about one mile east of the western side of the frame, and 3) the "Y" intersection of field trails in the approximate center of each frame and south-east of an old improved pasture area which lies between the "Y" and the main east-west road.)

Figure IV comes from Mission #67, March 1968. Note the contrasting tones in this frame. Yellows, greens, reds, and pinks are discrete and highly visible. The char from burns of September 1967 through March 1968 is represented by dark green tones and can be differentiated from the greens representing bayheads and cypress domes by both texture and tone variations. Older burned areas exhibit greater amounts of yellow and light green tones while regrowth upon recently burned areas exhibits more reds. This frame is from #8443 film.

Figure V is from Mission #81, October 1969. It exhibits fair to good tonal contrast. The green-blacks of the "recent" burns have diminished as the ages of these burns have increased and have been replaced by reds overlying subdued gray-green tones. Older burned areas lack the bright red tones which represent those areas burned within the last year. Note the pinkish tones of the improved pasture north of the road in comparison to the greyish tones of the older pasture south of the road. Vegetal regrowth subsequent to fires obviously can be discerned when these two frames are employed in echelon.

Figure VI from Mission #90, March 1969, contains a high proportion of overriding red tones and lacks sufficient contrast among yellows and greens to be of optimum value. Recent burns may be recognized by blackish tones. Differentiation of burns that are one year old from those two or more years old is virtually impossible. The weaknesses of this frame are more apparent when compared with Figure IV (Mission #67). Since the area represented by each frame is the same, and the season of the year is the same, approximately the same imagery signatures for essentially the same phenomena were expected. The obvious differences in signatures appear to result from a change in film type and from variations in film age and processing.

Figure VII, from Mission #92, April 1969, again is an example on the #S0117 film. Recent burns (September 1968 to March 1969) scarcely are visible. When compared with Figure VI (Mission 90) the increase in red tones recorded from March to April 1969, is striking. The boundaries between vegetation categories (areal "compartments") are less distinct than in the antecedent imagery. Differentiation of burned areas from others, and particularly the relative ages of burns, is extremely difficult and cannot be done with confidence. Although more intense red tones were to be expected during a period of peak plant activity, it is impossible to determine what proportions of the increase in red tones resulted from increased plant mesophyll activity and what proportion resulted from the highly sensitive cyan layer of the #S0117 film.

Where does the project stand today, in terms of this year's objectives?

1. As indicated, problems associated with scale change could not be attacked for want of imagery from high altitude platforms.
2. Imagery coverage of nearly all relevant vegetation categories for the Florida ranching area has been obtained.
3. Much of the coverage had to be reprocessed. This, coupled with quite recent delivery of late spring and summer flights, has meant delays in imagery analysis. The project is behind schedule. Analysis in the form of finished maps is at least a couple of months off-pace.
4. Analysis to produce interpretation index "families", consisting of indices covering the phytomorphic classes in seasonal sequences, has produced inconclusive results. Unfortunately,

the index families are the most important aspect of this year's program. The parameters of the problem involved are fairly simple. It is logical to presume that the increased plant mesophyll activity associated with the March to July "peak" in plant growth would record in proportionately increased tones of red on color infrared. However, with the switch to #S0117 film with its fast cyan layer and suppressed magentas and yellows, we are unable to determine what proportions of the increased tones of reds result from the stage of vegetative growth and what proportions are attributable to the film, or what proportions are attributable to the freshness of the film, or to variations in the film processing medium. At this stage there is no answer. 5. The test of imagery analysis without ground control is partially completed. Because of imagery quality problems, no analysis could be made to ascertain the distribution of burns prior to the 1968-69 winter season. On excessively red imagery, burns that are more than one season old are nearly impossible to detect. Ground checks of the 15 square miles involved, made in July-August, are incomplete because torrential rains left much of the area inaccessible. Checks were completed on the outer, more accessible portions of the test area. The results look good to date in terms of recent burns and recognition of phytomorphic types. Completion of the ground checks now is scheduled for October and November.

The summary observation on the research of the project for 1968-69 is simple. There have been many variations in the quality of the infrared imagery that this project has received. These variations have reduced the scientific results which the project has obtained since last September, compared to what it could have obtained. I would like to hope that MSC could institute a quality control program that would insure imagery whose properties are genuinely uniform. If this were done, an investigator then could know that the variations in the imagery are associated with phenomena under test, instead of the result of a new lab process, a new film type, or uncontrolled storage time in the deepfreeze. If this were done, the morale of the investigator would improve and some of his faith in both the scientific process and the folkways of the bureaucracy would be renewed.

The immediate goals for this project are clear. The analysis of imagery signatures through the full post-burn cycle--that is, through a full sequence of seasons--must continue until firm results are obtained. The problems of scale, hence analysis of imagery from a high altitude platform that in some measure simulates the returns that may be expected from ERTS-A and B, have to be resolved. The Florida test sites are not bona fide savannas, they are the best domestic approximations, only, of savanna conditions. There is a genuine need for experimentations with imagery derived from bona fide savannas such as those of Latin America, in association with ground control data from the same savannas. Finally, this project needs to examine the results it has obtained, since inception and on through 1969-70, in terms of probable instrumentation at the satellite stage.

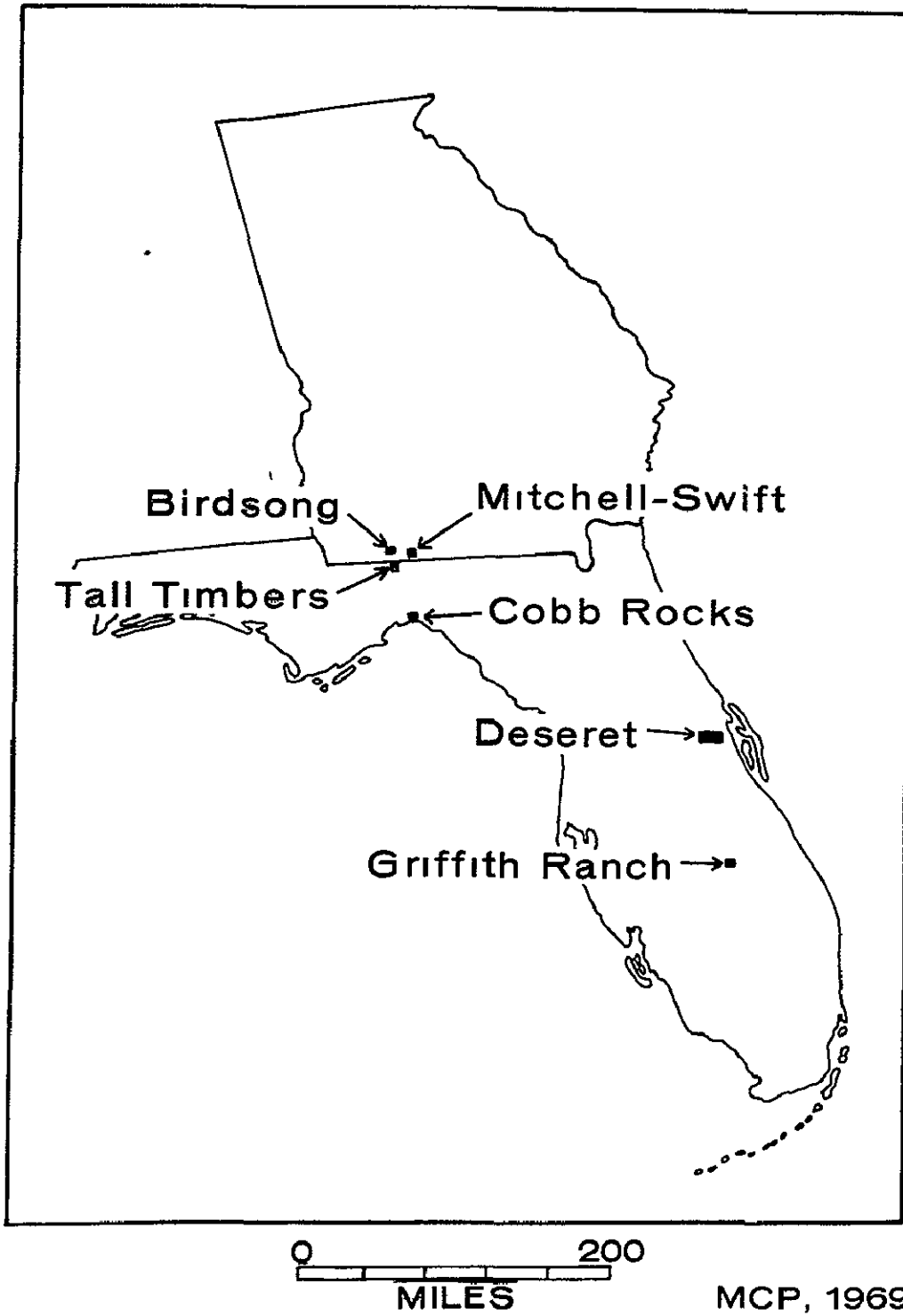
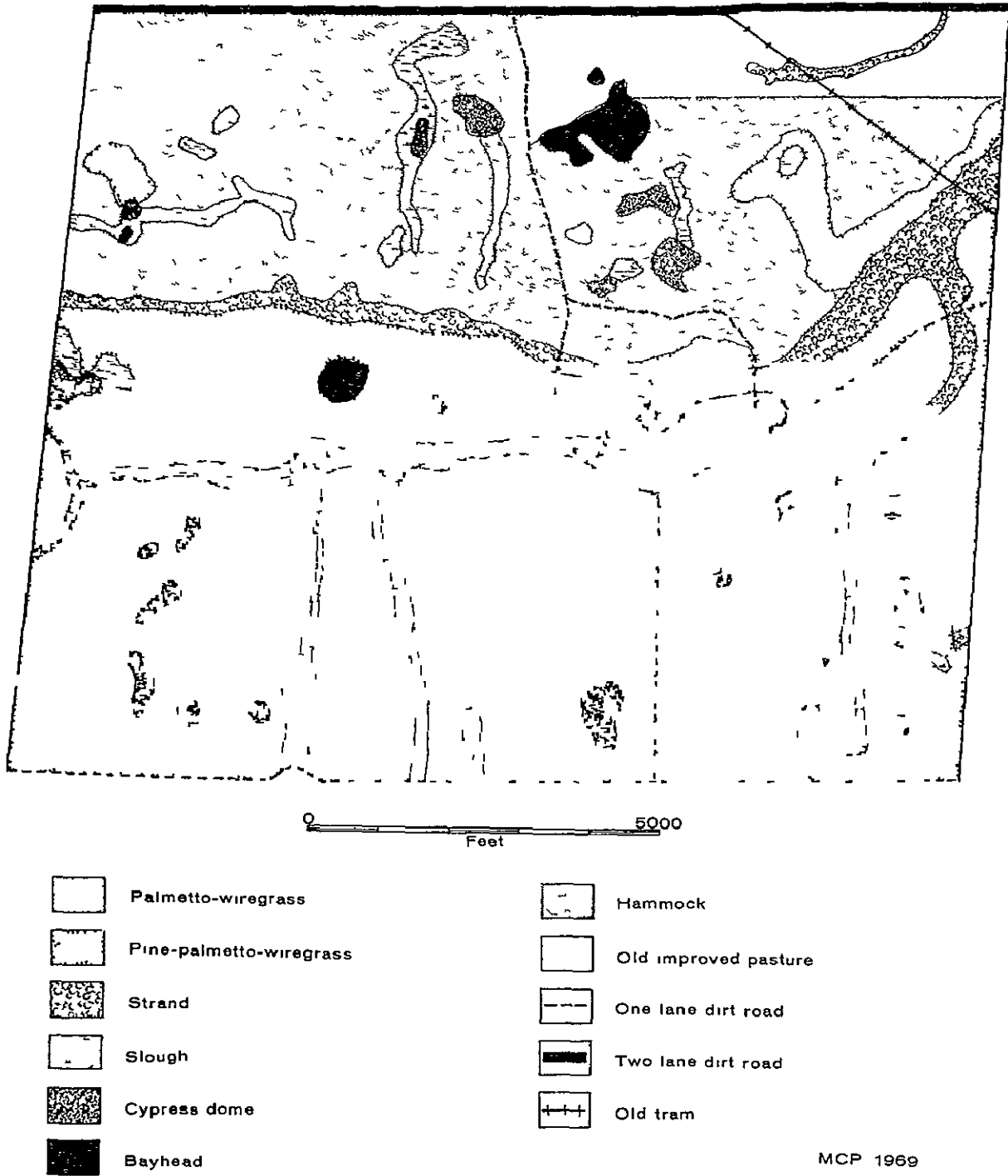


Figure 12-1 - Location of test site areas in Florida and Georgia.



MCP 1969

Figure 12-2 - Vegetation types, Pipeline Road, Deseret Farms, Florida.

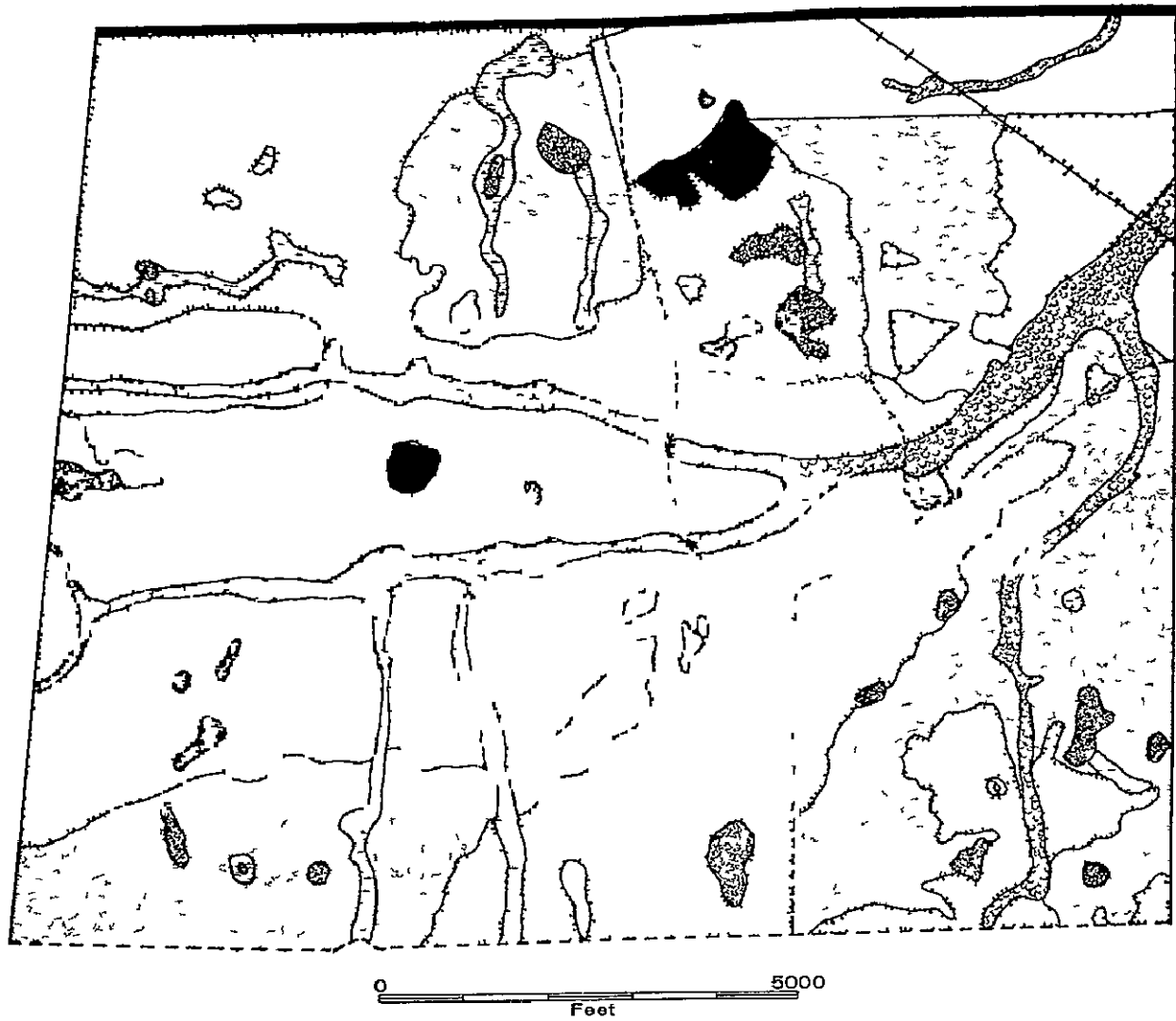


Figure 12-3.- Burns, Pipeline Road, Deseret Farms, Florida, 1967-1968



Figure 12-4.- Pipeline Road Area, Deseret Farms, Florida, March 1968, MSN 67; Color infared, Roll 4, Frame 7224.

12-10

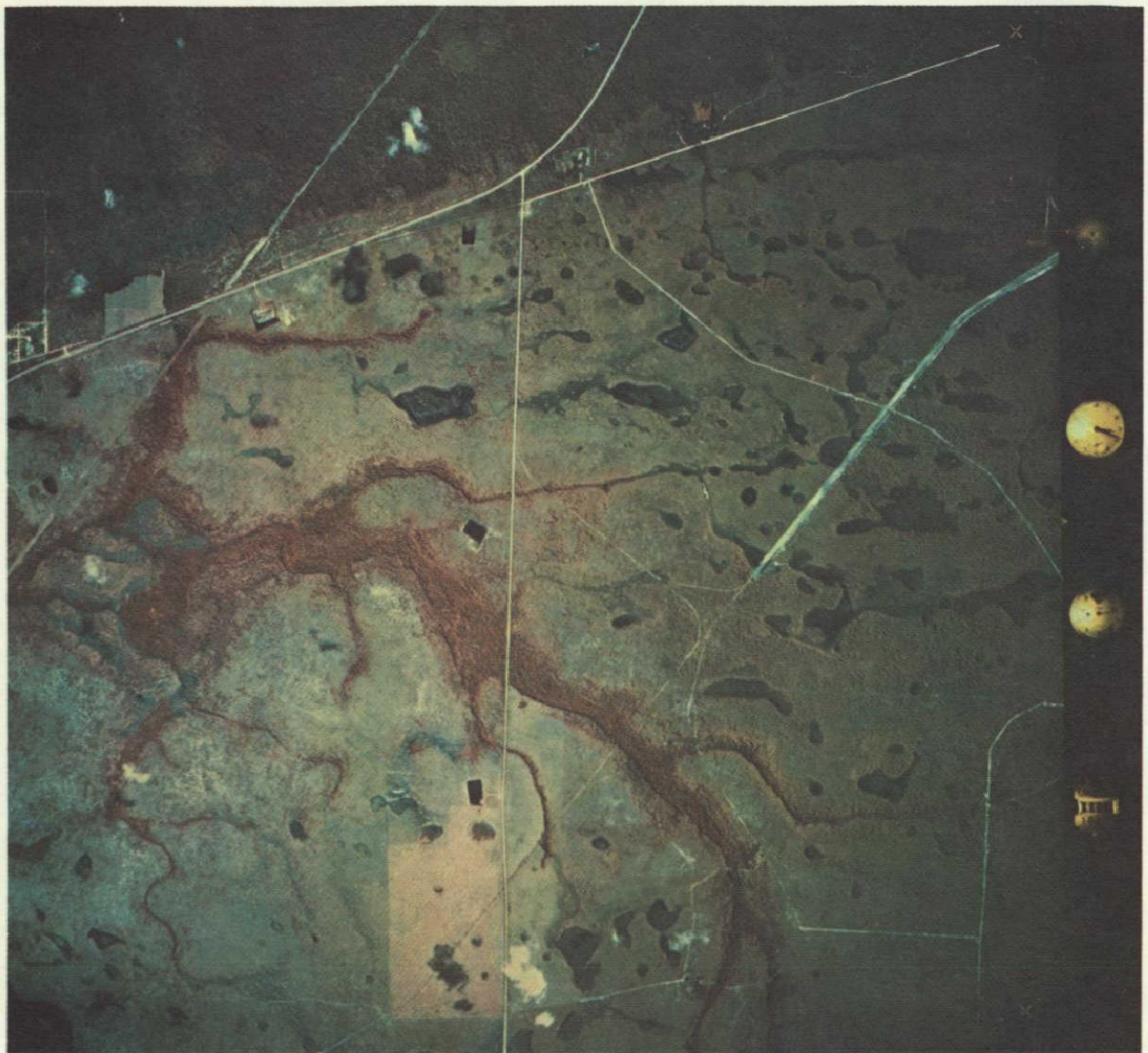


Figure 12-5.- Pipeline Road Area, Deseret Farms, Florida, October 1968,
MSN 81; Color infared, Roll 1 of 3, Frame 6402.

V

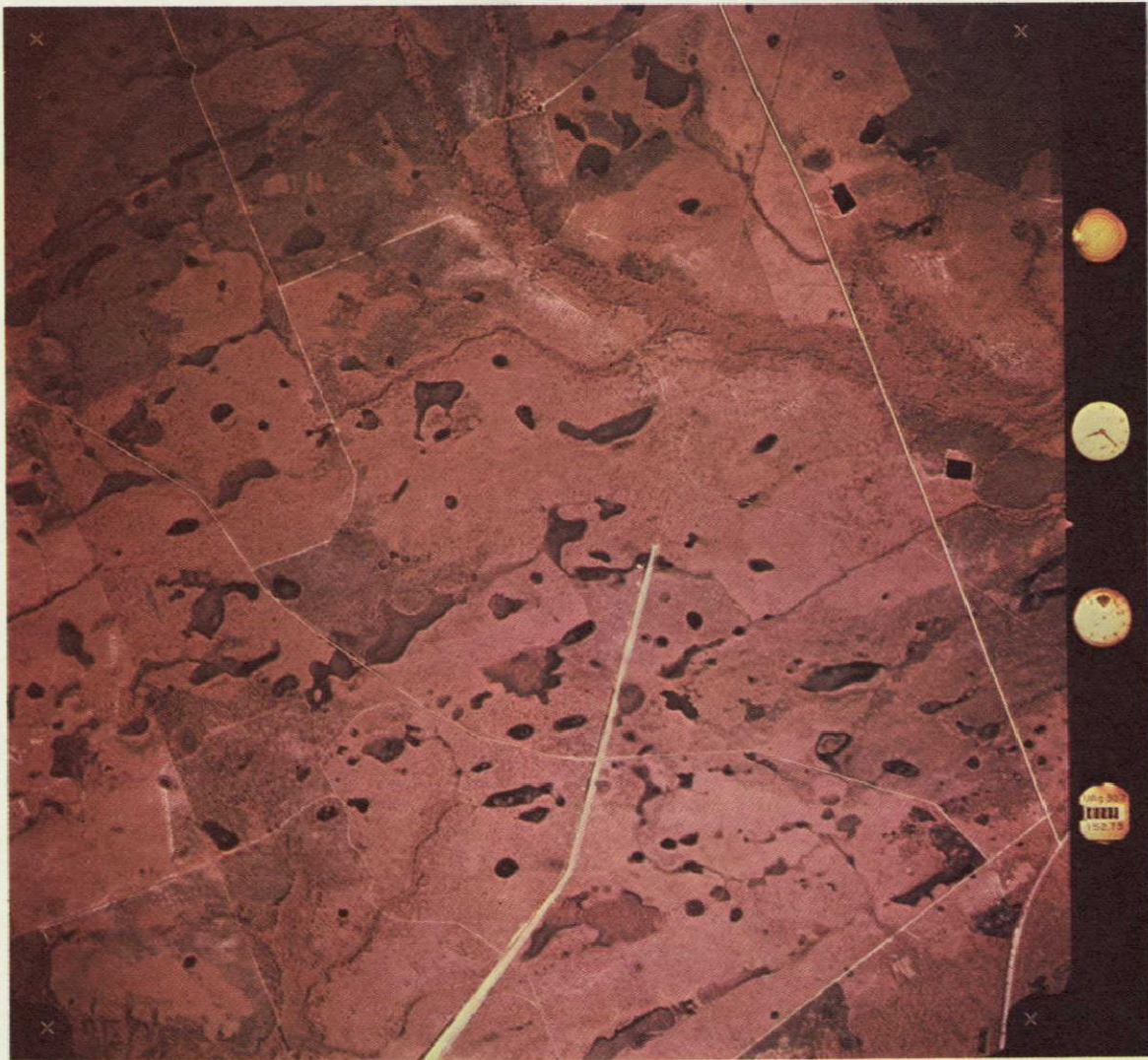


Figure 12-6.- Pipeline Road Area, Deseret Farm, Florida, March 1969, MSN 90; Color infared, Roll 1 of 2, Frame 9788.

12-12

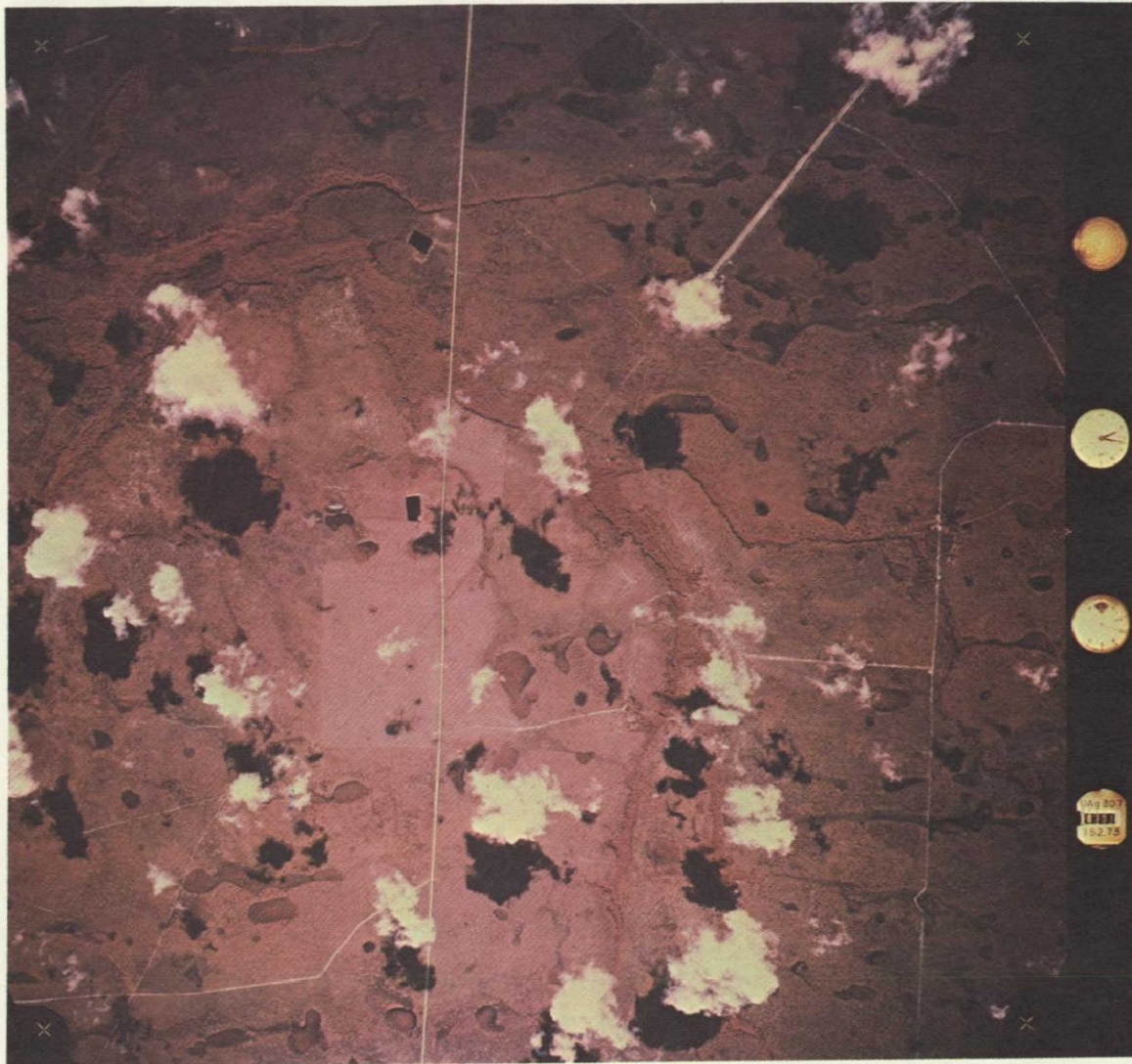


Figure 12-7.- Pipeline Road Area, Deseret Farm, Florida, April 1969 MSN 92; Color infared, Roll 1 of 8, Frame 0131.

SECTION 13

THEMATIC LAND USE MAPPING SOME POTENTIALS AND PROBLEMS

David S. Simonett
Department of Geography
and
Center for Research, Inc.
University of Kansas
Lawrence, Kansas 66044

NTI 19264

INTRODUCTION

In this presentation I propose to discuss the work carried out in my project in three broad groups. The first group involves studies using Gemini and Apollo photography for boundary and road detection. This is followed by three studies dealing respectively with the feasibility of making existing thematic maps from spacecraft data, some comments on the resolution needs for thematic maps in different environments and lastly, a comparison of time available for radar and photographic imagery obtained over the United States. Finally, statements are given on the results to date of the analyses of NASA aircraft data obtained over the Garden City and Lawrence sites.

Running through these studies are a number of themes of relevance to early ERTS or EROS type satellites. One theme relates to comparisons between 100 foot and 300 foot resolutions for thematic mapping. I once argued vigorously for a relatively coarse resolution and there is no doubt that for certain studies resolutions of 300 to 400 feet will be adequate, however, for thematic land use mapping, the evidence presented here indicates that broad-area coarse-resolution (300 feet) imagery should be carefully compared and contrasted with finer resolution imagery (100 feet) which may of necessity need to be coverage of smaller areas. I believe the evidence to hand indicates that the coarser-resolution may not be as acceptable for as many problems as I once thought.

A second thread running through this discussion relates to the nature of boundary delineation between land use entities on space photographs, and the discrimination between entities. The type of data which might be collected in a number of environments during the northern hemisphere mid-summer months are examined and some of the implications are explored in the Lawrence area in Kansas.

The third thread is that multi-channel data has considerable redundancy and that with three or four channels we may obtain almost as much information as with a dozen. If it can be demonstrated that for certain times and places three or four channels are incapable of effecting more than a most minimal separation of data for land use mapping it is imperative that the alternative of multiple looks through time should be thoroughly studied, even though there will be considerable problems in retaining data in a geographic spatial coordinate frame for comparisons of the time-sequential data.

A further concept is that information transfer is environmentally modulated. In short, a single resolution fitted to a very large area will not convey the same class of information in all regions. The size and spatial distribution of the entities making up an environment will substantially influence the character of the information transferred particularly if the resolution is close to a critical level.

Finally, the last theme is that of the consistency with which information may be obtained from the same environment at various times and circumstances.

These five themes are deliberately and provocatively stated in a negative manner, for I am concerned if we obtain too-few looks with a too-coarse resolution, that there will be serious problems in terms of the consistency with which we will be able to prepare thematic land use and related maps from spacecraft photography, that the amount of ground checking required may prove excessive for many problems, and that even the most elementary forms of automatic processing may prove to be so error-prone as to be a hindrance rather than a help.

I will be glad to be proven too conservative. However, the questions I raise are serious and they will not go away by ignoring them. The evidence I present is neither as fully researched nor as secure as I would like it to be. Yet it is sufficiently suggestive for me to wish to share with you this mixture of conclusions, some reasonably supported, others less so.

A standard format is used in the following discussions. Succinct summaries are given of 1) data used, 2) items investigated, 3) context of the investigation, 4) results of the investigation, 5) discussion of the illustrations and tables employed, and, finally, 6) possible implications of these results for spacecraft thematic land use mapping. The implications where appropriate are keyed to the five themes sketched above.

STUDIES WITH SPACECRAFT PHOTOGRAPHY

1 STUDIES IN THE ALICE SPRINGS AREA, CENTRAL AUSTRALIA

Data

Gemini V color photograph No. S-65-45568, color separation plates of same, IDECS color combinations for field checking (IDECS is an acronym for Image Discrimination Enhancement Combination and Sampling system, a hybrid analog-digital system developed at the University of Kansas), 8 weeks field observations.

Items Investigated

- 1 Nature of boundary delineation

- 2 Constitution of entities within boundaries
- 3 Field check of IDECS boundaries and interpreter-delineated boundaries

Context of the Investigation

This semi-arid to arid-region has a considerable range in topography, lithology, plant communities, plant community structures, and densities. It is representative of very large areas of interior Australia and has close affinities with similar environments in millions of square miles of Africa and Asia. In environments such as these there tends to be a very close tie between lithologies, soil types, and plant communities. These areas may well be among the easiest to derive relatively straight-forward relations suitable for space photography thematic mapping. Much more humid environments will be correspondingly more difficult, because the relationships between soils, lithology and vegetation are notably less direct.

Results

Boundary Delineation

1 Almost all boundaries discriminated on the space photography by trained interpreters proved to be meaningful when they were field checked. Many more boundaries were discriminated than by CSIRO (Australian Commonwealth Scientific and Industrial and Research Organization) investigators.

2 First and second order boundaries were meaningful at the major landscape type or plant structural level. By first order we mean high contrast and sharp boundaries. Second order boundaries are of medium contrast, and are not as easy to determine as to their exact location.

3 Third order boundaries were meaningful mainly at the plant density level within a community or at the ecotone level between communities. There is no guarantee that this relationship would hold in other situations. Third order boundaries are diffuse boundaries for which not all interpreters agree as to their existence or their precise location. Those we delineated were based on haggling and majority decisions between interpreters.

Nature of Entities Within Boundaries

4 Many entities which are of considerably different character in the field cannot be separated on the color photograph. Prior to field work many unlike entities were grouped together because of similar color tones on the space photograph. It may be that at other times of the year some of these entities which are confused could be separated because of differences in plant responses. My guess would be that this is doubtful and that probably not much better could be done in this environment with multiple looks through time. However, many of the areas which are confused are regions in which better spatial resolution would enable some of the entities to be separated.

5 A hundred foot resolution would certainly resolve some ambiguities by enabling patterns within an entity to be discriminated and it would be possible then to separate them on the basis of patterns if not on multispectral color differences

IDECS - Delineated Boundaries

6 Field checking of IDECS-delineated boundaries showed that the IDECS consistently separated out certain entities which were equally consistently missed by photo interpreters Also, in many cases the location of first order boundaries by the IDECS and sometimes second order boundaries was closer to the field boundary distributions than those delineated by the photo interpreters

7 Conversely, problems of spurious contouring are present with the IDECS as with any level-selecting analog or digitizing device Spurious contouring takes place in areas where there are diffuse natural boundaries and where there is a gradual change within a class which is not sufficient for a photo interpreter or a ground mapper to segregate them into different entities In short the IDECS, as is also true of a digital system is capable of generating nonsense boundaries

Discussion of Illustrations and Tables

Figure 1, shows the relative ease of discriminating major boundaries on the red separation plate of the Gemini space photograph for the Woodford Creek (upper) and Napperby and Day Creek (lower) areas, in comparison to working with black and white air photo mosaics The relative ease of boundary delineation indicates that space photographs of even this resolution will serve a useful part in an orderly system of double and triple aircraft and ground sampling designed to make effective use of the space photograph

Figure 2, Gemini V color photograph of the Alice Springs region A number of areas of like-color on this photograph represent regions of very unlike entities For example, straw colored areas include Mitchell grass savannahs on alluvial fans, various depauperate Mitchell grasslands now invaded by Kerosene grass, or by ephemerals, complex mixtures of red and white ironstone and kaolinitic lateritic residuals with occasional scattered trees, and mixed shrub and grassland on granite hills

Figure 3, shows the landscapes northwest of Alice Springs, Central Australia based upon a map by R A Perry (1961)

Figure 4, shows the landscapes northwest of Alice Springs, Central Australia delimited without field work and based upon the space photograph Comparisons of Figures 4 and 3 will show boundaries shared by the two maps.

Figure 5, is a comparison of the boundaries shown on the space photograph compared to those on R. A Perry's pasture map Boundaries shared are

in solid lines, those found only on the space photograph are in gray lines. The map is conservative in that only boundaries which are clearly identical on both photograph and map are shown as shared. This illustration is currently under revision for we believe that we have been too conservative in our comparisons. There is a substantial subjective element in such mapping which raises questions on the subjectivity of so-called ground truth. In this respect we may legitimately ask to what extent Perry's map reflects both his unique perception of the environment and the data sources available to him. Other persons may produce different maps by being either more of a lumpener or a splitter than Perry, or in perceiving the environment differently or by having different data available. It is hard to believe that with the space photograph in hand, as well as selected aircraft photographs, that investigators would not indeed find and map these boundaries and thus ground truth and space truth become more nearly the same.

Possible Implications

1 Most, if not all, of the boundaries normally delineated in reconnaissance type surveys of natural plant communities should be detected on space photographs in comparable environments.

2 It is very probable that more — (perhaps many more) — boundaries, may be discriminated on space photos than ground investigations would ordinarily erect. The boundaries will lie at all hierarchical levels in a classification. Thus while most first order boundaries should cleanly separate lithologies, soils, and natural vegetation communities, many second order and certainly most third order boundaries will represent cross cutting relationships, depending on the basis for the boundary delineation. Some may represent merely changes in soil color in the surface which are of no consequence to either land use or to the plant communities there. Such boundaries may not be then necessarily ones we wish to delineate.

3 The meaning of boundaries once delineated will still have to be checked on the ground, and with sample aircraft photography. Many tropical arid, and semi-arid plant communities show little change throughout the year (nothing anywhere near as drastic for example as leaf fall or fall coloration in temperate latitude deciduous communities) and furthermore they are rather random in their occurrence through the years depending on chance unique and heavy rainfall. Thus, it may be necessary to use higher resolutions to obtain information needed on the entities these boundaries separate. One thing we may reasonably state. The coarser the spacecraft resolution the greater the uncertainty as to whether the entities which appear similar on the photograph are indeed similar. The greater the uncertainty the more serious the problem of sampling. If it is not known, for instance, how many subcategories within an entity which are seen as similar on the space photograph really exist, then their spatial distribution cannot be forecast with assurance. How then does one decide on a rational sampling strategy? The implication from this, of course, is that a much heavier investment of

time spent in aircraft and ground sampling will be necessary to resolve these difficulties. For the Alice Springs area I have looked into the spatial distributions of patterns within the entities as seen on the space photograph and I believe that a 100 foot resolution would quite significantly improve the ability to delineate subsets within what is on the present resolution almost indiscriminable.

4 If one thinks of the entire data base as part of a system (the system consisting of space photography, intermediate altitude aircraft photography designed on some rational sampling basis, and lastly ground checks also employing some orderly sampling basis) the pluses and minuses in a systems framework needs to be evaluated. It may be more sensible to seek a higher resolution in spacecraft data and perhaps therefore cover a smaller portion of an area to insure that the investment of time in aircraft and ground work may be rational rather than based upon random possibilities. Certainly the trade-offs require study.

2 STUDIES ON ROAD DETECTION IN THE DALLAS-FT WORTH AREA, TEXAS

Data

Apollo VI and Apollo IX color photography SO65 false color and multi-band photographs, field checking, Texas highway department county road maps, color separation plates, Philco-Ford density level slicing. At a contrast ratio of 1.6 to 1 the best resolutions are probably of the order of 200 feet, the poorest of the order of 500 feet. Average weighted areal resolutions lie in the main from 300 - 400 feet depending on the film, based on data from IESD NASA/MSU, and from Keenan and Slater (1969).

Items Investigated

Detection and delineation of roads as a function of road type, width, and adjacent land use.

Context of the Investigations

It has been suggested that space photography may be used to update changing road networks. This study was designed to determine for the Dallas-Ft Worth area at the Apollo photography resolutions what class of roads were fully and unambiguously discriminated and what the transfer function was for lesser classes of roads in terms of percent detected and errors of commission and omission. A further part of the study is to determine the consistency with which the data may be obtained on sequential or time separated space photography and also to detect between-environment variations in detectability within a single photograph. Differences in road detection will obviously be found in environments as unlike as the arid southwest, intensively cultivated areas in the Great Plains and hilly mixed farming and forest regions in the Eastern United States. However, this study was specifically designed to sample within-photograph variation to assess its possible magnitude and consistency.

Results

1 All super highways of the Federal Interstate System were detected unambiguously

2 Lesser roads were variably detected on different parts of the same photo and on different photos in a time sequence. Some of this is random but others appear to relate to the nature of the background against which the road is viewed. Pasture and highly heterogeneous landscapes make for difficulty of detection.

3 Road width is the most important factor influencing detection and the next is the background (pasture is the worst background for detection)

4 In order unambiguously to detect not only divided highways of the Federal Interstate System but also U S highways we believe that resolutions of perhaps 100 feet will be required. Lower orders of roads especially those that consist of gravel and earth surfaces will require even better resolution for unambiguous detection. The resolution should certainly be no poorer than 4 times the road and shoulder width and it may be necessary in some areas because of complex topography and backgrounds to use resolutions as good as equal to the road and shoulder width.

Discussion of Illustrations and Tables

Figure 6, shows the roads detected on a space photograph and color separation plates of the Apollo VI obtained March 31, 1968

Figure 7, shows four areas delineated on the Apollo VI photograph for detailed comparisons

Figure 8, shows the Apollo VI color space photograph which may be compared to the illustrations in Figures 6 and 7

Table 1, is a table showing the detectability of roads by width on the Apollo VI photograph. Obviously the widest roads are the most visible and the narrowest roads the least visible.

Table 2, shows the percentage of roads visible by class on the Apollo VI space photograph for each of four areas in the region. Note that while there is, in general, a consistent decrease in detectability as road width and quality deteriorates there are some peculiar and certainly some non-random major fluctuations. Fluctuations of this magnitude can occur on a single photograph. It is difficult to see how such photographs can be used reliably to detect roads except those of the super highway system.

Table 3, shows the source of errors in false identification of roads in the four county sample area. These fall into errors of omission (not visible

miles) and errors of commission (false alarm miles) The total percentage of errors from both sources average out to 57 per cent and range as high as 69 per cent

Table 4, shows the percentage of roads that are visible and false alarms on a variety of Apollo space photographs including the Apollo IX SO65 experiment There is obviously considerable between-time and between-film variations

Table 5, shows the comparison of road detection using multiple space photographs in different combinations Again there is considerable variation although many seem to cluster about 40 per cent of the miles being visible

Figure 9, is a comparison between 8-fold enlargements of a portion of the Dallas-Ft Worth area photograph (300 foot resolution) and a portion of the Cape Kennedy area (100 foot resolution) The gain in detectability of roads is substantial with the improved resolution

Possible Implications

1 One possible implication which follows from this analysis depends on the quality of data one desires on road detection and delineation A highway engineer who demands to know exactly what is where and cannot accept a probabilistic statement would find this information intolerable for all except the super highway system I am not prepared to say that all super highways everywhere in the U S would be unambiguously detected with similar resolutions to those used in the Dallas-Ft Worth area

2 In detecting line elements in a landscape, multiple looks through time and multiple channels will aid in their detection However, the ambiguities which reside in detecting line elements below the resolution limits of a system are such that the multi-time or multi-band approach will not consistently and unambiguously give the data required In short, this is a case where I think there is no substitute for resolution In order unambiguously to detect both the Federal Interstate System and the U S highway system I doubt whether resolutions poorer than 100 feet could be used with spacecraft photography with the dynamic range found in hard copy color film

3 The cartography-geodesy panel, (Panel 13) of the National Academy of Science Summer Study on Space Applications (1969) recommended that a 20 meter resolution photographic system could be utilized for updating maps normally issued at a scale of 1 250,000 In regard to transport systems, such maps will include Interstate and U S highways and a number of State highways. The study in the Dallas-Ft Worth area lends strong support to the view of the cartography-geodesy panel

4. We were not able to detect railroads on this photography, nor was Barry Wellar (1969) in studies he has made in the Houston and San Antonio areas Consequently we cannot make any estimates as to what the critical resolutions may be for detecting railroad systems

STUDIES EMPLOYING DATA FROM NON-NASA SOURCES

Three studies are reported in this section, the first dealing with the feasibility of constructing thematic maps from space data, the second, with the resolution needs for thematic mapping in different environments and the last with a comparison of time available for radar and photographic imagery obtained over the United States

FEASIBILITY OF CONSTRUCTING EXISTING OR NEW THEMATIC LAND USE MAPS WITH SPACE PHOTOGRAPHY

Data

A sample of about 100 thematic land use maps taken from the University of Kansas map library were studied in general and a representative subsample of 23 were studied in detail.

Items Investigated

The categories shown on each map were studied to determine what proportion could be mapped with a spacecraft photograph using 100 foot resolution and what proportion could not be mapped either because they represented synthetic categories, required too fine a resolution, or would need to be based on inference rather than direct observation

Context of Investigation

No systematic study of thematic land use maps has ever really been attempted. The utility of existing maps is usually not clearly stated nor it is apparent from the map itself. A rational classification of such maps is also lacking and perhaps infeasible to produce. In our preliminary study of thematic maps we found no systematic relationship existed between the scale or the subject matter of the maps and their complexity. The makers of the maps, mostly government agencies, do not state the reason for providing such a map in most instances, but the existence of these and similar maps would indicate that they are the types most used in resource studies, regional planning, policy decisions, and other economic and governmental functions. It is virtually impossible to give either a full justification or a cost accounting for the production of such maps. About all one can argue from then in the spacecraft case is that these maps exist and presumably serve a useful purpose. It is our task now to see how many of the maps could be produced with spacecraft data.

Results

Very few existing land use maps at any scale could be exactly duplicated from spacecraft data. This arises because practically every map we have inspected mixes some categories which could be observable using space data with others which are non-observable. The non-observable categories

may require a) to fine a spatial resolution, b) information which is not obtainable from space, being obtained from statistical sources or inferences, or c) it represents a synthesis of material often from statistical sources

However, this evaluation has been based on traditional types of land use maps and the kinds of categories they have always employed. It is further apparent that no consistent and rational theme of land use categories runs through the maps we have studied. Many of the maps are composed of illogical and inconsistent categorization schemes. Most reflect the peculiarities of their locales and the idiosyncracies of their compilers as well as the diversities of their data sources. They frequently give emphasis to land uses which would be of little importance considering the world scale.

It will be unrealistic to expect that traditional detailed land use categories with all their peculiarities may be mapped with space data. Very general schemes of categorization such as those being developed for space photo use by the land use commission of the Association of American Geographers, those used by Thower and Associates in the University of California of Los Angeles, and those developed by us in Kansas will require considerable testing on their applicability over large regions. The single format imposed by space photography is both an advantage and a constraint in the construction of land use maps.

Discussion of Illustrations and Tables

Table 6, is a summary of the capability to duplicate sample maps using space data. It may be seen that of the 23 maps only 3, each with a small number of exceedingly simple categories, could be completely mapped from space. The capability for mapping from space using about 100 foot resolution is broken into 5 classes

- 1 readily done with few and slight errors
- 2 can be done with moderate but normally "acceptable" error
- 3 can be done with large, but "possibly acceptable" error
- 4 unreliable can be done only with great difficulty, errors are rarely acceptable
- 5 cannot be done

Only one additional map (of Craighead County in Arkansas) could be reproduced with moderate but normally acceptable error (Class 2). More than half of the maps fit into categories between 3 and 4. One is forced to conclude from this analysis that there will be no facile slipping of space photography into an existing system of producing land use maps. Completely new schemes of categorization and methods of handling will be required. It is instructive to take a few of the categories in each of these maps for comparison to show the types of problems we face in duplicating categories with spacecraft data: horticulture, unproductive land, Borneo Ironwood Forest, Casuarina Forest, dry fields, Arid Hummock Grassland, Arid Scrub, Tropical Layered Forest, Alpine Complex, Orchards and nursery gardens, yards, cemeteries, pit quarries, shifting

cultivation, coffee, cotton, forest and woodland grazed. It is equally instructive to consider the categories which can be essentially fully done from space. The Craighead County (Arkansas) map has three categories — forest, settlement, other, the French North Africa map has six categories — cultural zones, plateaus and mountains, desert, erg, woods and forest, oasis, the map of China has two categories — over 40 per cent of the area in cultivation, and 20-40 per cent of the area in cultivation, the map of U S S R has three categories — forest or wooded area, principal cultivated areas, and all other categories.

Possible Implications

The overriding implication of this study has already been stated, namely that it will not be possible to duplicate many existing land use maps and that new systems of categorization compatible with space photography and capable of consistent application will require to be developed and tested.

RESOLUTION NEEDS FOR THEMATIC MAPPING WITH SPACECRAFT PHOTOGRAPHY

Data Used

Aerial photographs of the following locations: Western and Eastern Kansas, Virginia, Puerto Rico, South Vietnam, Costa Rica, New Guinea, Tanzania, Panama.

Items Investigated

The number of discrete entities in resolution cells of different size were counted in each of the sample photographs. The resolution cell grid size ranged over the following steps: 1000 ft, 400 ft, 200 ft, 100 ft, and in some cases 50 ft. Transparent overlay grids were placed over the photograph and the number of discrete entities which fell in a single resolution cell at these sizes were counted and tallied and then expressed as a percentage of the total number of cells of a size-class investigated. The cells were broken into 4 classes containing one, two, three, or four or more entities in a single resolution cell. An entity as used here represents apparently different objects such as cropland, water, forest, brush land and so on. For example, some of the larger cells may contain as many as 5 entities — bare ground, crop A, crop B, forest, water, settlement.

Context of Investigation

Predictions on the resolutions which may be acceptable with spacecraft photography have generally been based upon considerations of the dimensions of the objects being investigated. Frequently these studies have implied that the entities to be resolved exist in units which are both of sufficient size and so distributed in space that the same information will be obtained consistently with a single resolution in many regions. This is an exceedingly simplistic notion and is incompatible with our knowledge that land use entities vary

markedly in size from place to place. Sizes of fields cropped is the most obvious of these, but there are many other entities which also have different size distributions in different environments. To illustrate this comment the sample air photographs from a number of environments have been studied as noted above.

The second point of concern in tabulating the number of entities within resolution cells of different size and in different locations relates to the question of unambiguous identification of entities using pattern recognition techniques with multiple channels. If the pattern recognition process is to be "successful" (or at least as successful as the technique allows with a given set of data) ideally each cell should contain but a single entity, or, if it contains more than one, the others should constitute such a minor part of the total as not seriously to perturb the value for the dominant entity. Obviously the coarser the resolution the more boundaries will be contained within a single cell or entities. This is the familiar problem of cell size in any statistical sampling procedure.

Results

The tables of number of entities per resolution cell for the areas studied indicate that for each environment there is a critical resolution size, at which, and for finer resolutions, a high level of detection of a homogeneous entity becomes possible. The term, homogeneous entity, is relative, it does mean that only one kind of crop or plant is discriminated. Some generalization is necessary. It implies distinction between fields rather than distinctions within a field, it implies distinction between clumps of trees rather than between different tree species.

It is too early to specify at what level we should choose to have resolution cells contain single entities. If for example we choose that 50 per cent of all resolution cells should contain but a single entity, the resolutions which would be required to obtain this level would be 400 feet in large irrigated fields near Garden City, Kansas, approximately 200 feet in the mixed farming regions near Lawrence in Eastern Kansas, approximately 150 feet in mixed farming areas in Orange County, Virginia, approximately 120 feet in a sample area in Costa Rica, about 100 feet in the Agua Buenas area of Puerto Rico, smaller than 50 feet in intensely irrigated areas in South Vietnam and of the order of 100 feet in two areas each in New Guinea and Tanzania. Only in the rain forest region of Darien Province in Panama where virtually the whole landscape is covered with rainforest would quite poor resolutions be acceptable.

From this analysis we conclude that the resolutions needed to obtain a particular class of information will change from environment to environment and that if consistency is required then the most limiting environment to be covered should be chosen to set the resolution constraints. The alternative is to apply a fixed coarse resolution to a variety of environments, and accept the fact that the results obtained will be acceptable in some areas, but not in others. Potential users of such data should be warned of the limitations.

within which they must work, so that they are not misled by results obtained in large irrigated fields in southwest U S A where most studies with space photography have been carried out to date

The consequences of applying a 400 foot resolution to a number of environments are rather disturbing, particularly when it is realized a 400 foot resolution is likely to be close to the average weighted areal resolution (AWAR) of some of the systems which will be proposed for ERTS satellites. With this resolution and a contrast ratio of 1.6:1, 50 per cent of the resolution cells would contain only a single category in Western Kansas, 36 per cent in Eastern Kansas, 10 per cent in Eastern Virginia, 10 per cent in Costa Rica, 5 per cent in Puerto Rico, none in South Vietnam, 22 per cent in New Guinea, 12 per cent in Tanzania and another site in New Guinea and about 90 per cent in Panama. Of those cells which contain more than one entity, many will contain 3 or 4 or more. Consequently, since a single value only is obtained from a single resolution cell in a given wavelength band the chances for acceptable discrimination drop, and that for serious errors in prediction increase correspondingly. Study of the tables given in the following illustrations leads me to repeat that there are indications that 300 - 400 foot resolution will be unacceptable in substantial areas of the United States, let alone those areas where man's activities are cut from a bolt with smaller patterns. We have a larger study underway on this problem.

Discussion of Illustrations and Tables

Figure 10, shows 6 photographs reduced to a common scale of 1) Western Kansas, 2) Eastern Kansas, 3) Virginia, 4) Costa Rica, 5) Puerto Rico, and 6) Darien Province, Panama. The sizes of the land use classes obviously differ considerably in these environments.

Table 7, shows the proportions of the resolution cells which contain specified number of categories for different resolution grid sizes in commercial agricultural areas of Eastern Kansas, Western Kansas and Eastern Virginia.

Table 8, shows for mixed commercial and subsistence agriculture in Costa Rica, Puerto Rico, and South Vietnam, the same matrix of resolution grid size tabulated against the percent of the decision/resolution cells containing a specified number of categories. It is obvious in comparing Tables 7 and 8 that the scales at which man patterns his landscapes varies widely from locale to locale and consequently no single resolution will give the same level of information in different environments.

Possible Implications

1. The most important implication is that if the figures in these tables hold over a greater variety of circumstances then we should be very careful in accepting the notion that 300 - 400 foot resolution with an ERTS satellite will be equally useful throughout the United States. While it may be adequate in

areas of large irrigation agriculture in southwestern United States and Western Kansas, I wonder whether it will be satisfactory in the Mid West and southeastern and northeastern United States

2 It would be premature at this time to say that the above conclusion is certain. I propose to carry out numerous further studies throughout the U S so that we can tabulate adequately the range of possibilities involved. By the time the next aircraft review rolls around I expect to have a much more thorough study on this subject to present to you

COMPARISON OF TIME AVAILABLE TO RADAR AND PHOTOGRAPHIC SYSTEMS IN THE UNITED STATES

Data Available

Data on precipitation rates per hour and percent cloud cover per hour for each hour during the day, by month, averaged over a 10 year period for 150 stations in the United States. This data is obtained from Tables C and E in Climatology of the United States, the Decennial Census of the United States Climate, Summary of Area Observations, 1951-1960. These data were used with astronomical tables and computer programs were written to calculate the amount of time when cloud cover of less than 30 per cent existed with the sun 30° above the horizon. This enabled calculation of the time available for photographic systems. The amount of time lost to radar was estimated at those number of hours during the month in which the rainfall rates exceeded 0.25 inch per hour. This value represents those cases when a 3 cm radar system would suffer between 8 and 10 db 2-way attenuation.

Items Investigated

- 1 Time available to photographic systems by month in the United States
- 2 Time lost to radar systems as a result of rainfalls in excess of 0.25 inch per hour by month for the United States
3. Ratio of time available for radar in comparison to photographic systems by month in the United States

Context of Investigation

There have been many comments in the literature on the utility of photography and radar in different environments. This study quantitatively shows the variations in time available to these sensors in different regions of the United States. Using this data it will be possible to compare areas realistically.

Results

The results of this investigation are a series of maps showing respectively the amount of time available for photography with 3/10 cloud or less in the United States by month and a series of maps for radar showing the number of hours lost per month with rainfalls exceeding 1/4 inch per hour. A third series of maps are now being constructed which give the ratios of time available to radar in comparison to photography by month.

Discussion of Illustrations and Tables

Figure 11, shows the time available to photography with cloudiness of 3/10 or less and solar azimuth of 30° or greater for the month of July

Figure 12, shows the number of hours lost to X-band radar in July through precipitation equal to or exceeding 25 inches/hour. In the mid west and southeastern agricultural regions, the ratios of time available for radar in comparison to photography on a 24-hour basis range from 10:1 to 15:1. On a daylight-hour basis it ranges from 6:1 to 9:1.

Possible Implications

1. In one sense this investigation demonstrates the obvious, namely, that there are many more hours available for radar imaging of the United States than for photographic systems and that there are considerable regional differences in the times available. In demonstrating the obvious, however, it forcefully reiterates that radar is virtually an all weather sensor when an X-band system is employed and that it is indeed the only sensor which can meet the dual requirements of moderate to high resolution coupled with an on-demand capability for obtaining information except under extreme weather conditions.

2. There is a second implication to this study. That is, if time turns out to be a better discriminant for land use identification than multiple channels (see later discussion on the Lawrence area in Kansas) then optimal use of aircraft would favor a system which could obtain the data without hindrance of clouds. This point can hardly be over emphasized.

STUDIES USING NASA AIRCRAFT DATA

MISSION 54, JULY 1967

SITE 85, LAWRENCE AND VICINITY, KANSAS

Data Used

With RC8 color infrared photography 2436 data points were obtained, five to a field for 487 fields, using a 1 mm spot size on a MacBeth Quantalog color densitometer. (This gives an equivalent resolution of 75 feet). At each data point densitometer readings were made of the blue, green, and red values in the photo corresponding to the bands sensitive to the green, red, and infrared spectral regions in the film. The data was digitized in 10 levels of gray for each band and was randomly divided into two data sets for training and Bayesian predictions. Predictions were made both with raw (unnormalized) data and unnormalized categories, and with normalized data and normalized categories. Normalizing the data enables one to obtain ratios which are not subject to vignetting and perhaps some processing errors, while normalizing the categories gives equal weight to all crop classes. Normalization by categories enables one to test what would happen when one trains in one area and predicts into an adjacent region which contains a different population.

distribution of the entities within the sample. The cleaner and sharper the predictions for all categories in the training region the less likely are we to obtain serious degradation in prediction quality as we move away from the training set. However, if particular categories are not well predicted even in the original training set, with increasing change in the population distribution of the various crops, predictions can rapidly become meaningless.

Items Investigated

Training and Bayesian prediction for land use categories with only single entities contained within a resolution cell. Thus each cell was measured well away from field borders.

Context of Investigation

One proposal for an ERTS satellite suggested a three channel system with channels in the green, red, and infrared regions, essentially those contained in color infrared film. The proposal also recommended that the spacecraft be sun synchronous with the northern hemisphere summer solstice such a system would produce photography comparable in character and to some degree in timing to that investigated in this study.

Many studies have recently been carried out with a 12 channel scanner, and a 28 channel scanner is being built for continuing aircraft studies. However, in this study we wished to simulate what the situation would be at the peak of the summer flush growth in Eastern Kansas with either hard copy color IR space photography or — a less secure simulation — a 3 channel satellite system. In addition, we were interested in obtaining some indications of the problems which might be found in humid tropical environments where lush growth is common throughout the year.

Two further rationalizations lie behind this experiment. Studies at Purdue have indicated that there are substantial redundancies between channels and that the output of the 12 channel scanner commonly may be collapsed to 4 or even 3 channels which contain about as much information (sometimes more) as the full 12-channel set. The feature extraction program at Purdue usually tends to include a channel from one (or both) of the red and infrared regions. The second rationale arises from my concern about the quality of the information which will be obtained at this time of year, which represents a worst-case situation. Expectations which are based on studies in the spring, early summer, and fall, when conditions are better for discrimination, will probably not be met in mid summer.

Results

1. There is exceedingly poor discrimination between crops at the individual-crop level (14% identification), and even when crops were grouped into broader categories such as forage crops, large grain, small grains and

2 If a 3 channel system (or a 3 channel set selected from a larger number of channels) obtained results of this quality (or even twice as good) with space data we would be well-advised to temper our predictions as to the value of space photography at selected times and places. I do not claim that results as poor as these will be universally or indeed even commonly acquired, for crop variability is notoriously wide in Eastern Kansas. The results should however lead us to be cautious in predictions until we have a much wider range of data available.

3 These results also suggest that the bulk of the information about the environment at times of inadequate crop spectral contrast will be contained in contextual and geometric clues. This in turn leads to the notion that studies to determine critical resolutions would be required for tropical situations. We currently are engaged in such a study in Puerto Rico, using data collected in Mission 98 in late July 1969.

4. Finally, this study reinforces the notion that time-dependent variations in crop should be thoroughly studied in a wide number of environments.

NASA/MSC AIRCRAFT MISSIONS DURING FISCAL 1969

Three missions were obtained in fiscal 1969 over the Garden City and Lawrence sites in Kansas. These were missions 74, 77, and 80. The first two were obtained 6-21-68 and 8-2-68 respectively, over both Garden City and Lawrence, while Mission 80 was obtained 10-7-68 over Garden City only.

The missions were obtained to evaluate radar scatterometry data as such, and secondly to use scatterometry to substitute for a radar imager. The intention in using scatterometry as a substitute for imagery was to take data at angles from 30 to 40 degrees. These have been recommended for spacecraft and are also those which have been used in our earlier studies with radar imagers. All other sensors were supportive to the radar scatterometry data to aid in interpretation of the scatterometry.

Missions 74 and 77

The scatterometry data has been analyzed and reported in technical report 118-17 issued July, 1969 by Mr. Jerry Bradley. For both missions 74 and 77 the scatterometer data was obtained in the saturation region of the tape recorder. As a result only the low angle data of 5 and 10 degrees can be utilized. Also, even these angles require additional analysis of the frequency spectral response of the recorded data and the measured receiver-recorder transfer functions before it can be utilized. These two angles will neither apply to aircraft imagery of the sidelooking type nor will they enable any evaluation of scatterometry to be carried out. Consequently these two missions must be written off except for ancillary work which may be carried out with the other sensors at a later time.

soybeans the percent correct identification was still no better than 35 per cent for any combination of normalized or unnormalized data and categories. Of course, this "improvement" is in part an artefact of reducing the number of sets within the data.

2. With predictions as low as this it is really improper to use the word "predictions" for the Bayesian output. As shown in Figure 14 there is a great deal of overlap between the three dimensional probability distributions and it is only on the skirts of a few of these that clear cut identification is possible.

Discussion of Illustrations and Tables

Figure 13, is a color infrared photograph immediately south of Lawrence, Kansas taken on July 31, 1967. The letters on the photograph indicate the crops present. P = mixed pasture, B = brome grass pasture, C = corn, W = wheat stubble and weeds, A = alfalfa, O = oat stubble and weeds, H = hay.

Figure 14, shows the considerable overlap in the densitometry data for the six most commonly occurring crops (alfalfa, brome grass, corn, mixed pasture, sorghums, and wheat stubble). Only at the tails of the distributions is it possible to get clean discrimination. Not only are the means of the individual distributions very close together but the within-class variation greatly exceeds the between-class variation.

Table 9, is the Bayesian contingency table based on unnormalized data and unnormalized categories. Training was performed on one-half of the data, classification on the other. This table also demonstrates that there is little if any basis for discrimination between crops in this area at this time, because the within-crop variability greatly exceeds the between crop variability.

Table 10, shows the data arranged in crop-groups — forage, large grains, small grains, and soybeans — using unnormalized data and categories. Even with the data collapsed into these groups there is a great amount of confusion and prediction accuracy is about 35 per cent.

Table 11, shows the type of changes that occur through normalization of data and categories in the four group — forage, large grains, small grains, and soybeans — case. Comparison with Table 10 shows that while the predictions for forage have improved those for large grains have deteriorated substantially. Prediction accuracy remains about 35 per cent.

Possible Implications

1. It may be that this worst-case example is indeed just that! Thus, extending any conclusions from this study may prove to be as serious an error as extending single best-case examples! However, I suspect that other instances will be found when we collect mid-summer data in temperate latitudes, and almost any-season data in the wet tropics.

Mission 80

For Mission 80 a first draft of a technical report has been prepared. Digital and analog time-history plots were compared with ground-truth data.

Items Investigated

1. The resolution cells were averaged per field, excluding boundaries and these were then correlated with ground truth
2. We attempted to smooth high incidence angle data to improve data character

Context of Investigation

1. To find the operating character of the instruments and to find what angles contains sufficient data to be worthy of further analysis.

Results

1. The analog data is still better than digital data
2. Noise spikes are introduced into the digital data at high incidence angles
3. The Reconofax IV imagery is considerably better for plotting than the RC8 photography
4. Farm buildings give the highest return at all angles
5. Of the crops, recently irrigated bare ground and emerging wheat are the highest at all angles
6. Dry bare ground is the lowest at all angles
7. Inversions are common in the data, for example, sorghum is high at 5 degrees and relatively low at 55 degrees, sugar beets are medium at 5 degrees and relatively high at 55 degrees

We recently re-evaluated this data and intend to analyze it further during the coming year.

The noise in the system makes all angles greater than 15 degrees unusable. The 5° and 10° angles will be used in simulation studies of a Radscat type instrument.

ACKNOWLEDGEMENTS

In the preparation of this report, I have drawn heavily on unpublished manuscripts and theses in preparation by the following faculty and students at the University of Kansas: Studies in the Alice Springs Area, G R Cochrane, D E. Egbert, and S A. Morain, Studies in the Dallas-Ft Worth Area, D E Egbert and F M Henderson, Feasibility of Constructing Spacecraft Thematic Maps, G F Jenks and D E. Schwarz, Resolution Needs for Thematic Mapping with Spacecraft Photography, J Ratzlaff, Time Available for Radar and Photography in the United States, J R Eagleman, J Marshall, and S A Morain, Studies Using NASA Aircraft Data — Mission 54, W G Brooner, Studies Using NASA Aircraft Data — Mission 74 and 77, G A Bradley, Studies Using NASA Aircraft Data — Mission 80, W G Waite and R L Walters

REFERENCES

- Bradley, G A (1969), The effect of amplifier saturation on a doppler scatterometer, CRES Technical Report 118-7, Center for Research in Engineering Science, The University of Kansas
- Geodesy/Cartography Panel (1969), Useful applications of earth-oriented satellites, National Academy of Science, National Research Council publication
- I E S-D (undated), Camera System and Calibration Apollo AS-502 (Apollo VI), NASA Manned Spacecraft Center, Houston, Texas.
- Keenan, P B and P N Slater (1969), Preliminary post-flight calibration report on Apollo IX multiband photography experiment SO-65, Tech Mem 1, Optical Sciences Center, University of Arizona, 1-14
- Perry, R A (1961), Pasture lands of the Alice Springs area, map (1 1,000,000), Division of Land Research and Regional Survey, CSIRO, Melbourne, Australia
- Wellar, B S (1969), Hyperaltitude photography as a data base in urban and transportation research, Dept of Geography, Northwestern University, Evanston, Illinois

TABLE 1

DETECTABILITY OF ROADS BY WIDTH ON APOLLO SPACE PHOTOGRAPH			
ROAD TYPE	ROAD WIDTH	ROAD PLUS SHOULDER WIDTH	% VISIBILITY
Divided Roadway	46	70	100
Paved Roadway	25	37	80
Bituminous Surface	20	28	65
Metal Surface	19	19	38
Graded and Drained	16	16	18
Bladed Earth	16	16	15

TABLE 2

PERCENT OF VISIBLE ROADS ON APOLLO SPACE PHOTOGRAPH TEXAS COUNTIES				
ROAD TYPE	WISE	COLLIN	JOHNSON	HOOD- SOMERVELL
Divided Roadway	100	100	100	NONE
Paved Roadway	80	84	86	69
Bituminous Surface	77	70	65	48
Metal Surface	30	54	49	20
Graded and Drained	17	32	14	11
Bladed Earth	17	0	0	43

TABLE 3

ROADS NOT DETECTED AND FALSE ALARM* MILES IDENTIFIED
ON APOLLO SPACE PHOTOGRAPH (TEXAS COUNTIES)

COUNTY	ACTUAL MILES	NOT VISIBLE MILES	%	FALSE ALARM MILES	%	MILES TOTAL ERROR	%
Collin	1080	478	44	45	4	523	48
Wise	984	552	56	70	7	622	63
Johnson	1122	540	48	41	4	581	52
Hood- Somervell	597	371	62	41	7	412	69
Total	3783	1941	51	197	5	2138	57

*False alarms are lines incorrectly interpreted as roads

DALLAS-FORT WORTH AREA
 VISIBLE ROADS AND FALSE ALARM* ERROR ON COLOR,
 FALSE COLOR AND MULTI-BAND APOLLO SPACE PHOTOGRAPHS

PHOTOGRAPH	TOTAL MILES A	MILES VISIBLE B	% C	MILES NOT VISIBLE D	% E	MILES ERROR F	% G
AS-6-1462 (SO121)	1107 6	338 8	30 6	768 8	69 4	191 5	36.1
AS9-3298 (SO368)	1005 9	274 8	27 3	731.1	72 7	185 8	40.3
AS9-3299 (SO368)	1085 2	368 4	33 9	716 8	66 1	147 9	28 6
AS9-3583 (SO368)	842	204 8	24 3	637 2	75 7	138 5	40 3
AS9-26A-3811A (Color Infrared)	1006 8	99 2	9 9	907 6	90 1	65.5	39 8
AS9-26B-3811B (Green Band)	1006 8	170 8	17 0	836.0	83.0	108 6	38 9
AS9-26D-3811D (Red Band I)	1006 8	204 8	20 3	802 9	79 7	99 7	32.7
AS9-26D-3811D (Red Band II)	1006 8	220 8	21 9	786 0	78 1	108 6	33
AS9-26C-3811C (Black & White IR)	1006 8	74 8	7 4	932	92.6	65 7	46 8

$$C = \frac{B}{A} \cdot 100$$

$$G = \frac{F}{F + B} \cdot 100$$

$$E = \frac{D}{A} \cdot 100$$

*False alarms are lines incorrectly interpreted as roads

TABLE 5
COMPARISON OF ROAD DETECTION* USING MULTIPLE SPACE PHOTOGRAPHS
DALLAS FORT-WORTH AREA, TEXAS

COMBINATION	TOTAL MILES	MILES VISIBLE	%	MILES NOT VISIBLE	%
Red Multiband Prints I and II SO-65	1006 8	292 8	29 1	714	70 9
3 SO-65 Multiband Photos	1006 8	358 8	35 6	648	64 4
2 Apollo IX Color, Separate Revolutions	1005 9	338 8	33 7	667 1	66 3
2 Apollo IX Color, Adjacent Photos	1085 2	422 8	39 0	662 4	61 0
3 Apollo IX Color	1085 2	461 2	42 5	624 0	57.5
3 Apollo IX Color and Color IR	1005 9	440 4	43 8	565 5	56 2
1 Apollo IX Color and Multiband Photos	1006 8	426 4	42 4	580 4	57.6
Apollo VI Color 3 Apollo IX Color	1085 2	542 0	50 0	543 2	50 0
All Photos	1085 2	627 6	57 8	457 6	42 2

*The difference in total mileage arises because not all photos overlap to the same degree. Thus some combinations have fewer miles shared on all photos than others.

TABLE 6
SUMMARY OF CAPABILITY TO DUPLICATE SAMPLED MAPS
USING SPACE DATA

Map Location	Mean Capability to do From Space	Map Type	Number of Categories	Map Scale
French North Africa	1 00	Land Use	6	1 5,000,000
China	1 00	Agriculture	2	1 7,500,000
U.S S R.	1 00	Land Use	3	1 50,000,000
Craighead Co , Ark	2 00	Land Use	3	1 62,500
Australia	2 13	Forest	7	1 6,000,000
Kansas	2 27	Agriculture	11	1 2,000,000
Ecuador	2 44	Forest	9	1 4,000,000
Great Britain	2 50	Land Use	7	1 625,000
Southern Peru	2 83	Land Use	6	1 6,000,000
Northwest Africa	2 90	Agriculture	5	1 3,800,000
Portugal	2 94	Agriculture & Vegetation	9	1 1,000,000
Israel	3 08	Landscape Regions	38	1 150,000
Dumbarton & Lammermuir	3 13	Land Use	14	1 63,360
North Antrim	3 25	Land Use	6	1 63,360
Truro, Nova Scotia	3 38	Land Use	16	1 250,000
Malaysia	3 53	Vegetation	18	1 5,000,000
United States	3 58	Agriculture & Vegetation	12	1 5,000,000
Australia	3 60	Land Use	13	1 6,000,000
Australia	3 63	Vegetation	35	1 6,000,000
Isle of Thanet	3 64	Land Use	37	1 25,000
Malaya	3 69	Forest	8	1 760,320
Malaya	3 75	Land Use	8	1 760,320
Sao Paulo	3 75	Land Use	12	1 6,000,000

TABLE 7
COMMERCIAL AGRICULTURE

SITE Type of Agriculture	Resolution Cell/Grid Size	PerCent of Decision/Resolution Cells Containing Specified Number of Categories			
		1	2	3	4 or More
<u>Western Kansas</u>	1,000'	13.8	37.9	33.6	14.7
Irrigated	400'	52.0	36.5	11.2	0.4
Area	200'	71.5	23.7	4.8	--
(Garden City)	100'	83.8	14.7	1.4	--
<u>Eastern Kansas</u>	1,000'	10.1	31.9	39.5	18.5
Mixed	400'	35.9	37.8	21.7	4.5
Farming	200'	57.9	34.0	7.7	0.4
(Lawrence)	100'	84.0	15.5	0.5	--
<u>Eastern Virginia</u>	1,000'	6.1	9.2	3.0	81.6
Mixed farming	400'	10.7	15.6	17.7	56.0
	200'	29.0	31.0	25.0	15.0
(Orange County)	100'	64.7	20.8	11.0	3.5
	50'	77.5	17.5	4.5	0.5

TABLE 8
MIXED COMMERCIAL - SUBSISTENCE AGRICULTURE

SITE	Resolution Cell/Grid Size	Percent of Decision/Resolution Cells Containing Specified Number of Categories			
		1	2	3	4 or More
Costa Rica	1,000'	3 0	17 2	32 9	46 9
	400'	10 0	42.2	34 1	13 7
	200'	21 4	68 5	10 1	--
	100'	63 7	35 4	0 9	--
Puerto Rico (Aguas Buenas)	1,000'	--	2 9	4 8	92 3
	400'	4 7	18 5	17 5	59 3
	200'	12.7	22.6	16 7	48.0
	100'	47.0	39 9	11 4	1 6
South Vietnam Intensive	1,000'	--	--	--	100 0
	400'	--	0 6	2 2	97 2
	200'	6 2	21 8	37 4	34 7
	100'	15 0	55 0	22.0	8 0
	50'	36 0	45 0	11 0	8 0

BAYESIAN CONTINGENCY TABLE
 UNNORMALIZED DATA, UNNORMALIZED CATEGORIES
 (TRAIN ONE HALF DATA, CLASSIFY ON OTHER HALF)

	ALF	BRM	CRN	HAY	MLO	OAT	PST	RCL	RYE	SBN	WHT
ALF	7	16	20	1	4	--	38	--	2	--	19
BRM	1	14	102	--	2	--	21	--	--	--	28
CRN	10	22	53	2	6	--	126	--	--	1	58
HAY	--	--	11	--	--	--	3	--	--	--	11
MLO	5	10	37	1	2	--	28	--	--	--	19
OAT	--	--	7	--	--	--	6	--	--	--	5
PST	9	11	101	--	1	--	80	--	--	--	58
RCL	1	1	9	--	1	--	2	--	--	--	6
RYE	--	--	--	--	--	--	--	--	--	--	2
SBN	--	3	18	--	1	--	23	--	--	--	8
WHT	--	20	114	3	13	--	19	--	5	--	11

Table 9 Bayesian Contingency Prediction Table using unnormalized data and categories Crop types are as follows ALF = alfalfa, BRM = Brome grass, CRN = Corn, HAY = Hay, MLO = Grain and forage sorghums, OAT = Oat stubble and weeds, PST = Mixed pastures, RCL = Red Clover, RYE = Rye, SBN = Soybeans, WHT = Wheat stubble and weeds

BAYESIAN CONTINGENCY TABLE
UNNORMALIZED DATA, UNNORMALIZED CATEGORIES
(TRAIN ONE HALF DATA, CLASSIFY ON OTHER HALF)

	Forage	Large Grains	Small Grains	Soy-Beans
Forage	205	251	124	--
Large Grains	204	98	77	1
Small Grains	48	134	23	--
Soybeans	26	19	8	--

Table 10. Bayesian Contingency Prediction Table using unnormalized data and categories.

BAYESIAN CONTINGENCY TABLE
NORMALIZED DATA, NORMALIZED CATEGORIES
(TRAIN ONE HALF DATA, CLASSIFY ON OTHER HALF)

	Forage	Large Grains	Small Grains	Soy-Beans
Forage	317	65	96	102
Large Grains	236	31	55	58
Small Grains	114	40	42	9
Soybeans	28	4	10	11

Table 11. Bayesian Contingency Prediction Table using normalized data and categories.

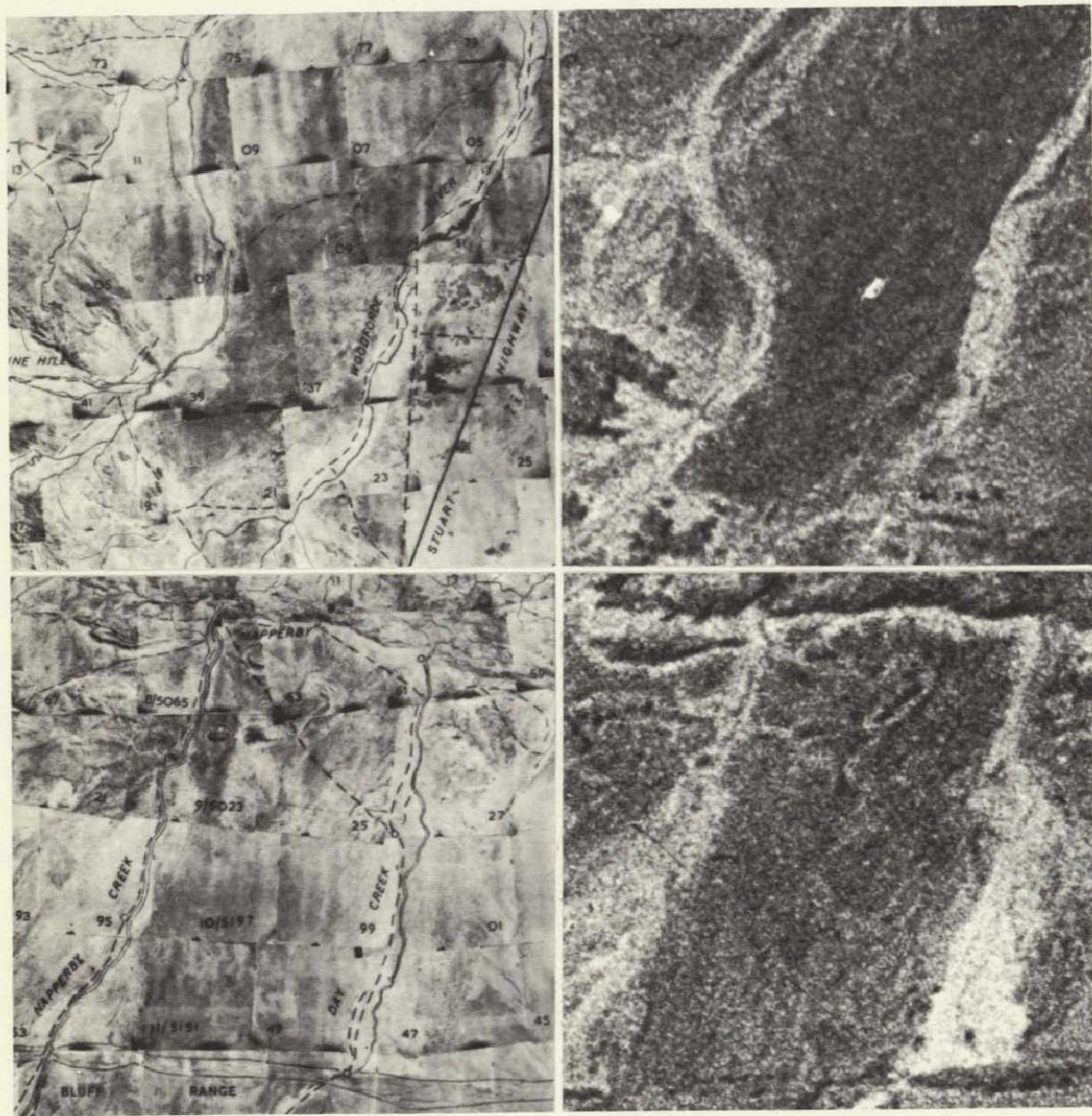


Figure 13-1.- Comparison of air photo mosaics with red separation plate enlargements of the Gemini color photo (Figure 2) of the Alice Springs region, Central Australia. Top, Woodford Creek area; bottom, Napperby and Day Creeks. Scale of reproduction 1:500,000.

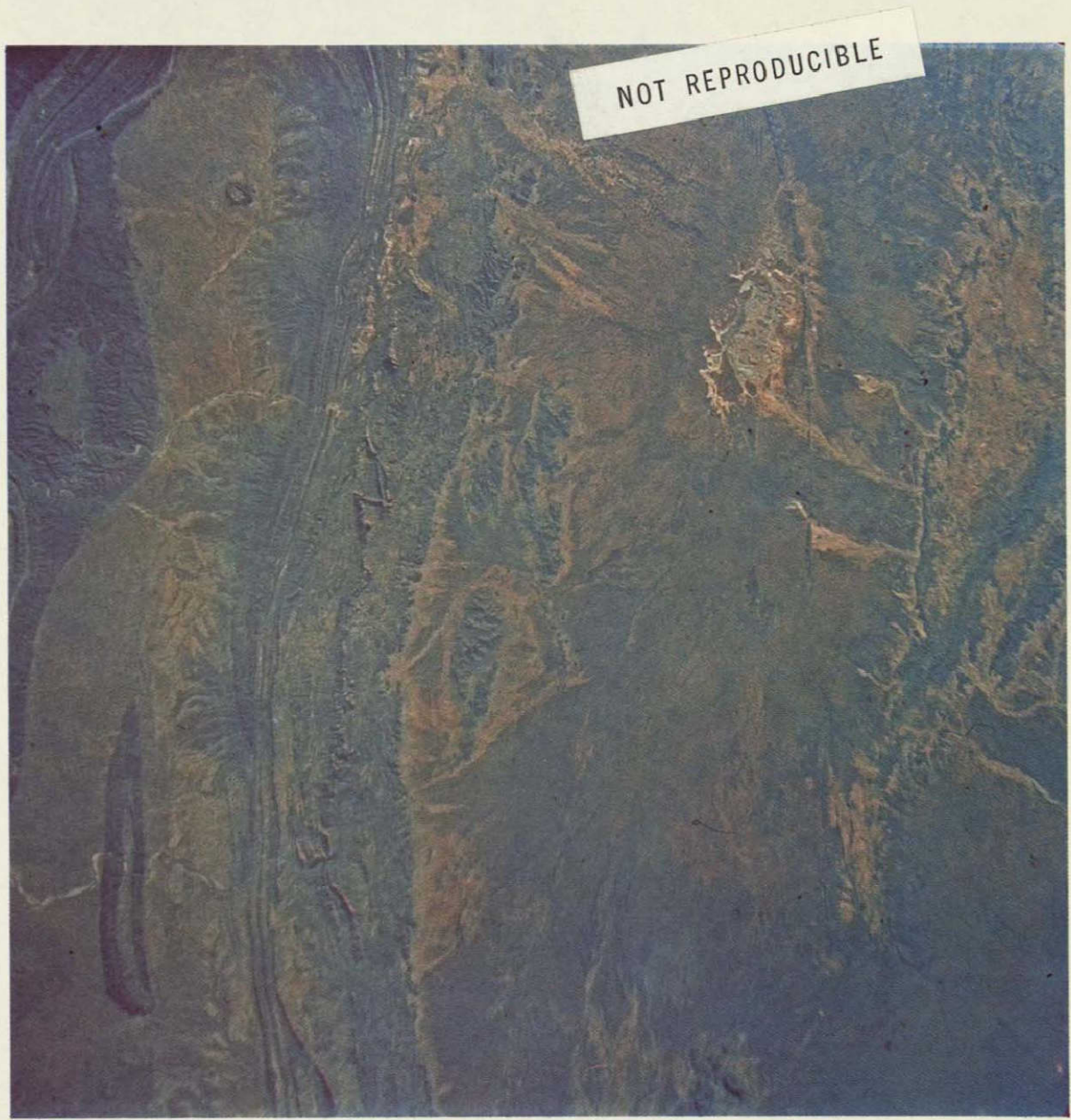


Figure 13-2.- Color photograph of the Alice Springs area, Central Australia. NASA photo number 5-65-45568, Gemini V.

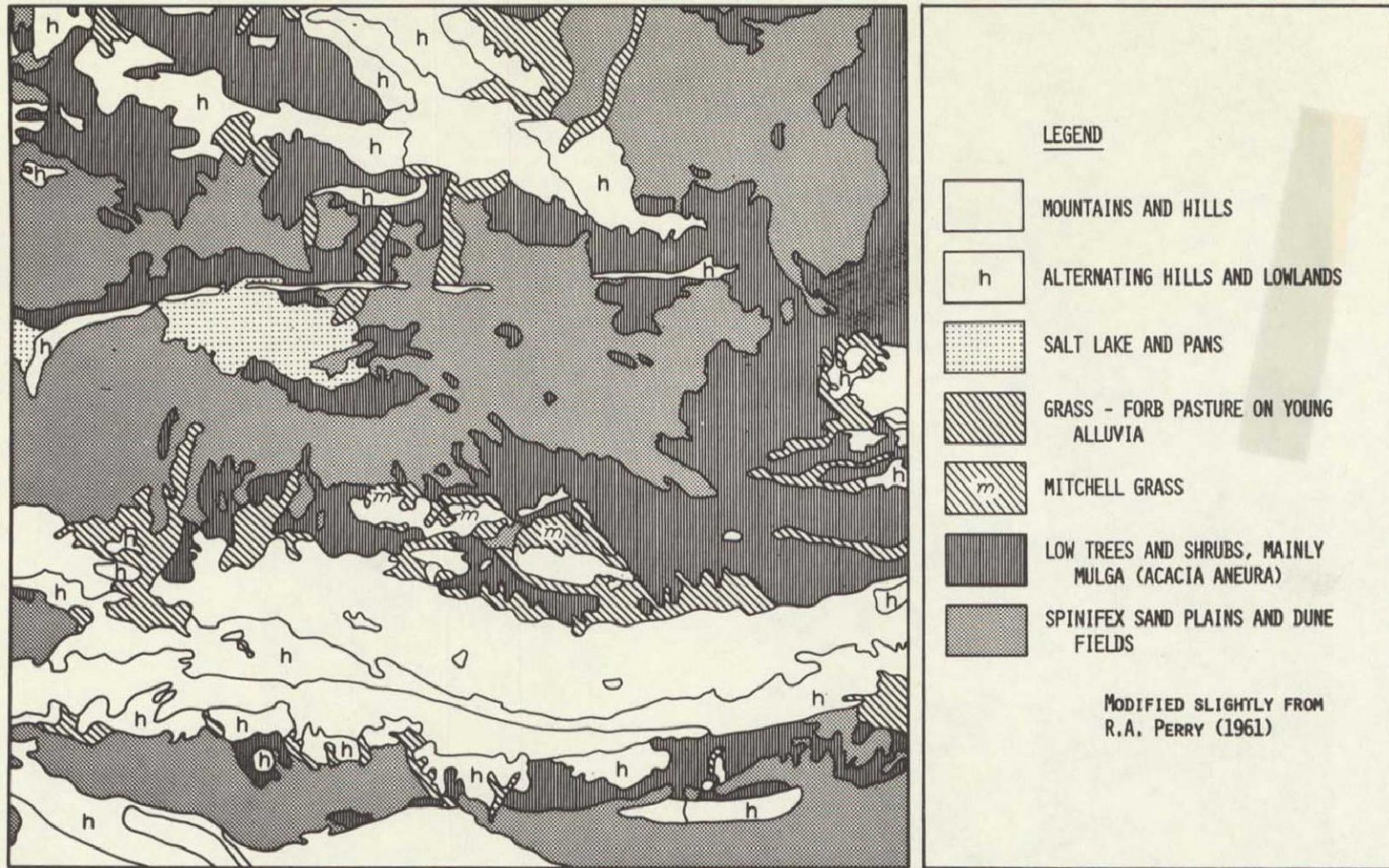


Figure 13-3.- Landscapes northwest of Alice Springs, Central Australia. Modified slightly from R. A. Perry (1961), Pasture Land Map.



PRIMARY TYPES:

- HILLS, MOUNTAINS; VARIOUS LITHOLOGIES, COMPLEX VEGETATION.
- SALT LAKE AND PANS, SPARSE HALOPHYTES.
- MAINLY GRASS WITH SOME SHRUBS, MOSTLY ON ALLUVIALS AND FANS.
- DRY CREEKS WITH RIVER RED GUM STRINGERS (E. CAMALDULENSIS).
- DUNE FIELD, MULGA ON LOWER AREAS, SPINIFEX ON FLANKS.
- WEAK DUNE FIELD, MOSTLY SPINIFEX.
- SPINIFEX SAND PLAIN (TRIODIA BASEDOWII).
- MULGA SCRUB (ACACIA ANEURA) WITH MIXES OF SHRUB AND SPINIFEX.

MOSAICS & TRANSITIONS:

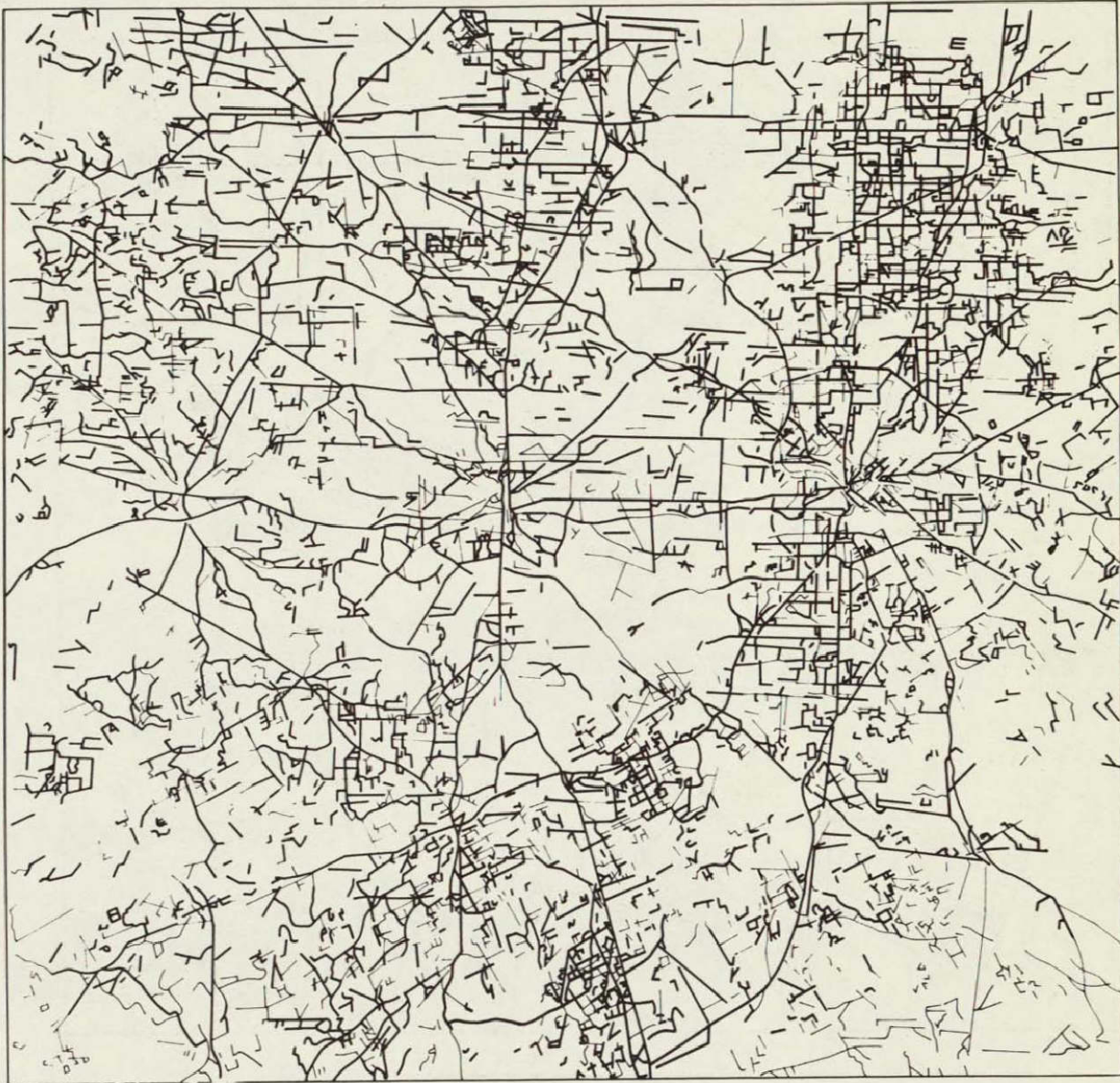
- GRASS - SPINIFEX - MULGA
- SPINIFEX - MULGA
- SPINIFEX - RIVER RED GUM
- GRASS - RIVER RED GUM
- SALT PAN - SPINIFEX

Figure 13-4.- Landscapes northwest of Alice Springs, Central Australia. Boundaries and categories based upon space photography.



—— BOUNDARIES SHARED
- - - SPACE PHOTO ONLY

Figure 13-5.- Comparison of boundaries delineated on space photograph and Perry's (1961) map of the Pasture Lands of the Alice Springs Region. The boundaries shared and those noted only on the space photo are given.



—— COLOR APOLLO VI PHOTOGRAPH, APRIL 13, 1968
—— ADDITIONAL ELEMENTS ON SEPARATION PLATES

Figure 13-6.- Roads detected on a space photograph and color separation plates of the Dallas-Fort Worth area, Texas.

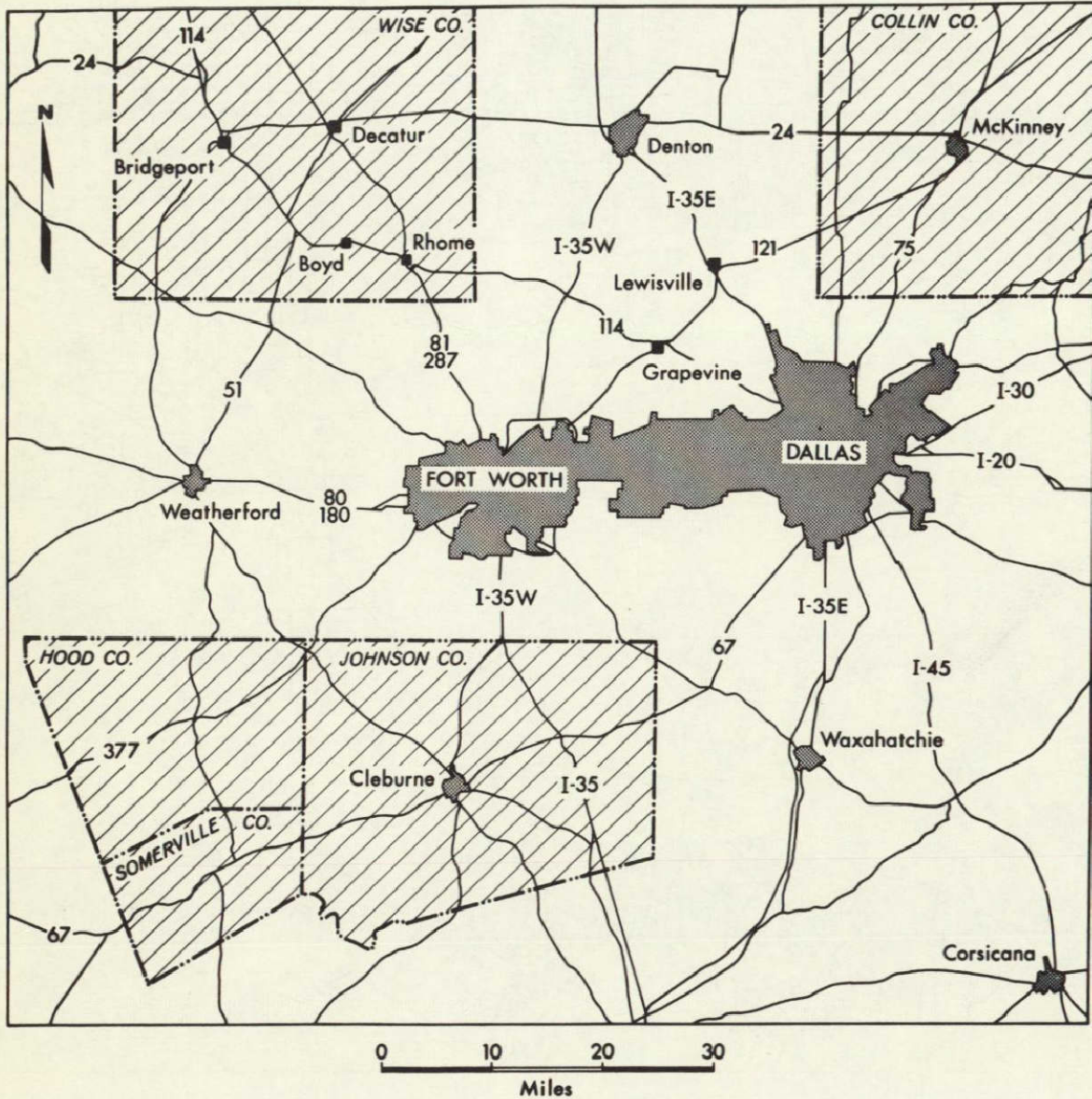


Figure 13-7.- This map depicts the area covered by the space photograph. The Dallas-Fort Worth Metropolitan area, excluded from the study, as well as a four county sample areas are shown by shading. By comparing the map with the photo it can be seen that each sample county is in a different land use area, and that even some of the major roads are not visible.



Figure 13-8.- Apollo VI color photograph of the Dallas-Fort Worth area, Texas. NASA photo number AS6-1462.

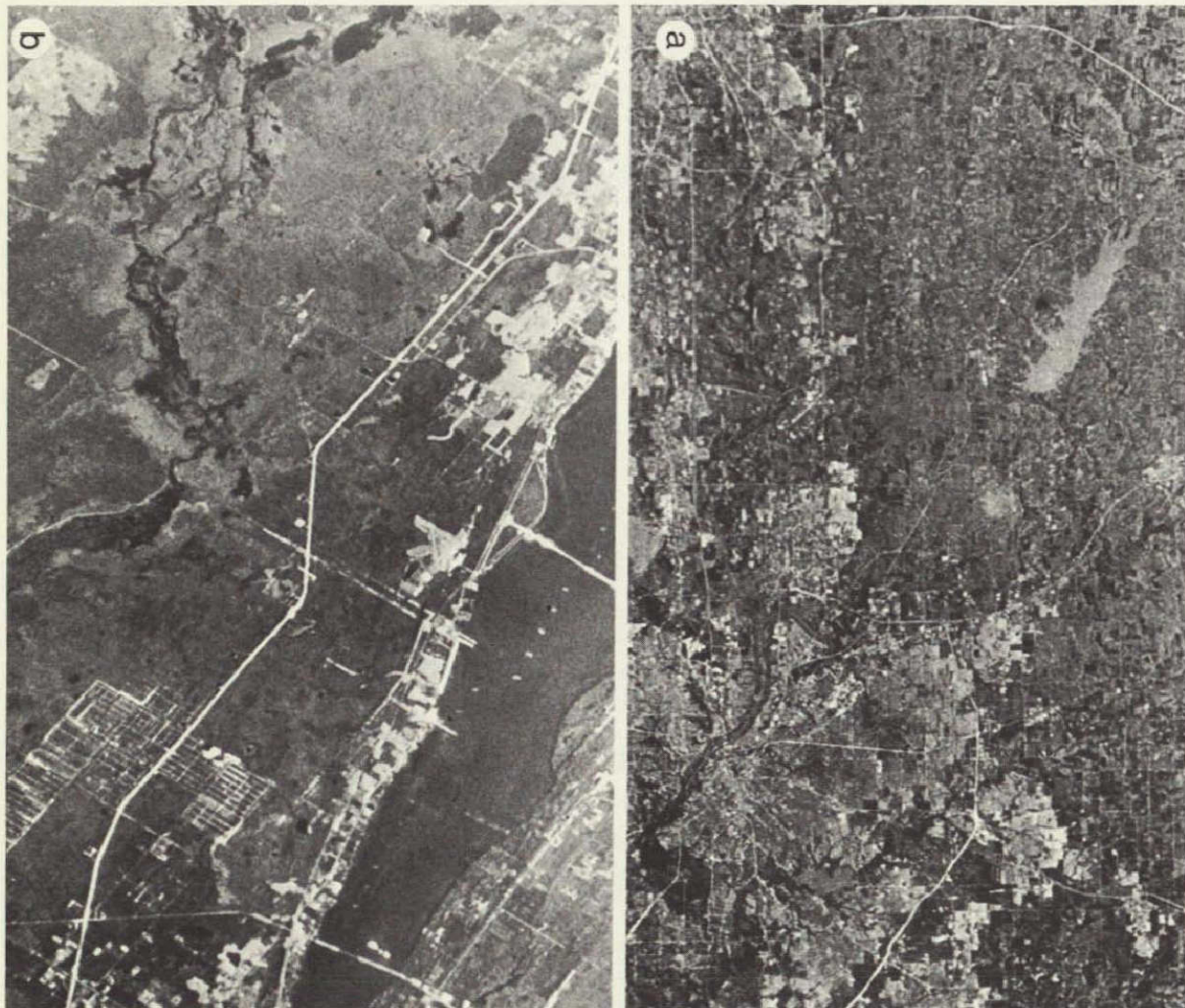
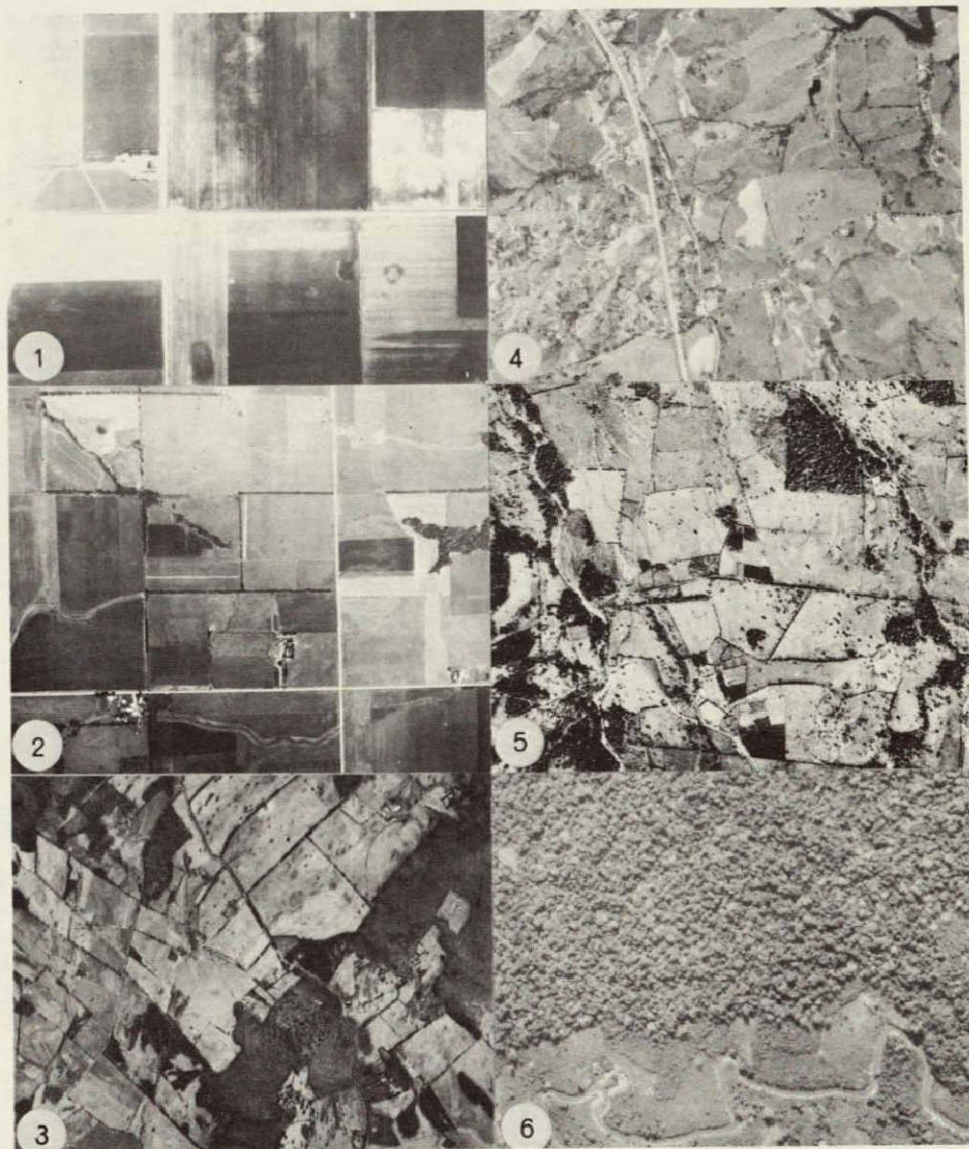


Figure 13-9.- Photographs of Dallas-Fort Worth, Texas and vicinity of Cape Kennedy, Florida, taken with 80 mm and 250 mm focal length lenses, respectively.

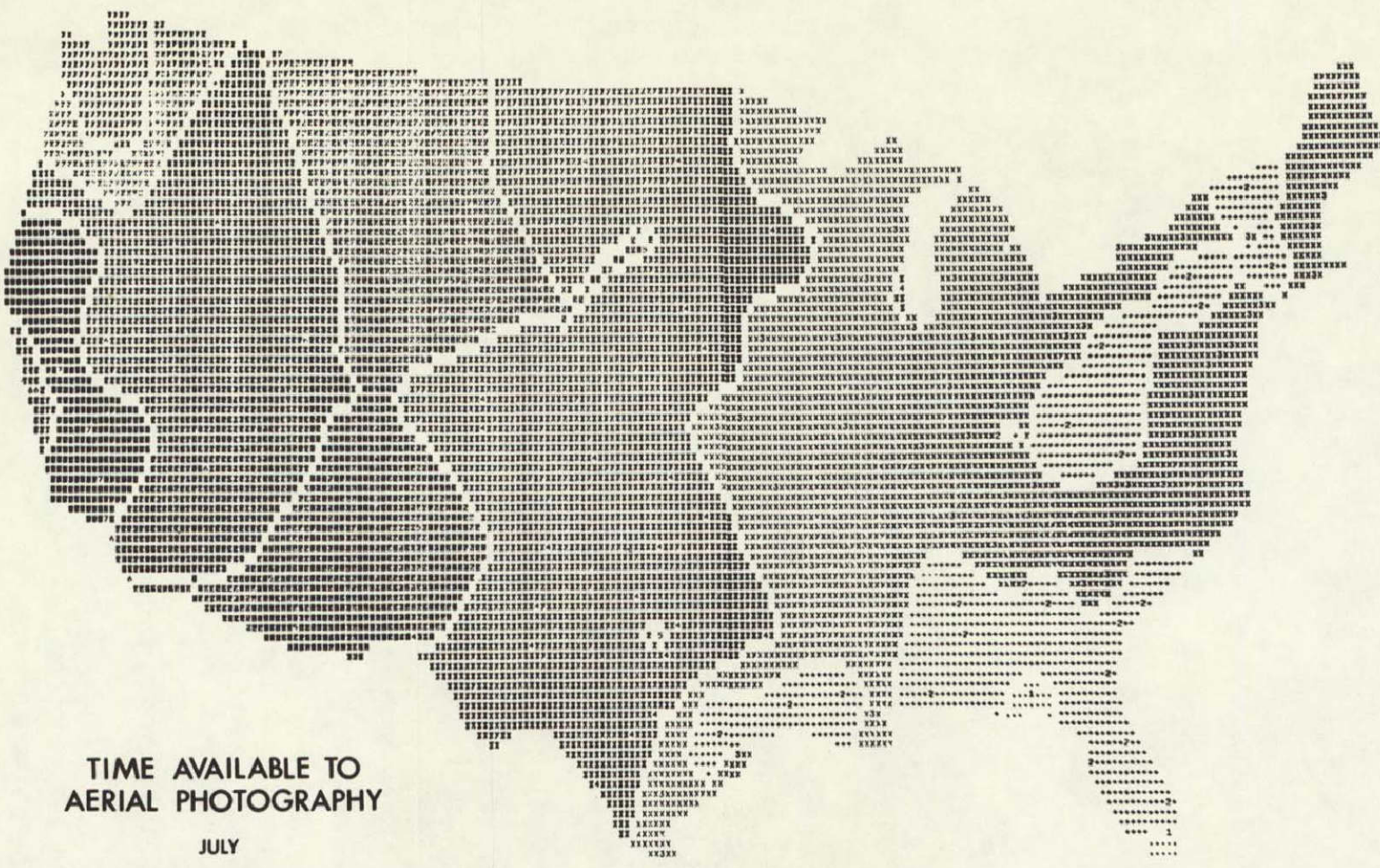
- (a) This 8X enlargement from an 80 mm focal length Ektachrome photograph of Dallas-Fort Worth, Texas area has a ground resolution of about 300 feet.

- (b) This 8X enlargement from a 250 mm focal length Ektachrome photograph of Titusville and vicinity near Cape Kennedy, Florida has a ground resolution of about 100 feet. This photo was taken from Gemini VII on December 6, 1965.



SITE	ORIGINAL SCALE
1. Garden City, Finney County, Kansas	1:15,000
2. Lawrence, Douglas County, Kansas	1:15,000
3. Gordonsville, Orange County, Virginia	1:20,000
4. Caguas, Agua Buenas, Puerto Rico	1:20,000
5. Venecia, Alajuela Prov., Costa Rica	1:43,000
6. La Palma, Darien Prov., Panama	1:35,000

Figure 13-10.- Aerial photographs, brought to a common scale of 1:25,000, illustrate the variations in the size, shape, and arrangement of spatial elements which occur in differing world environments.



TIME AVAILABLE TO AERIAL PHOTOGRAPHY

JULY

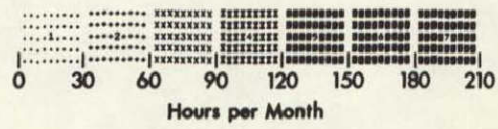
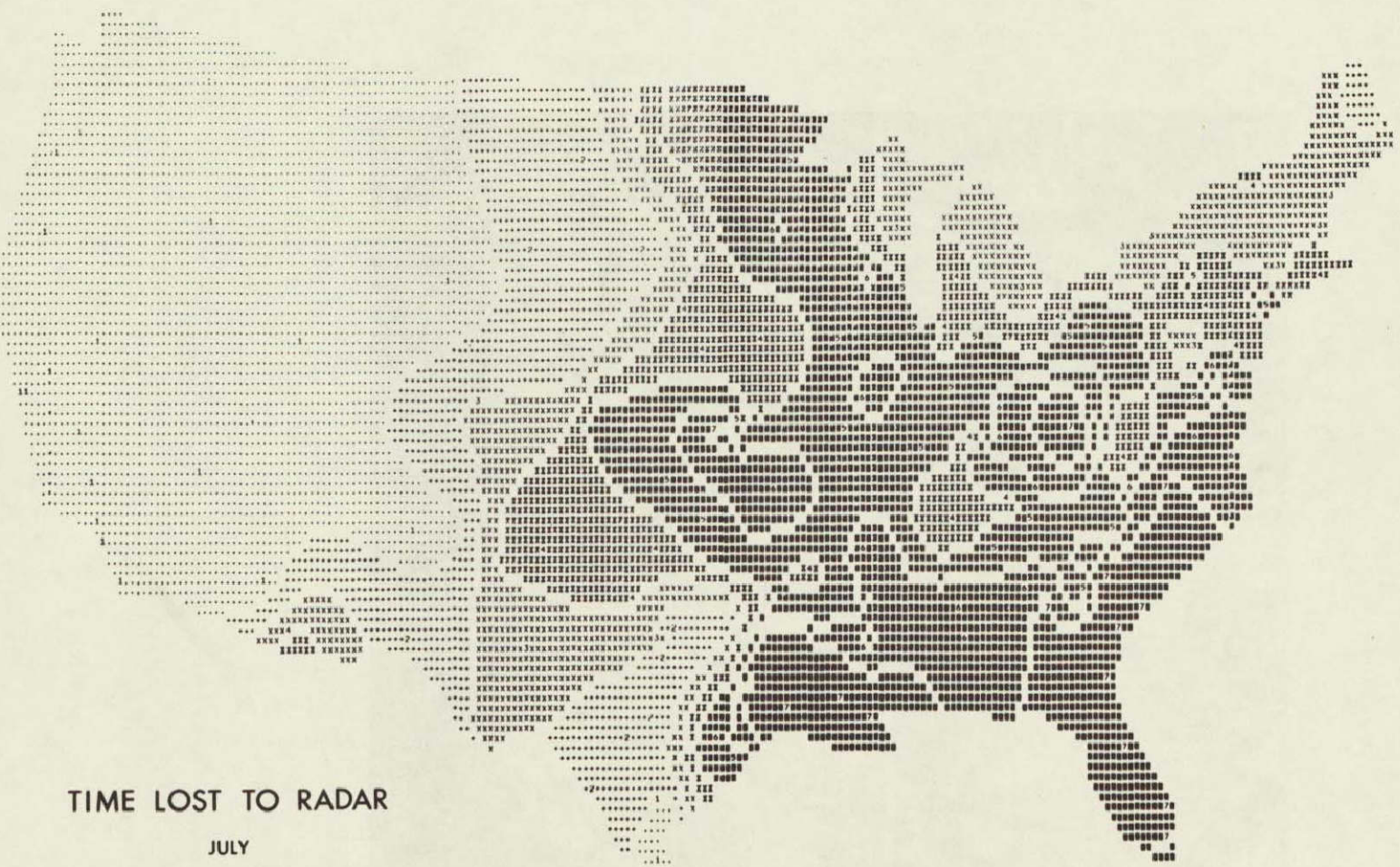


Figure 13-11.- Time available for aerial photography in July when the sun is 30° or more above the horizon and cloud cover percentage is 30 percent or less.



TIME LOST TO RADAR
JULY

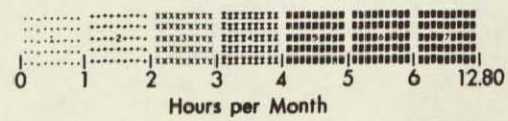


Figure 13-12.- Number of hours lost to radar in July through precipitation equal to or exceeding 0.25 inches per hour. In the Midwest and southeastern agricultural regions the ratios of time available for radar in comparison to photography on a 24-hour basis is from 10:1 to 15:1. On a daylight hour basis it is approximately 6:1 to 9:1.



Figure 13-13.- Color infrared photography of an area near Lawrence, Kansas July 31, 1967. The letters on the photograph indicate the crops present: P = mixed pasture; B = brome grass pasture; C = corn; W = wheat stubble and weeds; A = Alfalfa; O = oats stubble and weeds; H = hay.

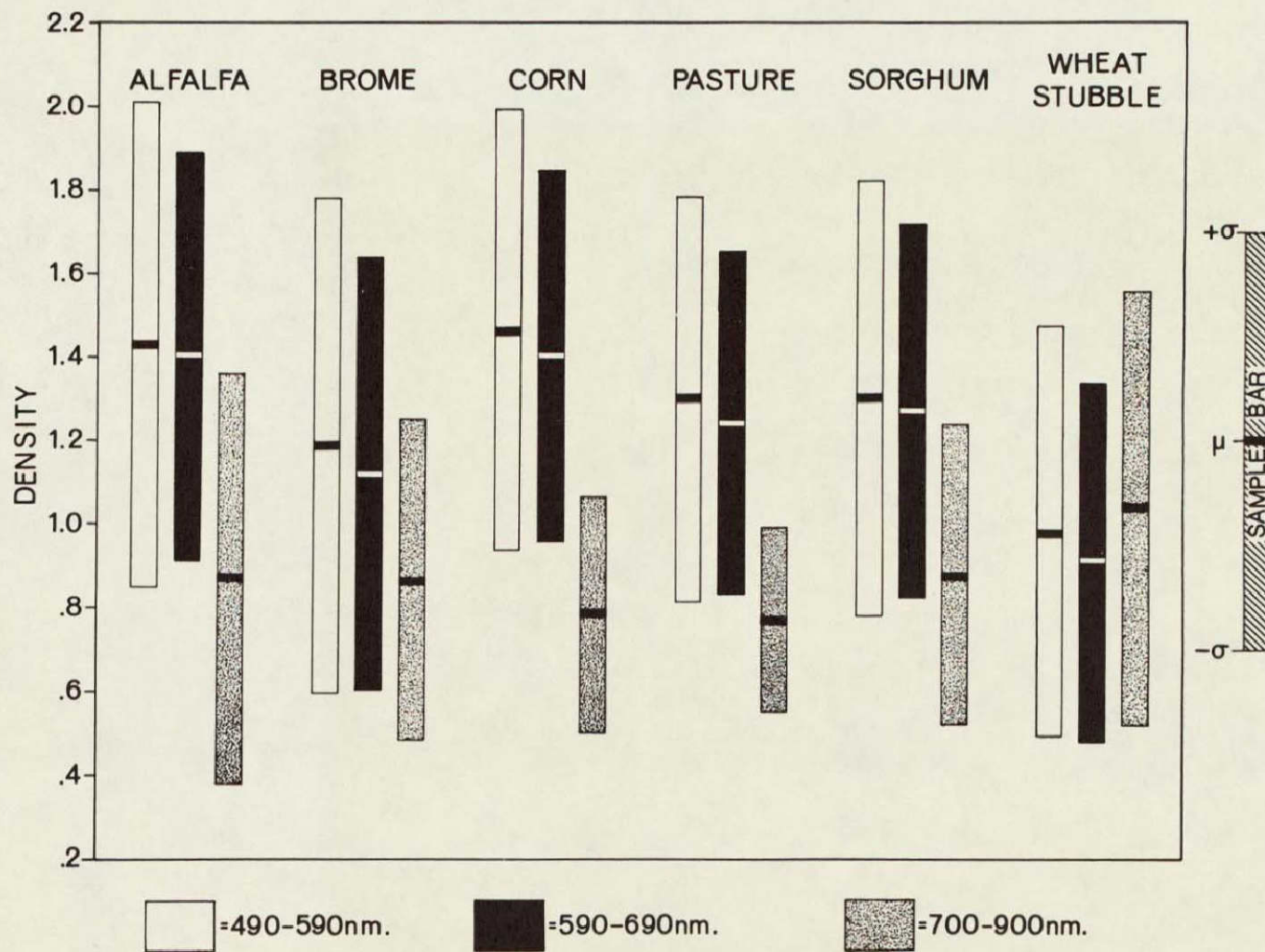


Figure 13-14.- Means and standard deviations for six crops, using unnormalized density data for the three dye layers of color infrared film. The spectral region corresponding to the dye densities (not color) are shown in the illustration. There is obviously considerable overlap in the densitometry data for the six most commonly occurring crops in the region.

SECTION 14

Imperial Valley Land Use Studies
A Continuum from Mission 7, to Apollo IXClaude W. Johnson
Department of Geography
University of California, Riverside

Introduction

N71-19265

Data obtained from Apollo IX helped produce some final stages in the long term program of geographic land use via remote sensing in the Imperial Valley. The aircraft program had helped support the investigation through overflights conducted during Mission 73. Mission 73 (and Missions 42 and 56) were used as training and evaluation models to set the stage for Apollo IX experiments. The combination of aircraft, spacecraft, laboratory and field investigations has made the Imperial Valley an exceptionally productive test site in the acquisition and application of geographic data.

Emphasis is, and has been, on use of color infrared photography and its application to land use studies. However, experiments with multi-band photography, side-looking radar imagery, passive microwave imagery, scatterometer data, and thermal infrared imagery have been conducted and partially evaluated. A significant step was the application of Apollo IX imagery to computerized programs (on land use) that developed from data acquired from Mission 73.

Discussion

The many variations which occur in the color record of agricultural crops imaged on color infrared (CIR) photography create one of the most perplexing problems in the design of equipment and systems for performing agricultural land use mapping from CIR imagery. An initial glance at the Apollo IX CIR photo (AS-9-26A-3798) taken of the Imperial Valley (California) on March 12, 1969, belies the true picture in that only slight evidence of color variation can be detected among the red false colors on the image. However, closer examination of the seven crops (barley, alfalfa, sugar beets, asparagus, carrots, lettuce, and onions) showing vegetative ground cover in the Apollo image demonstrated many color variations both within crop type and among crop types. A similar problem, peculiar to the March date of the imagery, is the lack of distinction among the six crops (cotton, sorghum, sudan grass, watermelons, cantaloupes, and tomatoes) which have been seeded, but have not yet shown any vegetative cover in the small scale satellite image. All of these crops show a blue color for moist or irrigated soil.

Analysis of the imagery from Mission 73 and the Apollo 9 has led to considerable insight into the how and why of crop color variations as displayed on CIR imagery. The understanding of the color variations

enabled considerably more accuracy to be achieved in interpreting the Apollo 9 photo as a test for the methods and techniques developed from Mission 73 imagery for a system of agricultural land use mapping

While the objective of the study which has led up to this report was the development of a computer-oriented agricultural land use mapping system, stress in this presentation is being placed on the problems encountered with the crop-color variations on CIR imagery. In addition to indicating some aspects of the methods and techniques developed in the study, some quantitative results obtained in spite of the color variation problem will also be reported. Evidence has shown that crop color and tone variations can be caused by

1. Technical deviations in film quality control, variables at time of exposure, storage history of the film before processing, and the processing itself. Personnel involved in these processes are aware of the problems and, hopefully, improvement in quality control will be noted in future imagery received.
2. Changes in resolution or scale, which indicate that these factors need to be standardized.
3. Changes occurring within the agricultural field units and the vegetation itself.

Mission 73 imagery taken at large scale (1 4,000) and medium scale (1 16,000) show examples of CIR crop color variations which have been noted to occur

1. within the same field,
2. among the same crop type in different fields,
3. among different crop types, but with the same resulting color and tone, and
4. in direct ratio to the soil background and its vegetative color

One investigator has suggested that the possible color combinations generated by use of three-color layer CIR film is over 10,000,000. Therefore, it seems amazing that many of the frames on the Mission 73 film taken by Western Aerial Surveys at a scale of 1 16,000 show so many crops with uniform color tones within the same frame and between the frames. One particular photo shows seven different crops in distinctive colors and patterns. The interpretation process would be greatly simplified if all images were as perfect as the 40 cm resolution of these CIR photos. It should be noted that the date of these images was June 11, 1968 at the end of the spring growing season when many of the crops show a maximum differentiation from each other.

The variation of color and tone within an individual crop can be illustrated by an alfalfa field being cut. One 160 acre plot was noted in the haying process, where one-third of the field had been cut and raked into windrows, and which displayed a very pinkish tone, with much of

the soil background integrated with the alfalfa stubble. Another one-third of the field displayed cut alfalfa that had been allowed to dry for a day after it had been cut. The color of the cut alfalfa had already begun to turn pink from the very vivid red hue of the fully matured, remaining one-third of the field which had not yet been cut. The 230-foot resolution of the Apollo 9 image does not permit the distinction within the field, and it is hard to imagine what type of integrated color this kind of field would present at small scale.

An illustration of the variation occurring among fields of the same crop type can be shown in an image which contains several alfalfa fields. Such an image might show alfalfa in six stages of maturity which are (1) cut and pastured (brownish to white color showing stubble and dry soil), (2) medium regrowth (white dry soil background with mottled red of regrown plants), (3) advanced regrowth (only small patches of white soil showing with strips of lush alfalfa between the brown colored flood borders), (4) mature regrowth (no soil background showing, but a trace of the brown flood borders between the lush red of the regrown alfalfa), (5) irrigated mature alfalfa (dark blue streaks of water showing between the vivid red of regrown alfalfa), (6) fully mature alfalfa (only dark vivid red showing). On the Apollo 9 photo, each of these different alfalfa fields would present a different color which would cause great difficulty in establishing a single color for alfalfa crops. In addition, some of the color represented for alfalfa would be indistinguishable from the color representation of barley or sugar beets at this time of year on the Apollo 9 image.

Two flights from Mission 73 provided illustrations of the differences of color tone caused by the high and medium resolution of the imagery. The 10 cm resolution of the NASA Convair flight at 2,000 feet taken on May 21, 1968, of a sugar beet field shows a very mottled brownish field with considerable background displayed in the photo. Sugar beets could not be identified from this photo. However, the medium resolution image taken three days later shows the same field as the very distinctive pink of mature sugar beets with no visible distinction between the plant and the soil background. A photo of the same field taken three weeks later (June 11) indicates the field had been harvested, which added to the proof that the crop was indeed sugar beets. The question arises, however, why does the low altitude or high resolution image have such a deleterious effect on the agricultural vegetation?

A CIR photo of a mature sugar beet field taken on the ground reveals that only the tops of the plant are reflecting infrared at the late date in the growing season, and much of the plant leaf is lying dead in the irrigation furrows. What apparently is happening is that the high resolution imagery is separating the infrared vegetation color reflectance from the other background colors. A similar situation has been found to exist with recently planted crops where the vegetative cover is only a few inches tall. Medium and low resolution imagery must, therefore, integrate the infrared reflectance of the vegetation with the other background color reflections into a single uniform color for each type of crop that has that particular soil background. Thus, the bright infrared reflectance of the sugar beets or new cotton becomes diluted with the background reflectance to record a very light pink on the CIR image. Maximum benefit of

the prime attribute of CIR film over black-and-white imagery, therefore, can only be obtained if the resolution is low enough to integrate all the colors present in a single field into a uniform color. Evidence indicates that the maximum resolution for agricultural CIR studies should be no higher than 40 cm.

During the middle of the particular growing season for the crops under study many of the crops will be at a stage of growth in which their infrared reflectance is nearly the same. On the Apollo 9 image this was true among many of the alfalfa fields, barley, wheat, and sugar beets. Later in the season alfalfa and sorghum yield similar infrared reflectance records on CIR imagery. The solution to differentiating among crops with the same infrared reflectance characteristics on medium and small scale imagery is to obtain time-lapse or sequential imagery. Carefully timed (approximately three to four weeks apart) imagery will permit separation of crop types through either a change in color, such as grain crops turning yellow, or evidence of the crop being harvested, such as sugar beets being dug. We should think of the time period in three parts: (1) the period just after vegetative cover has appeared and is six to nine inches tall, (2) mid-season when most crops are showing the same infrared reflectance, and (3) late season when the crop has matured to a different color or has been harvested. Timing of sequential agricultural images should be matched to these periods.

Unfortunately, time-lapse or sequential satellite photography was not available to test the hypothesis, but the results shown in Table I do indicate the need for more than one image. The poor 59.5% accuracy for specific crops was obtained only because of the availability of sufficient a priori information of the agricultural region. Even with sequential imagery, some prior knowledge of the region such as crop calendar is essential because of the many crop-color variations. The variations, both in technical processing and the vegetation itself, prohibit the design of a system which can train on a known area and transfer this training to a completely unknown area and achieve any satisfactory results in predicting crop types without additional information.

A previously prepared map overlay of the individual fields was used to interpret and identify the 7,801 individual fields of the Imperial Valley from the Apollo 9 image. The overlay permitted a form of edge enhancement which enabled some separation to be made of the colors between fields. Identification was made from the crop color on the image, the field size on the image, and the previously obtained and stored information about the individual field and area. The identification and location data were placed on machine record cards (IBM) from which summaries were prepared and future information retrieval can be obtained. The summary of total acreage, compared to the reported March 15, 1969 data of the Imperial Irrigation District, provided almost 98% correlation which is much more promising. In fact 2% error is well within the system error. Table II indicates the correlation between estimated and reported acreages by crop.

An element essential to the processing system design for individual field unit examination is that training on known fields must be performed.

On the Apollo 9 image, 7% of the fields were surveyed and identified from the ground on the date of the flight. After 50% of the image had been interpreted, another ground survey of 6% of the fields was conducted and the information reconstructed to March 12. Correcting personal bias, the remaining 50% of the image was interpreted, and a final survey of 6% of the fields was made and identification reconstructed back to March 12. Thus, the accuracies reported in Table I were obtained from a survey of 13% of the fields represented. (The total 20% of the ground survey data appears as corrected information on the final map which thus contains better than 59.5% accurate information.)

A necessary adjunct to any land use mapping scheme is a coding system. The system developed or adapted for this study was based upon the requirement of compatibility with a computer system. The Standard Land Use Code of the Urban Renewal Agency and Bureau of Public Works was so oriented, and slight modification as suggested by the agency provided a system for specific crop type identification. The adapted system eliminated any possibility of overlap between specific crop types or classes and provided a place (primary, secondary, or specific agricultural classification) for each crop no matter how poor the resolution of the imagery. An example of the system is shown in Table III.

The system outlined here provides for the preparation of many thematic maps, either by specific crop types or by secondary agricultural classifications. The completed agricultural land use map shows the 315,828 acres of field crops (principally barley, alfalfa, and sugar beets) which represents about 66% of the total 474,000 acres under cultivation. Vegetable crops which were showing vegetative ground cover in the Apollo 9 image, totaled 22,000 acres, and seeded crops which appeared as dark blue on the Apollo 9 image contained 51,160 acres.

Conclusions

In concluding this report a further word of caution needs to be stated. A regional agricultural land use map can be prepared from small scale satellite imagery utilizing the above described system only if adequate a priori knowledge has been obtained. Quite often the prior knowledge is available in the form of crop calendars or agricultural statistics. Also information about local conditions is accumulated with each successive mission over the area and, consequently, the accuracy of identification should increase with each mission.

Time-lapse or sequential imagery thus becomes a second method of improving the accuracy of agricultural land use mapping from the present small scale satellite imagery.

Finally, the effective use of CIR photography shows that ground resolutions should be no better than 40 cm in order to provide a uniform crop color integrated with the associated background.

Details of the study from which this presentation was made will be found in a Technical Report to the U S Geological Survey, under Department of the Interior Contract No 14-08-0001-10674, Status Report III, Technical Report V, to be published in the near future.

TABLE I

CORRELATION OF LAND-USE IDENTIFICATION WITH GROUND SURVEY CHECK
APOLLO 9 CIR IMPERIAL VALLEY IMAGE (MAR 11, 1969)

CROP TYPE	IDENTIFICATION ACCURACY WITHIN CLASSIFICATION (Digit Level)								
	SPECIFIC CROP (Fifth Digit)			CROP CLASS (Fourth Digit)			AGRICULTURAL TYPE (Third Digit)		
	NUMBER	CORRECT	PERCENT	NUMBER	CORRECT	PERCENT	NUMBER	CORRECT	PERCENT
<u>FIELD CROPS (811)</u>									
<u>GRAIN CROPS (8111)</u>									
111 Barley	140	53	37.9	150	57	38.0	150	129	
118 Wheat	10	0	0.0						
<u>FORAGE CROPS (8113)</u>									
131 Short Grass (Rye)	11	0	0.0	319	200	62.7	319	274	
133 Alfalfa	308	193	62.7						
<u>SUGAR CROPS (8114)</u>									
142 Sugar Beets	132	27	20.5	132	27	20.5	132	130	
<u>OIL CROPS (8117)</u>									
172 Flax	5	0	0.0	5	0	0.0	5	4	
Field Crop Totals	606	273	45.0	606	284	46.9	606	537	88.6
<u>VEGETABLE CROPS (812)</u>									
231 Lettuce	18	13	72.2						
272 Carrots	10	7	70.0						
284 Onions	12	3	25.0						
Vegetable Crop Totals	40	23	57.5						
<u>NON-PRODUCING & TRANSITION LAND</u>									
810 Fallow	32	26	81.3						
820 Plowed	130	120	92.3						
830 Leached	1	1	100.0						
840 Abandoned	39	37	94.9						
850 Harvested	0								
860 Prepared or Seeded	64	63	98.4						
Non-Prod & Trans. Land Totals	266	247	92.9						
GRAND TOTALS	912	543	59.5	912	554	60.7	912	807	88.5

SUMMARY OF CORRELATION BETWEEN REPORTED AND DETECTED
AGRICULTURAL CROP ACREAGE IN THE IMPERIAL VALLEY (March 15, 1969)

<u>Summary</u>	<u>Acreage</u>		<u>Difference</u>		<u>Percent Accuracy</u>
	<u>Reported</u>	<u>Detected</u>	<u>Over</u> ¹	<u>Short</u> ²	
<u>Agricultural Land Class</u>					
811 Field Crops	315,858	292,440		23,418	93
812 Vegetable Crops	21,162	20,574		588	97
813 Fruit & Nut Crops	2,309	668			
8186 Prepared & Seeded	51,160	50,980		180	97
816 Pasture Land	682	120			
Unidentified Ag Land		6,980			
<u>Total Land With Growing Crops</u>	<u>391,171</u>	<u>371,752</u>		<u>19,419</u>	<u>94 8</u>
818 Non-Productive Ag Land		93,180			
<u>Total Available Ag Land</u>	<u>474,437</u>	<u>464,932</u>		<u>9,505</u>	<u>98 0</u>
<u>Individual Crops</u>					
<u>811 Field Crops</u>					
111 Barley	72,829	68,350		4,479	94
115 Oats	2,423	140			
118 Wheat	9,932	1,100			
Total Grain Crops	85,184	69,590			
131 Short Grass (Rye, Bermuda)	14,714	4,490		10,224	31
133 Alfalfa	134,692	163,420	28,728		82
Total Forage Crops	148,714	167,910			
141 Sugar Cane	2				
142 Sugar Beets	79,679	54,350		25,329	68
Total Sugar Crops	79,681	54,350			
172 Flax	2,279	590		1,689	26
<u>TOTAL FIELD CROPS</u>	<u>315,828</u>	<u>292,440</u>			
<u>812 Vegetable Crops</u>					
211 Asparagus	2,832	3,100			
221 Beans, Green (Fava)	85	85			
223 Peas, Green	74				
224 Okra	51				
231 Lettuce	7,601	7,840	239		97
232 Celery	4	4			
234 Parsley	1				
236 Chicory	3	3			
237 Mustard	32				
Total Salad Crops	7,641	7,847			

* When no difference or percent accuracy is shown no valid comparison can be made

<u>Individual Crops (cont)</u>	<u>Acreage</u>		<u>Difference</u>		<u>Percent Accuracy</u>
	<u>Reported</u>	<u>Detected</u>	<u>Over⁷</u>	<u>Short[*]</u>	
241 Broccoli	289	72			
243 Cabbage	224	240			
244 Cauliflower	40				
Total Cole Crops	553	312			
272 Carrots	4,127	5,580	1,453		74
274 Potatoes (Chinese)	3				
Total Root Crops	4,130	5,580			
282 Garlic	391				
284 Onions	5,405	3,650		1,755	68
Total Bulb Crops	5,796	3,650			
<u>TOTAL VEGETABLE CROPS</u>	<u>21,162</u>	<u>20,574</u>		588	97
<u>813 Fruit & Nut Crops</u>					
314 Grapes	2				
322 Apricots	19				
330 Citrus, Undifferentiated	324	600			
331 Grapefruit	507				
333 Lemon	276				
335 Orange	611				
337 Tangerine	400				
Total Citrus Crops	2,118	600			
342 Dates	93	60			
363 Pecans	77	8			
<u>TOTAL FRUIT & NUT CROPS</u>	<u>2,309</u>	<u>668</u>			
<u>860 Prepared and Seeded Land</u>					
113 Corn	80				
114 Sorghum, Grain	9,510				
132 Tall Grass (Sudan)	1,145				
151 Cotton	20,888				
Total Seeded Field Crops	31,623				
250 Melons, Undifferentiated	1,053				
251 Cantaloupes	11,861				
252 Cucumbers	50				
253 Crenshaw melons	22				
255 Squash	336				
256 Watermelons	3,709				
Total Cucurbit Crops	17,031				
<u>TOTAL PREPARED & SEEDED LAND</u>	<u>51,160</u>	<u>50,980</u>	180		99.6

When no difference or percent accuracy is shown no valid comparison can be made.

	<u>Acreage</u>	
<u>Other Agricultural Land</u>	<u>Reported</u>	<u>Detected</u>
610 Pasture Land	682	120
Unidentified Ag Land		6,980
<u>818 Non-Productive Land</u>		
810 Fallow Land		35,110
820 Plowed Land		35,560
830 Land Being Reclaimed. Leached		1,540
840 Abandoned Ag Land		20,620
850 Harvested Land		<u>350</u>
<u>TOTAL NON-PRODUCTIVE AG. LAND</u>		<u>93,180</u>

TABLE III

AGRICULTURAL LAND-USE CODE

Digit Level
First Second Third Fourth Fifth

8		RESOURCE PRODUCTION AND EXTRACTION
81		Agricultural
	811	Field and Seed Crops
		8111 Cereal and Grain Crops
		81110 Undifferentiated Cereal and Grain Crops
		81111 Barley
		81112 Buckwheat
		81113 Corn (Maize)
		81114 Sorgham, Grain
		81115 Oats
		81116 Rice
		81117 Rye
		81118 Wheat
		81119 Other Differentiated Cereal and Grain Crops
	8112	Legumes for Seed Crops
	8113	Forage Crops
	8114	Sugar Crops
	8115	Fiber Crops
	8116	Beverage, Drug, Flavoring, and Spice Crops
	8117	Oil Crops
	8118	Rubber Crops
	8119	Other Differentiated Field and Seed Crops
	812	Vegetable Crops
	813	Fruit and Nut Crops
	814	Livestock
	815	Animal Specialties
	816	Pasture and Rangeland
	817	Horticultural Specialties
	818	Non-Producing and Transitional Crop Lands
	819	Other Differentiated Agriculture

SECTION 15
HOUSING QUALITY IN URBAN AREAS
DATA ACQUISITION AND CLASSIFICATION THROUGH
THE ANALYSIS OF REMOTE SENSOR IMAGERY

Frank E Horton, University of Iowa
and
Duane F Marble, Northwestern University

N 71 - 19266

Previous research on the application of remote sensors to the acquisition of urban data has been primarily concerned with an examination of sensor characteristics and qualitative evaluations of their usefulness in urban studies. However, the utilization of remote sensors for the acquisition for various types of urban data must be ultimately evaluated in terms of the sensor's relative capability to contribute quantitatively to the solution of substantive urban problems. One such problem, the potential of photographic sensors to contribute to the analysis and identification of housing quality areas in metropolitan regions, is the major focus of this paper.

Federal and local agencies have shown an increasing interest in methods for the rapid survey of housing conditions over large urban areas in order to (1) evaluate the magnitude of such problems within the city, (2) identify those neighborhoods most in need of immediate remedial action and, (3) to qualify for Federal funds for neighborhood improvement. At present expensive ground surveys covering a large number of parcels and involving many variables are currently required. The remote sensing project at Northwestern University has attempted to evaluate the following hypotheses with respect to housing quality surveys and potential remote sensing inputs: (1) due to high redundancy levels, an excessive number of variables are currently collected by public agencies in their attempt to identify housing quality areas, (2) a reduced set of these variables exists which are potentially observable via remote sensing techniques, (3) a viable classification algorithm can be developed utilizing the reduced variable set which would quantitatively assign a particular areal unit of observation to a unique class, and (4) measures of the reduced variable set can be extracted from remote sensor imagery.

*Analysis of Ground Data**

Data were obtained from a survey conducted by the Los Angeles County Department in the Spring of 1968 covering some 1300 blocks in three districts in the Los Angeles area containing some of the county's worst housing (see Figure 1). This data set constituted the basic

*The material in this section draws heavily upon the research carried out by Dr. Eric G. Moore of Northwestern University. A more extensive discussion of this work is found in his article "Applications of Remote Sensing to the Classification of Areal Data at Different Scales: A Case Study in Housing Quality" which is forthcoming in *Remote Sensing of Environment*.

ground truth information for the Northwestern University participation in NASA's Earth Resources Aircraft Mission 73 and were used to explore the hypotheses noted above

A 1% sample of parcels (478 parcels) was drawn from the Los Angeles housing data set. The 37 structural and environmental variables utilized are given in Table 1. It is unfortunate that many of these variables are subjectively defined and hence suffer from severe scaling problems. However, they are representative of the current state of the art in housing studies. Principle axes factor analysis of the sample set produced a factor structure whose interpretation is quite consistent with those conceptualizations of the nature of housing elements to be found in existing public agency statements. However, this analysis also shows that for each basic housing element, the variables acting as indicators of that element tend to be highly correlated with other variables within the element. This strongly suggests that a more critical evaluation is needed of the cost effectiveness of collecting data on large numbers of variables as practiced in existing housing quality studies.

Of particular interest was that, for the observations which made up the parcel sample, the structural dimensions emerged as a single cluster of variable which were uncorrelated with an identifiable environmental component. This leads us to reject, for this study area, the notion of estimating overall housing quality (as currently defined by public agencies) *at the parcel level* based only upon remote sensor observation of environmental variables. It is felt, however, that such a finding may be unique to Los Angeles (or at least to cities of the Southwest) which are dominated by single-family structures with a high degree of variation in the level of maintenance of individual parcels. In other U.S. cities, particularly those of the East and Midwest, the set of relationships between structures and environment may be substantially modified in the poorer areas possessing a predominance of multi-unit structures.

At the block level, a similar analysis was undertaken for observations on a 20% sample of blocks (268 units). The resulting factor structure was markedly different from that generated at the parcel level. Previous research has indicated that simple correlations between variables tend to increase with aggregation of the units of observation, in the multivariate case this also results in a larger proportion of the variance being accounted for by a given number of factors and also increasing correlation levels between previously uncorrelated variable clusters. In particular, in the present case, the structural condition component no longer represented an isolated variable cluster, but was associated with a number of environmental variables, primarily those which identify the level of upkeep of lots and the existence of land uses incompatible with residential development. This finding is extremely important since it implies that overall housing quality may be estimated *at the block level* utilizing observations on environmental condition variables alone.

The results of the two analyses indicate not only that the component structure defined at the individual parcel level has been lost, but also that the question of additivity in construction of housing quality indices must be examined anew at each level of areal aggregation, such as the origin-destination zone or census tract. The results of the factor analytic studies lead to a research concentration upon the assignment of quality values at the block level since it was here that remote sensor generation of data appeared most feasible.

The next stage of the investigation comprised an objective grouping of the sample blocks into five quality classes based on similar profiles of factor scores derived from an analysis of observations on all 37 variables (see Figure 2). Comparing this grouping with the subjective evaluations made by the ground enumerators, it was found that the general trends of the two classification structures were similar, with the most deficient blocks being well identified on both, however, considerable differences existed in the drawing of boundaries between the higher rated blocks. The objective grouping is more compact than that of the enumerators, suggesting that the latter did not utilize the full range of data recorded in making their subjective assignments. Further, it suggests that the ground enumerators tend to be somewhat conservative in assigning blocks to the highest or lowest categories.

Group assignments based on factor score profiles derived from a reduced set of 21 environmental variables were also made. The results showed a strong agreement with those of the previous stage with 75.4% of the block assignments being the same in both groupings. The errors occurred in the assignment of a number of marginal blocks and do not constitute a major problem.

The final stage of the ground data analysis examined the feasibility of further reducing the set of 21 environmental variables in effecting the classification. Using stepwise multiple discriminant methods it was found that a high level of performance (82.8% correct assignment) could be attained using only seven environmental variables, namely measures relating to

- | | | | |
|---|-----------------------------|---|---------------------|
| 1 | On-street parking | 5 | Refuse |
| 2 | Loading and parking hazards | 6 | Street grade, and |
| 3 | Street width | 7 | Access to buildings |
| 4 | Hazards from traffic | | |

(Table 2 displays the discriminant equations, pertaining to each of the five quality classes.)

Although it is not claimed that these results possess complete generality in the sense that an analysis of all urban areas would result in the same variables being selected for use in classification, particularly given the nature of housing in Los Angeles, it is highly encouraging that obtained by using all 37 environmental and structural variables in

combination This, in itself, is an extremely important finding of the research which could lead to large financial savings in urban data acquisition

Imagery Analysis

The imagery analysis consisted of an evaluation of black and white color, and color infrared photography obtained as part of NASA Aircraft Mission 73 with respect to the identification of the reduced variable set listed above Color infrared photography was found to be the most useful in defining the seven variables important in housing quality identification

After some interpreter training, sub-sample of 53 contiguous blocks in the Firestone area was chosen for an evaluation experiment. (see Figure 3) Definition of the variables and subsequent assignment via the generated multiple discriminant functions satisfactorily classified 50% of the blocks, when compared to the 37 variables classification, into the five housing quality groups Because of the subjective nature of some of the variables, we were forced to use three interpreters and go to a "majority rule" structure on the interpretation Further investigation indicated that within the area chosen, the differences between groups 2 and 3 were not critical and upon aggregating groups 2 and 3, thus reducing the number of housing quality classes to four, the level of accuracy was increased to 69% Thus, when remote sensor imagery was utilized to estimate the values of the seven variables, it was possible to correctly classify 69% of the blocks when compared to the classification generated using all 37 variables. Once again this percentage is based on a two out of three interpreter agreement, with individual interpreters scoring higher

Further evaluation of the seven variables utilized suggested that a further reduction in their number would remove some which suffered from severe interpretation difficulties The original 37 variable set was then reduced to four (1) street width, (2) on-street parking, (3) street grade, and (4) hazards from traffic, by methods identical to those used in the original analysis Comparison of the capability of the four variable discriminant functions to classify blocks correctly with respect to the 37 variable classification showed that use of the reduced variable set led to a correct assignment in 78% of the cases

Conclusions with Respect to Housing Quality

It is felt that small area classification of housing quality in the United States can definitely be accomplished via aerial photography utilizing the procedures similar to those outlined here The NASA aircraft program has successfully delivered imagery which has allowed us to accomplish this evaluation task and it appears that no further aircraft imagery will be required over U S sites Further calibration of the models and definition of necessary variables can be accomplished by

competent planning organizations within U S cities if they follow the procedures outlined here * The use of more highly trained interpreters should significantly increase the percentage of successful classifications Other problems which remain but which seem to fall outside the purvue of the Earth Resources Program are

- (1) Sharper definition of the housing elements used by public agencies and subsequent redefinition of observational variables in more objective form
- (2) Calibration of classification algorithms for major U S cities
- (3) More critical evaluation of the statistical grouping procedures used in the present study
- (4) Increased study in cooperation with public agencies to determine the sensitivity of classification schemes to differential weighting of the various housing elements

An extension of the housing quality studies into different cultural systems is an immediate task That is, can we apply the same basic study design and set of housing elements to the definition of housing quality in other parts of the world? Are the same types of variables relevant? Research oriented towards a partial answer of these questions currently underway utilizing San Juan, Puerto Rico as a study area (NASA Aircraft Mission 98)

Other Areas of Research Related to Urban Problems

Other research into the application of remote sensing to urban data acquisition problems is also underway at Northwestern and Iowa One task deals with the utilization of remote sensing for the definition of inventories of urban transportation systems, and another with the delineation and definition of commercial structure within urban areas Imagery of Phoenix, Arizona, will be the prime data source for these two task areas The solution of urban component definition will add greatly to our planning and scientific modelling capability However, because of the current lack of an integrative system allowing access and retrieval to the generated data by and for urban management, planning and scientific personnel, the time will be quickly upon us when this deficiency will dilute and significantly impede our capability to solve urban problems

Figures 4 and 5, an Apollo IX photograph of Phoenix and the derived land use map, provide a rough idea of our current capability to discern gross urban land use and other urban characteristics from low resolution space photography But clearly, we are faced with a major loss of useful information at this level of resolution The pattern of information loss, as resolution shifts from high to low, with regard to intra-metropolitan

* These are discussed in much greater detail in the forthcoming Northwestern University contribution to the Mission 73 Final Report

problems, is not well known. Experiments to define the level of information loss in problem specific contexts are being undertaken. It does seem clear, however, that both the quantity and quality of viable urban data which may be extracted from remote sensor imagery declines drastically as the size of the resolution element increases. This must be kept in mind in the design of future ERTS type systems.

TABLE 1

Structural and Environmental Variables Utilized
In the Los Angeles Study

1	Land Use - suitability for residential devt	} Variables Potentially Measurable Using Remote Sensors
2	Condition of Street Lighting	
3	Presence of on-Street Parking	
4	Street Width	
5	Street Maintenance	
6	Street Grade	
7	Condition of Parkways	
8	Hazards from Traffic	
9	Adequacy of Public Transportation	
10	Number of Buildings/lot	
11	Number of Units/lot	
12	Condition of Fences	
13	Adequacy of Lot Size	
14	Access to buildings	
15	Condition of Sidewalks	
16	Condition of Landscaping	
17	Refuse	
18	Parcel Use	
19	Adverse effects of residences	
20	Nuisances from loading/parking	
21	Unclassified Nuisances from industry etc	
22	Overall Block Rating	} Variables not Observable Using Remote Sensors
23	Noise/Glare (block)	
24	Smoke	
25	Condition of accessory buildings	
26	Premise Rating	
27	Noise, fumes and odors (parcel)	
28	Construction type	
29	Age of dwelling	
30	Condition of structure	
31	Condition of walls	
32	Condition of roofs	
33	Condition of foundation	
34	Condition of electrical installations	
35	Condition of paint	
36	Other exterior factors	
37	Overall parcel rating	

TABLE 2

Estimated Values of Seven Variable Discriminant
Function Coefficients for Five Housing
Quality Classes

Variables Entered	Group 1	Group 2	Group 3	Group 4	Group 5
Street Parking	11 98273	11 70921	14 29894	26 82691	33 83474
Street Width	9 58286	12 74884	12 83865	23 94130	29 37255
Street Grade	-0 09590	2 27461	-2 14395	-8 21800	-15.35324
Traffic	6 29865	6 97459	10 25828	14 83337	19 92107
Access to Bldgs	74106	7 53122	92118	4 81558	-23 01457
Refuse (B)	88833	31976	1 44861	2 78478	8 69098
Loading/Parking	-0 13313	15122	06021	19492	13 68095
Constant	-14 39145	-23 72600	-24 19998	-66 00233	-179 58047

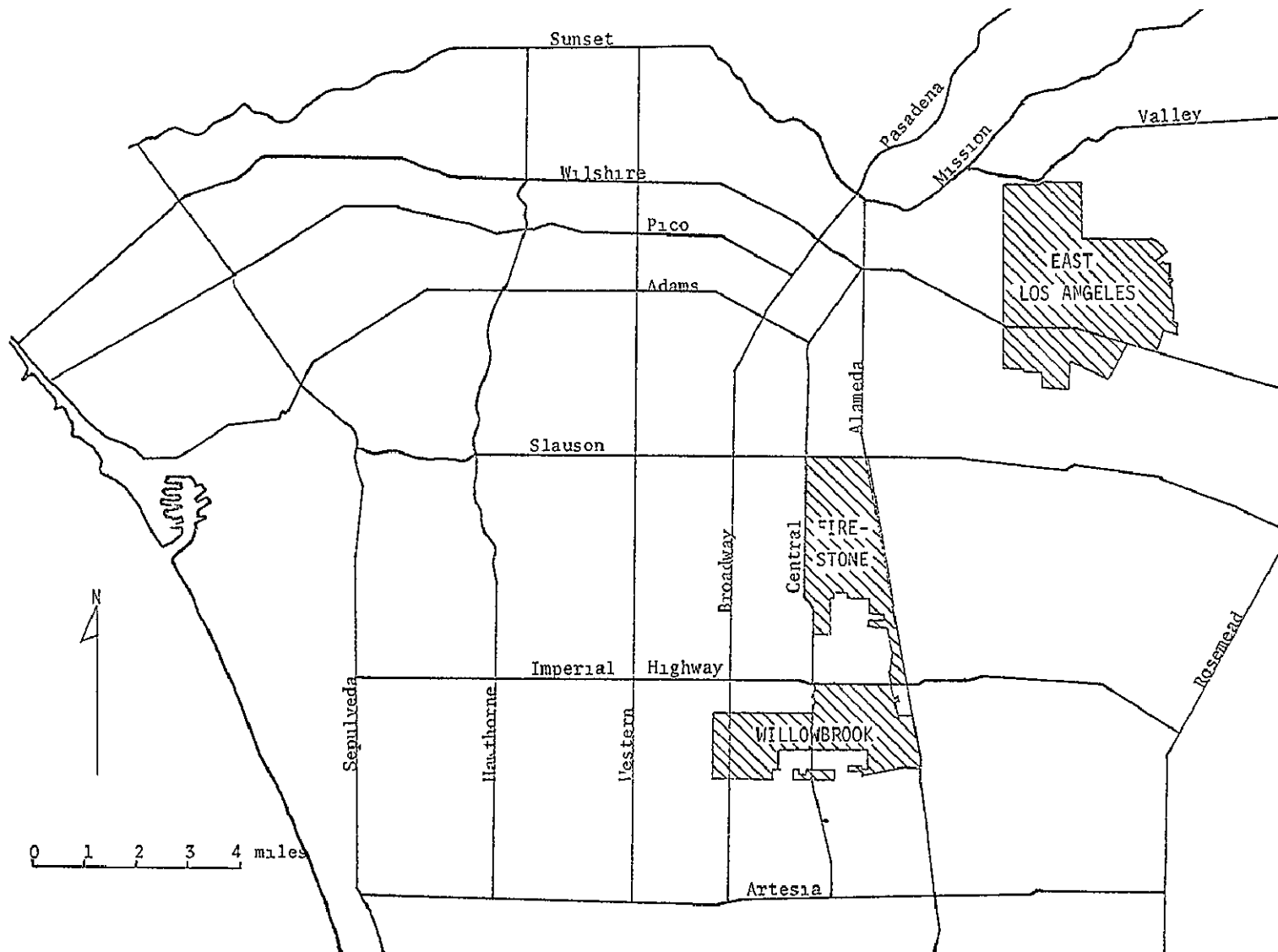


Figure 15-1.- Study areas in Los Angeles

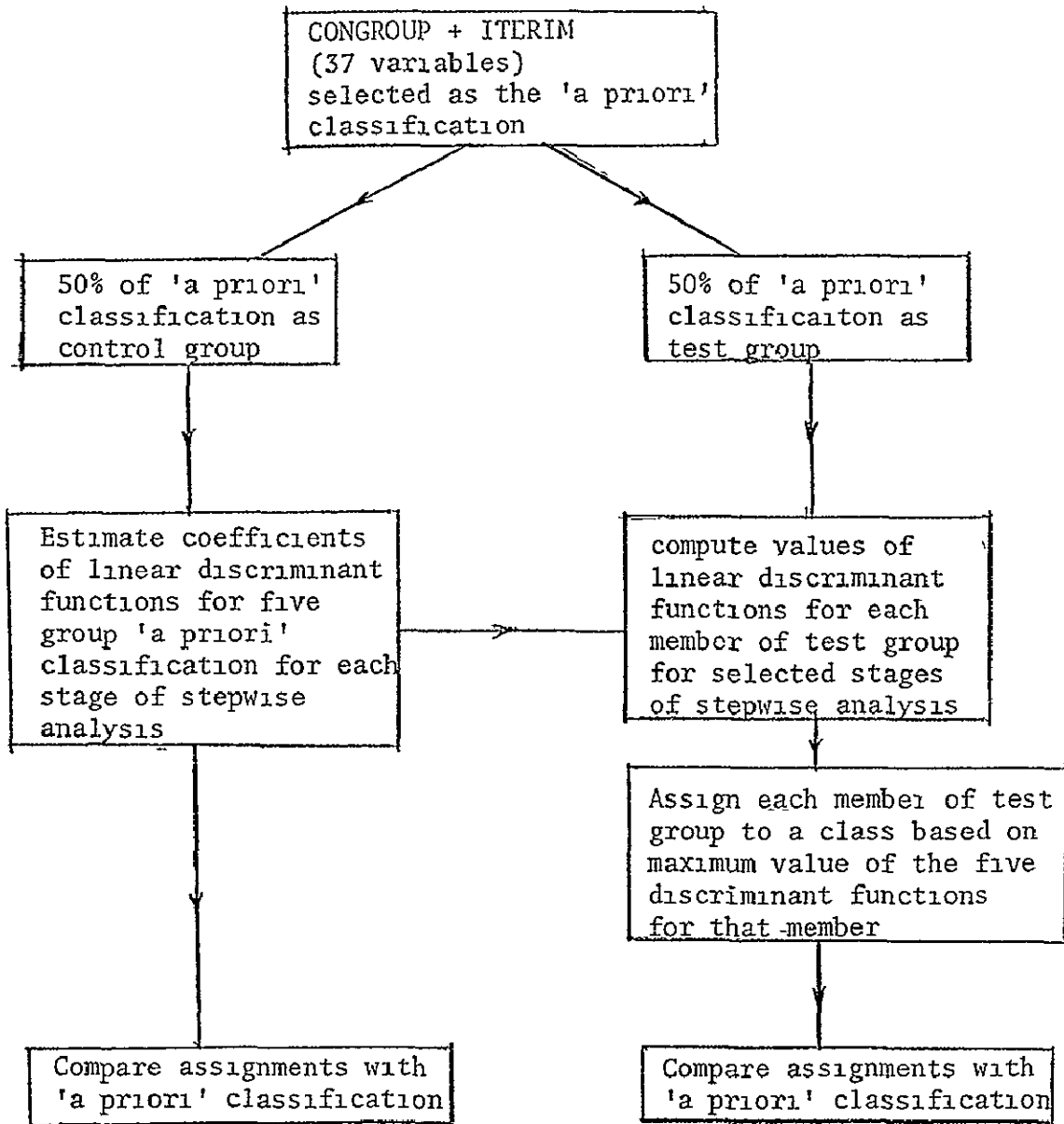
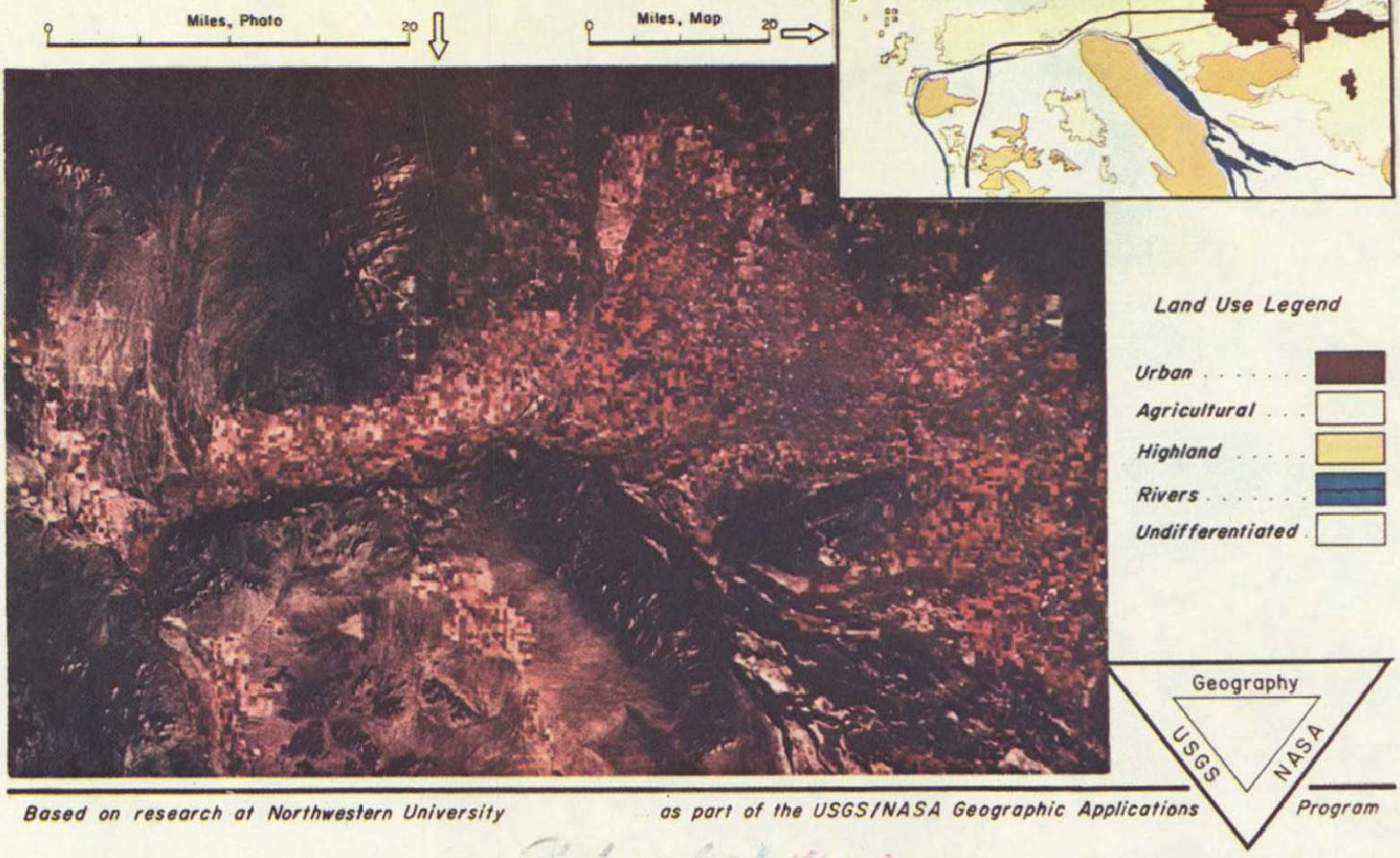


Figure 15-2.- Flow chart for steps in analysis.



Figure 15-3.- Color infrared image of Firestone Area NASA Aircraft
Mission No. 73

Mapping Metropolitan Land Use from Apollo Color IR Photo



Based on research at Northwestern University

as part of the USGS/NASA Geographic Applications

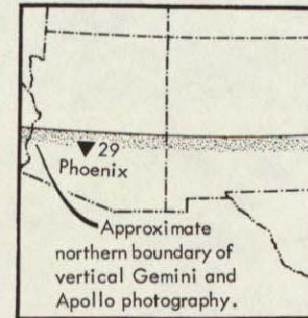
Program

Figure 15-4.- Mapping metropolitan land use from Apollo color IR photo.

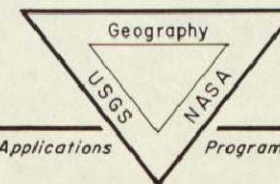
One of the Apollo IX photographs with color infrared film looks down upon Phoenix, Arizona. The entire photo, measuring slightly more than two inches by two inches, pictures an area measuring approximately 100 miles by 100 miles. An enlarged portion of this photo is shown at the left in the illustration. A land use map shown at the right has been compiled by interpreting the photo. The map covers exactly the same area, but at one-half the scale.

Because of the enhancement of vegetation by the color infrared film, the checkerboard pattern of large irrigated fields shows prominently from west to east across the center of the photo. This is mapped as agricultural land, yellow on the map. Highland areas in brown, drainage routes and flood plains in blue, and undifferentiated lands left uncolored (white) together block out the setting for the Phoenix urban area, which is shown in dark purple. Patches of outlying urban area also appear in this symbol.

Despite the coarseness of the land use classes listed in the legend, some further insight into the urban area can be interpreted. Major transportation routes, shown in black on the map, can be traced through the urban area to the limits of the area mapped. The Central Business District is the knot of most-blue, least-pink portion of the urban area where the transportation lines converge. The largest out-lying suburban area lies to the northwest. It appears more coarse-textured, and more pink, than the urban core. This area includes a growing retirement community, ringed by a red golf course bounding its pinkish center. Additional sections of this community are being developed. One use of time-sequence imagery from orbiting satellite is the monitoring of the peripheral growth of urban area. The false color imagery is useful in distinguishing urban from nonurban, and also in identifying intra-urban "green" space.



Geography Test Site 29
Phoenix, Arizona



Based on research at Northwestern University

... as part of the USGS/NASA Geographic Applications

Program

Figure 15-5.- Mapping metropolitan land use from Apollo color IR photo.

SECTION 16
SURFACE ENERGY EXCHANGE PHENOMENA
INTERPRETED FROM IR EXPERIMENTS

N71-19267

Robert W. Pease
Department of Geography
University of California/Riverside

Introduction

The title for this report is somewhat misleading. Two lines of inquiry are involved, only one of which fits the title. First to be discussed is a carry-over from previous work with false color film and could aptly carry the title "Multispectral Images from Multilayer Film."

This portion of the report is an outgrowth of previous NASA data flights, particularly Mission 73 and Apollo 9. It should be considered as a suggestion relating to information gathering systems of possible use in future aircraft or spacecraft flights.

Discussion

Data supplied by the NASA air and spacecraft programs must be viewed as input information to various systems of analysis. Instruments such as IDECS or those designed by Yost or Philco-Ford utilize multispectral black and white images as inputs. These have been obtained by camera clusters or multilens instruments, using appropriate spectral band pass filters, with images made directly onto mono-layered black and white films. But the existing bank of multispectral data is small and some like that from Apollo 9 has such poor contrast that practical use is limited.

It is only logical then, to explore objectively the feasibility of separating multispectral images from multilayer film, utilizing techniques that long have been a part of the graphic arts. Since ERTS-A will utilize essentially the three bands of CIR dye-layer sensitivities, it follows that separation analysis be made with color infrared film. Such an inquiry and evaluating of results has been carried out at the University of California, Riverside.

Advantages of the separation process are several: (1) The potential bank of multispectral data is greatly increased. (2) A single lens, single camera can be substituted for the more elaborate clusters. (3) Registration or congruency of images is automatic, and (4) better contrast is obtained in the green band, subject to deterioration by air luminance.

That multispectral images can be so made is shown in Figure 1. The cameras are the Apollo 9 Hasselblad cluster -- the target - the oft photographed Imperial Valley. The upper row contains multispectral images taken directly onto black and white film with three cameras of the cluster. The bottom row are the corresponding separations from the color infrared image made with the fourth camera of the cluster.

There are differences in both tone contrasts and resolution. The poor contrast of the B/W green band is readily apparent. There are also errors on the tone relationships of the separations. Note particularly the darker appearance of the cyan or infrared separation. The importance of these errors is being investigated and evaluated.

For those unfamiliar with the separation technique, in concept it is simple. In Figure 2 the spectral window of a separation filter has been superimposed upon the density curves of the three dyes that are formed in Ektachrome-type film. The window is placed at the point where the density of the desired layer is greatest, but also where the densities of the unwanted layers will be least. The filter here portrayed is a Wratten 93, one of the filters used in a color densitometer. Seventy-five percent of the exposure occurs in the clear area, all exposure within the light stipple. This diagram also illustrates one of the errors of the system. Densities of the unwanted layers are not zero in the spectral window no matter how narrow it is made, and thus a measure of interlayer- or cross-modulation occurs. In this example for a neutral target, the cross-modulation will amount to a density of about .05, a difference barely discernible by the average eye.

A second error results from the overlapping of layer sensitivities in the multilayer film. Figure 3 compares the multilayer and true multispectral systems. Of consequence is the overlapping of the infrared sensitive cyan layer into the red band recorded by the magenta layer. In theory this again should result in about an .05 density difference between a neutral and a vegetation target if both have the same infrared reflectance.

In Figure 4 two techniques are compared for a much enlarged portion of the Apollo 9 frame. It is to be noted that the general acutance of the black and white image is greater, but contrast in the green band is poor. Tonal differences tend to be greater in the separations due to the inherently greater contrast of the CIR film. Why the airbase has a lower reflectance than adjacent crops in the true multispectral, but appears lighter in the separations is being examined.

To check the utility of the separation technique, transparencies so made were used as inputs into the IDECS instrument at the University of Kansas (Figure 5,a). The area of the Imperial Valley shown on Figure 4 was used. Instructions were placed into the instrument so that areas with the greatest vegetative contrast would appear

as yellow or white. At the time of the Apollo 9 flight, these would be fields of uncut alfalfa, sugar beets, and barley. On the map above the readout, areas in solid black are fields within the yellow area that are not one of the three crops. Crosshatched fields are occurrences of one of the three crops outside of the light tone. This graphically records two types of errors which may ensue from the separations, but also may reflect harvested alfalfa and beets as well as barley in an early stage of development that exposes a large amount of soil.

Figure 5,b compares black and white multispectral imagery for an adjacent area, the images also from the Hasselblad cluster with transparencies furnished by MSC. Instructions were again placed in the machine as close to the former example as the subjectivity of this device allows. Errors are mapped in the same way. It is to be noted that the areal extent of fields of the three crops falling outside of the yellow tone is much greater than with the separations. Part of the problem appeared to stem from exceedingly low contrast of the green band which barely recorded on this video system.

This comparison makes no attempt to try to prove superiority for the separations. It merely demonstrates that they are useful and competitive in quality. For instruments like IDECS, the greater inherent contrast is a definite advantage.

A side endeavor to this inquiry has been the processing of CIR film to a negative from which positive multispectral images can be extracted without the need for an internegative. Ways have been developed to circumvent difficulties experienced by the Eastman Kodak Company in their endeavors to create CIR Aero-neg. Figure 6 shows a print made from a CIR negative and three multispectral separations the negative also yielded. Also shown (Figure 7) is an IDECS readout from derived multispectral separations with instructions placed in the instrument to emphasize plowed fields with a high moisture content (light tone). The correlation with ground truth is good.

Investigation of the separation technique for multispectral use is not complete. Attention at the moment is focussed upon obtaining the best infrared image possible from the cyan band. To answer such questions as posed by the airbase, graphic tests have been devised such as that shown in Figure 8. A strip of leaf was placed across a neutral gray wedge and photographed with various techniques mentioned. Shifts of tone match are indicators of inherent errors in the process.

In short, separation techniques are of interest to remote data gathering for the reasons previously stated. Simplification of instrumentation is a promising implication.

An observation made in the course of the investigation is of interest. The red and green multispectral bands give highly redundant information. Most significant is the contrast between "visual" and infrared images. Since variations of the red band are most significant

in the visual, perhaps 2 band B/W multispectral, red and near infrared, will supply most multispectral input needs.

The previous digression from the stated topic reports on the wind-up of earlier work. The immediate goal in the area of environmental impact has been the quantitative calibration of remote infrared radiometric sensors. This is a part of a longer range goal concerned with monitoring by remote sensing methods applicable to spacecraft, the energy resources of the planet.

Although the inquiry is still at embryonic stage of establishing instrument arrays, an opportunity was afforded in June to utilize NASA flown instrumentation on the island of Barbados in conjunction with the BOMEX project.

Although the BOMEX experiment was primarily concerned with the interchange of energy between air and sea, McGill University has established three sites instrumented with ground radiation sensors on the island of Barbados under the supervision of Dr. Ben Garnier. Since Seawell Airport on Barbados was the base for BOMEX flights, it was conceived that the calibration of remote radiation sensors through tropical air with high water vapor content could be explored by NASA aircraft engaged in the larger experiment. For the first time an infrared scanner with a potential for calibration was available in the program and attempts were made to calibrate it in order to obtain if possible, quantitative results. This scanner, the RS-14, not only produced a photographic record, but stored data on tape as well.

Figure 9 shows but a few of the ground instruments that were available. At the Waterford site (upper) there was a fairly comprehensive array of such instruments as a net radiometer and pyranometer (center) and an evaporation pan (lower). Waterford was only one of three sites instrumented with various weather data gathering gear.

In conjunction with the ground and NASA airborne instruments, the Barnes Engineering Company both provided precision ground radiometers and carried out ancillary airborne experiments of their own with the aid of a light airplane. In Figure 10 (upper left), a Barnes engineer is checking a small PRT-10 precision thermometer against its calibrating block with the more elaborate PRT-5 alongside. The upper right view shows the head of a PRT-5 attached to the landing strut of a light plane. Output was fed digitally onto tape. In addition, the principal investigators, Robert Alexander and myself, provided certain instruments of our own design. The lower left view is a small thermistor mast and measuring bridge which checked soil temperatures at, above, and below the soil surface as a part of ground truth. A broadband spectroradiometer for measuring albedo is shown in the lower right. Extensive instrumentation was thus available to attempt correlation of ground measurements with airborne sensors.

Fairly elaborate steps were taken to assure calibration of the various instruments to each other. A Leslie Cube (Figure 11, upper)

was used with the precision radiation thermometers, and these then checked against Barnes own calibration device and a simple water bucket (center). Recording devices were in turn checked out against the calibrated instruments.

In turn the ground instruments were calibrated to the instruments in the NASA aircraft. In Figure 10 (lower), Robert Alexander is holding a calibrating source under the RS-14 infrared scanner.

Conclusions

It would be gratifying to be able to give a definitive analysis of the data obtained by the NASA aircraft, but only yesterday was the first data made available to the principal investigators. However, visual monitoring of instruments at the time disclosed a significant finding relating to the quantitative remote measuring of radiation, which I am sure the data, when examined, will bear out. Briefly, the 8-14 micron "water vapor window" is not satisfactory for quantitative work under tropical moist conditions, and I now suspect for conditions where less water vapor is present. The airport runway which recorded a radiation temperature of 50°C at ground level had dropped 9°C when sensed from an altitude of 1000 feet. Clearly much of the runway emission was being masked out by absorption within the window and a considerable measure of cooler water vapor emission was being recorded. A similar effect was noted by the NASA aircraft over sea with known surface temperatures near the island.

To carry forward remote radiation measurement, it appears necessary to penetrate better the water vapor window. Barnes is developing an oscillating radiometer that sequentially doubles the optical path to determine and thus compensate for the vapor present. The U.C. Riverside project has on order a custom-built Barnes precision radiometer that will accept a 10-12 micron bandpass. As is commonly held, if the vapor intrusion occurs at the wings of the water vapor absorption bands at 8 and 14 microns, the narrower bandpass may give the desired better penetration. It is our understanding that a 10-12 micron instrument will be installed upon NASA aircraft in time for a planned spring flight in California and our own ground instrument arrays will be operational by that time. Better calibration can then perhaps be made. It would be desirable to try the narrower bandpass under the tropical conditions of the Barbados experiment. Our weather here today suggests that Houston, itself, might provide such a test site.

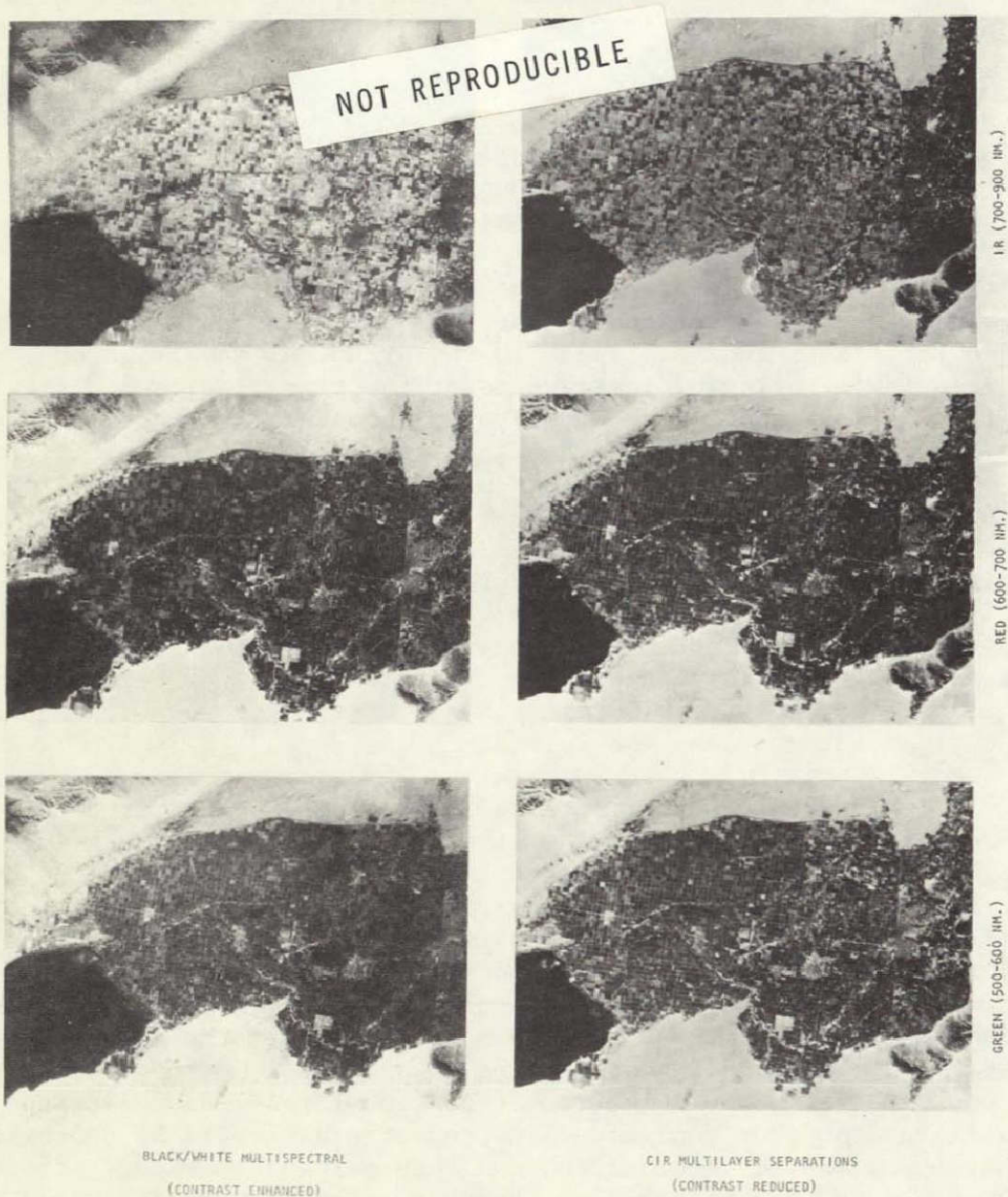


Figure 16-1.- A comparison of black and white multispectral photographs with multispectral separations from color infrared film. The three black and white spectral bands and the color infrared image were made at the same instant by a bank of four Hasselblad cameras mounted in the Apollo 9 command capsule orbiting the earth at an altitude of approximately 150 miles. Contrast of the B/W green band has been enhanced from the original. It has been necessary to decrease contrast in the separations since CIR is an inherently high gamma film. (Target-Imperial Valley of California. Mission S-065)

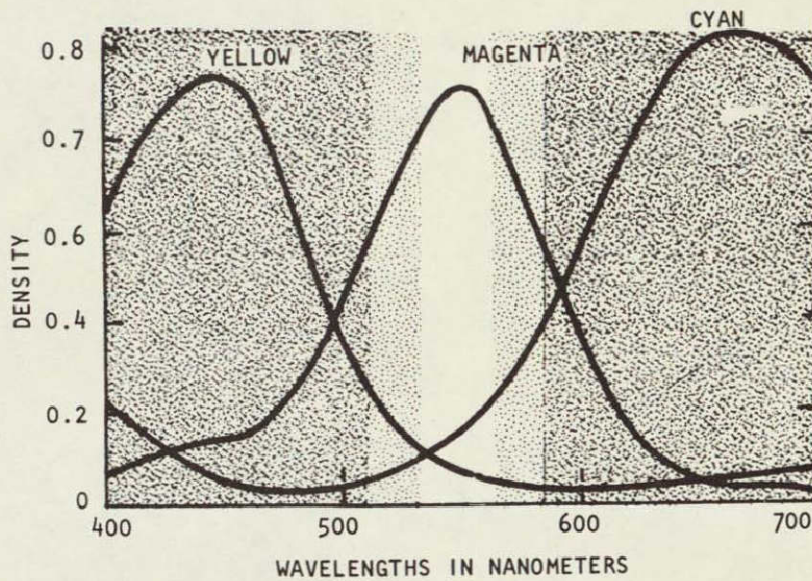


Figure 16-2.- The principle involved in making multispectral separations from multilayer film. Curves for the three dye layers of the multilayer film are plotted according to density and wavelength. The spectral window of the filter for separating the magenta modulations (red band on CIR film, sensitive to 600-700 nm.) is shown by lack of stipple. Seventy five percent of the separation exposure occurs in the clear area, all within the light stipple. Some cross-modulation between layers must occur since adjoining layers have some density within the spectral window.

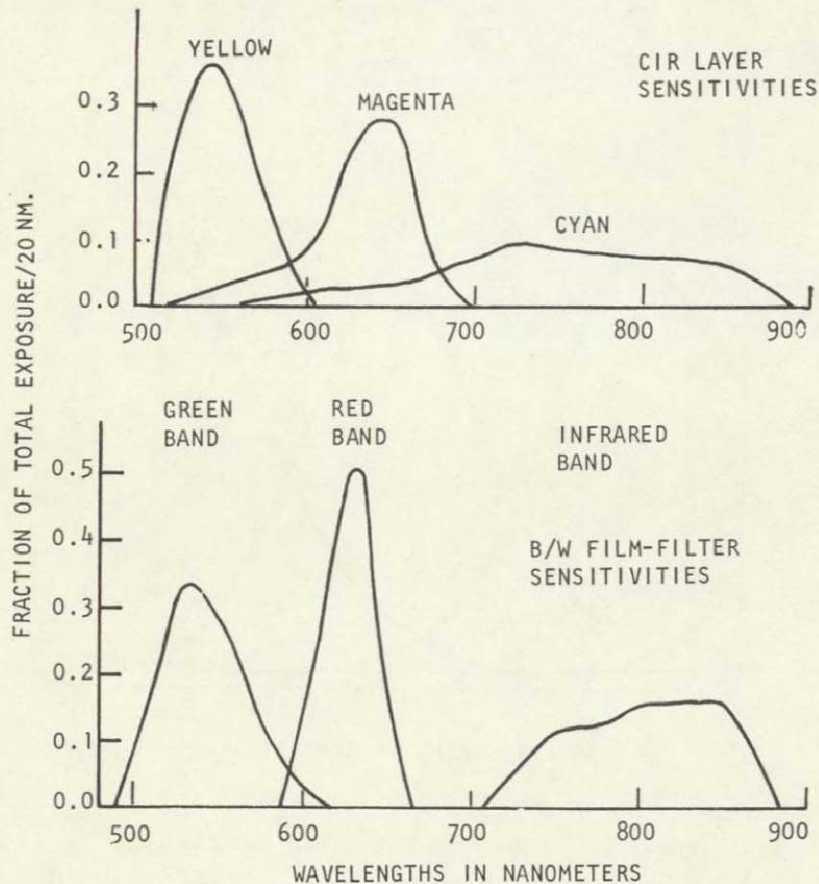


Figure 16-3.- Spectral sensitivities of the dye-forming layers of color infrared film compared with the effective sensitivities that occur in black and white multispectral systems. Overlap of sensitivities is a characteristic of the multilayer film which causes a small error in separation modulations. Uneven distribution of bands occurs in the black and white system because of the 650 nm. sensitivity cutoff of most panchromatic films. The B/W system for the red band (600-650 nm.) and an W89B for the near infrared (700-900 nm.) with the film sensitivity again setting the long wavelength limit.

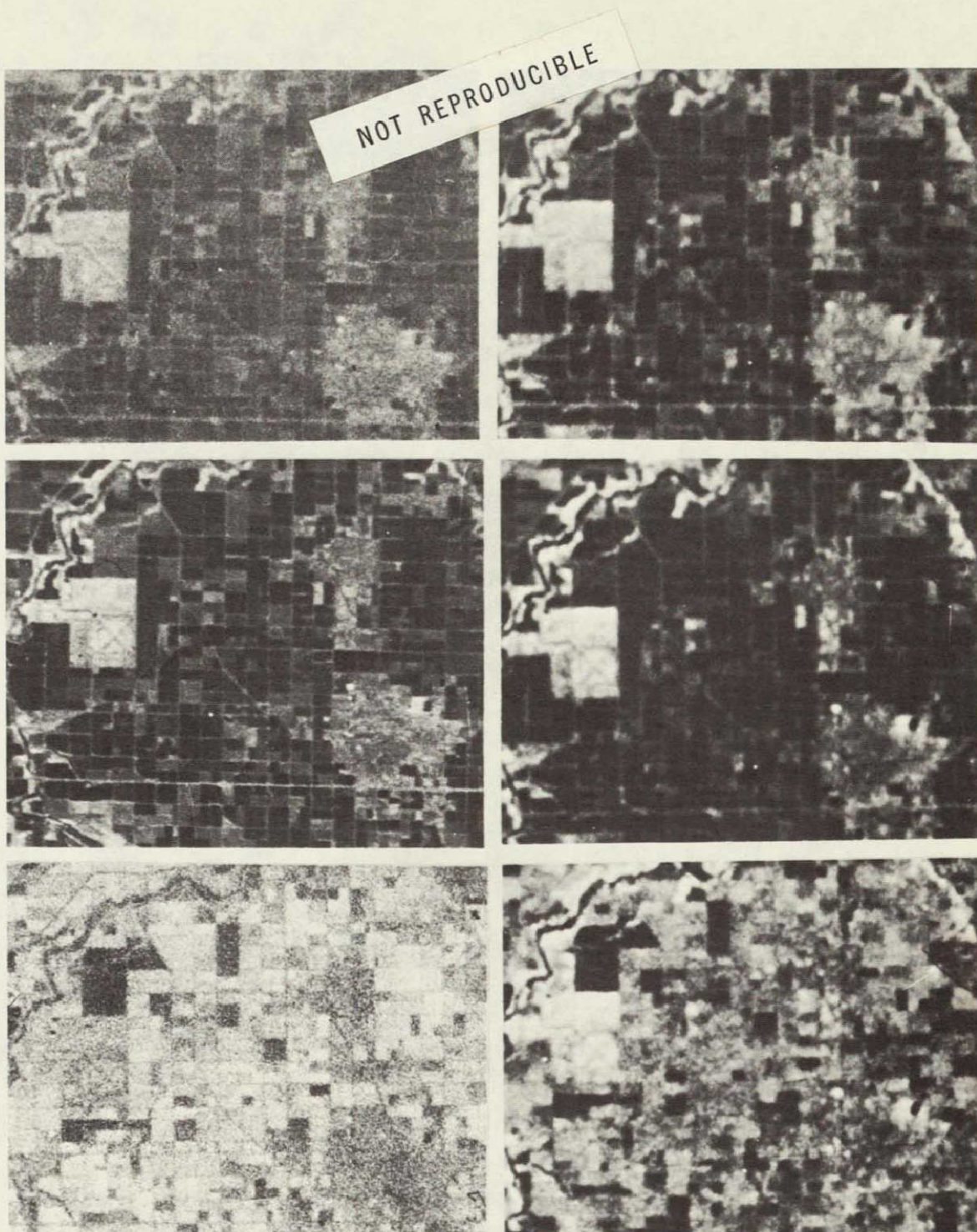
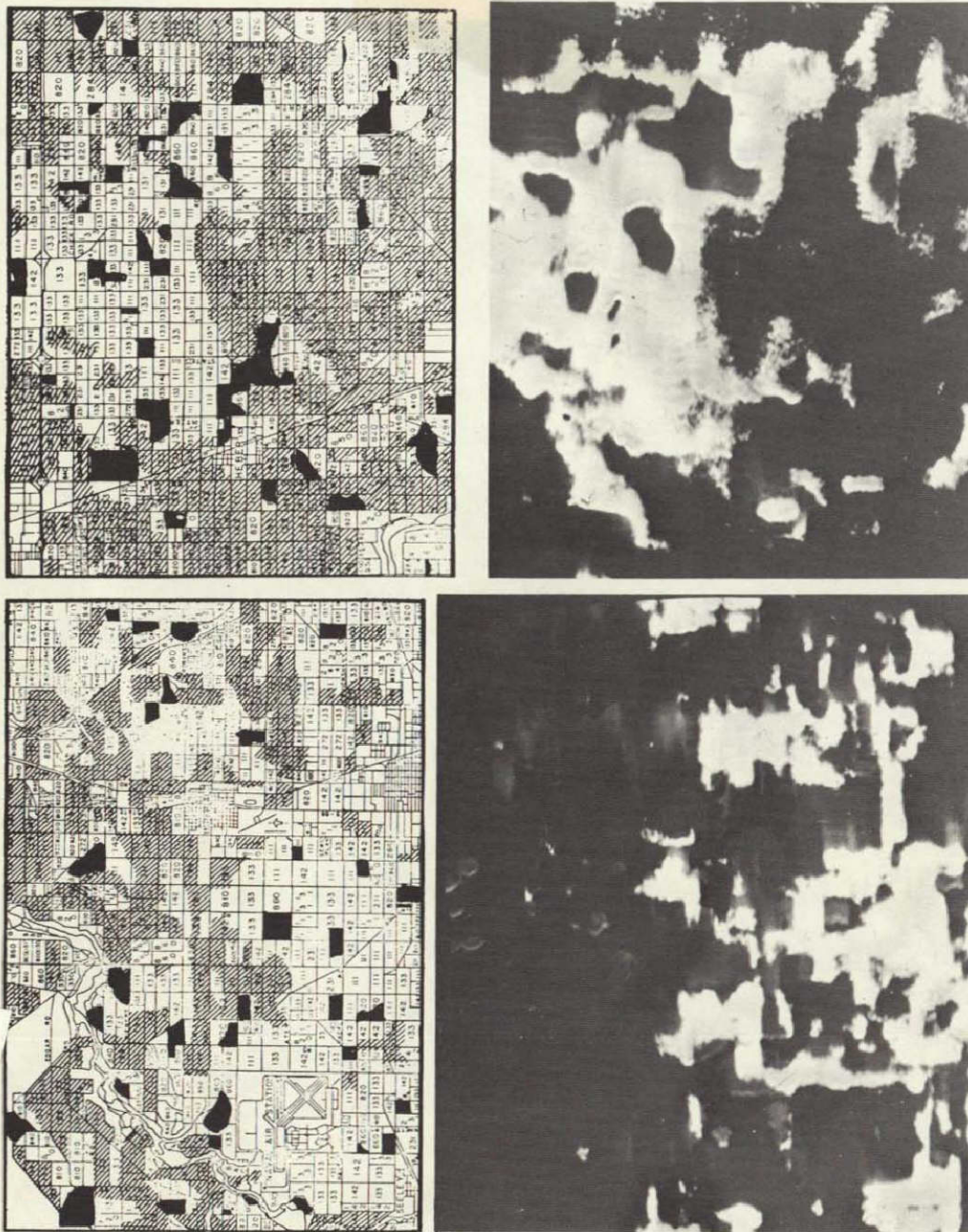


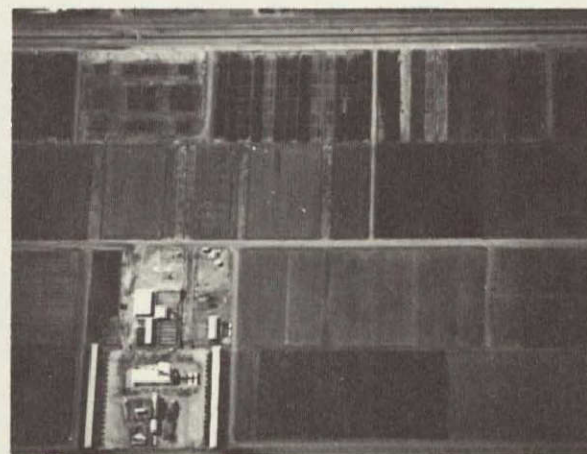
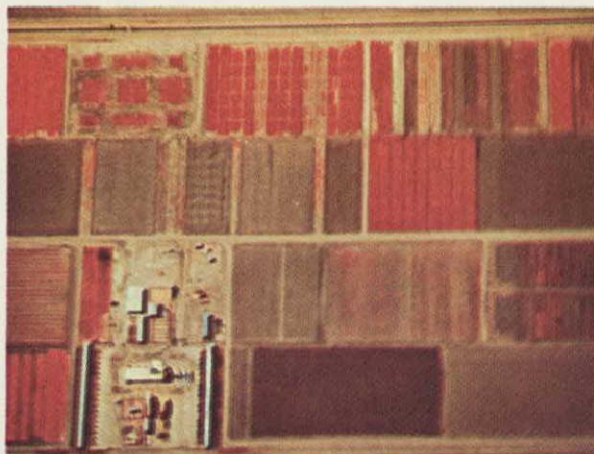
Figure 16-4.- Enlarged portions of Figure 1 (20 x) that compare resolution and tone. Note poor contrast of the B/W green band. Also compare the airbase and adjoining fields to the east in both infrared displays.



NOT REPRODUCIBLE

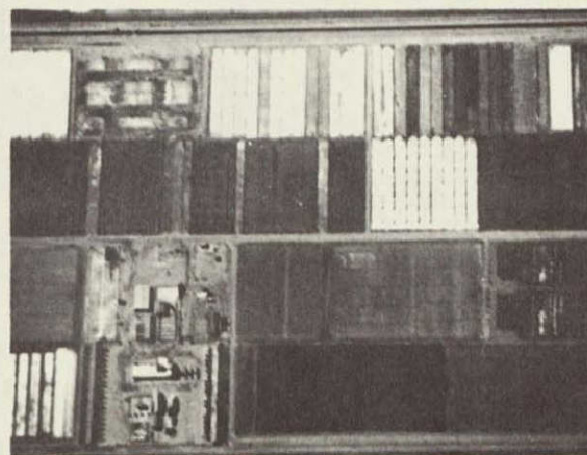
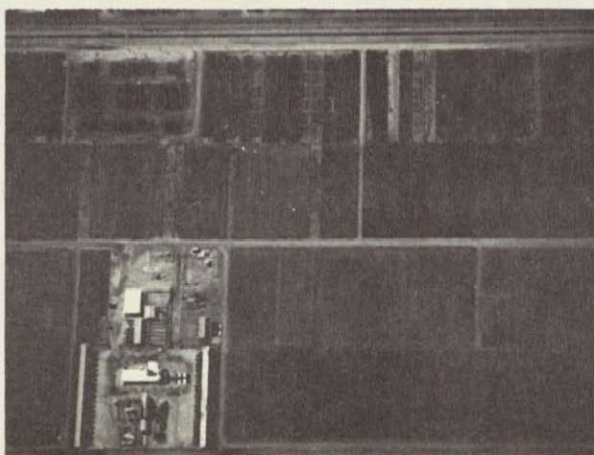
Figure 16-5.- A comparison of IDECS readouts from CIR multi-spectral separations of the area shown in Figure 4 (a.) with B/W multispectral readout for an adjoining area (b.). Above each video display is a map showing errors. The instrument was set in each case to cause highly vegetative crops to be light in tone. Other crops appearing within the light tone are black. Appropriate crops not within the light tone are crosshatched.

FROM
CIR
NEG.



500
TO
600
NM.

600
TO
700
NM.



700
TO
900
NM.

Figure 16-6.- A color print from type 8443 CIR film processed successfully to a negative and the set of multispectral separations derived from the same negative; green spectral band upper right, red spectral band lower left, and infrared band lower right.

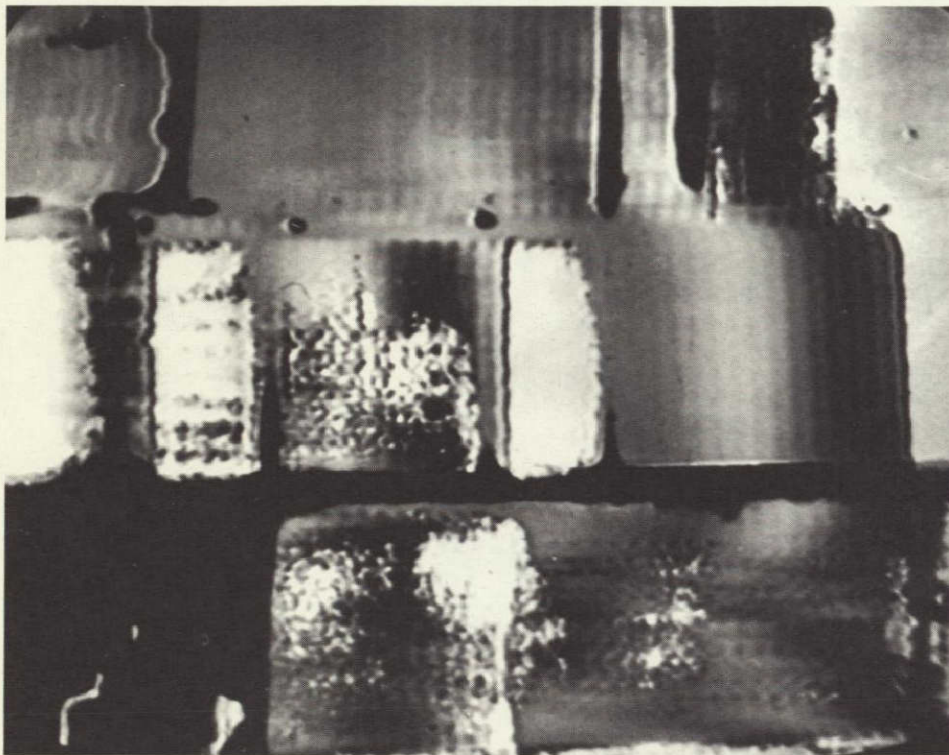


Figure 16-7.- An IDECS readout from transparencies derived directly by separation methods from the CIR negative of Figure 16-6. The instrument was so set that the light tone shows the moisture content of fields with no crop cover (plowed, seeded, fallow, etc).

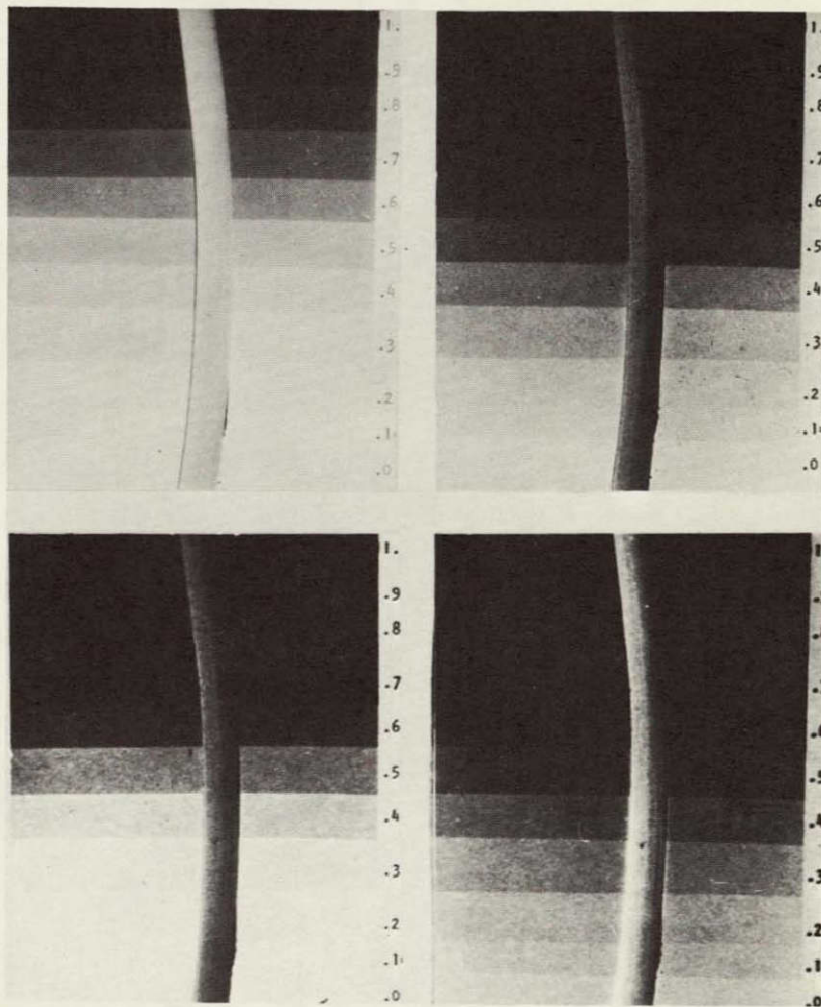


Figure 16-8.- Continuing investigation of value of multispectral separation process. A plant tissue target (lily leaf), placed across a neutral step-wedge, then photographed with the several techniques being used. Upper left is B/W multispectral (infrared film and 89B filter), upper right is cyan (infrared) modulation extracted from a CIR positive transparency using panchromatic internegative, lower photos made directly onto panchromatic paper from CIR processed to a negative. It is to be noted that the high contrast of the CIR film brings out variations in the plant leaf that made tone matching difficult and that the tone match of the separations varies with original exposure (lower). Ideally, the tone of target should have matched the same step in all photos.

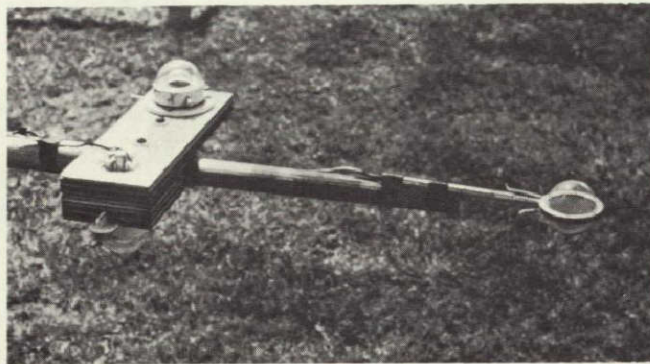
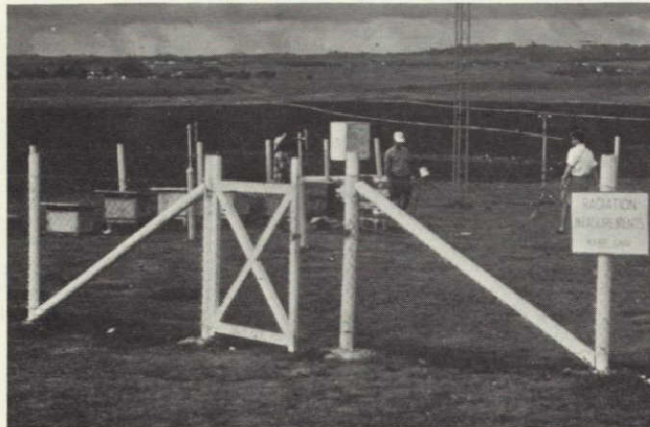


Figure 16-9.- Quantitative calibration of remote radiation sensors at Barbados. The Waterford site with ground instrumentation maintained by McGill University (upper), a net radiometer and pyanometer at Waterford (center), an evaporating pan at Waterford (lower), all representative of complementary instrumentation available from BOMEX participation.



Figure 16-10.- Other instruments for making ground to air correlations. Barnes Engineering Company representative with PRT-10 and PRT-5 radiation thermometers for ground use (upper left), PRT-5 sensing head mounted to light plane landing gear strut for airborne use (upper right), thermistor mast and bridge for soil and air temperature gradients (lower left), and broadband spectroradiometer for albedo measurements (lower right). Both of the instruments in the lower photos were designed and supplied by the principal investigators.

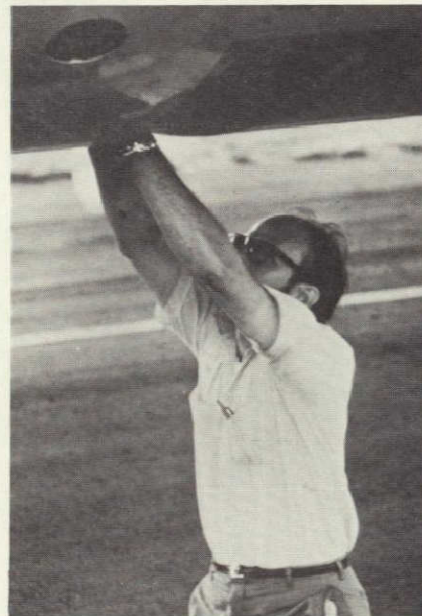
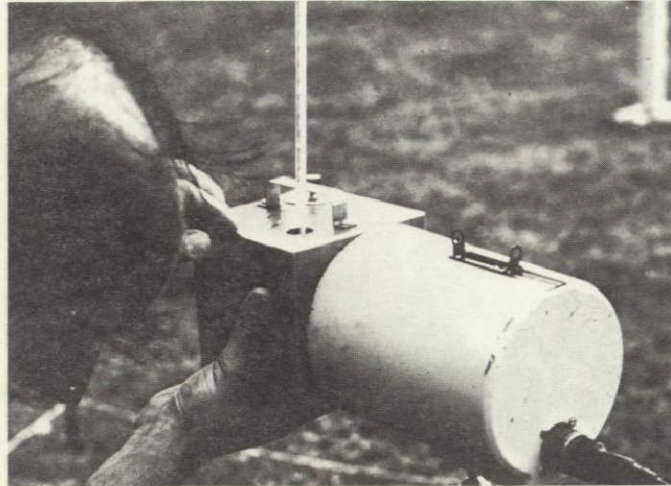


Figure 16-11.- Cross-calibration of radiation sensors. A basic calibrating device, the Leslie Cube is shown being applied to the ground PRT-5 thermometer (upper), a water bucket being used in calibration of the Barnes plane PRT-5 (lower left), and cross calibration of these devices to the RS-14 scanner of the NASA aircraft (lower right).

SECTION 17
GEOGRAPHY PROGRAM REVIEW AND INTEGRATION

By Robert H. Alexander
Geographic Applications Program
U S Geological Survey

N71-19268

ABSTRACT

The five substantive presentations of recent research results of the geography program are only a partial reporting of the progress of the past year. Advances in other projects of the geography program include the quarter million scale land use map of the southwest from Gemini and Apollo photographs, a new map and mapping procedures based on color infrared film for mapping montane vegetation in southern California, new comparisons of urbanized areas as depicted on radar imagery in New England, the application of spatial filtering to separate different terrain types from multi-spectral imagery, and new empirical evidence demonstrating the relationship of urbanized areas to population census data. Each one of these studies, along with the five examples presented at this meeting, fits into a tightly structured research program which is exploring a high priority topic leading toward a capability to use remote sensors in aircraft and spacecraft to obtain vital data on the effects of man's interaction with his environment and the quality of the environment that results from man's changes.

INTRODUCTION

The five geography projects reported on at this review form a part of an integrated geographic research program, reaching back five years and embracing a broad representation of physical and human environmental assessments of remote sensing techniques and applications. The goal of this effort is to establish the feasibility of incorporating data obtained from remote sensors into specific geographic and environmental information systems, so that an increased understanding of processes governing the spread of human populations and their environmental interactions will be available to resource managers and policy makers.

Following directly from this goal is the necessity for examining the whole sequence of operations which are required to prove feasibility of the sensors in an operational system (1) testing the prototype sensors in aircraft platforms over well-documented test sites, (2) establishing the detectability of the pertinent earth-surface features and environmental phenomena at various resolutions and scales of observation, (3) examining available spacecraft imagery as an aid in planning for utilization of early low-resolution earth resources satellites, (4) determining the tolerable limits of error and observation accuracy, (5) determining information systems requirements for enabling the remote sensing techniques, once proven, to be used meaningfully by the scientist or resource manager, (6) identifying the clients for the data to be produced by the ultimate operational remote sensing

system, and (7) assuring that adequate steps are taken for education, training, and retooling so that user groups will be ready and able to incorporate remote sensing data into their operations.

In the context of this required sequence of operations, the present status of the geography program can only be regarded as preliminary, having been largely confined to the first three stages. The need for an accelerated thrust into the remaining stages, backed by more stringent data-gathering requirements in our proposed use of the aircraft program, is indicated by results of the recent research, some of which have been reported by the other contributors to this geography presentation.

In this review and integration of the geography program the results of the aircraft missions (fig.1) flown over geography test sites (fig 2) are related to five topics or problem-oriented objectives which guide the research. These objectives derive from existing funding categories (Forms 1122) as follows:

<u>Objective</u>	<u>Funding Category</u>
1. Analyze land use changes and disaster effects	Land Use Analysis Task No. 160-75-01-32-10
2. Monitor and predict urban growth and environmental quality	Urban and Metropolitan Studies Task No. 160-75-01-35-10
3. Assess man-induced climatic change	Environmental Impact Studies Task No. 160-75-01-16-10
4. Supplement census information	Census Applications Project Task No. 160-75-01-58-10
5. Update small-scale thematic maps	Land Use Analysis Task No. 160-75-01-32-10 and Urban and Metropolitan Studies Task No. 160-75-01-35-10

OBJECTIVE ANALYZE LAND USE CHANGES AND DISASTER EFFECTS

Evaluation of remote sensors as gatherers of basic land use data have been a part of the geography program since its inception. Potential payoffs of this effort are improving the basic data inputs for regional planning and economic development, hazard and disaster assessment, recreation planning, and resource management in both the public and private sectors of the economy.

East Tennessee State University

The examination of remote sensing systems and their applicability to resource management problems in the Asheville Basin portion of the Tennessee

Valley Authority (Site 46) is complete and the final reports are being written. Missions 14, 23, 34, 53, and 65 were flown in support of this work. The reports detail a wide variety of remote sensing applications to rural land use, landslide studies, rural trade areas, water resources management, and broad-area assessments through remote sensor-aided classification of land types into functional subunits, each of which is related to a distinct Appalachian type of rural economy. A good information base has been developed for later assessment of spacecraft imagery. One important spinoff from this project has been the involvement of TVA in remote sensing programs and the establishment in TVA of a specific remote sensing function, with indications of beneficial applications from earth resources satellite data.

University of California, Riverside

Some recent results from regional land use analysis and sensor tests, at University of California at Riverside by Claude Johnson and Robert Pease, were reported on at this review by Johnson. It is important to stress that the analysis of the Apollo IX color infrared photography of the Imperial Valley was made possible by a sequence of studies extending through Missions 29, 42, 56, and 73 flown over the Southern California Test Site (Site 130), augmented by imagery from earlier Gemini and Apollo missions (fig. 3). The preliminary assessment of this complex series of operations is complete and the project is being terminated in its present form. As a result of the UCR studies, many potential "users" among local and regional resource agencies were brought into the program experiments. Several specific remote sensing applications in regional resource development and arid-lands assessment have been demonstrated. Among the new developments which have grown out of this project are a new research effort in surface energy exchange studies and a continuation under other sponsorship of the data processing implications of a capability to monitor regional land use changes by means of remote sensing surveys.

Florida Atlantic University

Land use assessment from low altitude aircraft data provided by Missions 66, 79, 85, 90, and 92, in the urban-dominated subtropical southeast (Test Site 164) is almost complete and the first reports have been submitted. Land use assessments have been carried out in the context of studies of improving automatic methods for handling and analyzing images for their land use content. Television measurements and simulation techniques have been employed, with particular attention being given to the effects of different scales on the automated analysis of the imagery. Having evaluated both low altitude aircraft and spacecraft photography, the investigators required two high altitude (RB57) flights to enable them to complete the analysis.

University of Georgia

Results of the analysis of recent data from this project were reported by Merle Prunty at the session. This project has been supported by the

following aircraft missions 964, 67, 81, 85, 90, 92, 93, and 95. Two or three high altitude flights (RB57) are requested to round out the seasonal coverage of the Florida test sites. The importance of improved control in the processing of the color infrared film, the most crucial single sensor for this project, has been stressed. It is also necessary for this project to obtain data from true savannas, preferably in Latin America, since the application to the tropical development and settlement problems has been the central concern of this project, and the Florida and Georgia test sites represent merely the best approximation to true savanna conditions in the continental United States

Land Use summary

The direction of the land use analysis task will be increasingly concentrated in areas where change is rapid and critical. This entails a focusing on the problems of dynamic changes in the vicinity of the large metropolitan areas, on economic development applications throughout the world, particularly in the tropics, and on hazard areas and disaster information management

OBJECTIVE MONITOR AND PREDICT URBAN GROWTH AND ENVIRONMENTAL QUALITY

The assessment of remote sensors as aids in data collection in urban environments has also been an integral part in the geography program since the beginning. Research has been conducted by Northwestern University, the University of California at Riverside, Dartmouth College, the University of Kansas, and the Office of Emergency Preparedness. There has been a high degree of interaction among the investigators in the urban field, with missions often shared jointly by more than one investigator. Therefore, this discussion will be arranged according to the applications area in urban studies rather than the contractor or principal investigator performing the work

Housing quality

A major portion of the effort in the urban program has been devoted to the assessment of housing quality by means of remote sensing data, some recent results of which were reported at this program review by Frank Horton. The following aircraft missions contributed to the housing quality effort. 12, 14, 19, 25, 31, 43, 73, 81, and 98. Data collection was accomplished or attempted at test site locations in Phoenix (Site 29), Chicago (Site 43), Los Angeles (Site 130), New Orleans (Site 132), and San Juan (Site 92). For United States cities we consider that an aircraft capability has been achieved for satisfactorily classifying residential areas into housing quality categories, in the sense that further testing of the ability to detect critical phenomena from low altitude aircraft flights is not required. To carry the aircraft housing quality surveys to the point of operational capability the next steps would be, as demonstrated by the results of the research performed to date, to improve the training of interpreters, train research teams to

calibrate the housing quality measurement procedure for use in different cities, and provide appropriate liaison among the remote sensing research program and the Federal and local agencies who are concerned with and responsible for obtaining data on housing quality. The method developed here for determining housing quality is only appropriate for low flying aircraft obtaining high resolution photography (resolution requirements in some cases exceeding 20 feet) and hence is not applicable for ERTS-A or other early proposed satellite systems.

Air pollution

Remote measurement of NO_2 and SO_2 through use of an absorption spectrometer has been considered feasible and worthy of further tests as the result of experimentation during Mission 73 in the Los Angeles area (fig. 4). Further experimentation with the spectrometer equipment is being performed by MSC, and the geography program contemplates no requirements for measurements during the coming fiscal year.

Urban planning applications

Remote sensing has been demonstrated to be an important data input to the urban planning process. Aircraft missions 29, 42, and 73, along with some radar missions, have demonstrated feasibility of utilizing various remote sensors to obtain data on, for example, residential land use, commercial land use, industrial land use, public and semi-public open space, institutional land uses, and transportation facilities, all of which may be needed in the preparation of data base for planning. Most of the urban planning requirements are for relatively high resolution information, indicating less application to the proposed early generation earth resources satellites than to either aircraft or higher resolution satellite data-gathering. More research is needed to establish the dependability and accuracy of the relatively low resolution imagery from projected space missions. There also needs to be a considerable amount of work with individual clients (specific city planning groups) and Federal supporting agencies. One of the most crucial needs is an information systems development capable of handling and managing the flow of remote sensing data which would result from an operational remote sensing connection to the planning process.

Urban change detection

The detection of change in an urban area is one task that can be considered for lower resolution systems. Aircraft missions 25 and 42, various Gemini and Apollo spacecraft missions, and radar missions have provided data for studies demonstrating recognition of gross features of urban areas, and hence the ability to detect changes in those features. Related research has been carried out at Northwestern University, the University of California at Riverside, and Dartmouth College (fig. 5).

Emergency Preparedness applications

Missions 40, 62, 66, and 81 have provided data in support of the study of remote sensing capability for improving emergency planning activities,

particularly in urban and industrial environments. Work has been carried out in cooperation with the Office of Emergency Preparedness, and a report on the first phase has been submitted. A proposed extension of this work would deal with the detection of various phenomena related to stockpiling of strategic materials.

Urban studies - future direction

Planned studies in urban applications of remote sensing will follow promising leads provided by the program results to date and will stress the following topics for further emphasis: change detection in fastest growing areas, for example the growth of suburbs of large cities, remote sensing applications to the population census, remote sensing applications to the study of urban environmental effects, such as pollution, climatic change, overcrowding, and other large-scale systems effects of urbanization, and the study of non-United States urban environments, which are much more poorly known than the American cities, but which have many of the same critical problems.

OBJECTIVE ASSESS MAN-INDUCED CLIMATIC CHANGE

One of the objectives of Mission 73 was to investigate the use of remote sensors for obtaining data on the surface heat and water balance. Sensors operating in the visible, thermal, and microwave (fig. 6) regions of the spectrum were included in the experiments. The results of those investigations were encouraging and led to the establishment of a new task, "Environmental Impact Studies" in the Geographic Applications Program, which was set up primarily to develop remote sensor capability for studying the too-poorly documented changes in the climate which are brought about by land use changes and other environmental effects of man's activities. The thrust of the new program is to be toward the study of urban climates and the effects of the urbanization process on climate.

The new investigation, to be conducted in part at the University of California at Riverside, was reported on by Robert Pease at this review. An important requirement is the flying of sensors with careful calibration and ground checks. An initial experiment was performed in Barbados during Mission 98 where a great deal of ancillary data was available for correlating with the measurements obtained by the NASA aircraft.

We foresee the need for much larger effort in this area. A more detailed sensor-ground truth experiment is projected for the coming fiscal year, probably in the vicinity of Houston. The importance of environmental studies of this kind will increase as environmental change brought about by man becomes more intense and widespread.

OBJECTIVE SUPPLEMENT CENSUS INFORMATION

The feasibility of a new thrust in the direction of census applications was demonstrated in a preliminary way by data from missions 14 and 25,

providing information on the relationship of remote sensing data at high resolution to the distribution of dwelling units and hence to distribution of population in urban areas. Other work based on Gemini and Apollo imagery has indicated the strong possibility of determining relationship between built-up areas, as observed on even low resolution imagery, and population living within those areas, a relationship which may be quantitatively valid for relatively large areas with the same cultural conditions. The United States may have a single "index" relating population to the built-up areas, it is clear that other cultures such as the Nile delta and Japan, where people characteristically live more closely packed together, will have different indexes. These promising indications have led to the establishment of a new task in census applications. New missions have tentatively been requested for Cedar Rapids, Iowa, and a portion of eastern Michigan, the locations of these missions may be changed depending upon availability of adequate ground survey teams to provide correlative information.

OBJECTIVE UPDATE SMALL SCALE THEMATIC MAPS

A number of investigations, primarily by the University of Kansas and the Association of American Geographers, have been conducted to determine the applicability of remote sensing imagery at various scales to the preparation of small scale thematic maps. Recent results from the University of Kansas program were reported at this review by David Simonett. The Association of American Geographers' effort has resulted in the preparation of a manuscript map at a scale of 1:250,000 of an extensive area in the southwestern United States covered by Gemini and Apollo photography (fig. 7). A fourteen-category, land use classification has been developed and adapted to the characteristics of space photography. This work is expected to lead to experiment definition for ERTS-A data utilization. An inescapable preliminary conclusion derived from this program, however, is that we need to supplement remote sensing engineering tests with more definitive information on the complex environments we are trying to observe. The variations in the environment, the very factors we are trying to map, are causing much more difficulty in developing remote sensing signatures for land use types than previously thought.

CONCLUSION

The sequence of operations required to progress from aircraft or satellite sensor tests to the operational goal of utilizing remote sensor data to increase our understanding and our prediction capability of the interaction between human and environmental systems is illustrated in a condensed form in Figure 8. Three matrices are used to display the relationships among the necessary stages of the research program, and incidentally to point out areas where future emphasis might profitably be projected.

The lower left hand matrix displays the combination of sensors and aircraft or satellite platforms that have been tested in the geography program. The lower right hand matrix relates information from remote sensors concerning

the critical geographical phenomena of interest with detectability as proven by the remote sensing program to date. The upper right hand matrix indicates the phenomena or combinations of phenomena obtainable from remote sensing, in relationship to their use in solving a particular research problem in geographic analysis or resource management. It should be emphasized that the list "Information from Remote Sensors" is highly abbreviated in this particular chart presentation and is included at this time to be indicative rather than exhaustive. The arrangement of phenomena of primary concern to the land use and urban projects has been devised to group together on the one hand larger-sized objects and phenomena which are expected to be visible from low resolution ERTS types satellites, and on the other hand higher resolution phenomena which to date have been detectable only from aircraft platforms. Assignment of a particular phenomenon to one category or the other is not firm and depends upon the continued results of the research program. The establishment of connections between information obtainable from remote sensors and the use of that information in a particular research or resource management problem may require a large research effort in itself. For example, in applying various kinds of urban data to the problems of urban land use mapping or city planning applications, it may be necessary to develop whole new information systems before the application becomes feasible. Hence each square is not a simple "yes" or "no" but is rather an indication of a major task that will be spelled out in detail in the future in the Geographic Applications Program.

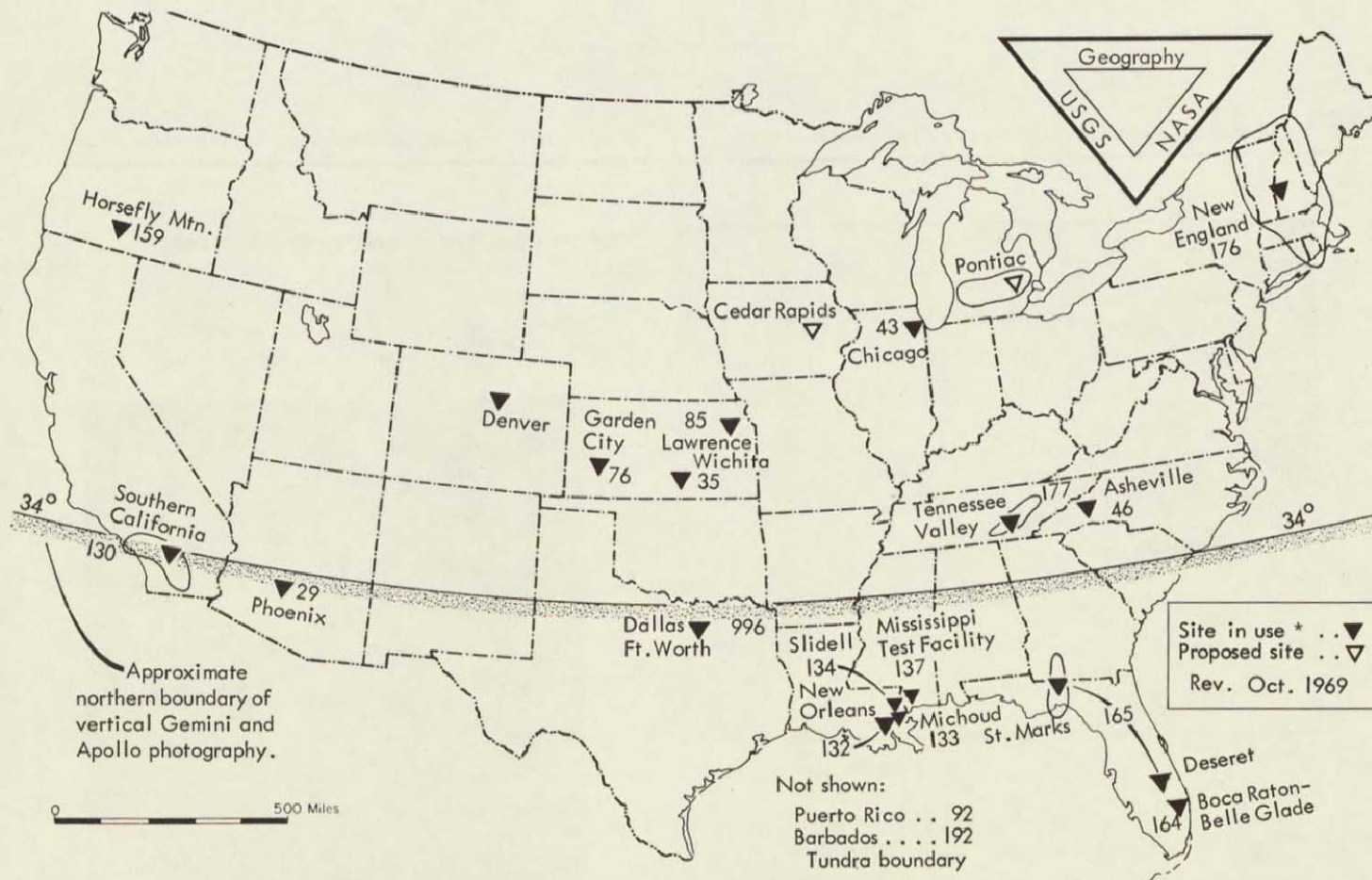
A shorter version of the chart, which uses the four-category rating scale (feasible, promising, not promising at present, and unknown) for the application of remote sensing instrumentation types to major geography program objectives is presented in Figure 9. The lower matrix on Figure 9 indicates the kinds of sensing experiments proposed or planned for future implementation in the Geographic Applications Program. Obviously not all of these are related to the activities of the coming fiscal year.

The sequence of research in the Geographic Applications Program has led us from a broad examination of a large number of geographic topics to a concentration on fewer topics in which we feel we can make a greater impact. The selection of these topics is based on what we consider to be high priorities for the agencies and the nation. These topics will stress those areas where we feel that our main competence lies, namely, in the area of environmental systems studies, involving interactions of physical and human factors. We call these "man-environment systems."

In the ensuing program we will need to maintain close connections, as in the past, with sensor experimentation, but must increase the relative emphasis on data analysis and information systems to make it possible to use the remote sensing data in practical projects. In terms of the chart of Figure 8, this would represent an increase of emphasis in the upper right hand matrix.

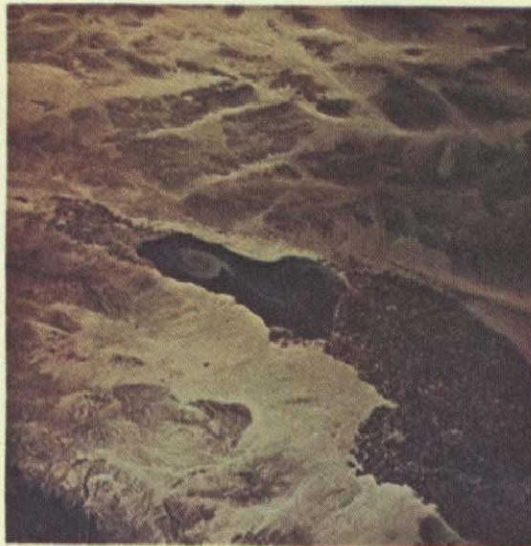
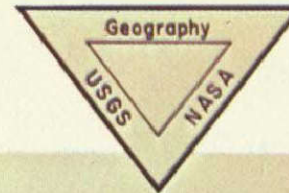
We shall continue to stress the study of time-variance of environmental phenomena and the importance of adding the time dimension to the spectral

dimension, and to developing remote sensing signatures for practical applications. At the same time we intend to stress the improvement of environmental models, for example, economic development models, urban growth models, spatial diffusion and interaction models, and energy exchange models, which will guide the design of the experiments and enable us to use the new remote sensing technology more effectively for the solving of critical environmental problems.



* Accompanying chart, arranged by Test Site number, shows contractor, mission number, and fiscal year.

Figure 17-2.- Geographic Applications Program; test sites.



Oblique view to Northeast
across Imperial Valley

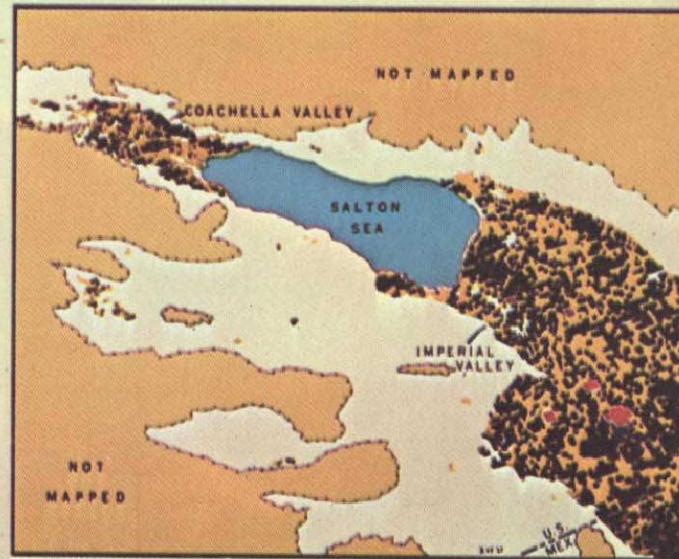


Land Use map of area in foreground of photo



Land Use Classes

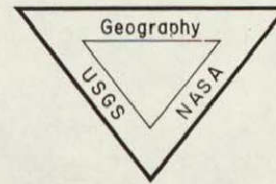
- Agricultural land (intense vegetation).... 
- Agricultural land (fallow)..... 
- Urban land unit..... 
- Vacant land..... 



Based on research at the University of California at Riverside ... as part of the USGS / NASA Geographic Applications Program

8.

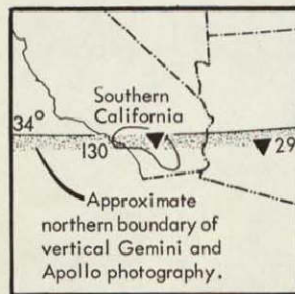
Figure 17-3.- Mapping land use from Gemini color photos.



Land use mapping from spacecraft imagery was attempted for the first time from this Gemini photograph. The scale of the imagery used in the study was 1/1,000,000.

The larger urban areas were easily identified, but no differentiation of urban land use was possible. The deep blue portions of the photograph were interpreted as crops in a high state of growth; the light blue portions as cropland in an early stage of growth, or after harvest; and the beige to white portions, similar in tone to the surrounding desert, as vacant land.

The accuracy of land use mapping in the Coachella Valley was estimated at 50 percent and in the Imperial Valley at 85 percent. To increase the accuracy of land use mapping from space, photographs of higher resolutions and closer to the vertical will be necessary. This land use mapping exercise has stimulated research efforts involving the Imperial Valley and led to the multi-sensor, multi-disciplinary USGS/NASA Mission 73.

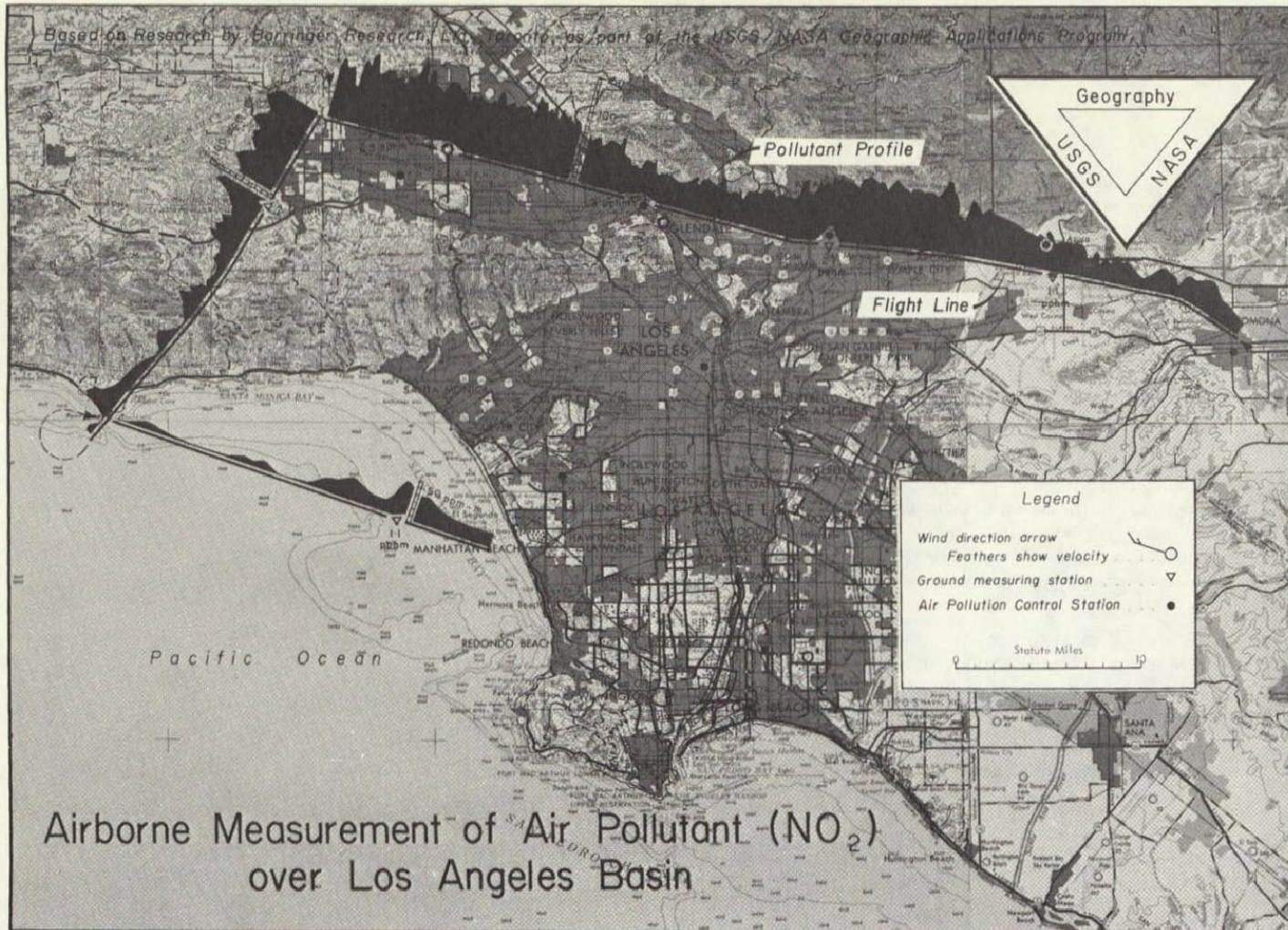


Geography Test Site 130
Southern California

Based on research at the University of California at Riverside ... as part of the USGS/NASA Geographic Applications Program

b.

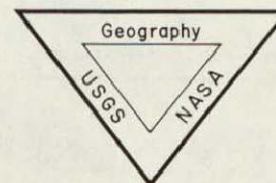
Figure 17-3.- Concluded.



a.

Figure 17-4.- Airborne measurements of air pollutant (NO_2) over Los Angeles Basin.

Based on Research by Barringer Research, Ltd., Toronto, as part of the USGS/NASA Geographic Applications Program

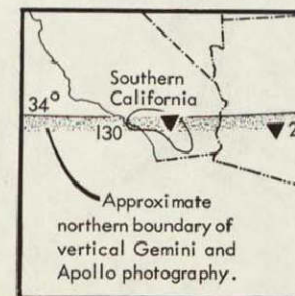


Airborne remote sensing of NO_2 over the Los Angeles basin showed a reasonable correlation between airborne measurements in parts per million per meter of atmospheric path length (ppm-m on height scale of graphed profile) and simultaneous ground measurements expressed in parts per hundred million (pphm). Ground measurements at selected points on line of flight are derived from observations recorded at Air Pollution Control District stations throughout the area.

Concentrations of NO_2 in the atmosphere increased over the city, but decreased over mountains, ocean, or farmland.

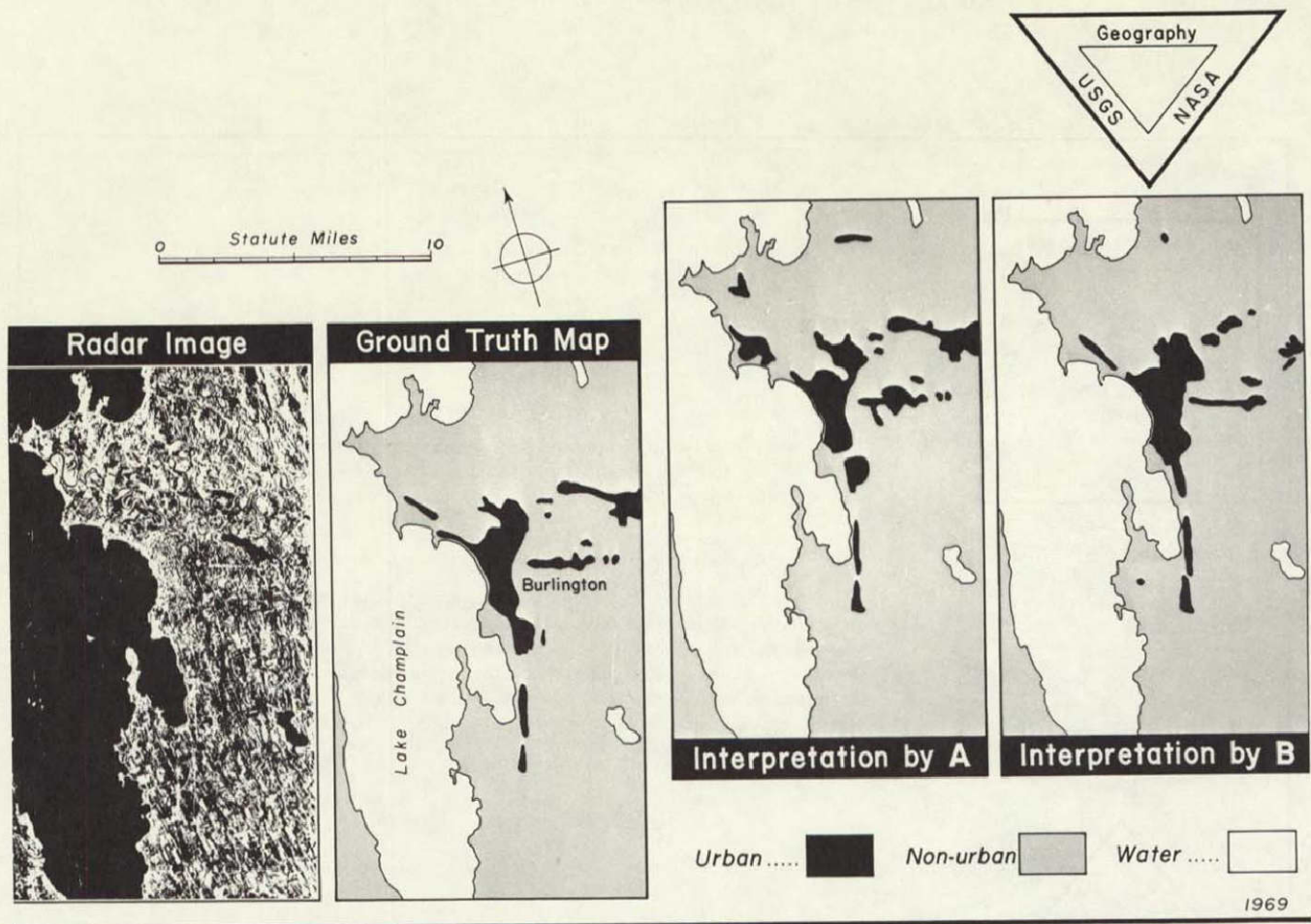
Air pollution influenced by man changes the energy flux through the atmosphere. High concentrations of NO_2 in the urban atmosphere may be injurious to health. Monitoring is one essential element in the control of air pollution.

Geography Test Site 130
Southern California



b.

Figure 17-4.- Concluded.

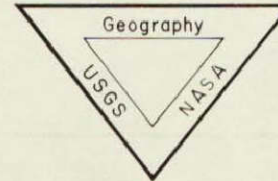


Based on research at Dartmouth College ...

... as part of the USGS/NASA Geographic Applications Program

a.

Figure 17-5.- Mapping urban areas from K-band radar.



In 1966, most Geography test sites were covered by relatively small scale, airborne, Side Looking Radar (SLAR), in the K-band portion of the electromagnetic spectrum. The application illustrated here investigates the use of this and supporting sensors to distinguish urban from nonurban area, and to recognize large bodies of water.

The pair of panels on the left in the illustration compare at the same scale the Radar Image and a corresponding Ground Truth Map. The latter shows the Burlington, Vermont urban area on the east shore of Lake Champlain.

The pair of panels on the right show two delimitations of the Burlington urban area and its outliers. Interpreters A and B, unfamiliar with the ground truth or the Burlington scene itself, submitted the separate interpretations shown. There is close agreement on delimitation of the central urban area. However, there are greater differences in the recognition and delimitation of the outlying portions of the urban area.

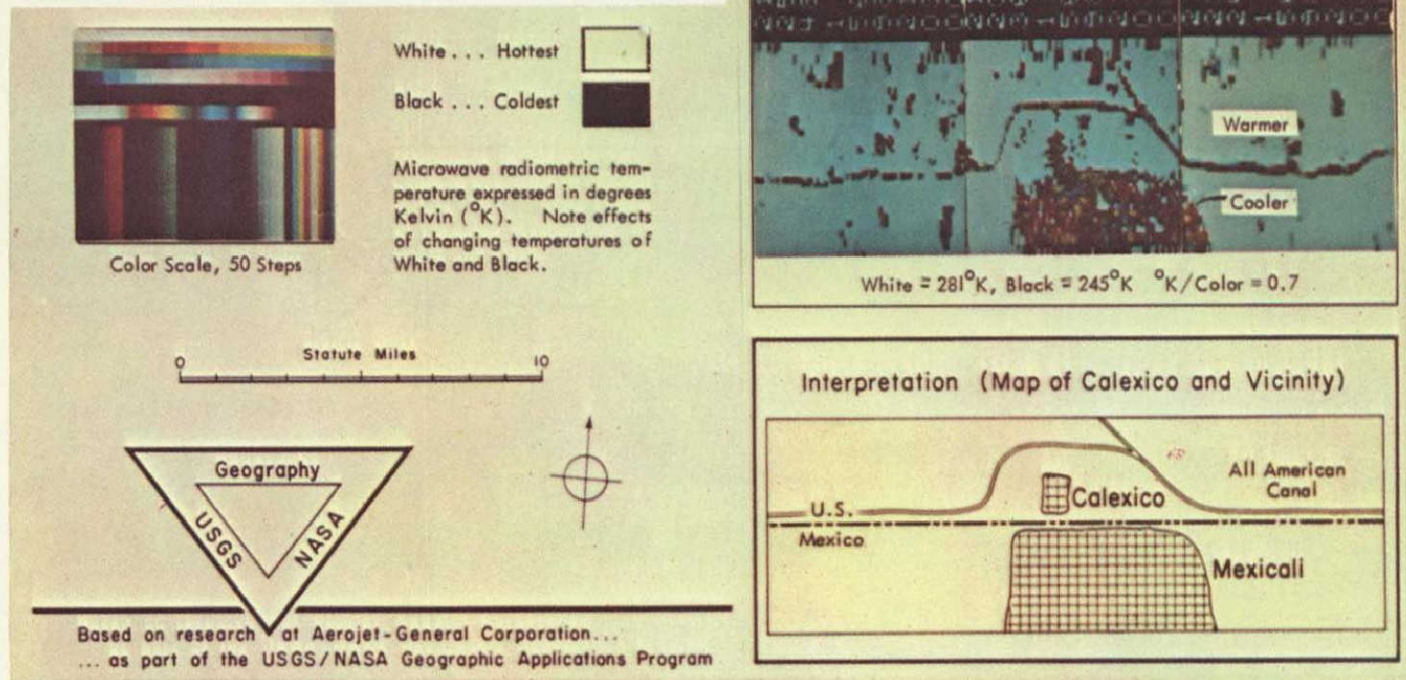
Research elsewhere has shown that there is a close correlation, in a given culture region, between population size of a settlement and the amount of area it covers. This research sheds some light on the magnitude of the task of recognition and delimitation, by different trained analysts, and on the effect this will have upon measurements of urban area and the resulting estimates of population size. To some extent, the small scale, airborne SLAR imagery also simulates that which might be procured with a higher resolution sensor from orbiting altitudes.

Geography Test Site 176
New England



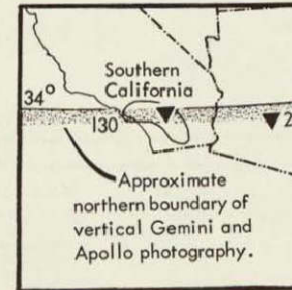
b.

Figure 17-5.- Concluded.



a.

Figure 17-6.- Recognition of gross surface temperature patterns by analysis of passive microwave radiometry.

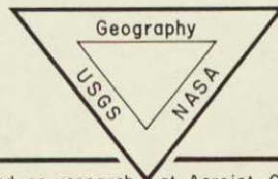


Geography Test Site 130
Southern California

Passive microwave images obtained from aircraft revealed gross land use, that is, urban from rural, open water, irrigated districts from non-irrigated.

Data are tape-recorded, and can be manipulated to highlight different features. Changing the temperature/color scale to a "colder" setting causes warmer agricultural areas to be rendered in white, while enhancing the temperature discrimination in the colder urban areas.

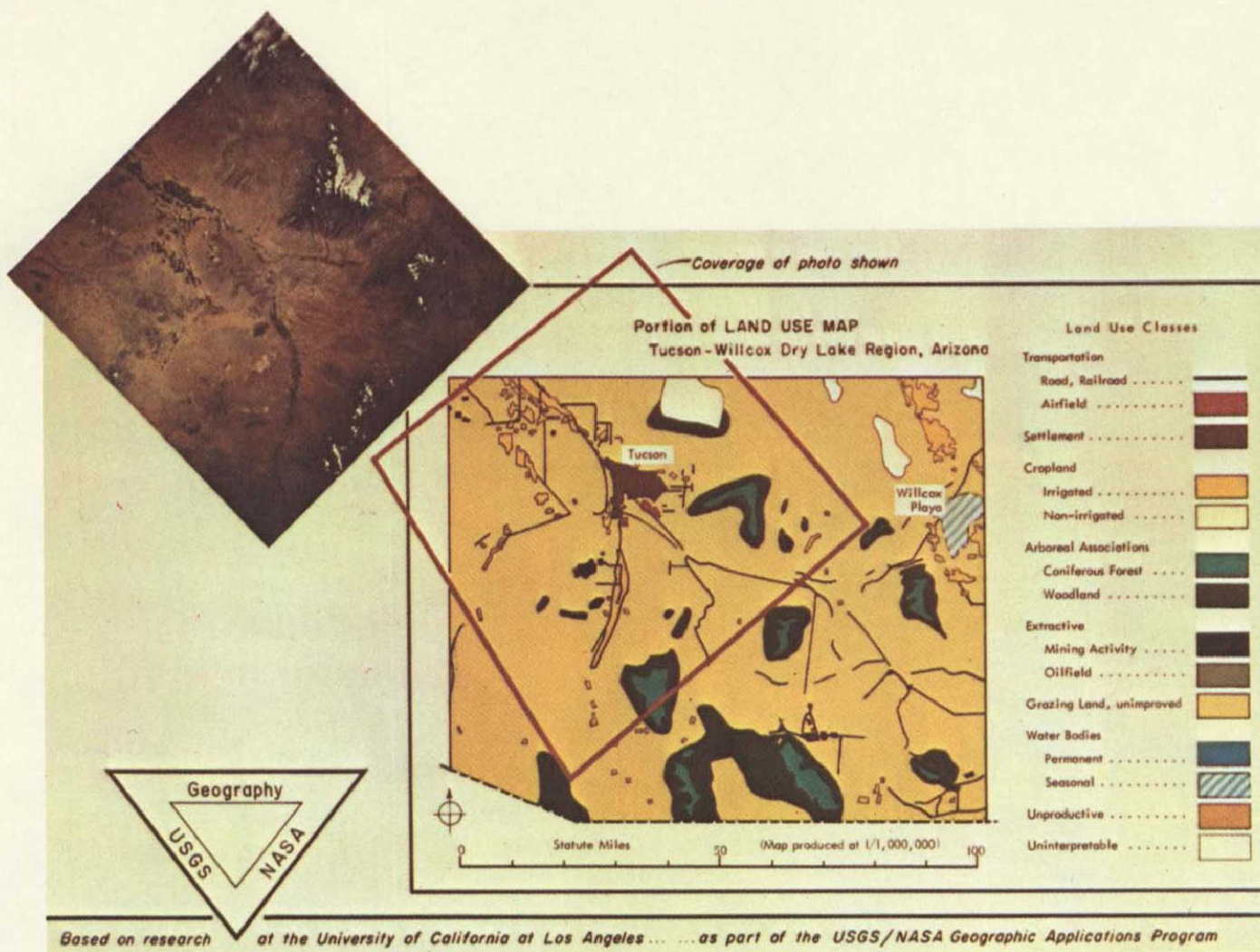
This research demonstrates the relationship of built-up urban areas to colder microwave temperatures. This might lead to a future capability to obtain quick estimates of urbanized areas in large regional surveys by means of passive microwave imaging techniques.



Based on research at Aerojet-General Corporation...
... as part of the USGS/NASA Geographic Applications Program

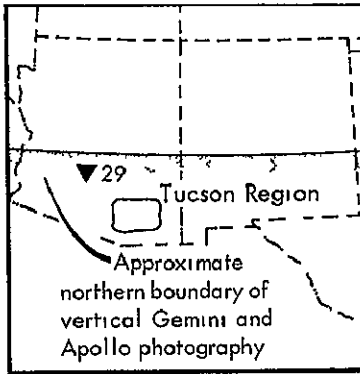
b.

Figure 17-6.- Concluded.



a.

Figure 17-7.- Regional land use classification from Gemini color photography.

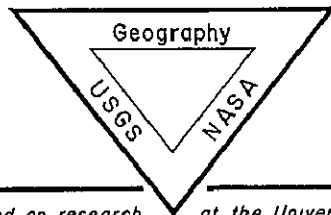


Tucson-Willcox Dry Lake
Region, Arizona

A land use map of the Southwestern United States is being prepared from Gemini imagery, supplemented by Apollo imagery. The finished map will be produced at a scale of 1/1,000,000. Representative portions of the imagery, the land use map, and the land use classification system, are shown in this illustration.

The irrigated agricultural areas are clearly visible on the photo, where their areal extent is sharply defined. The non-irrigated agricultural areas tend to blend into the landscape and were not detected within the area covered by the photo shown. Major transportation lines are generally visible, but roads and railroads cannot be distinguished from each other. Large urban centers can be identified by street patterns and a coarse-textured signature, however, small urban centers are easily missed because the street patterns are not visible and the coarse texture is easily overlooked. Nearly 10,000 square miles were ground checked in order to confirm positive land use interpretation, and to discover the significance of the color-textural patterns observed on the imagery.

The significant benefits derived from using satellite-borne imagery for land use mapping include wide coverage, scale, speed of interpretation, reduction of field work, and potential ease of periodic revision.



Based on research at the University of California at Los Angeles as part of the USGS/NASA Geographic Applications Program

b.

Figure 17-7 - Concluded.

GOAL
 Improve the management of our Land, Water, and Atmospheric Resources by increasing our understanding, and prediction capability, of the interaction between the human and environmental systems

Analyze land use changes and disaster effects	APPLICATION	A	A	A	B	A	B	D
Monitor and predict urban growth		A	A	A	B	A	B	D
Assess climatic change		C	B	B	A	C	B	D
Supplement Census information		B	B	B	C	B	C	D
Update small-scale maps		A	A	A	C	B	C	D
<p><u>Application Feasibility Code</u></p> Feasible A Promising B Not promising at present C Unknown D		INSTRUMENTATION						
		Conventional Color Film	Composite, IR Color Film	Multispectral Imagery	Thermal Infrared	Active Microwave	Passive Microwave	Low Light Level TV
Aircraft	OBSERVATION PLATFORM	//	//	//	//	//	//	
APOLLO / GEMINI								
ERTS A and B				//	//			
ERTS C and D								
Film Return Satellite A and B (FRS)			//					
Small Applications Technology Satellite								
NIMBUS / TIROS								
APOLLO Applications Program (AAP)		//	//	//	//	//	//	
Space Station		//						

Data obtained X
 Data acquisition planned // Revised Sep 69
 Data acquisition uncertain ?

Figure 17-9 - Discipline research matrix, geography and cartography